Univerzita Karlova v Praze, Přírodovědecká fakulta,
Ústav geochemie, mineralogie a nerostných zdrojů

REKONSTRUKCE PALEOKLIMATU Z ABIOGENNÍCH A BIOGENNÍCH PROXY ZE SEDIMENTÁRNÍHO ZÁZNAMU BAJKALSKÉHO A ARALSKÉHO JEZERA

disertační práce

Mgr. Anna Píšková

Vedoucí disertační práce: Dr. David Hradil
Konzultant: RNDr. Tomáš Grygar, CSc.

Praha 2009

Prohlašuji, že jsem tuto práci, ani její podstatnou část, nepředložila k získání jiného nebo stejného akademického titulu.

I hereby declare that neither this thesis nor its part was already used to obtain equivalent or another academic degree.

This thesis is based on the following papers:

I. **Píšková, A**., Grygar, T., Veselá, J., Oberhänsli, H., 2009. *Diatom assemblage variations in the Aral Sea core C2/2004 over the past two millennia.* Fottea. Accepted.

II. Grygar, T., **Bláhová, A.**[1], Hradil, D., Bezdička, P., Kadlec, J., Schnabl, P., Swann, G., Oberhänsli, H., 2007. *Lake Baikal climatic record between 310 and 50 ky BP: Interplay between diatoms, watershed weathering and orbital forcing*. Palaeogeography, Palaeoclimatology, Palaeoecology 250 (1-4) , p. 50-67.

III. **Píšková, A.**, Novotná, K., Veselá, J., Oberhänsli, H., Chabrillat, S., Nourgaliev, D.K., Sapozhnikov, F.V., *Environmental changes in the Aral Sea during past 1800 years: diatom and mineral based reconstruction.* Manuscript.

IV. **Píšková, A.**, Bezdička, P., Hradil, D., Káfuňková, E., Lang, K, Večerníková, E., Kovanda, F., Grygar, T., *High-temperature XRD as a tool for characterization of smectites, layered double hydroxides, and their intercalates with porphyrins.* Applied Clay Science. Submitted.

My contribution to the papers:

I carried out experimental work concerning diatom analysis as well as major part of interpretation and writing that was related to the papers I, III, IV. In the paper II I have provided diatom analysis.
I participated on all methods that have been carried out in the Institute of Inorganic Chemistry of the Academy of Sciences of the Czech Republic, v.v.i. (AS CR), I visited workplaces where external measurements have been provided, i.e. GeoForschungsZentrum (GFZ) Potsdam, Germany; Department of Paleomagnetism, Institute of Geology, AS CR, v.v.i.; Polymer Institute Brno, s. r. o., CR.

[1] maiden name of Píšková A.

TABLE OF CONTENT:

LIST OF FIGURES:

LIST OF TABLES:

LIST OF ABBREVATIONS:

AS CR ..... Academy of Sciences of the Czech Republic
AAS/AES ..... Atomic adsorbtion/emission spectroscopy
AMS ..... Accelerator Mass Spectrometry
ARM ..... Anhysteretic Magnetic Remanence
CEC ..... Cation exchange capacity
CCD ..... Carbonate compensation depth
CR ..... Czech Republic
DAZ ..... Diatom assemblage zone
D/O ..... Dansgaard/Oeschger event
DRIFTS ..... Diffuse reflectance infrared fourier transform spectroscopy
DRS ..... Diffuse reflectance spectroscopy
EDX ..... Energy Dispersive X-ray Analysis
ENSO ..... El Niño/Southern Oscillation
GFZ ..... GeoForschungsZentrum - Research Centre for Geosciences
HT-XRD ..... High temperature x-ray diffraction
IRM ..... Isothermal Remanent Magnetization
KY ..... Kilo years
LIA ..... Little ice age
LOI ..... Loss of mass during ignition
MIS ..... Marine isotopic stage
MS ..... Magnetic susceptibility
MWP ..... Medieval warm period
NAO ..... North Atlantic oscillation
NRM ..... Natural remanent magnetization
OIS ..... Oxygen isotopic stage
POM ..... Picked organic matter
SEM ..... Scanning electron microscope
SST ..... Sea surface temperature
TOC ..... Total organic carbon
UV-VIS ..... Ultra-Violet - Visible
VNIR ..... Visible/Near Infrared Reflectance
XRD ..... X-ray diffraction
XRF ..... X-ray fluorescence spectroscopy

ABSTRACT

1. ABSTRACT

Lake sediments represent an important source of valuable information about the past climate in continental environment. They consists of a mixture of autochthonous and allochthonous organic and inorganic components both responding to paleoenvironmental changes in the water bodies and watershed. Both the composition and relative content of individual sedimentary components mirrors the climate changes. The main inorganic components in lake sediments are quartz, carbonates, and clay minerals; organic matter embodies various plants and animal remains. Reconstruction of past climate is possible only when an efficient combination of analytical methods allowing characterization of all these components is used. We have provided such multi proxy and high resolution analysis on two cores from two lakes, Aral Sea and Baikal Lake. These two large Asian water reservoirs have got a large watershed, originated tectonically, and have grabbed scientific attention during the last decades.

Aral Sea represents a closed lake system in semi-arid area and therefore Aral Sea sediments mirrors even minor environmental changes. Research performed on Aral Sea sedimentary cores aims to unravel past lake level variations and to determine their leading forces. Ten radiocarbon dates have been used to construct the age model according to which yet unstudied core C2/2004 covers ~2000 years of continuous sedimentation. Lake level changes have been reconstructed based on the actualistic interpretation of diatom species analysis combined with mineralogical and chemical data. We identified four regression phases in periods of phases1900-2000, 1330-1450, 910-1060, and 0-250 AD that contributes significantly to the knowledge of past environmental changes in Aral Sea. However, further work would be needed to unambiguously decide what where the leading forces of past lake level changes.

Baikal Lake is a highly valuable archive of the continental climate of Central Siberia back to the Mesozoic period ideal for the comparison with glacial and marine archives. This open lake system surrounded by a mountainous area is especially sensitive to solar forcings. We have studied one core from Academician Ridge. The age model was based on a correlation of diatom concentration maxima to insolation maxima (high latitude, northern hemisphere); the age model was successfully checked by palaeomagnetic dating. This core represents continuous sedimentation from 300 to 60 thousand years before presence. A combination of diatom analysis, spectral, X-ray, magnetic, and chemical methods enabled us to define periods of enhanced weathering and to distinguish cold/dry and warm/humid phases. Exceptionally stable and most marked climatic optimum in the studied period was the MIS5e, known as Kazantsevo (the analogue of the European Eemian). Our high-resolution paleoclimatic reconstruction complements numerous previous studies focused on the characterization of climate in the Baikal Lake area in the last 150 kilo years (ky).

2. AIMS OF THIS WORK

This work is a part of complex research focused on paleoenvironmental reconstruction from sedimentary cores from Baikal Lake and Aral Sea provided thanks to the cooperation of Institute of Inorganic Chemistry, Academy of Sciences of the Czech Republic v.v.i. (AS CR) and GeoForschungsZentrum - Research Centre for Geosciences (GFZ) Potsdam, Germany.

The main aims of this work are

- to perform diatom analysis on two sedimentary cores / one from Aral Sea and the second from Baikal Lake. Diatom analysis is a traditional, powerful method for paleoenvironmental reconstruction, which is not common in the Czech Republic. This step includes managing of methodology of (i) diatom slide preparation, (ii) counting technique, (iii) proper diatom identification, and most importantly (iv) environmental interpretation of diatom assemblages.
- to understand diatom and inorganic records in order to get a more complex view to the past environment changes. Such multiproxy analysis is more and more required in paleoclimatology.
- to describe limitations and potentiality of methods used in our paleoclimatic reconstructions in two different sedimentary environments and different time periods.

INTRODUCTION

3. INTRODUCTION

3.1. Palaeoclimatic introduction

The major limitation of palaeoclimatic studies is time: there is no possibility to measure past climatic parameters directly. Therefore paleoclimatologists are trying to get as close as possible through proxy values which represents various parameters of the climatic complexity. Proxy parameters could be obtained by many paleoclimatic methods; however, each method has its own limitations which pull to find the effective combination of methods in order to get the most realistic picture of the past.

There are several factors influencing the climate change. These factors, e.g., solar activity, oceanic circulation, atmosphere circulation, continental drift are connected to each other and even separately complicated. I doubt that it is possible to describe these factors in a holistic view. There is always need of simplification, which naturally leads to increase the inaccuracy of the results. The more we simplified, the larger is our mistake. In order to get results as reliable as possible we need to combine results of different sample types, compare results from independently measured methods and moreover combine the more complex results with different studies from other environments. This goal could only be fulfilled by interdisciplinary and international cooperation. Nobody can do climatic study on his own but a team work and international communication is required.

Recently, also as a result of a large public attention to the climatic changes, many of the basic questions are reopened and reinterpreted, e.g. relation cause and effect - global warming vs. CO_2 values, human vs. natural impact in the past and recent - recent global warming as direct result of anthropogenic activity or natural instability at the end of interglacial climatic optimum. There is increasing pressure to gather very large amount of paleoclimatic studies to specify global climate of some periods or some trends in climate change. Although large amount of information about past climate have been already gathered (many very useful data are easily accessible online, e.g. http://www.giss.nasa.gov/research/; http://www.ncdc.noaa.gov/paleo/data.html) unambiguous answers are still missing and disputations among scientists from various disciplines seem to be never-ending.

3.2. Different time periods of climatic changes and their forcing

Past climate could be studied in various time scales beginning with the annual resolution and ending with millions and hundreds of millions years. Each time period has its own dominant forcing, e.g. continental drift did not influence short term changes or anthropogenic activities could not influence more than thousands of years (Figure 1). Climate has both long term trends and short term variability. In looking at longer time scales, major shifts in climate such as the ice ages are easily recognizable. The coexistence of short and long term trends through time complicates our ability to unravel the climate change. Time intervals covered by studied lake cores in this work are in the scale of several hundred ky at largest. The main projected forcings in these time scales are extraterrestrial forcings, i.e. changes in solar output and changes in Earth's orbit.

3.2.1. Earth orbital parameter variations

Variations of Earth´s orbital parameters have periodical character and were firstly calculated and described at the end of 19th century by Croll, than developed by Milankovitch and Berger as astronomical theory, and later proved by isotopic analysis in marine sediments (see chapter 3.5.1) (Bradley 1999). Variations in the shape of Earth´s orbit have been found in (i) the degree of orbital eccentricity around the Sun, (ii) the axial tilt (obliquity) of Earth from the plane of the ecliptic, and (iii) the timing of the perihelion with respect to the seasons on the Earth (precession of the equinoxes) (Figure 2). This wobbles lead to considerable fluctuations in the amount and distribution of incoming solar radiation, resulting in dramatic changes in climate over long time scales. Orbital forcings does not affect the solar radiation over the Earth in the same

Figure 1 Examples of potential processes involved in climatic fluctuations and their characteristic timescales (Bradley, 1999).

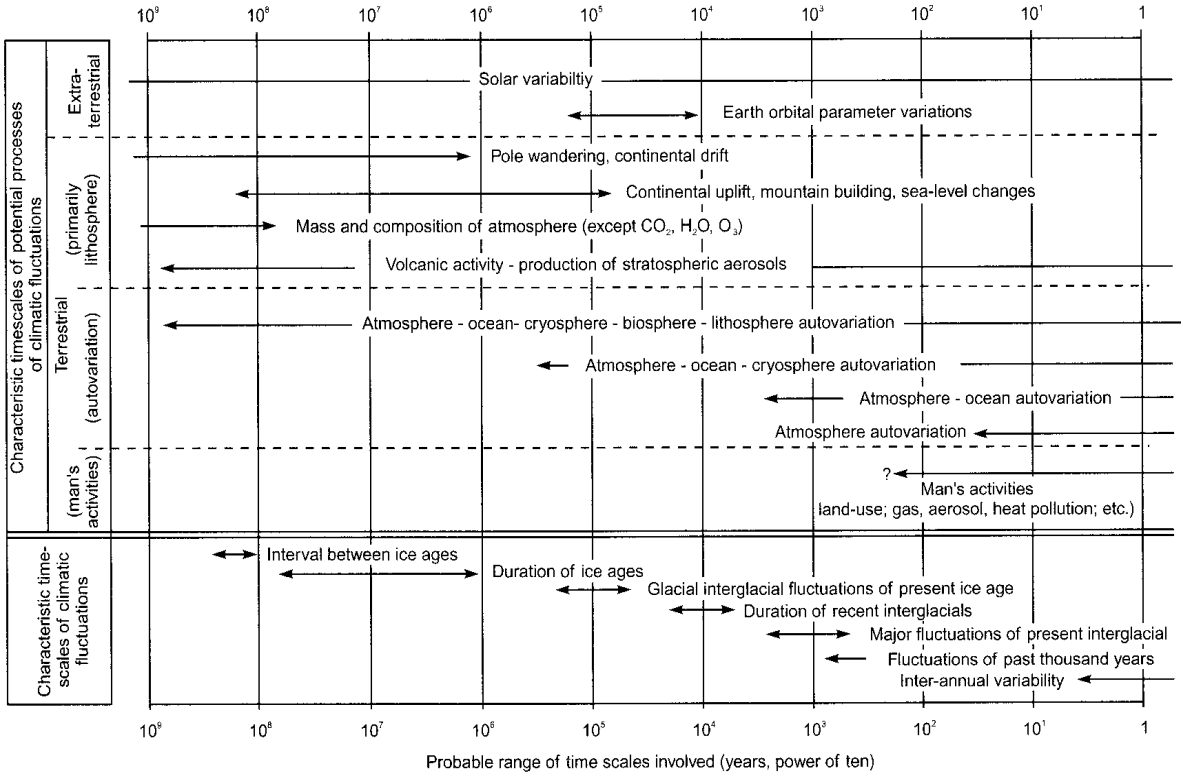

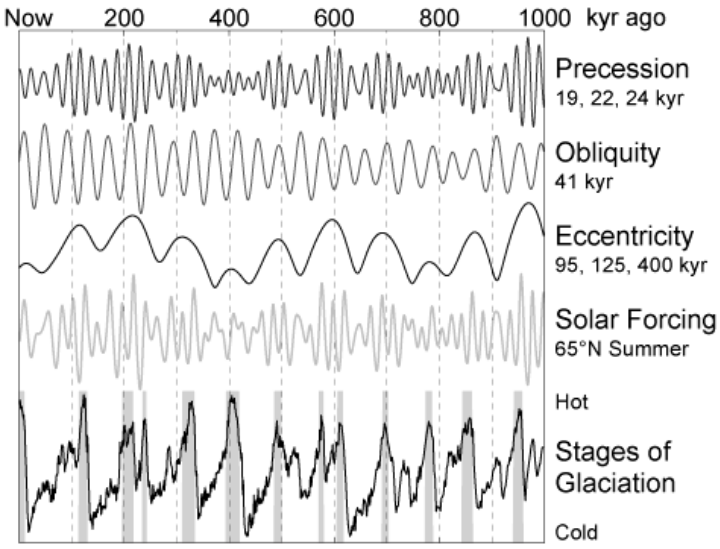

Figure 2 The orbital changes and their duration in comparison with changes in insolation and stages of glaciation. Grey rectangles represent interglacial maxima (Rohde 2005 - online) .

way – low latitude areas are principally affected by variation in eccentricity and precession of the equinoxes. By contrast, higher latitudes are mainly affected by obliquity changes (Dawson 1992). Such solar forcings are believed to be the major reason for Quaternary glacial/interglacial periods (Figure 2).

Past cold and warm periods covering glacial and interglacial periods and additionally fluctuations within glacial stages are very often demonstrated on the oxygen isotopic record (see chapter 3.5.1) divided to oxygen isotopic stages (OIS), or marine isotopic stages (MIS). In OIS curve each cooling and warming event is numbered. Interglacials are marked by odd and glacials by even numbers. Standardized chronology from many oxygen isotopic records is called SPECMAP (Mapping Spectral Variability in Global Climate Project). Each glacial and interglacial period had a different development (Figure 2). Generally it is remarkable that the terminations of glaciations occur rather abruptly, e.g. the transition from the last Ice Age to the warm Holocene climate took about 1500 years, with much of the change occurring in only 40 years (Rahmstorf 2001), on the other hand the crossing into glacial period is gradual.

3.2.2. Short term climatic variations

Within periods of glaciations shorter abrupt climatic changes could occur. One of them is known as Dansgaard/Oeschger (D/O) events. D/O are rapid and yet fully unexplained climatic oscillations described mainly from the last glacial period between 60 – 15 ky BP (Oldfield 2005). D/O events typically start with an abrupt warming around 5 °C within a few decades followed by gradual cooling over several hundred or thousand years (Rahmstorf 2001) with periodicity often around 1500 years. D/O events are linked to orbital forcings and are connected with the termohaline circulation of the ocean (Alley *et al.* 2003). Heinrich events represent the second major type of climatic events during glacials. Heinrich events occurred in a cold stadial phase of some D/O cycles (Rahmstorf 2001) and are traced in North Atlantic Ocean sediments as lithologically distinct layers of ice-rafted debris (IRD) deposited by icebergs. This coarse material originated from periodic instability of ice streams draining the North American Laurentide Ice Sheet over the past 60 ky (Scourse *et al.* 2000).

The most pronounced and recently studied are short term and abrupt climate changes because of their vital importance for our civilization, e.g., past hurricane frequency, changes in flood regimes, and especially prominent droughts. The most pronounced climate changes within the last 2 ky besides recent global warming event were Little ice age (LIA) and medieval warmth period (MWP) both documented mainly from Northern hemisphere archives. LIA was temperature decrease and climatic worsening from the 16th century to the mid 19th century. It is generally agreed that there were three minima, beginning about 1650, about 1770, and 1850, each separated by slight warming intervals. Forcings that have been found as possible reasons of such a marked climatic change are: decreased solar activity (mainly Maunder solar minimum), increased volcanic activity, and anthropogenic influence. MWP was a time of warm weather around AD 800-1300 during the European Medieval period. Although many documents as well as archives captured this temperature optimum its leading forcings is still not fully understood. Similarly to LIA is one of the possibilities solar forcing (Acot 2005).

The endeavour for present climate change development leave us with the essential question whether the recent global warming is caused by natural powers or by human. The answer now divides the world. Mankind influences natural systems in many ways and it is hardly possible to separate these influences. The paleoclimatologists challenge is to understand fully the past climate and its changes in order to understand the presence and potentially predict the future climatic changes.

3.3. Regional versus global studies

The data density for many regions now allows robust regional-scale reconstructions that avoid the problems of records from individual sites and improve communication between scientists from various paleoclimate subdisciplines and climate modellers. Comparing climatic studies from two different but potentially comparable regions, e.g. ice-cores from Greenland and Antarctica are quite uncertain because of often used relative dating (Bradley 1999). The climate of a given region is determined by the interaction of forcings and circulations that occur at the planetary, regional and local spatial scales, and at a wide range of temporal scales, from sub-daily to multi-decadal. Planetary scale forcings regulate the general circulation of the global atmosphere. This in turn determines the sequence and characteristics of weather events and weather regimes that characterise the climate of a region. Embedded within the planetary scale circulation regimes, regional and local forcings and mesoscale circulations modulate the spatial and temporal structure of the regional climate signal, with an effect that can in turn influence planetary scale circulation features. Examples of regional and local scale forcings are those due to complex topography, land-use characteristics, and inland bodies of water, land-ocean contrasts, atmospheric aerosols, radiatively active gases, snow, sea ice, and ocean current distribution. Moreover, climatic variability of a region can be strongly influenced through teleconnection patterns originated by forcing anomalies in distant regions, such as in the El Niño-Southern Oscillation (ENSO) and North Atlantic Oscillation (NAO) phenomena. The difficulty of simulating regional climate change is therefore evident. The effects of forcings and circulations at the planetary, regional and local scale need to be properly represented, along with the teleconnection effects of regional forcing anomalies. These processes are characterised by a range of temporal variability scales,

and can be highly non-linear. In addition, similarly to what happens in the global Earth system, regional climate is also modulated by interactions among various components of the climate system, such as the atmosphere, hydrosphere, cryosphere, biosphere and chemosphere, which may require coupling of these components at the regional scale (Giorgi *et al.* 2001).

El Niño-Southern Oscillation (ENSO) - represent the most prominent climate features in the low latitudes and directly affect life conditions and human welfare of more than one third of the Earth's population (Paeth *et al.* 2008). In the case of El Niño warm phases, weaker trade winds lead to a drop in the normal sea level pressure gradient across the Pacific and a consequent deepening of the thermocline on the eastern side. This leads to weaker upwelling, warm sea surface temperatures (SSTs), and further reduction in the zoned SST gradient and further weakening of the trades. The opposite set of feedbacks acts to maintain cold La Niña events: stronger trades enhance and shallow the eastern equatorial Pacific thermocline, driving colder and more intense upwelling, strengthening the zonal SST gradient (Labeyrie *et al.* 2003). According to palynological studies these oscillations did not occur during mid Holocene.

Monsoons - Major determinant in the timing and strength of East Asian monsoons are orbital variation, affecting most directly the winter SST portion of the East Asian climate system but also other additional possibly internal mechanisms are involved. At the 100-kyr frequency, maxima in East Asian monsoon precipitation are in phase with minima in the global ice volume (minima in Eurasian snow cover and albedo). At the 23-kyr frequency, East Asian monsoon precipitation responds to additional forcing (possibly latent heat) besides that provided though summer insolation (radiative forcing) and changing climate boundary condition (orbital forcing) (Morley and Heusser 1997). Thus it is not surprising that Asian monsoon is connected with interglacial periods starting in the time of insolation rise. During the last interglacial monsoon activity lasted ~9.7 ky (Yuan *et al.* 2004).

NAO (North Atlantic Oscillation) - During low (negative phase) NAO winters, the sub-tropical sea-level pressure gradient between the Iceland Low and the Azores High is weakened and Atlantic westerlies assume a more zonal trajectory, bringing moister and warmer conditions over the Mediterranean region (Hurrell *et al.* 2001) and even further east towards the Caspian Sea (Cullen *et al.* 2002).

Although mentioned phenomena could be termed as regional, their impact is often rather large. Regional studies in a strict sense deal with a far more detailed phenomena characteristic for smaller areas, in our case the lake watersheds. Mixture of effects typical for the regional studies is very characteristic for each area, e.g. the position and status of the territory from the climatic point of view, human impacts, mechanical weathering predisposition, relief division etc. Therefore the first thing that needs to be done before any climatic study is to know the study area from various points of view. To this purpose we set aside chapter 4 - Studied lake archives.

3.4. Paleoclimatic archives

Sedimentary archives contain climate related information of environmental changes. Each environmental archive has some limitation; most commonly in recorded time interval, resolution, and of its distribution on the globe (e.g. compare tree rings and ice core records). Sedimentary material from most of archives must be obtained by drilling and cores often provide laminated records. The information about past climate hidden in sedimentary cores can be revealed using various methods (see chapter 3.5).

In the following text we focus mainly on the lake sediments but also provide basic information about (i) glaciers, (ii) marine, and (iii) continental archives because we often refers to them in the discussion. High-resolution proxy climate indicators, including tree rings, corals, ice cores, and laminated lake/ocean sediments, can be used to provide detailed information on annual or near-annual climate variations back in time. Certain proxy information with coarser resolution (from e.g. boreholes, glacial moraines, and non-laminated ocean sediment records) can usefully supplement this high-resolution information (Folland *et al.* 2001).

3.4.1. Glaciers

Glaciers provide one of the most valuable climatic archive despite that the records are influenced by number of processes within the glacier. It has regional sampling bias (high elevation or high latitude where snow accumulation is continuous) and melted water and precipitation accumulation data are not easy to date accurately (Folland *et al.* 2001). Climate-related indicators provided by glaciers are summarized in Table 1. Most straightforward results from glaciers are $\delta^{18}O$ values representing past temperature records (see chapter 3.5.1).

Value of ice core information is in their high resolution (annual or even seasonal where accumulation rates are particularly high), availability in polar and high-attitude regions (where other types of climatic proxies like tree-ring data are not available), and their provision of multiple climate- and atmosphere-related variables (Folland *et al.* 2001). The oldest ice core records are from Vostok lake (up to ~420 ky) (Petit *et al.* 1999) and Dome C (up to 740 ky) cored by European Project for Ice Coring in Antarctica (EPICA) (Audustin *et al.* 2004), both in Antarctica. Currently scientists from International Partnerships in Ice Core Sciences (IPICS) are searching for the place where would be possible to get a continuous record of ~1.5 My.

Table 1 Environmental parameters and proxy values from glaciers (Bradley *et al.* 1999).

Environmental parameter	Proxy
Temperature - summer	Melt layers
Temperature – Annual? Days with snowfall?	Oxygen and hydrogen isotopes
Humidity	Deuterium excess (d)
Paleo-accumulation (net)	Seasonal signals, ^{10}Be
Volcanic activity	Conductivity, nss. SO_4
Tropospheric turbidity	Microparticle content, trace elements
Wind speed	Particle size, concentration
Atmospheric composition: long-term and anthropogenic changes	Gas content (CO_2, CH_4, N_2O), glaciochemistry
Atmospheric circulation	Glaciochemistry (major ions)
Solar activity	^{10}Be
Vegetation	Pollen analysis

3.4.2. Marine archives

Basically two different types of archives are studied within Ocean: (i) marine sediments, and (ii) corals.

Marine sediments

Ocean sediments may be useful for high-resolution climate reconstructions. Sedimentation rates usually varied from 45 cm/10^3 years (Richey *et al.* 2007) to less than 0.6 cm/10^3 years (in the Canada Basin, Schneider *et al.* 1996). In rare cases can be as high as in the case of lake sediments, i.e. 1.2 -1.5 mm/year (Rad *et al.* 1999). Therefore the resolution of marine sediments varied from annual to century-scale variability is resolvable.

Pelagic ocean sediments usually consist of i) remains of biological activity of the above water column, ii) usually very fine inorganic particles, iii) newly formed material depending on the actual local conditions, e.g. Mn-nodules. For summary of commonly examined environmental parameters studied on different marine material see Table 2. Inorganic part contains an information about ocean and/or atmospheric circulation at the time of the deposition as well as it captures riverine activity or/and floating ice presence (see chapter 3.2). For the paleoclimatic approach the organic part of sediment is used far more often. The preservation of shells of different species is strongly dependent on the depth of the water column. Two main groups according to the shell composition could be distinguished; these are carbonatic ($CaCO_3$) and siliceous (SiO_2) shells. Each group embodies large variability of both phyto- and zoo-plankton forming so called biogenic ooze. The most common calcareous shells preserved in marine sediments are Pteropod, Globigerinina (plankton group of foraminifera), and Coccolithophores whose presence is limited by aragonite compensation depth, lysocline, and calcium carbonate compensation depth (CCD), respectively. On the opposite the dominance of the siliceous shells such as Radiolaria (representing tropical high productive area) and diatoms (more common in boreal areas) are usually below CCD (Bradley 1999). The most famous group in paleoclimatic studies is Foraminifera (with carbonatic shell) that represents worldwide, numerous and easily distinguishable assemblage with species distribution strongly dependent on the water temperature. Present day distribution of Foraminifera varied from arctic (0-5 °C) with typical species *Globoquadrina pachyderma* to tropical (24-30 °C) waters with *Globigerinoides sacculifer* as a major species (Oldfield 2005). The analysis of oxygen isotopes ($\delta^{18}O$) forming their shell is largely used as paleotermometer and becomes a base of definition of OIS, i.e. Quaternary glacial – interglacial stages. OIS also served as one of the main proves of Milankovitch theory that explains the periodicity of marine record by extraterrestrial forcings (for details see chapter 3.2).

Figure 3 Age of the ocean floor (adopted from Müller *et al.* 1997)

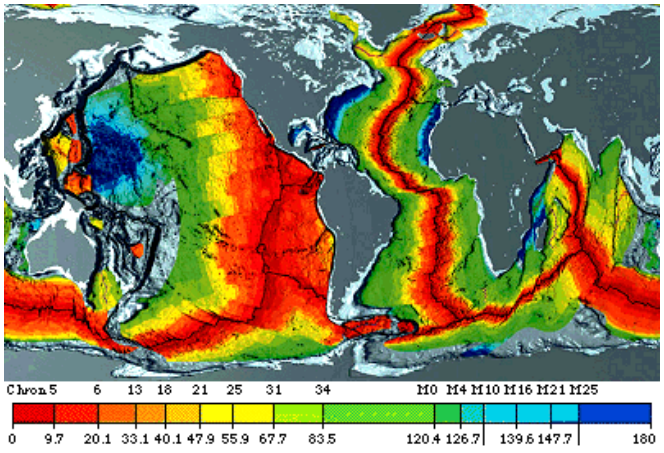

The paleoclimatic potential of the whole ocean floor above compensation depths

is largely limited by scouring bottom currents that cause catastrophic disturbances in sedimentation (Bradley 1999). In a long term view we must deal with non stationary reservoir as a result of plate tectonics. Time limitation of marine record is ~200 My. However, very small portion of ocean floor is older than 125 My (blue colour in Figure 3) and the structure of ocean floor age is not distributed linearly (Müller *et al.* 1997).

Table 2 Environmental parameters and proxy values from marine environment

Environmental parameter	Proxy
Temperature	Oxygen isotopes – foraminifera, corals, trace and minor elements, coral skeletal growth bands
Salinity	Oxygen isotopes - foraminifera, corals
Ocean and atmospheric circulation	Grain size, concentration; mineralogical content; trace elements
Tropical wind system, rainfall	Coral trace elements
Seasonal cloud cover, plankton intake	Coral carbon isotopes
Upwelling, wind anomalies	Coral trace elements
River outflow	Coral trace elements, luminescence of coral skeletons
Ocean productivity	Major elements, luminescence of coral skeletons

Corals

The coral archives used for paleoclimate reconstruction grow throughout the tropics in shallow waters, often living for several centuries. Accurate annual age estimates are possible for most sites by using a combination of annual variations in skeletal density and geochemical parameters. Paleoclimate reconstructions from corals generally rely on geochemical characteristics of the coral skeleton such as temporal variations in trace elements or stable isotopes or, less frequently, on density or variations in fluorescence (Folland *et al.* 2001). Corals represent relatively short term laminated archive of climatic changes. The oldest living coral is dated to 4200 y BP (Milius 2008). Paleoclimate reconstructions from corals provide insights into the past variability of the tropical and sub-tropical oceans and atmosphere at annual, seasonal, or even sub seasonal resolution (Grottoli and Eakin 2007) making them a key addition to terrestrial information (Folland *et al.* 2001). Reef building coral growth (usually in the range of 5-25 mm/year) is limited mainly by temperature. When mean SST fall below 18 °C the rate of calcification is significantly reduced and during lower temperature the colony dies. Intraannual temperature variability causes bands of different density that form a pronounced lamination (Bradley 1999).

3.4.3. Continental archives

All terrestrial geological records, i.e. aeolian, glacial, lacustrine, and fluvial deposits, convey paleoclimatic signal, though it is often difficult to identify the particular combination of climatic conditions leading to its formation. We present here the most often used continuous records including also purely biological.

Trees

The climate signals contained in tree-ring density or width data reflects a complex biological response to climate forcing. Tree-rings of both living and fossil trees provide annual record of past temperature and precipitation in particular terrestrial area with most records in the last 1500 years but also possibility of reconstruction of most of the Holocene when cross-dating samples from lakes and bogs (Bradley 1999). Trees most often used for climate reconstructions are pine and spruce (e.g., D'Arrigo *et al.* 2005). Unique pros of the tree records is its chronology because of possibility of dating wood itself by radiocarbon method (see chapter 3.5.4). Tree-ring networks are also now being used to reconstruct drought and fire frequency that are linked to atmospheric circulation, and also the relationship between ENSO events in the Pacific and anomalous rainfall patterns in different parts of the world (Bradley 1999). Climate reconstructions based entirely on a tree-ring data are susceptible to several sources of contamination or non-stationarity of response. For these reasons, investigators have increasingly found tree-ring data most useful when supplemented by other types of proxy information in "multi-proxy" estimates of past temperature change (Folland *et al.* 2001).

Caves

Cave calcite is one of the few terrestrial climate proxies with potential of continuous information about the isotopic composition of meteoric precipitation. Cave calcite is usually dated with ^{230}Th methods (see chapter 3.5.4). Thus caves may yield well-dated, low-latitude, low-elevation records that characterize atmospheric moisture earlier in its transit from source region, and additionally mean annual temperature. Cave stalagmites posses in many aspects similar records as ice cores but from complementary areas. Cave records were successfully used for reconstruction of, e.g. East Asian monsoon activity in the last 160 ky from caves Dongge and Hulu, China (Yuan *et al.* 2004), for characterization of humidity in Mediterranean area in the last 185 ky from Soreq cave, Israel (e.g. Orland *et al.* 2009).

Loess-palaeosol

Soil development from parent loess is climate related, i.e. soil development is bound to a warming event. Therefore units of buried soils covered usually by loess could form well preserved sequences with applicability in the stratigraphy. The Loess Plateau of North China is a key region for the study of records of Quaternary climatic change. Various techniques to abstract climatically sensitive data were first applied to the classic loess-palaeosol site at Luochuan, and current views on climatic change in Asia have been strongly moulded by results from this central part of the Loess Plateau. Data including the magnetic susceptibility, granulometry, mineralogy, geochemistry, micromorphology, fossil content, and inorganic and organic carbon content of Asian loess-palaeosol series have been used, singly and in combination, as surrogate measures

of paleoclimate to infer climate changes with particular reference to changes in the East Asian monsoon (Derbyshire *et al.* 2009).

3.4.4. Lakes

Lakes accumulate material from their surrounding environment; therefore their sediments can provide a record of an environmental change, i.e. climate change, usually with high resolution (Bradley 1999). In addition to recent lakes there is also possibility to study fossil lake sediments. These sediments could provide old valuable environmental record with a very high resolution (Lojka *et al.* in press). Wider knowledge of the lake sedimentation processes as well as the relation of climate and lake system is crucial for this work. We provide here an introduction to the lake problematics, for further information we recommend following literature: Limnology by Wetzel, 2001, Paleolimnology by Cohen, 2003, and Sedimentary Basins by Einsele, 2000.

Lake types

Classifications of lakes could be based on many points of view with focus to the different characteristics, i.e. residence time (water quality), biological (trophy state); but the most often used classification is based on the lake origin, which influence geomorphologic and other lake parameters:

1. Tectonic lakes are formed by filling up a depressions that originated by tectonic movements. They have very often elongated shape. We distinguish two types of tectonic lakes (Figure 4) i) Graben lakes formed by faulting movements, e.g. Baikal Lake, Tahoe, African rift (Wetzel 2001) and ii) Earthquake lakes, e.g. Quake Lake (Laval 2006 - online)

2. Volcanic maar lakes are formed by volcanic activity, tend to be relatively small. Volcanic lakes may form within the crater of a formerly active but then quiet volcano, in a caldera produced by explosion and collapse of an underground magma chamber, e.g. Crater Lake, Oregon, on collapsed lava flows, e.g. Yellowstone Lake, and in valleys dammed by volcanic deposits, e.g. Sea of Galilee, Israel (Allen and Collinson 1986).

3. Glacial lakes – formed on, below (lake Vostok, Antarctica), or within existing glaciers; their variability is described in four types: i) ice-scour lakes - countless small lakes formed in depressions caused by ice-scouring of rock, e.g. Canadian Shield region. Where glacial-scouring of weak rock regions occurred, large, deep lakes may form, e.g. Laurentian Great Lakes (largest lakes in the world, combined contain 25 % of the world's liquid freshwater); ii) cirque lakes – formed by ice-scouring in mountainous regions frequently result in amphitheatre shaped valleys known as cirques, which may contain lakes usually small and shallow (< 50 m deep); iii) fjord lakes – in ice scoured valley, usually with

Figure 4 Tectonic types of lakes (Zanden 2008 - online).

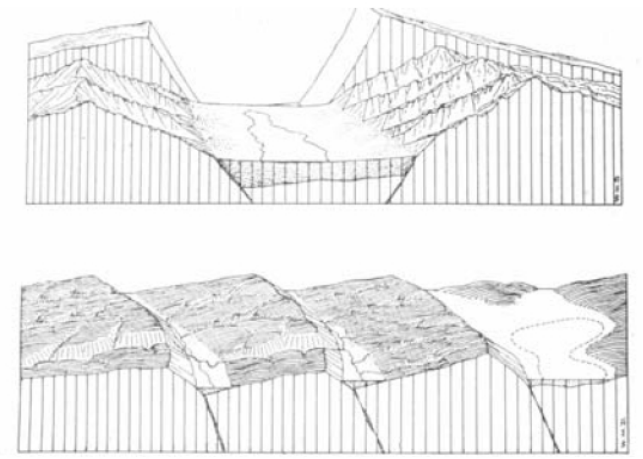

a morrainal dam at one or two ends, typically, long, narrow, and deep; iv) kettle lakes – ice blocks buried in glacial debris during regression of glaciers, thousands of small lakes in northern North America, they rarely exceed depth of 50 m.

4. Other – mainly small shallow lakes could be formed by one of the following processes: a) landslides – damming due to landslides (usually temporary); b) solution – depressions created by dissolution of soluble rock, common in limestone regions, e.g. in Florida, Puerto Rico, and in the former Yugoslavia (Allen and Collinson 1986); c) river-formed – isolated depressions formed by erosional and depositional action of rivers, e.g. plunge-pool lake (below former waterfalls), oxbow lakes, and floodplain lakes; d) wind-formed – including deflation basin lakes formed by wind erosion, e.g. northern Texas, New Mexico, parts of Australia, and lakes in low areas between sand dunes, e.g. Sand Hills, Nebraska; e) coastal – completely enclosed bar-built estuaries, e.g. Coorong lakes, south-eastern Australia f) meteorite – impacts can form lakes, e.g. Lake Bosumtwi, Ghana; and Manicouagan Lake and Chubb Lake, Quebec) (Allen and Collinson 1986). g) organically-formed – impoundment by massive vegetation growth or biologically mediated $CaCO_3$ precipitation; h) reservoirs – beavers and humans (Laval 2006 - online).

Lakes as climate archives

Not all lake types provide valuable climate archive; each type offers a different kind of information depending also on their age, water input, volume, and depth. Exceptionally valued are annually laminated (varved) lake sediments as symbol of a stable environment and well dated sediments. They offer a considerable potential as high-resolution archives of palaeo-environmental conditions where other high-resolution proxy indicators are not available (e.g., in arid terrestrial regions) and latitudes poleward of the treeline. Varved sediments can be formed from biological processes or from the deposition of inorganic sediments, both of which are often influenced by climate variations. Three primary climate variables may influence lake varves: (i) summer temperature, serving as an index of the energy available to melt the seasonal snowpack, or snow and ice on glaciers; (ii) winter snowfall, which governs the volume of discharge capable of mobilising sediments when melting; and (iii) rainfall. Laminated lake sediments dominated by summer temperature can be used for inferences about past high latitude summer temperature changes, while sediments dominated by the latter two influences can be used to estimate past drought and precipitation patterns (Folland *et al.* 2001). Sedimentation rate differs within lake types depending on the watershed and also within one lake, e.g. sedimentation rate of glacial lake Seneca, USA, varied from 0.5 to 200 mm/year (Halfman, 2006 - online).

Lake basins may be termed overfilled, balanced fill, or underfilled, depending on the balance between potential accommodation spaces (mostly tectonic) with sediment + water fill (mostly a function of climate). According to Caroll and Bohacs (1999) climate and tectonics exert coequal influence on lake deposits at both mesoscales (1 m to hundreds of meters) and macroscales (hundreds to thousands of meters). The climate change directly affects important characteristics of lake systems such as lake levels; water temperature; thermal stratification; water quality; productivity; and biodiversity in water reservoirs. Some most common generic relationships between climate and lacustrine systems are outlined in Hulme *et al.* (2003). For Holocene climate change and its impact to the various hydrological systems over the world see Issar (2003).

Lake size and depth can change over the time, due to various reasons. Through natural processes, lakes will ultimately fill with sediment, thereby "evolving" into a terrestrial ecosystem. Human influences can accelerate the process. For example, Lake Chad, once one of Africa's largest bodies of fresh water, has largely decreased in size due to an increasingly dry climate and human demands for irrigation water (Bradley 1999), another example is Aral Sea discussed in chapter 4.1. Lake burial by sediments or drying out could be completely natural processes, e.g. short-term lakes are: seasonal lakes, playas, coastal lakes or small glacial lakes formed after deglaciation. Information about area, depth and salinity of the largest lakes in the world has been gathered by Williams (2006-online).

Physical properties of lakes

The amount of **light**, i.e. solar energy incoming to the lake influences predominantly lake productivity and the composition of water organisms. Light penetration through water depth has various trends depending on the light scattering that is related mainly to a number of suspended particles. Light transmission through ice is very similar to liquid water, however, snow cover reduces the transmission greatly, e.g. 1 m of snow cover lead to zero light attenuation that affect an entire metabolism of the lake (Wetzel 2001). **Heat** distribution profile is governed mainly by action of wind, only 10 % by direct absorption of solar radiation. Contrasts in seasonal conditions within lake lead to pronounced changes in thermal stratification during each year, i.e. spring turnover due to increased heat income, summer stratification to epilimnion, metalimnion, and hypolimnion layers with different characteristics, loss of stratification in the autumn, and inverse stratification when colder water lies over warmer during winter period (Wetzel 2001).

Depending on the latitude several thermal lake types can be divided: (i) amictic – perennially ice-covered, (ii) cold monomictic – water temperature below 4°C and summer circulation, (iii) dimictic – circulation twice a year (spring, autumn) and stratified in summer and winter, (iv) warm monomictic – circulation in winter, not ice-covered, (v) oligomictic – stratified most of year, (vi) polymictic – frequent or continuous periods of mixing per year. Also further classification within each group is possible, e.g. such polymictic lake that do not undergo a complete circulation (usually the primary water mass does not mix with a lower portion of the lake) are termed meromictic (Wetzel 2001). **Oxygen** profile depends on the stratification but also on the nutrient income. If the nutrient income is low than the lake is termed oligotrophic, on the other hand high nutrient income results in eutrophic and in that case the oxygen content of the hypolimnion is depleted by oxidative processes, i.e. often anaerobic.

Lake sediments

Lake deposits are particularly well horizontally bedded or laminated and, in addition, show frequent vertical changes in lithology and colour. Two principal reasons for these phenomena are: (i) lake sediments are little affected by waves and currents and (ii) very sensitive to changes in climate and other environmental factors (Einsele 2000). Lake sediments are usually composed of a combination of autochthonous (formed within the lake basin) and allochthonous (detrital, formed outside the basin and transported to the lake) materials. Chemical and mineralogical composition of lake sediments is largely controlled by the geology of the lake watershed, transport mechanism, facies deposited in lake, and early diagenetic processes.

Allochthonous sedimentary components

Transport of sedimentary materials from land to lakes is provided by water inflows as well as by wind. The leading source of types of allochthonous particles has the primary rock compositions in the watershed. Mineralogical characteristic of allochthonous particles is governed by weathering processes. Several types of minerals are usually present: (i) residual minerals of primary rocks – primary minerals- often stable minerals, most commonly quartz, and also secondary minerals – already products of weathering, i.e. kaolinite, (ii) secondary minerals formed on the way within the rivers, e.g. calcite. The amount of transported materials is also influenced by the growing vegetation. In lake sediment mineralogy clay mineral composition has fundamental position as fine grained materials pointing to the specific climatic conditions in watershed, where they are formed, environmentally driven transport to the lake, and hydrologically driven sedimentation in the lake. Šucha (2001) divided several main environments with different temperature and precipitation conditions and defined the clay mineral genesis for each group. Hydrolytic process has the crucial role in clay mineral formation that could be divided into 3 types with decreasing intensity of weathering processes that are connected to increasing activity of precipitation and temperature: (i) bisialitization characterized by incomplete degradation of both Si and alkalic cations that are basis to nascent 2:1 clay minerals, most commonly smectites, (ii) monosialitization with incomplete degradation of Si but complete of alkalic cations causing an enrichment in 1:1 phyllosilicates, e.g. kaolinite and halloysite; (iii) allitization with total degradation of Si and also alkalic cations (K, Na, Ca...) leading to the formation of Al-rich minerals, particularly hydroxides, e.g. gibbsite. In formation of clay minerals the different processes could lead to the same mineral, e.g. illite could be formed by illitization of smectite but also by illite neoformation (Šucha 2001).

Autochthonous sedimentary components

Due to weathering processes water incoming to the lake is enriched in cations that serve as the main source of nutrients as well as their concentration governs chemical precipitation of minerals in the lake. Classification of the lakes based on their salinity was reviewed by Hammer (1986) who collected 8 salinity systems and ended with the following classification: (i) freshwater lakes have 0.5 ‰ or less of dissolved salts, (ii) subsaline lakes are those with salinity range from 0.5 to 3‰, and (iii) the saline lakes are categorized in three major groups according to salinity: hyposaline (3-20‰), mesosaline (20-50‰) and hypersaline (equal or greater than 50‰).

The amount of dissolved ions concentrated in inland waters determines its salinity values, usually four major cations (calcium, magnesium, sodium, potassium) and anions (bicarbonate, carbonate, sulphate, chloride) are present (Wetzel 2001). With increasing mineralization, i.e. salinity, four steps of minerals precipitation occur: (i) at the beginning low Mg-calcite, (ii) subsequently according to the lake chemism –Mg-calcite, aragonite (carbonate lakes), gypsum (sulphate lakes), gaylussite, trona (soda lakes), (iii) gypsum (carbonate lakes), mirabilite, thenardite, glauberite (sulphate lakes), and (iv) finally halite and other salts (see Table 3) (Einsele 2000). Concurrently with the first salt precipitation step the incoming clay minerals, degradated by weathering in the drainage areas, react with lake water and take up cations, hydrogen carbonate and silica. This so-called "regradation" of clay minerals (or reverse weathering) consumes a significant amount of

the incoming dissolved matter. It may lead to the formation of illite, montmorillonite, and smectite at the expense of kaolinite. In addition, small amounts of new clay minerals can be formed in the lake already at very low salt concentration. These processes have been largely neglected in previous studies on lake evaporites (Einsele 2000).

Important part of autochthonous material is formed by living organisms. Chemical and mineralogical composition of biologic material is dependent on the lake water chemism. Water rich in carbonates are more inhabited by organisms forming carbonatic shells, e.g. *Charophytes* and typically blue-green algae. These organisms take CO_2 for photosynthesis from water and it causes precipitation of $CaCO_3$ on the surface of their body. On the other hand lake rich in dissolved silica and high amount of nutrients is favoured by organisms having siliceous shells, e.g. diatoms. Usually both types of organisms are present in each lake (Einsele 2000).

Table 3 Autochthonous minerals in lake sediments with their formulas (compilation from Okada *et al.* (1994), Boomer *et al.* (2000), Einsele (2000), and Kilic and Kilic (2005)).

Carbonates			
Calcite/Aragonite	$CaCO_3$	Trona	$NaHCO_3.Na_2CO_3.2H_2O$
Magnesite	$MgCO_3$	Gaylussite	$Na_2CO_3.CaCO_3.5H_2O$
Huntite	$CaMg_3(CO_3)_4$		
Sulphates			
Gypsum	$CaSO_4.2H_2O$	Epsomite	$MgSO_4.7H_2O$
Anhydrite	$CaSO_4$	Konyaite	$Na_2SO_4.\ MgSO_4.5H_2O$
Glauberite	$CaSO_4.\ Na_2SO_4$	Polyhalite	$K_2SO_4.MgSO_4.2CaSO_4.2H_2O$
Thenardite	Na_2SO_4	Antarcticite	$CaCl_2.6H_2O$
Bloedite	$Na_2SO_4.MgSO_4.4H_2O$	Hexahydrite	$MgSO_4.6H_2O$
Mirabilite	$Na_2SO_4.10H_2O$	Starkeyite	$MgSO_4.4H_2O$
Langbeinite	$2MgSO_4.K_2SO_4$	Astrahanite	$Na_2Mg(SO_4)_2$
Kieserite	$MgSO_4.H_2O$		
Chlorides			
Halite	NaCl	Sylvite	KCl
Carnalite	$KMgCl_3.6H_2O$	Bischofite	$MgCl_2.6H_2O$
Silicates			
Illite	$(K, H_3O)(Al, Mg, Fe)_2(Si, Al)_4O_{10}[(OH)_2, H_2O]$		
Montmorillonite	$(Na,Ca)_{0.33}(Al,Mg)_2(Si_4O_{10})(OH)_2{\cdot}nH_2O$		

3.5. How to study paleoclimatic archives

This chapter will briefly go through individual methods used in paleoclimatology. Not only measured data but also data from historical records or data derived from observations by geomorphologists, sedimentologists (e.g. insitu glacial material, satellite data), and/or biologists are valuable for paleoclimatic reconstruction. However, we focus our attention to those methods which are applicable to various sampled material and brought to laboratory. We do not intend to present here all the methods but mainly those that are used in lake sediment studies as well as methods that we have used in our experimental work.

In the following text we used term "proxy" climate indicator in the meaning by Folland *et al.* (2001) as a local record that is interpreted using physical or biophysical principles to represent some combination of climate-related variations back in time. Paleoclimate proxy indicators have the potential to provide evidence for large-scale climatic changes prior to the existence of widespread instrumental or historical documentary records. Typically, the interpretation of a proxy climate record is complicated by the presence of "noise" in which climate information is immersed, and a variety of possible distortions of the underlying climate information (Bradley 1999). Careful calibration and cross-validation procedures are necessary to establish a reliable relationship between a proxy indicator and the climatic variable or variables. This relationship is often provided through a "transfer" function (Folland *et al.* 2001). The usage of each proxy method is depended on the composition of studied material and some proxies are connected exclusively to only one environment.

3.5.1. Inorganic analytical proxies

Magnetic methods

Besides their chronostratigraphic application (chapter 3.5.4), magnetic methods point to presence or absence of minerals with various magnetic properties. Magnetic techniques are in general non-destructive, highly sensitive, and fast. This allows processing large numbers of samples in relatively short time in order to establish high-resolution paleoclimate records. Usually a combination of following magnetic methods is used: (i) magnetic susceptibility (MS); (ii) remanent magnetization; (iii) anhysteretic magnetic remanence, and many further parameters. Volume normalized magnetic susceptibility (κ) can be used as the first estimate of the abundance of ferromagnetic minerals, such as magnetite/maghemite. Because κ is also influenced by ferrimagnetic, paramagnetic and diamagnetic minerals, its interpretation may be less straightforward than the interpretation of magnetic remanence parameters. Isothermal Remanent Magnetization (IRM) reflects the presence of ferrimagnetic and, to a lesser degree, imperfect antiferromagnetic minerals (Geiss *et al.* 2003).

Magnetic methods are/were largely used in Ocean drilling projects for magnetostratigraphy. This systematic work has resulted in the enlargement of knowledge about past reversal phases of Earth´s magnetic field. Less frequently but for this work more importantly these methods are used in other environments, such as lake sediments or loess deposits. E.g. Sun *et al.* (2006) applied Magnetic susceptibility (MS) in Chinese loess plateau to indicate monsoon evolution in the last

few My using the relationships of MS as a proxy of rainfall. Geiss *et al.* (2003) proposed a model that explains variations in magnetic parameters of lake sediments in the following way: During periods of forest growth within the watershed, deposition of terrigenous material is low and the sediment magnetic properties are characterized by low concentrations of mainly authigenic minerals (low values of Isothermal Remanent Magnetization (IRM), high ratios of Anhysteretic Magnetic Remanence (ARM)/IRM. During dry periods, deposition of terrigenous material increased due to intensified dust deposition and the erosion of lake margins caused by lowered water levels. Concentration of magnetic minerals increases (high IRM, χ) simultaneously with the grain-size of the magnetic fraction (low ARM/IRM).

Mineralogy

From mineralogic point of view, sediments are mainly composed of quartz, clay minerals and carbonates. Besides these major components, presence of specific minerals could point to specific environmental characteristic, e.g. gypsum or other salts that could be formed only if salinity exceeded known level. Presence of type of clay minerals and their mixtures point to the type and intensity of the weathering in the time of sedimentation (see chapter 3.4.4). For example the presence of mixed-layered clay mineral illite–smectite point to diagenetic conditions (Šucha 2001). Mineralogic signatures mirror several processes, e.g. weathering, erosional changes, and changes in transport mechanisms.

Particle size analysis

Granulometry is irreplaceable whenever a mechanism of transport of siliciclastics is in a focus of study. The characterization of grain sizes could give us valuable climate related information about the flow intensity, the presence of turbidity and the presence of coarse glacial material (e.g. Heinrich layers). Varve thickness has also been used as climate proxies after time series calibration (Oldfield 2005). The sortable silt mean size proxy, i.e. the mean grain size of the 10–63 μm terrigenous sediment fractions with biogenic carbonate and opal removed, is an indicator of bottom currents flow speed. Generally, coarser values of the sortable silt mean size reflect stronger near-bottom flow and selective deposition and winnowing (Mackensen 2004). Particle size analysis, in larger extension facies analysis is one of the main methods used in sequence stratigraphy to characterize sedimentation processes and their changes in individual sites and more importantly to compare them and produce larger scale models of processes (Cohen 2003).

Geochemistry - major elements

Multi elemental analysis of the samples from the cores or excavated profiles points to the geochemical characteristics of the sedimentary environment. This kind of analysis can be easily compared with other geochemical datasets (Freund, 2004).

Silica and aluminium (**Si, Al**) as relatively unreactive and insoluble minerogenic elements became concentrated in soil profiles as weathering intensifies. Therefore, increases in terrigenous Si and Al in lake cores have been used as indicators of warmer and/or wetter climatic conditions. Both these elements analysis in lake sediments have some disadvantages. In the case of Si concentration there is need to separate terrestrially derived (minerogenic) and biogenic Si (Cohen 2003). In many lakes, diatom frustules constitute a considerable part of the sediments. If the

diatom production in the water column changes it proportionally affects the Si/Al ratios in the suspended matter, and later on in the sediment (Peinerud *et al.* 2001). The interpretation of Al profiles is mainly affected by increased Al solubility under acidic conditions (Cohen 2003).

Magnesium to calcium (**Mg/Ca**) ratio in foraminiferal calcite shows temperature dependence due to the partitioning of Mg during calcification. Elderfield and Ganssen (2000) have found that past temperatures reconstructed from Mg/Ca ratios followed the two other palaeotemperature proxies: faunal abundance and alkenone saturation. Moreover, combining Mg/Ca and $\delta^{18}O$ data from the same faunal assemblage, they show that reconstructed surface water $\delta^{18}O$ represents changing hydrography and therefore global ice volume.

Carbon to nitrogen (**C/N**) ratio in sediments quantifies the relative abundance of terrestrially and aquatically derived organic material in the sediment. The usefulness of this proxy is based on the fact that terrestrial organic material consists of high-order plants with a more complex, cellulose-rich structure, while aquatic organic material such as plankton have a less rigid structure. These differences cause terrestrial organic material to be rich in C and aquatic organic material to be rich in N, allowing the C/N ratio to track the relative abundances of these two classes (Sampei and Matsumoto 2001)

Phosphorus (**P**) is a key macronutrient being strongly enriched in the deep ocean as a result of continuous export and remineralisation of biomass from primary production. Montagna *et al.* (2006) show that phosphorus incorporated within the skeletons of the cosmopolitan cold-water coral *Desmophyllum dianthus* is directly proportional to the ambient seawater phosphorus concentration and thus may serve as a paleo-oceanographic proxy for variations in ocean productivity as well as changes in the residence times and sources of deep-water masses. However according to Cohen (2003) long term phosphorus accumulation only rarely mirror phosphorus loading due to high diagenetic mobility and biological reactivity of phosphorus at the sediment-water interface and therefore do not recommend phosphorus usage in paleolimnology.

Aluminium to titanium (**Al/Ti**) ratio calculated from the total concentrations of these metals in sediment samples can be used to identify source types of detrital material, as different rock types have different Al/Ti ratios. Generally, Al/Ti ratios of ocean sediments may provide information about whether detrital sources are continental or oceanic (Mackensen 2004).

Geochemistry - trace elements

Strontium to calcium (**Sr/Ca**) ratio in corals has been shown to be a function of sea surface temperature, with minimal sea water Sr/Ca influence (Evans *et al.* 1998). The same valuable information could be got from uranium to calcium (**U/Ca**) ratio.

Individual non-marine ostracod valves contain **Sr** in proportion to the Sr content of their host lake water. If the relationship between salinity and the Sr content of a hydrologically simple lake is known, palaeosalinities can be calculated from fossil ostracod analysis (Chivas *et al.* 1985).

Niobium to titanium (**Nb/Ti**) – was used for example in Lake Malawi to trace windy periods that brought a material from volcanic eruptions (Johnson *et al.* 2002).

Cadmium to calcium (**Cd/Ca**) ratios in foraminiferal tests reflects Cd water concentrations in which they were grown. Dissolved Cd in seawater, in turn, is correlated with dissolved phosphate concentrations. Thus Cd/Ca ratios of benthic and planktonic foraminifera are extensively used as a nutrient proxy. Only recently it has been found that the incorporation of Cd into planktonic foraminifera relative to seawater is temperature sensitive (Mackensen 2004).

Stable isotopes

Isotopic fractionation is based on many processes (biotic and abiotic) that sequester, precipitate, metabolise, or release preferentially one stable isotope resulting that a known process lead to a typical ratio of isotopes. Ideally analyzing these ratios in various environments provide reconstruction of these processes and states. The isotopic fractionation is a result of both thermodynamic and kinetic constrains of so many physical and chemical processes that the interpretation of a given signature in sedimentary series must be very thorough. Listing all the principles exceeds the scope of this work.

Oxygen isotopes ($\delta^{18}O = {}^{18}O/{}^{16}O$): This proxy, i.e. the ratio ^{16}O (99.76%) and ^{18}O (0.20%), results from isotopic fractionation during evaporation and condensation of water. Lighter $H_2{}^{16}O$ evaporates more easily from the water body resulting that the atmospheric H_2O vapour is poorer in $H_2{}^{18}O$ than oceanic water. Similarly as water molecules travel up on an ice sheet (water changes from vapour to liquid) $H_2{}^{18}O$ is precipitating first. Ice on the top of the glacier has less $\delta^{18}O$ than at the base of the mountain. Similarly to altitudinal also a continental effect could be observed (Folland *et al.* 2001). The usual sample types where it is reasonable to measure $\delta^{18}O$ are ice-cores, calcite of planktonic foraminifera, aragonite from corals, lake snail shells (Wu *et al.* 2002), and also deep-lake ostracods (von Grafenstein *et al.* 1999). Most commonly $\delta^{18}O$ is used as a proxy of temperature because fractionation of oxygen isotopes during the formation of calcium carbonate is temperature depended. Additionally $\delta^{18}O$ can be used to reconstruct past changes in the effective moisture (precipitation minus evaporation) (Epstein *et al.* 1953). $\Delta^{18}O$ itself is an indicator of global ice volume and salinity (Elderfield and Ganssen 2000). Anderson *et al.* (2001) inferred effective moisture from oxygen isotope ratios in sediment cellulose from Meli Lake. Stable isotopes $\delta^{18}O$ Evans *et al.* (1998) used seasonal range of sea surface temperature based on $\delta^{18}O$ measurement for the characterization of ENSO variations in past. In lakes with optimum hydrology (size and precipitation/evaporation regime) there is a simple relationship to $\delta^{18}O$ precipitation but in other cases the water composition is strongly influenced by processes such as evaporation within the catchment and within the lake itself. $\Delta\ ^{18}O$ precipitation is increasingly being shown to be an important indicator of climate change: it typically changes with mean annual temperature but non-linear responses to climate change are increasingly being recognised (Leng and Marshall 2004). $\Delta\ ^{18}O$ method limitations are linked to the presence of shells and that only few species of foraminifera could be used as they precipitate calcite in equilibrium with ocean water (Evans *et al.*1998). Moreover Bradley (1999) point to dependence of $\delta^{18}O$ on the salinity.

The $\delta^{18}O$ value of inorganic phosphate ($\delta^{18}O_P$) has been proposed as a useful proxy and tracer of biological reactions and P cycling in natural environments (Liand and Blake 2005).

Carbon isotopes ($\delta^{13}C = {}^{13}C/{}^{12}C$) are most often analyzed in carbonatic skeletons. Carbon isotopic fractionation processes in lakes are far more complex than in the case of oxygen. Most of problems in interpretation of carbon isotopic composition are caused by presence of mixture of organic and inorganic carbon sources, i.e. mixture of fractionation pathways. Additionally mixing dynamics and diagenetic processes affects the final isotopic ratio (Cohen 2003). $\Delta\ {}^{13}C$ at high latitude location is strongly linked to the air temperature whereas in tropics to the changes in source and available volume of moisture (Oldfield 2005). $\Delta\ {}^{13}C$ in corals represents past light conditions, e.g., seasonal cloud cover and plankton intake (Grottoli and Eakin 2007). In marine sediment they could stand for the source of carbonates and organic matter (Oldfield 2005).

The concentration of **boron isotopes** ($\delta^{11}B = {}^{11}B/{}^{10}B$) in marine carbonates is highly dependent on pH. $\Delta\ {}^{11}B$ values of fossil foraminifera calcite are therefore sensitive pH indicators of ancient sea water. For a given pH of sea water the aqueous CO_2 concentration can be calculated and thereby the atmospheric pCO_2 can be quantitatively estimated (Mackensen 2004).

Nitrogen isotopes ($\delta^{15}N = {}^{15}N/{}^{14}N$) of marine organic matter produced in the euphotic zone serve for the reconstruction of ocean productivity and nutrient utilization in ocean surface waters. This is based on the fact that assimilation of nitrate by phytoplankton is accompanied by nitrogen isotope fractionation, leaving organic matter depleted in ${}^{15}N$ (Mackensen 2004). Similarly the nitrogen isotopes can trace lake productivity especially in the cases of long term reconstructions and/or marked increase in the anthropogenic influence to the nitrogen concentration (Cohen 2003).

Strontium isotopes ($\delta^{87}Sr = {}^{87}Sr/{}^{86}Sr$) in planktonic foraminifera are thought to reflect changes in the flux of Sr to seawater from mid-ocean ridge basalts and continental rocks. Sr fluxes from the continents mainly depend on the weathering conditions on land and on the nature of the source rocks (Palmer and Edmond 1992 in Mackensen 2004).

3.5.2. Organic analytical proxy methods

This chapter includes proxies from primary biological material with a valuable relationship to the climate. Paleoclimatic inferences from biogenic material in sediments derive from assemblages of dead organisms (thanatocoenoses) from the past overlying water column (Bradley, 1999). Output of most of organic proxy methods are counts of identified taxa, genders etc. plotted in diagrams vs. depth, and/or age.

Bulk organic matter indicators

Total organic carbon (TOC) content could be estimated in several different ways, (i) loss of mass during ignition (LOI) at high temperature, (ii) chromatographically, (iii) with CHN analyser, which uses separated chromatographic column and thermal conductivity detector, (iv) coulometrically. The most widely used technique for organic rich sediments is LOI. LOI often serves as paleoproductivity proxy, e.g. demonstrate substantial changes in association with glacial advances (TOC decreases) and deglaciation (TOC increases) (Cohen 2003).

Carbon to nitrogen (C/N) ratio is a useful tool for distinguishing long-term transitions between terrestrial to algal-input dominance in lake sediments because organic matter from phytoplankton

is much richer in N (has much lower C/N ratios) than terrestrial organic matter. Such transition might occur as a result of lake level fluctuation or a migration or progradation of a large river delta (Cohen 2003).

Compound specific indicators

Lipids comprise large class of organic compounds that can be isolated by organic solvent extraction, and quantified using gas chromatography mass spectrometry. Various lipids are nowadays used as paleolimnological indicators, because many are indicative of specific organic sources (Cohen 2003). **Alkenone paleothermometry** uses an index (U^k_{37}) derived from the response of certain coccolithophore species to changes in water temperature. It is based on the relative proportions of long-chain alkenones with different number of carbon atoms (Oldfield 2005). However, according to Hinrichs *et al.* (1997) there are discrepancies in paleotemperatures based on alkenones from *Prymnesiophytes* (coccolithophore) and those derived from analysis of foraminiferal assemblages probably caused by foraminifera living in deeper (colder) water than Prymnesiophytes. The applicability of alkenone concentrations is restricted by variations of O_2 concentration in bottom waters combined with the susceptibility of alkenones toward oxidation (Hinrichs *et al.* 1997). Also other molecular technique trace marine productivity, e.g. concentration of most of the **steroidal alcohols** originated from marine plankton organisms, and total **free sterol concentrations** (Hinrichs *et al.* 1997). All three methods are performed using gas chromatography.

Photosynthetic pigments preserved in lakes sediments are biomarkers. Total pigment concentration has been numerously used as trophic status indicator (the highest pigment values occur in eutrophic lakes). However, pigment concentration in sediments is alterated most commonly in the presence of oxygen, and elevated temperatures, i.e. diagenetic conditions. On the other hand pigment preservation is promoted by: low O_2, low light conditions, rapid deposition in fecal pellets, deep water burial environments, and cold hypolimnetic water. Therefore pigments can provide information about stratification history in lakes, and in some cases also about lake acidity (Cohen 2003).

Remains of organisms in sedimentary record

This group of methods embodied analysis based on optical counting (using microscopy) of various objects that had its origin in organic materials. Studied organic group must fulfil several conditions – (i) have morphological characteristics that are specific to a particular genus or species, (ii) be produced in vast quantities, (iii) be distributed widely within its environment, (iv) be extremely resistant to decay in certain sedimentary environment, and most importantly (v) must reflect some climate related information. Most of the paleoenvironmental and paleoclimatic application are governed by preservation of remains of organisms in the sedimentary record.

Pollen analysis reveals the natural vegetation at the time of pollen deposition, which can yield information about past climate. Pollen grains range in size from 10 to 150 μm and are protected by a chemically resistant outlayer (exine). Thus, the organic or inorganic matrix in which the pollen grains are trapped can be removed by chemical means without destroying the pollen itself

(Bradley 1999). Reconstruction of facies and vegetation changes is only possible for organic rich sediments (Freund 2004). Similar applications have spore analysis for sediments older than higher plants. The ratio of two common pollen species called *Artemisia* and *Chenopodiaceae*, known as A/C ratio, shows the water availability at the time, because *Artemisia* requires more water to grow as it is documented from Tibetan Plateau Lake by Zhao *et al.* (2008).

Algae analysis The most widely studied algae group in paleoclimatology is diatom group **(**for further information see chapter 3.5.3). Diatoms could serve as indicators of palaeo-salinity, morpho-dynamics and environmental changes in fine sediments (Freund 2004). Other algae groups are used far less often. *Chrysophycean* algae represented in fossil record by siliceous resting cyst with species specific morphology can be used as paleoindicators. However their classification system as well as ecological demands system is poorly developed. Similarly resting stages and vegetative remains of *Chlorophycae* (e.g. *Pediastrum*), blue-green algae, dinoflagellates, and charophytes could be in some cases used in paleoecological interpretations (Smol 1987).

Zoological macro-remains Remains of fossil *Coleoptera* (beetles) that are often found in lake sediments and peats could provide record of past temperature variations (Oldfield 2005). **Ostracod** shells are often dominant benthic invertebrates in the lakes with excellent preservation in sediments, relatively easy to identify and traceable back to Palaeozoic lakes. Their assemblages are sensitive to several environmental characteristics, e.g. water chemistry, temperature, oxygen, nutrients, and water depth. These qualities make ostracod analysis extremely important for paleolimnologists. Similarly **mollusc** group has a long and rich fossil record and can trace mainly water temperature, salinities and water level changes; however they are not much used in freshwater environments (Cohen 2003).

3.5.3. Diatoms

Diatoms are photosynthesing algae with a siliceous skeleton (frustule). They are found in almost every aquatic environment including fresh and marine waters, soils, in fact in almost any place with enough moisture. Diatom presence in water is governed by physical and chemical environmental parameters. Main limiting physical factors are light, temperature, and currents (wind, water). Main chemical variables are nutrients, pH, oxygen, salinity, and pollution (Round *et al.* 1990). The new classification of diatoms from the biological point of view is following: superregnum: *Eucaryota*; regnum: *Chromista*; evolutionary line: autotrophic chromista; division: *Chromophyta*, brown algae (Zelený 2005). According to the traditional classification developed by Round *et al.* (1990) belongs to the division *Chrysophyta*, Class *Bacillariophyceae*. The *Chrysophyta* are algae which form endoplasmic cysts, store oils rather than starch, possess a bipartite cell wall and secrete silica at some stage of their life cycle. Diatoms are commonly between 10-200 μm in diameter or length, although sometimes they can be up to 2 mm long. The cell may be solitary or colonial (attached by mucous filaments or by bands into long chains).

Cell description

Diatoms are divided into two Orders. The Centrales (now called the *Biddulphiales*) which have valve striae arranged basically in relation to a point, an annulus or a central areola and tend to appear radially symmetrical, and the Pennales (now called *Bacillariales*) which have valve striae arranged in relation to a line and tend to appear bilaterally symmetrical. The valve face of the diatom frustule is ornamented with pores (areolae), processes, spines, hyaline areas and other distinguishing features. It is these skeletal features which are used to classify and describe diatoms, which is an advantage in terms of palaeontology since the same features are used to define extant species as extinct ones (Olney 2002 - online). Centric/pennate ratio could be used as a tracer of environmental productivity (the more centrics are present in the sample, the more productive the environment was; with the exception of a species called *Cyclotella*).

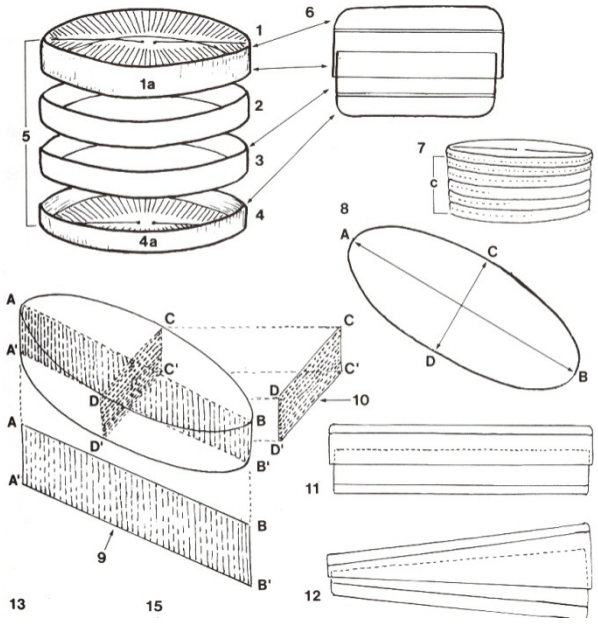

Diatom frustule is often likened to a pill-box or agar dish with an epitheca (larger upper valve), and a hypotheca (smaller lower valve). The vertical lip or rim of the epitheca is called the epicingulum, and the epicingulum fits over (slightly overlaps) the hypocingulum of the

Figure 5 Frustule structure: 1 – face of the epivalve; 1a - mantle of the epivalve; 2 - epicingulum (composed of one or more bands or girdles) which overlaps the hypocingulum and is attached to the epivalve to form the epitheca; 3 - hypocingulum which is attached to the hypovalve to form the hypotheca; 4 – the hypovalve; 4a – hypovalve mantle; 5 – epitheca and hypotheca together constitute the frustule; 8-10 – planes of the frustule: AB = apical axis; CD = transapical axis; ABCD = valvar plane; 11- 12 – cingulum, side or girdle views (Barber and Haword 1994, modified).

hypotheca (Figure 5). The epicingulum and hypocingulum with one or several connective bands make up the girdle. Many diatoms are heterovalvate, i.e., the two valves of the frustule are dissimilar (Round *et al.* 1991). The identification of diatom frustule into genus level is possible using light microscopy, in many cases also into species level but often (mainly small species but also most of centric species) it is necessary to use Scanning electron microscope (SEM) microscopy.

Ecological preferences and systems

The environmental preferences of diatom species can be described by ordering each species into various systems separately for each ecological characteristic. Species categorization is provided on the basis of measured variables and the presence of diatom species. The most usual tool of ecological studies for the demonstration of the relationships between diatoms and environment is canonical correspondence analysis (CCA) where both the most depended variable and the relativity of dependence of each species are shown (Battarbee *et al.* 2001). Species categorization is usually published for individual sites and put together in datasets typical for some area or an environmental indicator. Automatic data evaluation using programs that contains information about diatom preferences, such as Omnidia database is commonly recommended in ecological studies (Lecointe *et al.* 1993). Ecological preferences of individual species can also be described using the ecological codes, where each ecological category is numbered and the order of numbers specifies type of the category (Vos and Wolf 1993).

Salinity characterization: Some species are restricted to a very narrow range of salinities and are known as stenohaline species; others have no such restrictions and are known as cosmopolitan species or tolerate a broad range of salinities (eurysaline). Freshwater species that tolerates a little salt are known as halophilic (Hammer 1986). Van Dam *et al.* (1994) provided own salinity classification with four categories applicable preferably to freshwater environment (Table 4). Wider salinity system used for transition to marine salinities is the Kolbe – Hustedt system. It has also four categories (Table 4, Figure 6) although often is used without α and β differentiation. For hypersaline systems (such as playas, shore lakes, and lakes in subtropical areas) any further classification of diatom tolerances does not exists.

Similarly several systems of classification exist for trophic, pH, and saprobity levels. Relatively unified are classification for moisture, currents, oxygen saturation, and temperature (warm, moderate, cold) (Table 5).

Diatoms in lakes

Regarding only diatoms in lakes it seem to be useful to point out also categorization of diatoms according to their living strategy based on Denys (1992). Euplanktonic diatoms only live in the planktonic habitat, i.e. metabolise and reproduce in the water column. Tychoplanktonic diatoms occur in the plankton, but originated primarily from other habitats. Epontic diatom species are sessile and normally live firmly attached to substrata, i.e. epiphytic live attached to plants and episammic (epilithic) species live attached to sand grains. Benthic diatoms live within the sediment, but not attached to it (Horton 2006). Plankton/non plankton ratio is used to describe littoral zones because usually with increasing depth increase number of planktonic species.

Diatoms are non-motile, or capable of only limited movement along a substrate by secretion of mucilaginous material along a slit-like groove or channel called a raphe. Being autotrophic they are restricted to the photic zone (water depths down to about 200m depending on the clarity) (Olney 2002 - online).

We have already stated the different environmental characteristics that influence diatom assemblage. Depending on the lake type we can define the basic characteristic of water column and therefore basic algal composition. Two types of lakes have dominance of diatoms above the other phytoplankton: (i) oligotrophic, slightly alkaline, nutrient-poor lakes (*Cyclotella*, *Tabellaria spp.*) (ii) eutrophic, usually alkaline, nutrient-rich lakes (*Asterionella*, *Aulacoseira granulata*, *Fragilaria crotonensis*, *Synedra*, *Stepnahodiscus*, and *Melosira granulatea*). Other lake types are dominated by other plankton, e.g. desmids, Chrysophycean algae, Dinoflagellates, Cyanobacteria (Wetzel 2001). Bennion and Battarbee (2007) add to the previous classification following usual major diatom assemblages: (i) shallow lake = mainly non-planktonic taxa: *Achnanthes* spp., *Cocconeis* spp., *Cymbella* spp., *Fragilaria* spp., *Navicula* spp., (ii) acidophilous – circumneutral nutrient poor lakes: *Achnanthes minutissima*, *Brachysira vitrea*, *Cyclotella comensis*, *Cyclotella kuetzingiana*, *Tabelaria flocculosa*, (iii) mesotrophic lake = mostly planktonic species – *Asterionella formosa*, *Aulacoseira subartica*, *Fragilaria crotonensis* (Bennion and Battarbee 2007).

Table 4 Salinity and moisture systems used in diatom evaluation

SALINITY						**MOISTURE**
	VanDam (Van Dam *et al.* 1994)			Kolbe (1927)-Hustedt (1937-39)		VanDam (Van Dam *et al.* 1994)
		Cl^- (mg/l)	salinity (‰)		salinity (‰)	
1	fresh	< 100	< 0.2	oligohalobous	< 1	strictly aquatic
2	fresh brackish	< 500	< 0,9			mainly in water bodies
3	brackish fresh	500 - 1000	0,9 – 1,8	α mesohalobous	1-10	regularly on wet and moist places
4	brackish	1000 - 5000	1,8 - 9			moist or temporarily dry places
				β mesohalobous	10-30	
				polyhalobous	> 30	

Figure 6 Salinity system published by Simonsen 1962 (from Schrader 2007) with improved categories of tolerances within the previously stated Kolbe and Hustedt salinity system (right part). Modified.

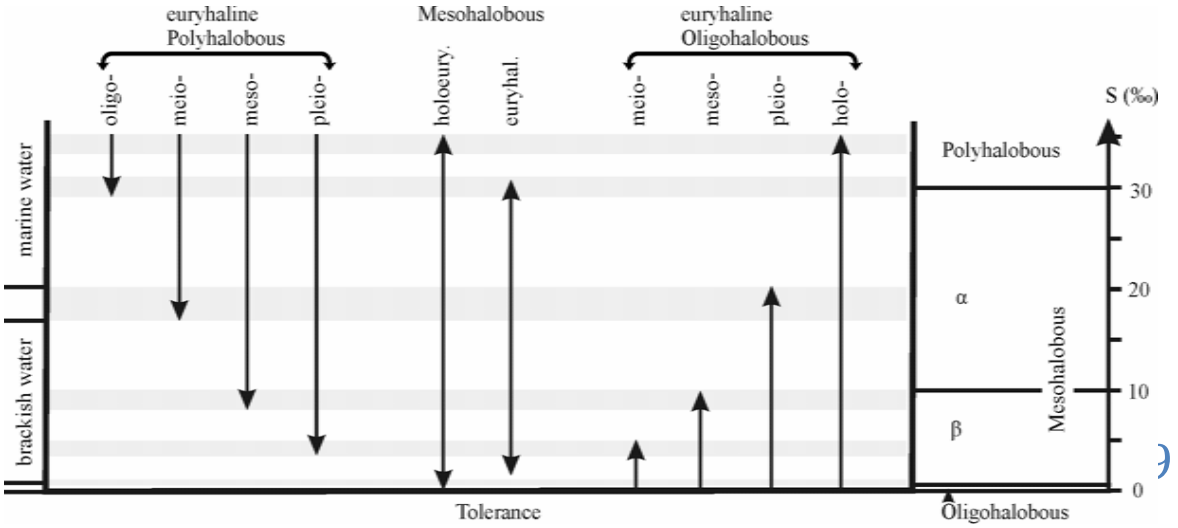

Table 5 Grouping of diatoms according to ecological indicators: trophic state, current, pH, oxygen saturation, and saprobity.

TROPHIC state				CURRENT
	Van Dam *et al.* 1994	Hoffman (Omnidia)	Schiefele (Omnidia)	Denys (Omnidia)
0		unknown	unknown	unknown
1	oligotraphentic	oligotraphent	most tolerant	not relevant
2	oligo-mesotraphentic	oligo-b-mesotraphent	highly tolerant	rheobiontic
3	mesotraphentic	oligo-a-mesotraphent	tolerant	rheophilous
4	meso-eutroaphentic	a-meso-eutraphent	less sensitive	indifferent
5	eutraphentic	eutraphent	eutrophic	limniophilous
6	hypereutraphentic	tolerant	sensitive	
7	indifferent	indifferent	oligosaprobic	

pH				OXYGEN SATURATION
	Van Dam *et al.* 1994		Hakansson (Omnidia)	Van Dam *et al.* 1994
1	acidobiontic	pH optimum < 5.5	acidobiontic	continuously high (100% sat.)
2	acidophilic	pH optimum 5.5 - 7	acidobiontic to acidophilous	fairly high (> 75% sat.)
3	neutrophile	pH optimum about 7	acidophilous	moderate (> 50% sat.)
4	alkaliphilous	mainly occurring at pH > 7	indifferent to acidophilous	low (above 30 % sat.)
5	alkalibiontic	exclusively occurring at pH > 7	indifferent (neutral circumstances)	very low (about 10% sat.)
6	indifferent	no apparent optimum	alkaliphilous to indifferent	
7			alkaliphilous	
8			alkaliphilous to alkalibiontic	
9			alkalibiontic	

SAPROBITY					
	Van Dam *et al.* 1994		Hoffman (Omnidia)	Lange-Bertalot (Omnidia)	Watanabe (Omnidia)
0		oxyg. sat (%)	unknown		indifferent
1	oligosaprobous	> 85	oligosaprob	most pollution tolerant	saprophile
2	β- mésosaprobous	70-85	oligo-mesosaprob	α – mesosaprobic a	saproxene
3	α- mésosaprobous	25-70	b-mesosaprob	α – mesosaprobic b	
4	α- méso-polysaprobous	10-25	b-meso-b-a-mesosaprob	ecological questionable	
5	polysaprobous	<10	b-a-mesosaprob	more sensibel (abundant)	
6			b-a-meso-a-mesosaprob	more sensibel (less frequent)	
7			a-mesosaprob		
8			a-meso-polysaprob		
9			polysaprob		

Diatoms in sediments

Diatom frustules are enriched to the acid polysacharide diatotepin that increase its stability; therefore diatom frustules are often preserved in sediment. The oldest known diatoms are from Lower Cretaceous; evolutionally younger are freshwater species that occurred in large numbers from Mid Eocene, however, there are some sedimentary evidences of freshwater diatoms from Upper Cretaceous (Sims *et al.* 2006).

Not all diatoms present in a water body may settle out after their death, they can be lost via outflows, dissolve, be crushed or eaten (Round *et al.* 1990). Diatoms sinking rates varied from X – 0,0X (mean 0,3) m per day depending on the cell size, volume, and surface texture (Wetzel 2001). Dissolution of diatom frustules during descent through the water column, on the sediment surface and during diagenesis, may seriously alter the preserved assemblage by preferentially dissolving more lightly silicified forms. High alkalinity of pore waters and burial temperatures in excess of 50 °C are also known to increase dissolution of silica (Olney 2002 - online). Additionally diatoms sedimented from littoral zone have a higher dissolution rate (Wetzel 2001). Incorporation into fecal pellets or muciligenous aggregations, rapid burial and the formation of heavily silicified resting spores tend to counteract these problems, however, in marine samples only 1% to 5% of the living assemblage of the surface plankton is represented in the death assemblage found on the sediment surface (www.ucl.ac.uk). These problems must be regarded when interpreting fossil diatom assemblage.

Another disagreement in composition of diatom assemblage in sediments and their previous assemblage in water column may be caused by contamination by diatoms washed in from outside the sample area, from soils, animal droppings, or tributaries. The sample becomes augmented, and in the worst case scenario may include indicator species contrary to the actual palaeo-environmental conditions (Round *et al.* 1990). Another interpretation problem may be caused by insufficient silica dissolved in the water body for diatoms to produce robust, preservable frustules, resulting in a complete absence in the sample.

Biogenic silica largely influences Si cycle. 16% of the gross riverine Si load is delivered to the world ocean as biogenic Si. Most of this biogenic Si would be remobilized by dissolution in marine environments (Conley 1997). Michalopoulos *et al.* (2000) observed the occurrence of conversion of biogenic silica to authigenic clays throughout the Amazon deltaic deposits. Biogenic silica alteration provides proof for a direct link between the biogeochemical cycle of silica in nearshore environments and the neoformation of cation-rich aluminosilicates, and it may prove to be important for oceanic geochemical cycles as a sink for Si, K, and other elements incorporated in the authigenic aluminosilicates. Rapid formation of authigenic K-smectite may also represent a reaction stage leading to eventual formation of illitic clays during later diagenesis.

Diatoms as paleoindicators of sedimentary environment

The practical usage of diatoms in paleosciences covers biostratigraphy mainly of marine high latitude sediments, where calcareous microfossils are often poorly preserved, sparse, or of low diversity (www.ucl.ac.uk). Biostratigraphical usage of diatoms is also possible in Baikal Lake sediments because there are known several major periods of diatom extinctions (Khursevich *et al.*

2005). Review of major climate related limnological variables studied in paleolimnological records by diatom analysis, such as ice cover, river discharge, dissolved organic carbon, water colour, dissolved inorganic carbon and/or alkalinity, pH, nutrients, temperature, conductivity and salinity, lake level, and water column stability was provided by Smol and Cumming (2000).

The most sophisticated method for **paleo-salinity** interpretation is via transfer function – that means the recounting of each species into conductivity values using some reference dataset (Reed 1998). One of the main problem of salinity inferred interpretation are classification systems discrepancies. However, paleo-salinity interpretations are widely used, mainly in estuarine environment with expected shifts from freshwater to marine salinities in the past (Witkowski *et al.* 2005, Witak and Jankowska 2005, Witak *et al.* 2006). **Paleo-pH** is perhaps the most important and most widely used application of diatom studies because diatoms are highly sensitive to pH, i.e. can illustrate differences of as little as 0.1 pH units (Round *et al.* 1990). On the other hand diatoms are not very useful in determining changes in **palaeo-temperatures**. Although the large majority of species tolerates very wide ranges of temperature (typically from 0°C to 20°C) different assemblages are present when comparing warm and cold waters. However, this is almost certainly due to other overriding factors such as: incident solar radiation, water chemistry, pH, and nutrient availability (Round *et al.* 1990). Winder *et al.* (2009) studied assemblages of Lake Tahoe over the last decades and found that together with temperature increase the diatom community structure changed: increased stratification and reduced nitrogen to phosphorus ratios selected for small-celled diatoms, particularly within the *Cyclotella* genus. There are several ways of deducing **palaeotrophic** status using diatoms, (i) total diatom counts (the more diatoms there are in the sample the more productive a given body of water was), (ii) individual diatom species interpretation – it require diatom species counting and presence of sensitive species to trophic status (Round *et al.* 1990).

Main disadvantages of usage diatom analysis in paleoclimatology (according to Round *et al.* 1990)

- Taxonomy, especially in poorly preserved specimens, can often be difficult resulting in mis-identification and a chain of consequent errors.
- The ecology is not well known for all species, causing problems and/or errors with interpretation. Especially abundance of extinct and/or endemic species is difficult to interpret.
- The Equifinality Conundrum - different events give rise to the same outcome. For instance interpretation of a diatom assemblage in given sediment core indicates a rise in nutrients, however, there are more explanations: (i) increased precipitation causing excessive run-off into the lake (ii) warmer weather causing an algal bloom, thereby releasing nutrients as they die off? (iii) a plethora of human activities - increased soil erosion from deforestation or ploughing, increased live-stocking densities in the catchment area resulting in higher effluent run-off, or accidental sewage/pollutant spillage.

3.5.4. Dating of lake sediments

Following text provide a compilation of dating methods (Figure 7) with focus to dating possibilities of lake sedimentary records in different time scales.

Figure 7 Principal dating methods used in paleoclimatic research (adopted from Bradle 1999).

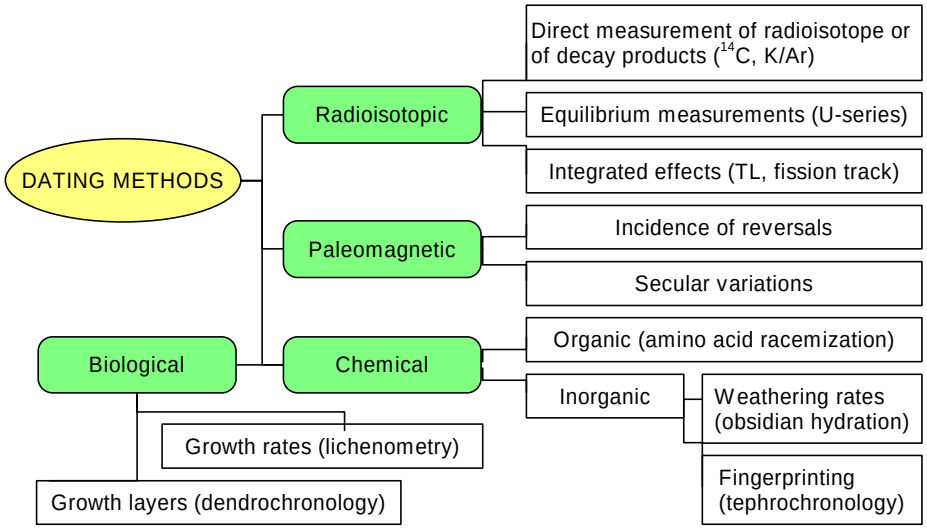

Radioisotopic

^{14}C – the atmospheric concentration of radiocarbon (^{14}C) has varied through time, partly as a result of changes in the rate at which the radioisotope is received at the Earth's surface, partly because of changes in the residence time of ^{14}C in the ocean, which in turn affects ^{14}C concentration in the atmosphere. It follows that organisms incorporating ^{14}C at different time will have different starting values from which decay begins. Therefore the ^{14}C ages must be calibrated usually according to the tree ring records (Oldfield 2005). Radiocarbon dating is only suitable for organic material, e.g. peat, salt marsh deposits, snails, shells, etc. Dating accuracy of bivalves has to be proven; contamination with modern and reworked material is possible (Freund *et al.* 2004). Half-life of radiocarbon isotopes is 5730 years. Therefore technique is most often used in dating Holocene samples. Nevertheless in some cases can be dated material 75 ky old but it's very exceptional. Dating of the last 350 years is problematic because repeated variations of ^{14}C in atmosphere occur and results of calibration can be therefore ambiguous (Bradley 1999). Special Accelerator Mass Spectrometry (AMS) technique, which is also used in this work, offers possibility to date samples 1000 times smaller, and in much shorter time than with the formerly used (conventional) technique (radiation detection of ^{14}C isotope). It enables dating of samples, which are difficult to get in amount required for conventional dating (e.g. plant remnants (including seeds), fragments of hair, rests of food on ceramics, shells of foraminifera), of absolutely not available in amount bigger than a few milligrams (e.g. fragments of cultural monuments or art pieces made from wood, pergamine, paper, tissue, paints, etc.).

^{238}U/^{230}Th – for dating carbonates (corals, speleothems, and lacustrine carbonates) up to ca 350 ky BP. Using thermal ionisation mass spectrometry (TIMS) increases precision and decreases needed

sample size. The method is based on radioactive decay of ^{238}U that is converted to ^{230}Th (Oldfield 2005).

$^{210}Pb/^{222}Rn$ – for sediments not older than 150 year. The method is based on radioactive decay of ^{210}Pb to gaseous ^{222}Rn.

The artificial radionuclides such as ^{137}Cs, ^{241}Am, ^{239}Pu, ^{240}Pu, ^{90}Sr can be used as tracers of past nuclear weapon testing (last 57 years) (Cohen 2003, Oldfield 2005). ^{226}Rn- ^{210}Pb radionuclides can trace up to 150 years (Oldfield 2005).

Paleomagnetic

Principle of magnetic methods has already been mentioned (see chapter 3.5.1). Paleomagnetic methods provide two types of dating according to (i) changes in polarity and (ii) characteristic continuous pattern of paleomagnetic secular variations with different timescales. Magnetostratigraphy studies, in conjunction with correlation of susceptibility records to the orbitally tuned marine $\delta^{18}O$ record, can provide global dating resolution of ~10 ky for studies of lake sediments in the timescales of 10^6–10^7 years. A combination of secular variations and radiocarbon provides dating and correlation with centennial resolution for Holocene lakes (King and Peck 2001). Paleointensity studies of suitable sediments provide an independent approach to dating sediments on similar timescales as radiocarbon dating. On the other hand, studies of excursions/short events hold promise for increasing dating resolution of the lake sediments in timescales of 10^5–10^6 years. Intensive study is underway that will clarify the excursion/short event stratigraphy of the last 1 Ma (Oldfield 2005).

Chemical

Amino acid racemization – can be applied to organic material (most often wood, speleothems, coral, marine and freshwater shells) ranging in age from few thousand to a few million years. It requires very small samples – several mg (2 mg in the case of molluscs and foraminifera). Amino acid molecular structure changes specifically (process called racemization) after organism death in relation to time and also temperature (Bradley 1999).

Tephrachronology – fingerprinting of volcanic ashes. Each major eruption has its unique geochemical signatures and therefore its ashes found in sedimentary records of various ages can be used as chronostatigraphic marker to date associated deposits and to correlate events of wide areas (Bradley 1999).

Seasonal signatures – varved sediments, that are typical for certain lake sedimentary environments can be successfully dated by visual counting of growth increments. This technique is usually used in combination with other dating techniques in order to get absolute values (Sims *et al.* 2006).

STUDIED LAKE ARCHIVES

4. STUDIED LAKE ARCHIVES

This work is concerned to provide climatic studies from Aral Sea and Baikal Lake sedimentary record. Both studied lakes are situated in Asia (Figure 8) representing two large lakes with continental climate with a potential to provide valuable climatic record. In following chapter we will introduce both lakes from geographic, geologic, hydrologic as well as climatic point of view. The lakes differences in depth, age, watershed etc. gave us a potential to compare the reliability of various methods in different environments.

Figure 8 The general view to studied lakes Aral Sea (left) and Baikal Lake (right red circle).

4.1. Aral Sea

4.1.1. Geography

Aral Sea is located in central Asia on the border of Kazakhstan and Uzbekistan (Figure 9) eastern from the Caspian Sea. The Aral Sea watershed covers most of the territory of Tajikistan, Uzbekistan, Turkmenistan, three provinces of the Kyrgyz Republic (Osh, Jalalabad and Naryn), the southern part of Kazakhstan (two provinces: Kyzyl-Orda and South Kazakh), and northern Afghanistan (Figure 10). Aral Sea was in 1960 fourth largest lake in the world with the area of about 67 000 km^2 until now the Aral Sea area has been gradually reduced simultaneously with the lake level fall (Table 6, Attachment 2.2) leading to subdivision of single water body into three basins that are connected only with small channels: small Aral Sea at the north, deeper Western and shallow Eastern Basin (Figure 9).

The natural freshwater input to the lake is governed by two tributaries, the Amu Darya, currently feeding the Eastern Basin at the south, and Syr Darya, currently feeding the Small Aral Sea at the northeast (Figure 10). Both tributaries are originating in Tien-Shan and Pamir Mountains. Aral Sea water body, a typical closed lake, mirrors sensitively even weak environmental changes in the watershed (Sorrel *et al.* 2006). Two additional sources of the Aral Sea water are precipitation transported from central Asia and occasionally from Mediterranean area (Sorrel *et al.* 2007b) and groundwater originating in the Pamirs and Tien-Shan mountains (Lètolle and Mainguet, 1996; Austin *et al.* 2007). However, the sedimentary record of the Aral Sea does not only register climate signals but has also been impacted by geomorphologic changes and more importantly also men actively impact on the river course of the lower Amu Darya by reactivating and increasing the discharge into the Caspian Sea (Tolstov 1965).

Table 6 Hydrological and salinity characteristics of Aral Sea from 1960 AD (after Micklin 2007).

Year	Level [m asl]	Area [km^2]	% 1960	Volume [km^3]	% 1960	avg. salinity [g/l]
1960	53.4	67.499	100	1089	100	10
1971	51.1	60.200	89	925	85	12
1976	48.3	55.700	83	763	70	14
1989	39.6	39.734	59	364	33	30
2006 (whole Aral Sea)		17.382	26	108	10	
Large Aral Sea	30.0	14.325	23	81	8	Eastern - >100 Western 70-80
Small Aral Sea	40.5	3057	50	21	26	12

4.1.2. Geology

The relief of the territory can be divided into two types: plain and mountainous (Figure 10). The plain-lands belong to the Turanian plate of the Gercian platform, where a deep covering layer (more than 10 km thick) of Mesozoic and Cenozoic sediments lies upon highly rugose Palaeozoic sediments. The mountainous areas of the region (the Pamirs, Tien-Shan, Pamiro-Alai) comprise of newly formed rugose geological structures, which originated from the same plate formed during the Neogene period of the Cenozoic aeon. Continental Neogene-Quaternary sediments are found above this layer, which were formed by river processes and temporary water flows, as well as sea transgressions and aeolian processes (UNEC, 2005).

Figure 9 Satellite image of Aral Sea from 2007 - red line represents state borders; black line represents the lake level in 1960.

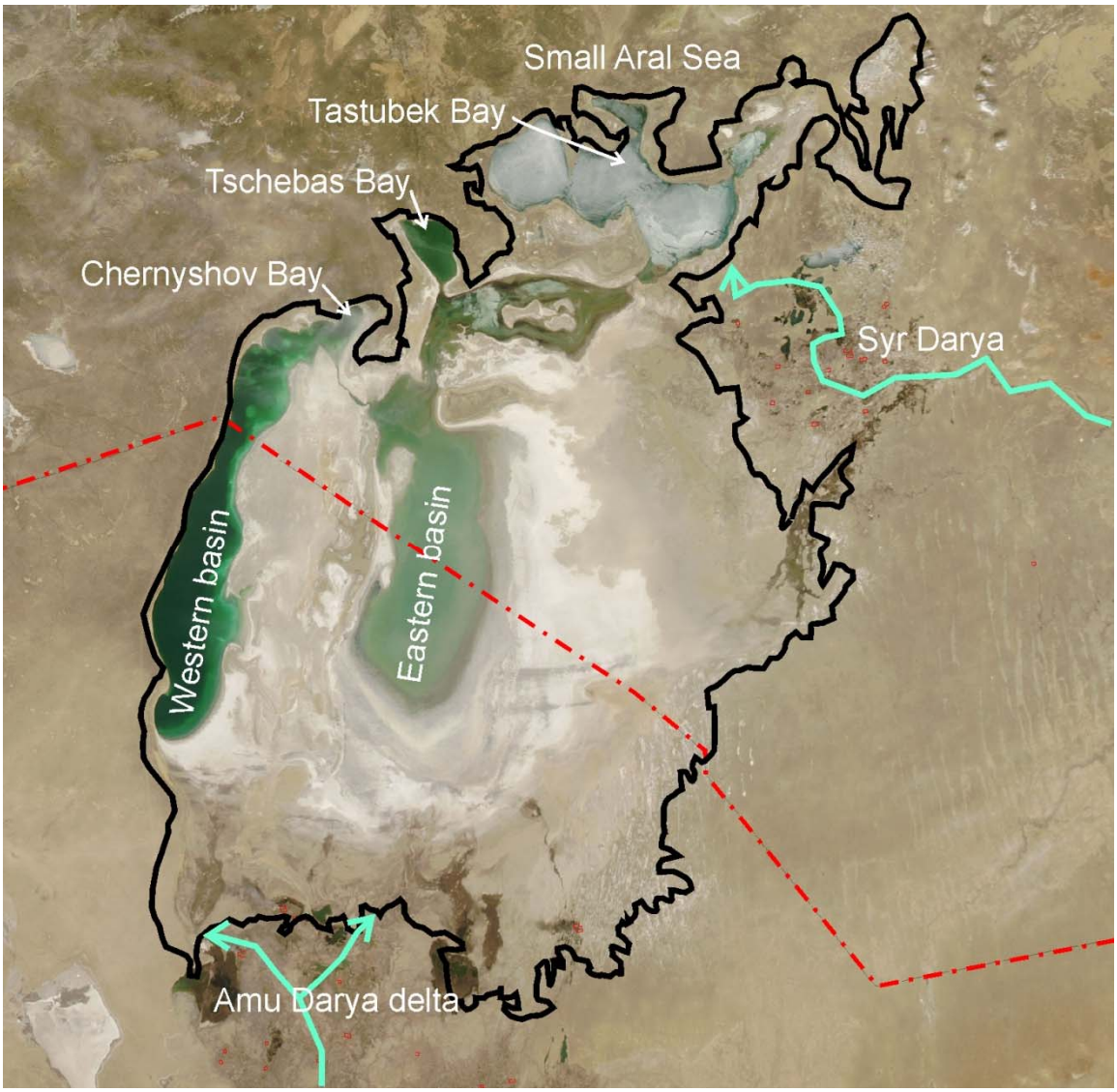

Figure 10 Geomorphologic map of Aral Sea catchment area (after UNEP 2005).

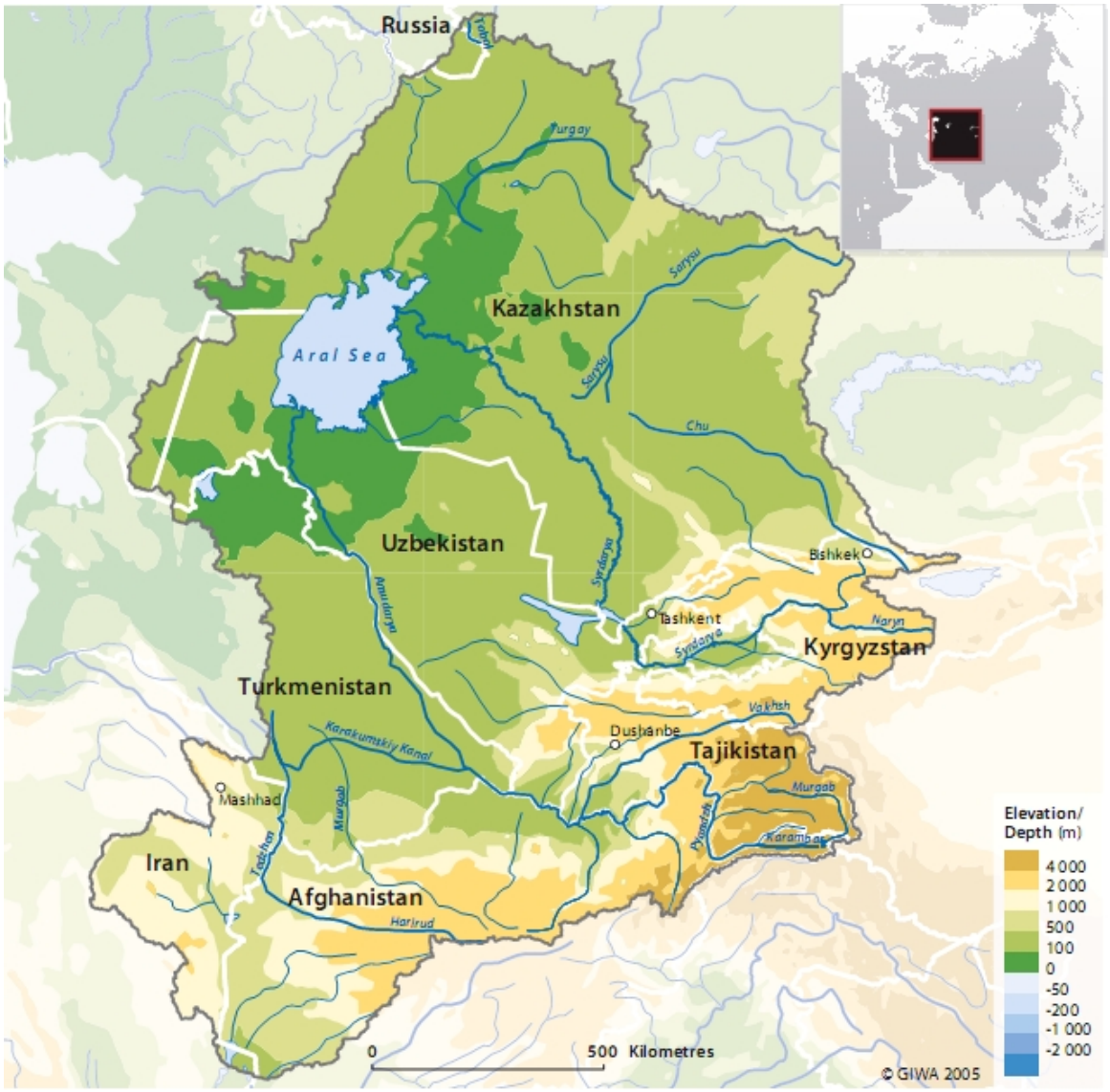

4.1.3. Lake origin

The origin of the lake is tectonic. The basin is bounded to the west by a number of normal faults that may have been active during the Neogene. These structural controls probably explain the relatively steep western boundary of the basin and also the presence of the structural high of Vozrozhdenie Island in the centre of Large Aral (Létolle and Mainguet, 1993). Boomer *et al.* (2000) suggested that the Aral and Sarykamysh depressions would have been flooded at some time between the mid- and late Akchagylian (2Ma) due to a transgression of the Caspian and possibly Black seas. Alluvial deposits associated with paleo-valleys in the bed of the Aral Sea indicate a major lowering of the lake. Rubanov (1991 in Tarasov *et al.* 1996) suggests that the lake was most extended probably during the late Neogene, when it stood at a level of 73 m a.s.l. The time of the last flooding of the Aral depression is debated: estimates vary from some time after 24,000 yr BP to the beginning of Holocene, ~10 ky BP (Tarasov *et al.* 1996).

4.1.4. Recent climate

The deserts and semi-deserts of Central Asia have a strong continental climate. The temperature pattern for winter is largely influenced by high pressure resulting from a cold anticyclone centered over eastern and northern Asia (i.e., the Siberian High) with pronounced temperatures from 0 to -15°C in average down to -40°C for the minimal values (Lioubimtseva *et al.* 2005). Although this area is often struck by humid winds, the mountains trap most of the moisture, leaving little precipitation for other area of the Aral Sea Basin. At lower elevations, the climate is characterised by dry, hot summers and moderately mild, rainy winters. Average temperatures range from 0 to 4 ^{0}C in January to 28 – 32 ^{0}C in July. Annual precipitation is generally low; about 150 to 500 mm, which usually occurs in winter and spring. Prevailing ecosystems are steppes (including shrubs). Some isolated trees (e.g., poplar, tamarisk, elm, oak), which are typical for riparian ecosystems, are restricted to the banks of two major Central Asian rivers (Sorrel 2007b).

Two other important controls on precipitation changes over Central Asia are the levels of the Caspian and the Aral seas and their contribution of moisture and heat to the lower atmosphere, especially during summer when evaporation greatly intensifies (Lioubimtseva *et al.* 2005). According to the observations recent Aral Sea regression changed the climate of the Aral Sea region by decrease of relative humidity and marked temperature increase (Martius *et al.* 2004).

4.1.5. Water budget and riverine salinity

Water budged of Aral Sea is naturally impacted by a combination of global teleconnections, e.g. Asian monsoonal activity, NAO, ENSO (Sorrel *et al.* 2007), implying the complexity of the natural forcings assessment in the past. Oberhänsli et al. (2009) recently published data from Aral Sea hydrological budget before 1960th: evaporation 44-64 km^3/year, annual precipitation 100-140 mm (6-9 km^3/year), river discharge 56 km^3/year, underground water sources 1-10 km^3/year. Schiemann et al. (2007) point out that only Amu Darya River is influenced by Indian summer monsoon and counted this contribution as 10% of Amu Darya runoff. However, the relationships of Aral Sea water income and Indian summer monsoon is rather than by direct precipitation in the watershed governed by temperature changes related to monsoonal activity.

The Amu Darya Basin is a typical endorheic basin under arid conditions. Precipitation rates on Amu Darya catchment area vary from 100 mm per year in the desert plains to 2000 mm in the high mountain areas. Most of the water of the Amu Darya derives from the high mountain glaciers of the Pamir-Alai-System, while the desert plains that cover about two thirds of the basin do not receive significant amounts of water. In the opposite, the evaporation rate is very high in the plains and the river loses most of its water through evaporation, infiltration and withdrawal for irrigation. High water levels occur twice a year, the first in April/May after the snowmelt, which is quite short; the second is in June/July after the glacial melt. The largest water share of the river originates in Tadjikistan (72.8 %), 14.6 % of Amu Darya water comes from Afghanistan and Iran and about 8.5 % of the water is formed in Uzbekistan. Today, water withdrawal for irrigation purposes amounts to 90 % of the water flow of the Amu Darya. This development resulted in a decrease of the water discharge to the Aral Sea and finally to its desiccation (NeWater project report, 1995). During dry years, the mean annual salinity of the Amu Darya water entering into

the sea reaches 0.8-1.6 g/l, and salinity in the Syr Darya amounts to 1.5-2.0 g/l. In some seasons, higher salinity levels are observed (Schutter and Dukhovny 2003). Le Callonnec *et al.* (2005) present differences in water chemistry of the Amu Darya and Syr Darya rivers as follows: Syr Darya water in comparison with Amu Darya are enriched in sulphate and impoverished in Fe. From the mountains downstream to the Aral Sea, the main course of the Syr Darya and the Amu Darya across the deserts has not significantly changed. Chemical analysis can therefore indicate river discharge.

4.1.6. History of research

Aral Sea problematic was before 1990 discussed mainly in Russian language. One of the first non Russian complex study was published in French (Létolle and Mainguet, 1993) lately (1997) translated to English. This book provides very valuable summarization of that time knowledge. From 1995 several books concerning to Aral Sea has been published (e.g. Glantz 1999, Schutter and Dukhovny 2003, Valentini *et al.* 2004, UNEP 2005, Micklin 2007) the main topic of these books were recent environmental-political situation of the area and solution of the Aral Sea budget problems. Recently (2009) special issue of Journal of Marine Systems (Volume 76, Issue 3) with title: Aral Sea Basin, Hydrological, Chemical, and Biological dynamics today compared with trends of the past 50 years (edited by H. Oberhänsli and P. Zavialov) has been published proving that the Aral Sea theme is topical and many questions have not been answered yet.

Past lake level changes in Aral Sea basin have been studied from sedimentary cores (Le Callonec *et al.* 2005, Sorrel *et al.* 2006), archaeological excavations (Boroffka *et al.* 2006), morphological features (Reinhardt *et al.* 2008), and historical documents (Boomer *et al.* 2000). These studies generally agree on 4 major regression phases in the last 2 ky with variable timings and durations (Figure 11).

Figure 11 Aral Sea lake level reconstructions for the variations in the last 2 ky.

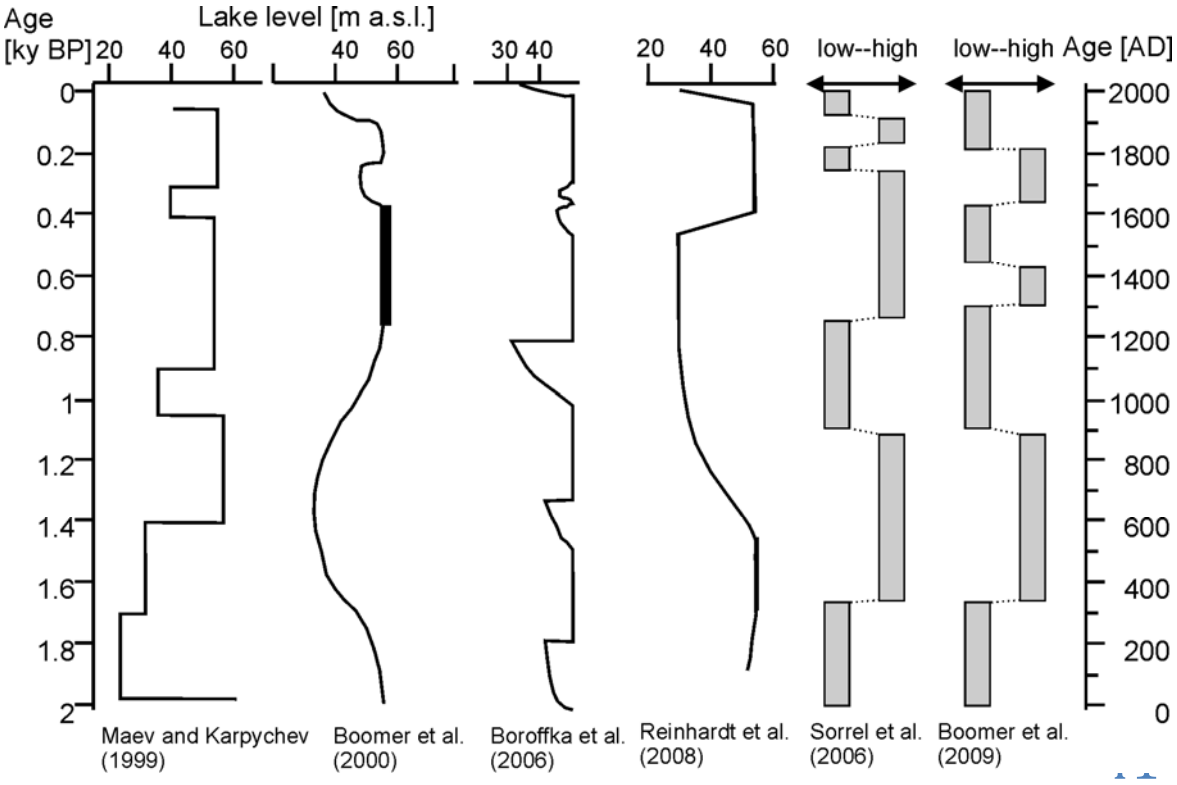

4.2. Baikal lake

4.2.1. Geography

Lake Baikal is situated in eastern Siberia, Russia (Figure 8). The lake is completely surrounded by mountains; large part of the watershed is situated in Mongolia (Figure 12, Figure 13). It is known as the oldest (20- 30 million years), the deepest (1,637 m) and the largest by volume (holds 1/5 of the world's unfrozen fresh water) freshwater reservoir in the world. More than 330 rivers feed into Lake Baikal but the main tributaries are: Selenga River, Barguzin River, Upper Angara River, Turka River, Sarma River, and the Snezhnaya River. It is drained through a single outlet, the Angara River in the south western part. Another major feature that sets Lake Baikal apart from other deep lakes is that the entire water column is saturated throughout with oxygen (Mackay *et al.* 2002).

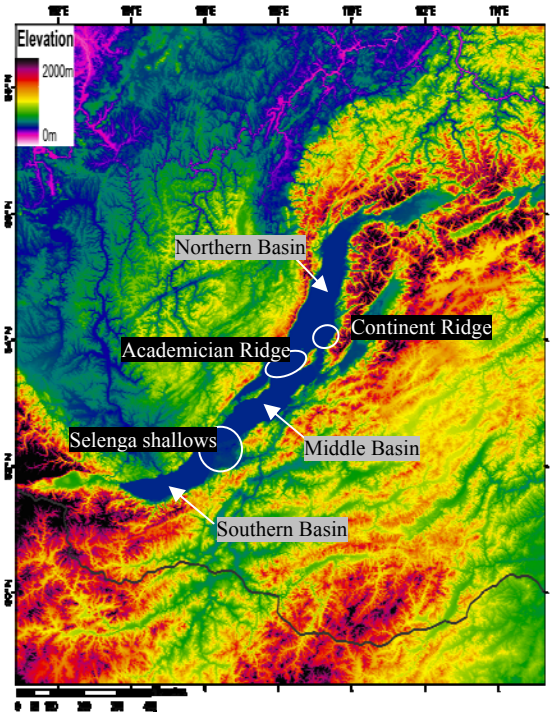

Figure 12 Digital elevation model of Lake Baikal. The *bl*ack line is the Russia-Mongolia boundary (http://www.ngdc.noaa.gov/mgg/topo/globega2.html).

4.2.2. Geology

Lake Baikal is located in the central portion of the Baikal Rift System at the southern margin of the Siberian Platform. The Baikal rift zone separates the tectonically stable Siberian Craton from the seismically active tectonic belts in the Trans-Baikal region and Mongolia (Callender and Granina 1997). From investigations of palaeostress fields in the Lake Baikal area, two major stages during the Cenozoic can be distinguished: (i) a Late Oligocene–Early Pliocene palaeostress stage that is related to the rift initiation with a compressional to strike-slip regime, and (ii) a Late Pliocene–Quaternary palaeostress stage starting around 3.2 My that is related to the major stage of rift development with a pure extension regime in the Central Basin and an acceleration of vertical movements (Müller *et al.* 2001). Recently the rift widens ~ 2 cm/year. Three large basins, i.e. Southern, Central, and Northern, are separated by two underwater highs: the Selenga Shallows in the south, and Academician ridge in the north (Figure 12) (Mackay *et al.* 2002).

Mountains that surround Lake Baikal are composed of Precambrian crystalline rocks, mostly granites and granodiorites. The Selenga river basin is underlained by bedrock composed mainly of Proterozoic granites. There are many depressions filled with Mesozoic sediments, and Tertiary basalts crop out on the tops and crests of mountains. On the west side of the lake, the bedrock is composed of metasandstones, metaconglomerates, tuffs, gneisses, and granites (Callender and Granina 1997). Present-day sedimentary environments in Lake Baikal comprise, in general, three types of facies: i) turbidite depositional systems, which occupy mainly the floors of the basins, ii) large river deltas, and iii) isolated ridges and banks, with mainly hemipelagic sedimentation. The sedimentation rates vary between these systems from less than 3 cm/kyr (on ridges) to more than 30 cm/kyr (on basin floors) (Sapota *et al.* 2004).

Figure 13 Lake Baikal watershed (Brunello *et al.* 2006).

4.2.3. Recent climate

The climate of the Siberia region has high degree of continentality characterized by sharp contrasts between summer and winter temperatures (Rioual and Mackay 2005) but Baikal Lake region has some signs of a maritime climate, i.e. seasonal temperature variations are smoothed over. Thus, there is a comparatively mild winter and cool summer (bww.irk.ru). The leading factor controlling the climate of this region appears to be the strength and expansion of the Siberian High which affects how much moisture the Westerlies can bring from the North Atlantic and how far from the south the summer monsoon can reach into China (Rioual and Mackay 2005). Siberia is highly sensitive to the supply of moisture from the North Atlantic (the main driving force of global cooling events), most likely related to changes in the thermohaline heat flux at glacial/interglacial transitions and therefore there is a high probability for Lake Baikal to record shorter episodes as Heinrich events (Prokopenko *et al.* 2001b). Winter monsoon generates cold and dry conditions. On the other hand East Asian summer monsoon related to tropical ocean, generates warm and moist conditions. However, its moisture did not affect the Baikal Lake water budget. Domination of these two monsoonal systems varied in the past (Rioual and Mackay 2005). Other moisture income to the region is transported from the Barents Sea and other parts of the Arctic (Williams *et al.* 1997). The temperature of the water in the surface layer changes from ~14 °C (in August) to 0 °C (in December-January). In coastal regions the temperature can achieve ~16 °C, mostly in eastern part and in shallow bays and shores the temperature can rise up to 22 °C. In general Baikal begins to freeze on 21st of December and melt on 16th of January (mapstor.com).

4.2.4. Water budget and chemistry

The water budget is especially notable for the predomination of river influx (83 %) over atmospheric precipitation and the dominance of drainage from the lake (81 %) over evaporation (Mackay *et al.* 2002). From chemical analysis of Baikal Lake water we can conclude that total mineral concentration is relatively low. Falkner *et al.* (1991) presented that water is highly calcinated with the major ion hydrogencarbonatic. The rest ionic concentration (Mg^{2+}, Na^{+}, K^{+}, and Cl^{-}) is below 5% but according to Granina (1997) water is rich in Fe, SiO_2 and Cl^{-}, Ca^{2+} and HCO_3^{-} poor. The latter analysis is supported by Swan and Mackay (2006) who point to the lack of carbonates within the sedimentary record and therefore increasing importance of biogenic silica measurement to obtain palaeoclimatic information. Biogeochemical silica mass balance important for this work shows that the production of diatoms in the lake is supported mostly by remineralisation processes in the water column and is accompanied by a significant contribution of dissolved silica from the riverine inputs (Mackay *et al.* 2002).

On the basis of high oxygen concentrations throughout the water column and other hydrologic observations, Lake Baikal has been presumed to be dimictic with the entire water column turning over twice annually. Complete renewal that has implication for nutrient cycling takes ~8 years (Falkner *et al.* 1991).

4.2.5. History of research

Large interdisciplinary projects have been concerned in Baikal Lake sediments as valuable climate archive, e.g. Past global changes (PAGES) program – namely International geosphere-biosphere program Pole-Equator-Pole (PEP II) transect through Asia (Williams *et al.* 1997), Baikal International Centre for Ecological Research (BICER), the Baikal Drilling Project–ICDP programme with target to complete paleoclimatic record of the last 2.5 to 3 Ma (Oberhänsli and Mackay 2005), and finally CONTINENT (High-resolution CONTINENTal paleoclimate record in Lake Baikal) project that funded core analysed in this work. CONTINENT project results in special issue of Global and Planetary Change (Volume 46, 1-4) in 2005 containing 22 articles summing up the Baikal lake problematic with focus mainly to the last 150 ky.

Diatoms in Lake Baikal have been commonly used to reconstruct palaeoclimatic and palaeoenvironmental changes over glacial-interglacial cycles (e.g., Khursevich *et al.* 2001) as well as within interglacials (e.g., Rioual and Mackay, 2005) and glacials (e.g., Swann *et al.* 2005). Works that use diatom analysis are is based on the often distinct environmental characteristics of individual taxa, the strong first-order relationship which exists between insolation patterns and diatom abundance (Prokopenko *et al.* 2001a) and the diversity, appearance and extinction of individual species (Khursevich *et al.* 2001). The palaeoenvironmental interpretation of individual diatoms species is often limited by the unknown ecological characteristics of both endemic and extinct diatom taxa. This is particularly true prior to the Holocene with many of the dominant species from the Pleistocene now extinct (Khursevich *et al.* 2001).

EXPERIMENTAL PART METHODS

5. EXPERIMENTAL PART — METHODS

Our choice of methods was governed by the composition of studied sediments. We tried to use traditional methods and compare them with other simpler mainly chemical methods with potential to have a palaeoclimatic output faster and in the better resolution. Methods are ordered according to their broad classification (see below). We did not use all the methods for both studied sites; therefore we marked at each method the site where it was used. All methods were performed in Institute of Inorganic Chemistry Academy of Sciences of the Czech Republic (AS CR), v.v.i, 250 68 Rez, Czech Republic unless another institute is clearly denoted.

Broad classification of used method:

1) Microscopic – diatom analysis, Scanning electron microscope (SEM)
2) Chemical – Cu-trien
3) Spectral – Diffuse reflectance infrared fourier transform spectroscopy (DRIFTS), Ultra-Violet - Visible (UV-VIS) Diffuse reflectance spectroscopy (DRS), Visible/Near Infrared Reflectance (VNIR)
4) Magnetic – Magnetic susceptibility (MS), Natural remanent magnetization (NRM), Anhysteretic Magnetic Remanence (ARM)
5) X-ray – p-XRD (X-ray diffraction), High temperature x-ray diffraction (HT-XRD), X-ray fluorescence spectroscopy (XRF)
6) Radiocarbon dating

5.1. Microscopic methods

Diatom analysis – Aral Sea, Baikal Lake

Sample preparation: The method of the sample preparation depends on the type of analyzed material. The standard procedure (described in more detail in Battarbee *et al.* 2001, see also Figure 14) consists of several cleaning steps of sediment suspension from organic matter, salts, and carbonates. In the case of organic poor sediments the procedure is simpler. With respect to high fragility of fossil frustules in Baikal Lake sediment, Mackay *et al.* (1998) recommended not to use any leaching steps (e.g. with acids such as HCl, or oxidizing agents, such as H_2O_2). Therefore we used following simplified procedure while preparing diatom slides of Baikal Lake as well as Aral Sea sediments: usually 0.1 g of dried sediment was enough to provide sufficient diatom concentration. In order to get the quantitative information of diatoms as well as each species we add exact amount (~0.5 ml) of divinylbenzen microsphere (diameter of 7-10 μm) suspension with a concentration of 6.81 $x10^6$ to the sediment suspension. After mixture completion we dropped ca 150 μl of it to a cover glass and allow to dry covered in order to prevent contamination. A dried cover glass was carefully turned and pressed to the drop of honey-like liquid Naphrax glue (BrunelMiroscopes, UK) on the microscopic slide. We always put two pieces of cover glass with different concentration of the same sample onto one microscopic glass (in order to double our chance to get the ideal diatom concentration). Naphrax glue is toluene diluted and in order to solidified it the toluene needs to evaporate, to speed up and control this

process we heated each glasses in the flame burner several times until the glue was solidified. Flame temperature should not rise above 130°C when the spheres may begin to melt. The microspheres also contain mercury iodine so we strongly recommend careful manipulation (instruction for microsphere uses).

Figure 14 Diatom slide preparation steps - in this work we started from the "add microspheres" step (adopted from Battarbee *et al.* 2001).

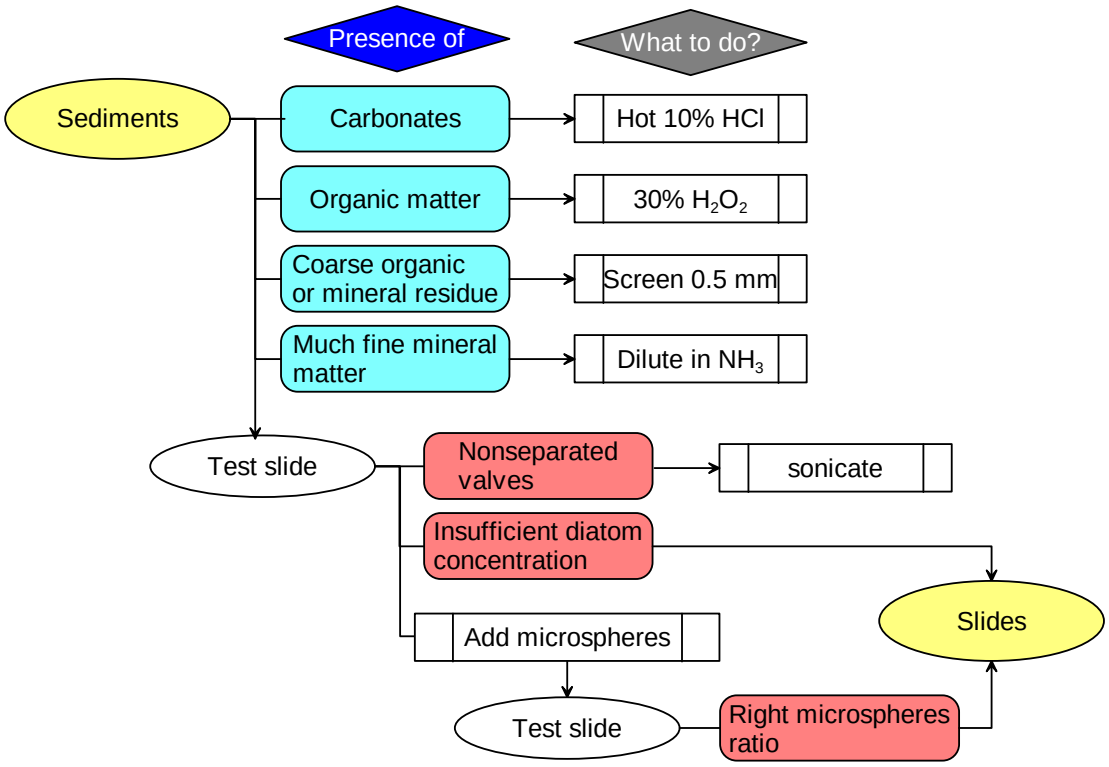

Used equipment and counting procedure: Counting area was at least one systematic vertical traverse across the diameter (20 mm) of the cover glass. In sample with a low diatom concentration this traverse were repeated 3times at different levels and in samples with high diatom concentration we ended counting with ~300 counts. We noted stage co-ordinates in order to continue in counting if necessary. We counted both - the individual species and microspheres. For diatom counting we used an optical microscope Olympus BX 40 with oil immerse lens at ×1000 magnification. Immersion oil has refractive index of 1.515-1.516 and together with the Naphrax (1.65) it provides the essential contrast. We follow the counting technique described in Battarbee *et al.* (2001) - countable frustule must have at least half of the centre or in the case of tubular species one complete end (and at the end their counts are divided by two).

Program for evaluation: We used Microsoft Office Excel 2003, OriginPro 7.5 as well as database produced by V. Píška in Microsoft Office Access 2003.

Expected result: Diatom assemblage reacts very fast, usually within the season, to the changes of the lake environment. Reconstructing fossil assemblages allow tracing the main environmental changes and moreover the species analysis can provide additional information about the changed parameters.

Main advantages of the method: Obtained results provide complex information about changes in water environment. Diatom analysis as a traditional method could be compared within authors, lakes, etc.

Methodical uncertainty: Large amount of mistakes could be produced during every step of the procedure, i.e. contamination of slides during slide preparation, inaccurate counting of valves as well as microspheres, misidentification of diatom species, misinterpretation using wrong sources. Diatoms as the unicellular organisms with high mobility (often carried by wind) require the absolute clearness of used instruments. Ideally usage of new in every analysis but at least really careful cleaning of used equipment is essential.

Diatom identification: In both lakes the diatom identification (see attachments 2.7 and 3.3) was aggravated by the uncommon diatom assemblage in the case of Baikal Lake it was mainly due to species endemitism and in the case of Aral Sea salinity communities. There was not possible to get almost any diatom literature in Czech Republic concerning these two types of diatom communities. Therefore we relied primarily on specialized articles and also on consultations with more experienced diatomists: G. Swann (British Geological Survey, UK), P. Austin (University College London, UK), G. Khursevich (National Academy of Sciences of Belarus, Republic of Belarus), V. Houk (Institute of Botany, AS CR), and J. Veselá (Department of Botany, Faculty of Sciences, Charles University in Prague, CR) and secondly were diatoms identified following Krammer and Lange-Bertalot (1986 - 1991). For identification of small species, especially in the case of Aral Sea we used Nomarski differential interference contrast. Very often was the identification difficult because of broken valves with only central part left. We gave special attention to the identification of Aral Sea species *A. octonarius*. We produced SEM images (Attachment 2.5), and also contacted P. Austin, who has identified this species in fossil assemblage previously (Austin *et al.* 2007). *A. octonarius* is known to be in Aral Sea even nowadays (Sapozhnikov *et al.* 2009) but we must admit that we are not experts to *Actinocyclus* identification into species level.

Co-workers: K. Novotná, G. Swann, P. Austin, V. Houk, J. Veselá, T. Grygar

Scanning electron microscope (SEM)/ Energy Dispersive X-ray Analysis (EDX) – Aral Sea, Baikal Lake

Place of measurement: 1. IIC AS CR, Rez; 2. Department of zoology, Charles University in Prague, Faculty of Science, Czech Republic, Viničná 7, Prague.

Sample preparation: Traditional way of diatom samples preparation for SEM analysis is very similar to the slide preparation except we used a special metal underlay according to each SEM machine instructions instead of glass and we do not use naphrax. In the case of Baikal sediment traditional leaching steps cause frustule damage so the procedure must have been adjusted. So we compared samples that were in raw state and those dispersed in a drop of water. We found that the dispersed sample was covered by clay matrix resulting low visibility of morphological features. Therefore we used raw samples to observe present diatoms.

In the case of Aral Sea samples we used both samples dispersed only in distilled water and followed standard methodology for diatom sample preparation (Battarbee *et al.* 2001) cleaned

sample with distilled water in order to wash present salts and with NH_3 and after settling remove supernatant to minimize content of clayey matrix (Figure 15).

Used equipment and measurement conditions: Rez: electron microscopy Philips XL 30 CP; Prague: electron microscopy Jeol JSM-6380LV in vacuum; in both cases we metalized samples with gold to get the best possible images. Only in the case of ostracod samples we did not use the gold cover because we wanted to study elemental composition of shells using Robinson Backscattered Electron Detector. Presence of elements was analysed by Energy Dispersive X-ray Analysis (EDX).

Program for evaluation: Zoner Photo Studio 9, XnView, CorelDRAW X4

Expected result: Identification of diatoms into species level. Also provide photo documentation of some found and already identified species.

Main advantages of the method: Provide very detailed images of the frustules.

Methodical uncertainty: Diatom frustules are often in position and state that is not ideal for their identification and their motion in SEM machine is impossible.

Co-workers: V. Grünvaldová, S. Švarcová, J. Veselá

Figure 15 Comparison of SEM pictures of *T. compressa* prepared by different methodology: a) only dispersed in drop of water (covered by sediment matrix); b) using standard methodology (Battarbee *et al.* 2001). Scale 10 µm

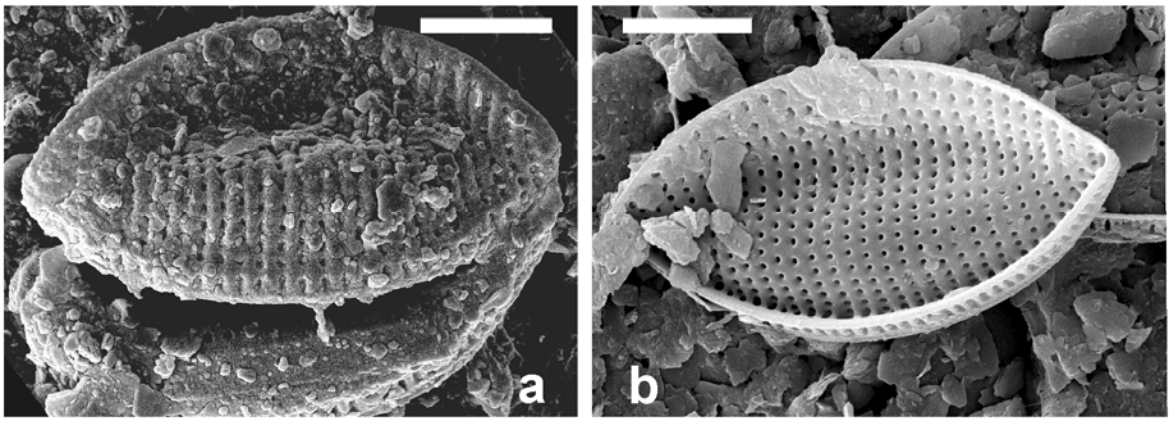

5.2. Chemical methods

Cu-trien – Aral Sea, Baikal Lake

Sample preparation: Before any treatment all samples were dried, homogenized, and manually powdered. The preparation procedure was described in Grygar *et al.* (2007, 2009). 250 mg of sample was re-suspended in 5 ml of water before the addition of 5 ml of 9 mM solution of Cu(trien)SO_4 (trien=1,4,7,10-tetraazadecane). The suspension was then stirred for 10 min and filtered into 50 ml flasks. Under these conditions, with ~ 50% of the Cu-trien consumed for the exchange, Cu^{2+} ions replace exchangeable cations in the expandable structures.

Used equipment and measurement conditions: The difference in concentration of Cu^{2+} (ΔCu^{2+}) as well as the concentration of evolved Ca^{2+} and Mg^{2+} were determined by atomic absorption or emission spectroscopy using Atomic adsorbtion spectroscopy (AAS) 3, Carl Zeiss, Jena.

Expected result: ΔCu^{2+} is proportional to the amount of expandable clay minerals in the samples and therefore it produces a proxy for the changes in important part of allochthonous sedimentary components. Moreover, higher amount of expandable clay minerals should be in the correlation with higher weathering in the watershed, and also with the climatic changes.

Main advantages of the method: Fast, low-cost, efficient, moderate instrumental requirements.

Methodical uncertainty: The mean error given by a possible adsorbtion of Cu^{2+} or dissolution of calcium or magnesium salts expressed as a molar non-equivalency of ions involved in the reaction (ΔCu^{2+}–Ca^{2+}–Mg^{2+})/ΔCu^{2+} was 3%, i.e., the systematic error for Cation exchange capacity (CEC) determination was insignificant. CEC determined by Cu-trien method

Co-workers: T. Grygar, J. Dorflová, P. Vorm

5.3. Spectral methods

Diffuse reflectance infrared Fourier transform spectroscopy (DRIFTS) – Aral Sea

Place of measurement: Polymer Institute Brno, s. r.o.; Tkalcovska 36/2, 656 49 Brno, CR

Sample preparation: We acquired the spectra of the powdered and homogenized samples. Sampling resolution was 1 cm.

Used equipment and measurement conditions: Nicolet Avatar FTIR (ThermoNicolet) spectroscope with aluminium cells filled by sample.

Program for evaluation: Reflectance were recalculated to absorbance, and then processed by Microsoft Office Excel to isolate the height of the bands of kaolinite (3696 cm^{-1}), gypsum (2230 cm^{-1}), calcite (875 cm^{-1}), and aragonite (856 cm^{-1}).

Expected result: Analyses of abundance of minerals using the height and ratio of the height of the above mentioned bands as proxies of mineral concentrations in the sediments with high resolution.

Main advantages of the method: Non-destructive, fast, small amount of the sample needed.

Methodical uncertainty: The band could be similar with other minerals, require very good homogenization.

Co-workers: T. Grygar

Ultraviolet – visible (UV-VIS) diffuse reflectance spectroscopy (DRS) – Baikal Lake

Sample preparation: Powdered and homogenized samples filled to the glass cuvette.

Used equipment and measurement conditions: Perkin Elmer Lambda 35 spectrometer equipped with an integrating sphere (Labsphere). White standard - $BaSO_4$ plate.

Program for evaluation: OriginPro 7.0 with peak fitting module, OriginLab Corporation

Expected result: DRS spectra could be used for the evaluation of content of Fe-bearing clay minerals and oxides (Grygar *et al.* 2003; Hradil *et al.* 2004; Grygar e al., 2006). We used two characteristics based on reflectance (%): R_{UV}, reflectance in UV–Vis region at 270 nm (charge-transfer bands of total Fe^{3+}), and R_{Vis}, mean reflectance in visible-light region (400–700 nm, total lightness). For statistical analyses, R_{UV} and R_{Vis} were recalculated to absorbance using the Kubelka–Munk formula. Additionally another parameter, B/C, was obtained based on the amount of absorption calculated from the Kubelka– Munk formula (Grygar *et al.* 2006). B and C are gaussian components of the spectra corresponding to Fe^{2+}-O-Fe^{3+} IVCT and Fe^{3+} d-d electrons transfer, respectively. The bands are centered at 13900 cm^{-1} (~720 nm) and 16000 cm^{-1} (625 nm), respectively. As detailed within Grygar *et al.* (2006), the B/C ratio is a good measure of Fe oxidation state within detritus minerals.

Main advantages of the method: Non-destructive, fast, differentiation between Fe^{2+} and Fe^{3+} without need of use the traditional Mössbauer spectroscopy. Analyse a presence of even a very small amount of materials containing Fe^{2+}–Fe^{3+} and distinguishing between phases (e.g. goethite, hematite).

Methodical uncertainty: Samples must be well homogenized; gaussian deconvolution fitting of reflectance plots require certain experience.

Co-workers: T. Grygar

Visible near infrared spectroscopy (VNIR) – Aral Sea

Place of measurement: Department of Climate Dynamics and Landscape Evolution, Helmholtz-Centre Potsdam - GFZ German Research Centre for Geosciences, Potsdam, Germany

Sample preparation: We sampled the core by plexiglas boxes (with inner size of 115x28x5 mm) (Attachment 1) arranged along two parallel stripes with 5 cm overlapping. In order to minimize oxidation and drying of sediments the boxes were covered with a thin polymer foil and thereafter immediately scanned at the VNIR spectral device.

Used equipment and measurement conditions: FieldSpec® portable spectrometer. The spectra were measured between 350 -2500 nm (28571-4000 cm^{-1}) with a 1 nm step. The reflectance was converted to Kubelka-Munk scale. Kubelka-Munk remission function ($F(R_\infty)$) is $F(R_\infty) = (1-R_\infty)^2/(2*R_\infty)$,where R_∞ is reflectance. Method optimization as well as comparison with UV-VIS diffuse reflectance spectra was performed in GFZ, Germany during one year study stay of K. Novotná in 2006.

Program for evaluation: Microsoft® Office Excel 2003; OriginPro 7.0 with Peak Fitting Module, OriginLab Co. The adjustment (the correction to white reference; the jump deletion of detectors; the transformation to ascii data) of spectra were performed by software ENVI 4.2.

Expected result: High resolution record (2 mm) of some of the present sedimentary components analysed using material standards (e.g. mica, biotite, chlorite, kaolinite, gypsum).

Methodical uncertainty: Analysed bands could be similar with other minerals – misidentification. Peak fitting of reflectance plots require a lot of experience.

Co-workers: K. Novotná, T. Grygar. All results of this method are unpublished results of K. Novotná. Author has assisted to the core measuring only in the processing of the last core section (400-432 cm).

5.4. Magnetic methods

MS, NRM, ARM – Baikal Lake

Place of measurement: Department of Paleomagnetism, Institute of Geology, AS CR, v.v.i.; 252 43 Průhonice, CR

Sample preparation: Magnetic measurements were done after sediment sampling into boxes in a naturally wet state. All samples were demagnetised in 5–6 steps with a maximum alternating field of 100 mT by the LDA-3 device.

Used equipment and measurement conditions: Low field volume magnetic susceptibility (MS) was measured using the Kappabridge KLY-3S (sensitivity of 1.2·10-8 SI units). The natural remanent magnetisation (NRM) components were measured with the JR-6A or JR-5A spinner magnetometers after each demagnetisation step in order to gain the primary components of the NRM. The relative magnetic field palaeointensity values were calculated as the ratio of NRM value at 20 mT in the demagnetisation field to the anhysteretic remanent magnetisation (ARM) value gained at 20 mT in the demagnetisation field combined with a 0.05 mT constant biasing field. The ARM was imparted to the samples using a AMU-1A device and measured on the spinner magnetometers.

Program for evaluation: OriginPro 7.0, OriginLab Corporation

Expected result: Age model construction based on the comparison of measured data and variations of the relative palaeointensity of the Earth magnetic field in the past. Magnetic susceptibility was expected to be used as a proxy of changes in detrital material (e.g. magnetite) and also for the interval estimation where diatom analysis should be provided with higher resolution (where diatom high abundance was expected).

Magnetic susceptibility of Aral Sea samples was measured directly on the surface of split core halves with a Bartington MS2E sensor (GFZPotsdam) at a resolution of 1 to 2mm (H. Oberhänsli, unpublished results).

5.5. X-ray methods

X-ray diffraction methods (p-XRD, HT-XRD)

Sample preparation: Powdered, homogenized sample was (i) spread to standard non-diffractive plate (p -XRD); (ii) suspended in ethanol and water mixture spread onto a heated support - Pt plate (HT-XRD).

Used equipment and measurement conditions: 1. Siemens D5005 diffractometer (Bruker). Diffractograms were measured in the 2Θ range 2–70° (CuKα) with 20 s counting at 0.02° steps, resulting in a total measuring time of almost 19 h. The content of biogenic silica was estimated

from the height of the extremely broad diffraction (shoulder with width FWHM ~5° in 2Θ scale) centred at 2Θ 22°, as was also done by Fagel *et al.* (2003).

2. Diffractometer PANalytical X'Pert PRO (CoKα, X'Celerator multichannel detector) equipped with Anton Paar HTK16 high-temperature chamber. Analyses were performed between 25 and 300 °C with 5 °C steps in the 2Θ range 4–40° with 0.017° steps resulting in a total measuring time of almost 23 h (for the details on methodology see Grygar *et al.* 2006)

Program for evaluation: X´Pert HighScore, PANalytical B. V.; OriginPro 7.0, OriginLab Corporation

Expected result: Identification and quantification of main mineral phases (p-XRD) including clay mineral mixtures (HT-XRD).

Main advantages of the method: Non destructive (except for HT-XRD), standard method, excellent phase database

Methodical uncertainty: Relatively low detection limit (5%)

Co-workers: P. Bezdička, A. Petřina, T. Grygar

X-ray fluorescence spectroscopy (XRF) - Aral Sea

Sample preparation: We analyzed sediments averaging the core with 1 to 2 cm steps after drying and grinding to analytical fineness.

Used equipment and measurement conditions: XRF spectrometer MiniPal4.0 (PANanalytical) with Rh lamp and energy dispersive detector. The spectra were not recalculated to concentrations and only integral signals in diagnostic Kα lines were processed, namely K, Ca, Mg, Si, P, S, Cl, Ti, Al, Cr, Mn, and Fe. Cl signal is partly overlapped with primary radiation but the Cl content was sufficiently large to characterization its trends within the core.

Expected result: Changes of elements in the core leading to identification of present phases.

Main advantages of the method: Non-destructive, and fast method, small amount of sample is required.

Methodical uncertainty: Used spectrometer cannot identify elements lighter than Mg.

Co-workers: Z. Hájková, T. Grygar

5.6. Radiocarbon dating – Aral Sea

Place of measurement: Poznań Radiocarbon Laboratory, ul. Rubież 46, 61-612 Poznań, Poland

Sample preparation: Depending on the type of dated material. Mollusc shells and organic remains were carefully picked up and washed as was possible. Another carbon rich organic materials were only picked up from the wet sediment and then dried. Ostracod shells were separated using set of sieves, on the sieve 250 μm these shell were concentrated but still mixed together with other organic and inorganic particles. Flow separation and manual separation was then used in order to get only ostracod shells.

Used equipment and measurement conditions: 5 SDH-Pelletron Model "Compact Carbon AMS" ser. no. 003, produced in 2001 by the National Electrostatics Corporation, Middleton, USA. To determine carbon isotopic ratios ($^{14}C/^{12}C$ and $^{14}C/^{13}C$), the AMS machine simultaneously measures number of ^{12}C, ^{13}C and ^{14}C atoms released from cathode earlier produced from the sample (www.radiocarbon.pl).

Program for evaluation: Calibration of radiocarbon ages was performed using OxCal v4 produced by Christopher Bronk Ramsey. For more information about OxCal as well as links to other calibration programs and radiocarbon laboratories please use following website: http://www.radiocarbon.org/Info/.

Expected result: Age of each sample with low error and production of age model of the core C2/2004.

Main advantages of the method: Very little organic material needed (2-50 mg depending on the type).

Methodical uncertainty: Do not trace quite well last 350 years because of repeated fluctuation of ^{14}C within the atmosphere; calibration of these ages is very difficult and often produces several possible results.

EXPERIMENTAL PART
ARAL SEA

6. EXPERIMENTAL PART — ARAL SEA

6.1. Materials—Core C2/2004

The core C2/2004 has been obtained by D. Nourgaliev (Department of Geology, Kazan State University, Kazan, Russia) in 2004 with a Mackereth-type corer (Mackereth, 1958) from Chernyshov Bay in the Large Aral Sea (Figure 16; Nourgaliev *et al.* 2007) within the broader context of EU-INTAS project CLIMAN (2002-2003): Holocene Climatic Variability and Evolution of Human Settlement in the Aral Sea Basin.

The core was sectioned into 5 core fragments with various depths together forming 4.34 m of sediments. Core photo documentation as well as sampling of the core sections (Attachment 2.4) has been done in GFZ Potsdam.

The cored sediment sections consist mainly of bluish, olive, or greenish silty clays intercalated with darker organic-rich muds and occasionally with sandy and gypsum-rich layers of variable thickness (Figure 20). The cored sections are mostly finely laminated except for the organic-poor intervals at core depths 87-104, 125-150, and 210-305 cm, respectively. Mollusc shells and algal remains are confined to organic-rich layers. According to descriptions of the individual core sections, a part of the core representing the interval 214-220 cm is missing.

The core was sampled for biogenic (diatoms), minerogenic (clay minerals), and chemical components by sampling 0.5x1x1 cm of sediment, and VNIR analysis measurement was carried out using 115x228x5 mm large boxes. For VNIR measurement we used raw samples and for other analysis were the samples before processing dried at room temperature and for minerogenic and chemical analysis were grounded in an agate mortar.

Figure 16 From the left: Aral Sea location in Asia, Aral Sea satelite image 2007 and detail to Chernyshov Bay with location of the core C2/2004 and also the most studied core by CLIMAN group

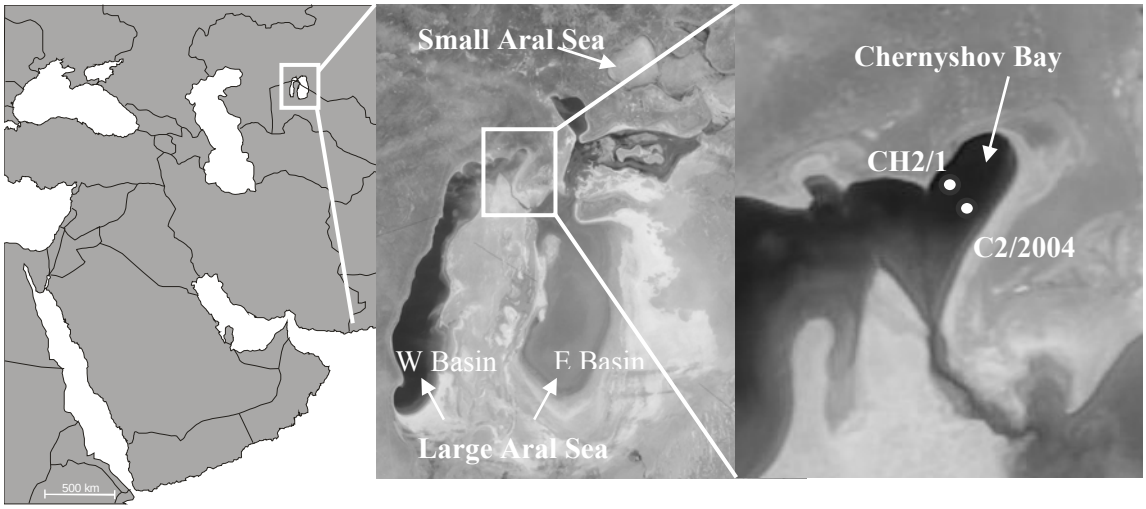

6.2. Results

6.2.1. Chronology

Various types of material (Table 7, Figure 17) were dated in order to get the best age model as possible. The age model is based on dating of shell rich layers. Secondly we dated filamentous algae and other organic remains, including one charcoal (254-256 cm). Two ages from intervals 27-29 cm (Picked organic matter - POM) and 119-121 cm (ostracod shells) are expected to be known during September 2009. The least contaminated material was from mollusc shells because they are easily manipulated and washable. We dated single shell if the weight was sufficient; otherwise we put several shell pieces together and formed a composite sample (316-318 cm). Composite samples were also used for dating plant remains (204, 290-298 cm). The most common contamination was carbonates and clayey matrix that was unsepararable from the dated material although several cleaning steps were carried out. Last obtained data (254-256 cm and 290-298 cm) was at the limit of detection because very little organic matter was found in the interval 210-306 cm.

The AMS radiocarbon ages from recent down to 1820 ±40 years BP plotted versus depth are almost linearly distributed (Figure 20). From our age model we have excluded age from the core depth 254-256 cm that was derived from carbon rich material of unknown origin (Figure 17b). The average sedimentation rate for the topmost undisturbed 3 m of the core is 0.17 cm per year, which is much below sedimentation rates 1.6 to 0.3 cm/y reported by Sorrel *et al.* (2006). The radiocarbon dating of the lowermost about 1 m of the section provided ages of about 5000 years BP (Figure 20). Similar or older ages have been reported from cores retrieved during an earlier CLIMAN field campaign in the western Chernyshov and Tchebas Bay (4860 ±80 y; Sorrel *et al.* 2006; and Oberhänsli, unpublished data). Sorrel *et al.* (2006) confirmed reworking in all horizons with older ages from organic-rich Palaeogene sediments outcropping at the W shore. Based on these previous observations, we could expect that the sediment unit below ~315 cm with radiocarbon ages between 5100-5500 y BP documents phases with intensive reworking of older material from the shore or a major hiatus between the upper and the lower sediment units. From the lithology of the core section (Figure 18) and from observed abrupt changes in most proxy logs at the level of 300-315 cm (Figure 21,Figure 25, Figure 30) we suggest thelatter possibility as more probable. However, we cannot prove this hiatus. Opposite to observations in the core CH2/1

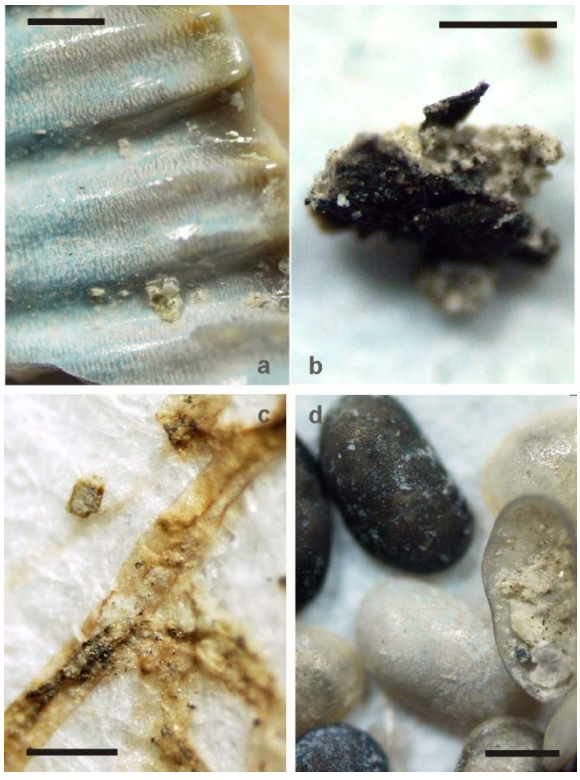

Figure 17 Types of dated material: a) mollusc shell; b) carbon rich material – small charcoal; c) remains of filamentous algae; d) ostracod shells. Scale = 3 mm.

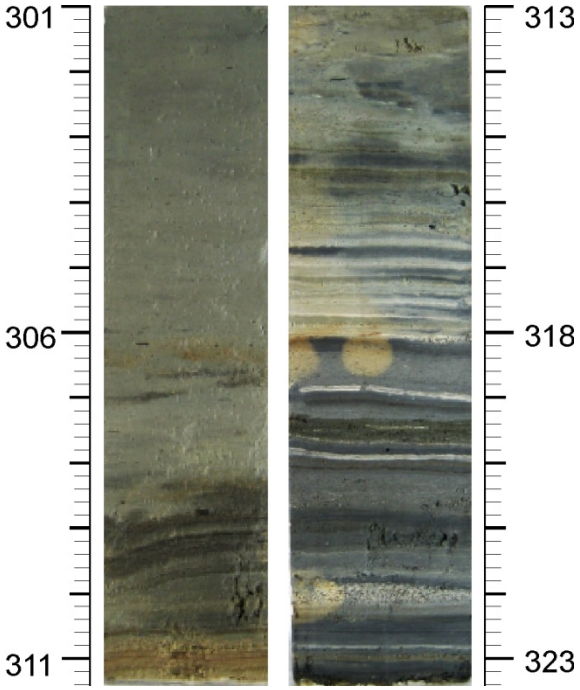

Figure 18 Part of the core part with probable hiatus or the beginning of the contamination by reworked material. Unfortunatelly 312 cm is the end of the fourth core section. Units = cm. Photo taken in GFZ, Potsdam by Kateřina Novotná, 2006; modified by Anna Píšková, 2008.

(they excluded about one third of dates) no reworking could be documented from the upper level of the studied core through. Comparing coring depth and the lithology of cores CH2/1 (Sorrel *et al.* 2006) and C2/2004 (Figure 19) sedimentation occurred in a generally shallower environment and with less steep slope at the shore of the Chernyshov Bay.

We need to keep in mind possible age shift due to reservoir effect as well as due to interpolation in the age model construction. The reservoir effect should be especially important in highly mineralized lakes with changing water level and particularly during low stands (Sylvestre *et al.* 1999). Kuzmin *et al.* (2007) performed a ^{14}C dating of mollusc shells collected alive at the Aral Sea shore in the 1930's and 1940's and subsequently stored in a museum in St. Petersburg. Based on the radiocarbon dates of the molluscs the authors showed that due to the reservoir effect an overestimation of radiocarbon ages of about 130 years should be expected in Aral Sea sediments during high stands. In previous studies of CLIMAN, they dated green algae (*Vaucheria* e.g., Sorrel *et al.* 2006) and did not include any reservoir effect in their age model. We did not observe significant differences between radiocarbon ages derived from mollusc shells and algae collected in the same depth (Table 7). We decided not to use in the text corrected radiocarbon ages for the reservoir effect which are for the comparison listed in Table 7.

Table 7 Radiocarbon ages of the core C2/2004, Chernyshov Bay.
[b] Radiocarbon dates were calibrating using OxCal 4.0.
[c] Corrected ages have had 130 yr subtracted due to a reservoir effect for mollusc shells (Kuzmin *et al.* 2007).
[d] POM, picked organic matter; CARB, organic carbonate (mollusc shells).

Depth [cm]	^{14}C Age [years BP]	Error [1σ]	Calibrated age [b] [AD]	Corrected age [c] [AD]	Material [d]	Lab. no
7.5	112.8 [pMC]		modern		CARB	Poz-20031
11	118.6 [pMC]		modern		CARB	Poz-20032
112-115	775	30	1215 to 1281	1345 to 1410	CARB	Poz-22433
119-121	980	30	993 to 1155	1123 to 1285	CARB	Poz-22920
125-126	915	30	1031 to 1206	1161 to 1336	CARB	Poz-22432
204	1400	30	590 to 670		POM	Poz-24846
207-208	1415	30	584 to 663	714 to 793	CARB	Poz-22431
254-256	3080	70	-1496 to -1136	-1366 to -1006	Charcoal	Poz-29059
290-298	1820	40	85 to 323		POM	Poz-29025
316-318	4875	35	-3750 to - 3538	-3620 to -3408	CARB	Poz-24750
337	4405	35	-3312 to -2913	-3182 to -2783	CARB	Poz-20033
370	4705	35	-3632 to -3372	-3502 to -3242	CARB	Poz-20034
388	4720	35	-3634 to -3375	-3504 to -3245	CARB	Poz-20036

Figure 19 Seismic profiles of coring sites C2/2004 and CH2/1, respectively (D. Nourgaliev, unpublished results).

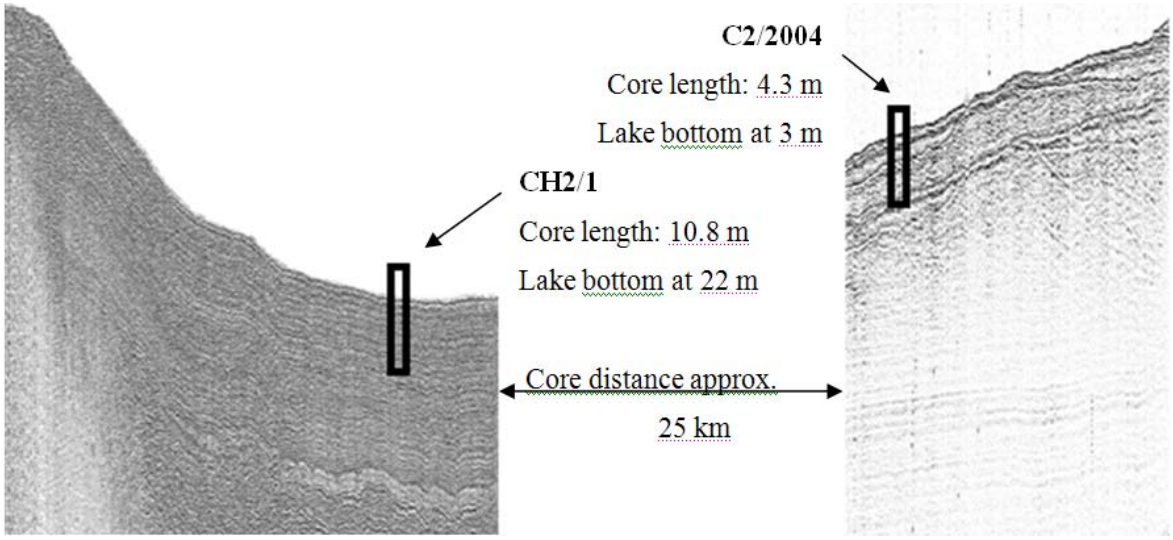

Figure 20 Linear age model up to 2ky with marked radiocarbon data (right side) and simplified core lithology (left side).

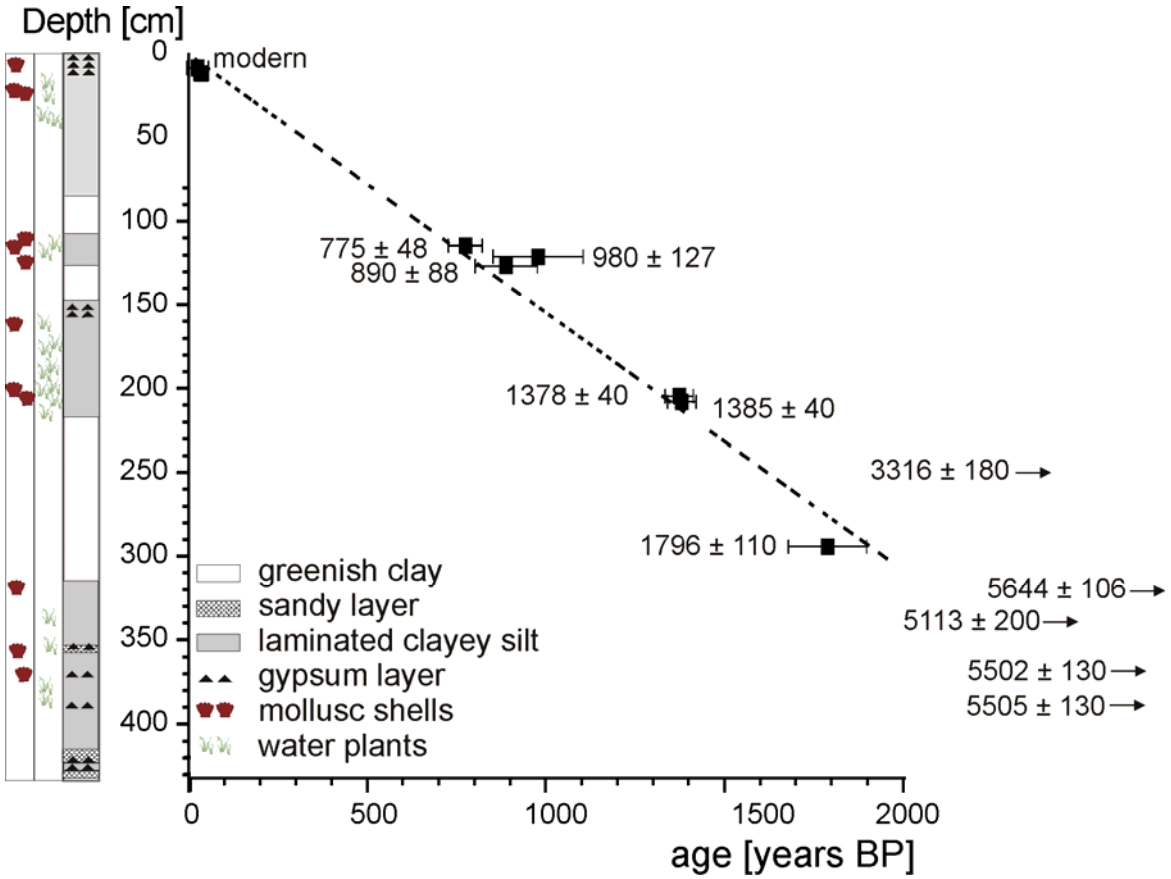

6.2.2. Inorganic sedimentary components

Elemental analysis

We split the elemental data from the XRF analyses into two main groups reflecting their autochthonous and allochthonous origin. Changes in concentration of elements „minerogenic“ elements (Ti, Al, Cr, Mn, and Fe), which reflects abundance changes in allochthonous particles, are shown in Figure 21a. The trend of „minerogenic“ elements have been constructed by normalizing curves of minerogenic elements via recounting them to percent values and then averaged. Potassium concentration also follows the trend of the „minerogenic“ elements approving that illite is a major component of clay minerals in detritus while salt precipitates incorporating potassium are negligible. Si, which is partly fixed in opal of biogenic origin, follows the „minerogenic“ trend except between 58 and 110 cm (Figure 30). The trend of „minerogenic“ elements resembles independently produced CEC changes, which is not surprising as high total concentration of minerogenic elements as well as high CEC values traces the increased detrital components. Their dominance is interrupted by a few discrete intervals with abundant allochthonous precipitates which lower the CEC values (Figure 30).

Elements of the second group (Ca, Mg, Cl, S, and P), shown in Figure 22, are typically enriched in autochthonous precipitates, which cluster in discrete levels. From XRF data, it was possible to identify main chemogenic precipitates. The elemental analysis by XRF completed the information previously obtained by CEC, VNIR, and XRD. The most common chemogenic precipitates were carbonates. The interval 292-311 cm is enriched in Mg-carbonates (e.g. magnesite, huntite) and/or epsomite ($MgSO_4$) that appeared with gypsum layers in the rest of the core (see below). Calcite and/or aragonite are present in increased concentrations at core depths 44-68.5, 113-165 and 275-320 cm. We spotted also sulphates: two massive gypsum layers are located at the core depths of 0-20 cm and 147-158 cm and than in the lowermost part of the core in 353, 368, 388, and 420-424 cm. The VNIR absorbance maximum at 1445 nm considered to reflect the band of gypsum (VNIR pattern; Figure 22) shows more than mentioned layers indicating that besides gypsum other salts are present and contribute to the same band. We checked these intervals (14-54 cm and 103-124 cm) with p-XRD (not shown) and together with XRF, neither Mg nor K but Cl is increased in these depths. We hence concluded that these intervals are rich in halite.

Phase analysis

The sediments consist of clay minerals (chlorite, illite, kaolinite, and smectite), quartz, halite, calcite, and aragonite, gypsum and other salts. The ratio between autochthonous and allochthonous components within the core is very variable (see the intervals of enhanced chemogenic precipitation - Figure 30, and intervals rich in organic remains - Figure 20). Based on HT-XRD data we found smectite to be the most common expandable clay mineral in the sediments of the core C2/2004. These results are in agreement with previous analyses reported by Zhamoida *et al.* (1997). DRIFTS analysis confirmed that the siliciclastic detrital components, mostly clay minerals, are diluted by organic material, carbonates, and gypsum, as documented by low CEC values and XRF results.

Figure 21 "Minerogenic" elements analyzed by XRF.

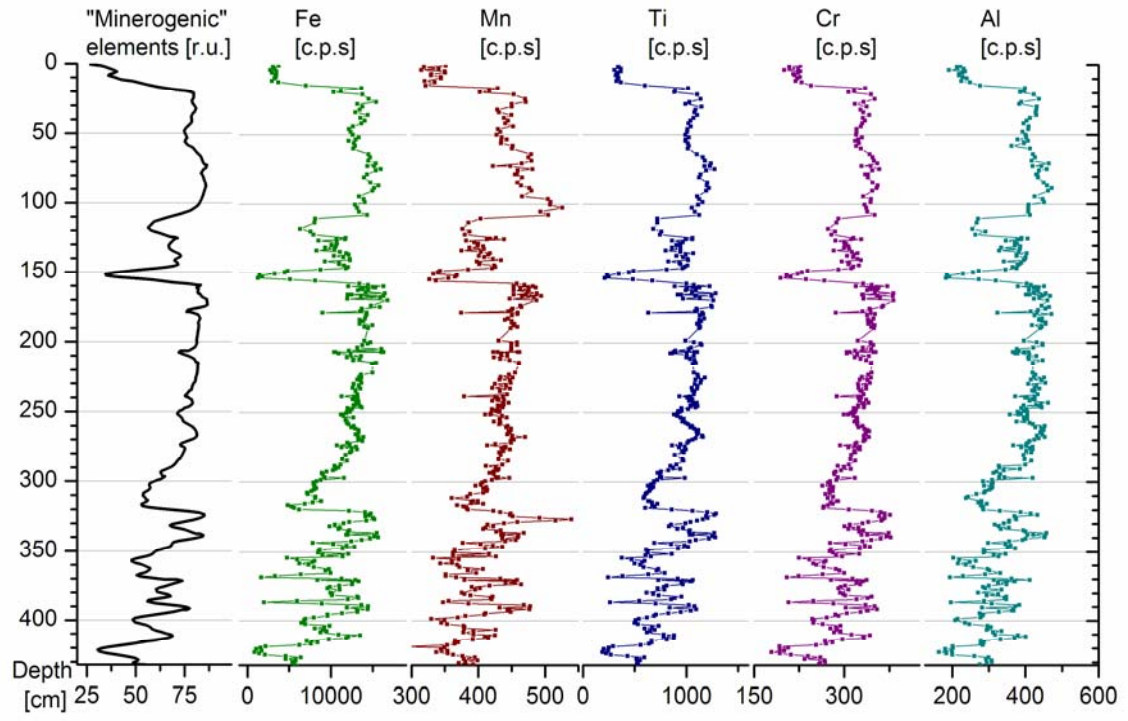

Figure 22 Major precipitates formed within the core: Cl most probably represents halite, Ca represents calcite and/or aragonite (after theoretical gypsum is subtracted), Mg represents epsomite. Last three plots show gypsum proxies obtained by three independent methods - XRF, CEC, VNIR.

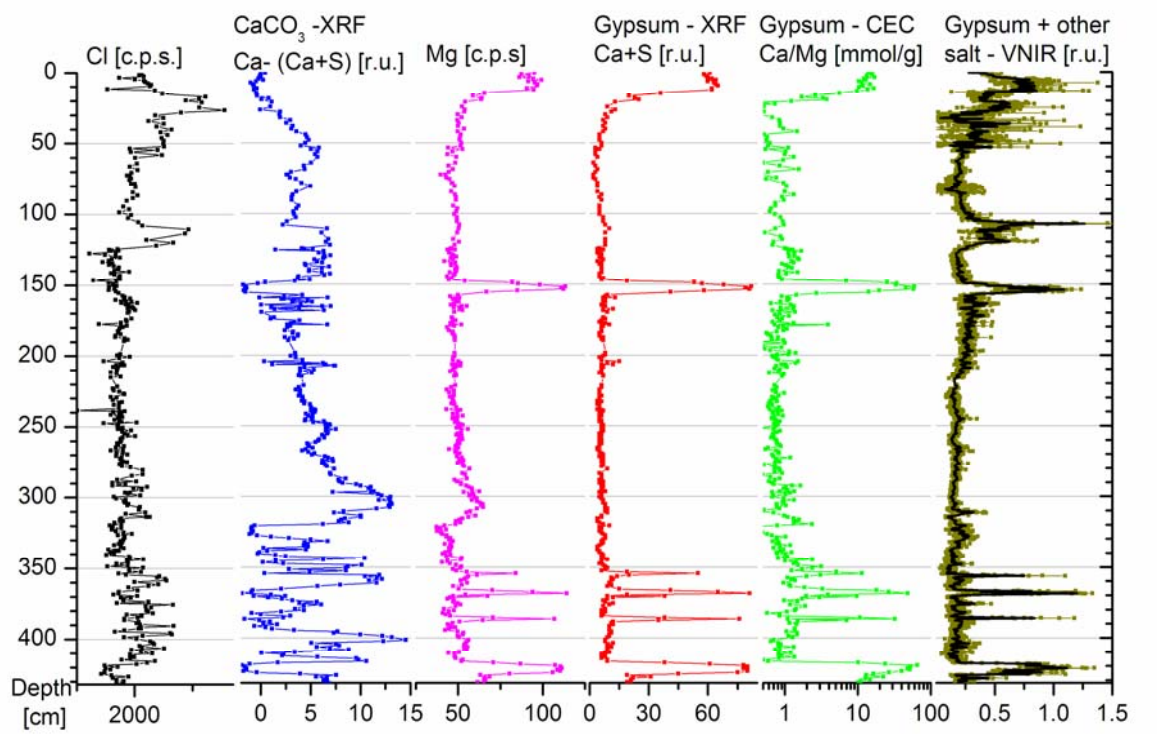

Periods of calcite/aragonite presence appears to be complementary to the trend of "minerogenic" elements. Therefore we suggest that thay are mainly of autochthonous origin. That would be supported by long term HCO_3^- saturation of Aral Sea water (Friedrich and Oberhänsli, 2004; Létolle *et al.* 2005). Some part of the calcite could be also allochthonous similarly as was observed by Maev and Karpychev (1999). We observed (by SEM) many pyrite particles in some samples, e.g. 306-307 cm, that prove the low oxygen periods connected probably with lake meromictic stage as it is observed today (Friedrich and Oberhänsli, 2004).

6.2.3. Organic sedimentary components

We observed several indicators corresponding to the lake biological productivity (i) macroscopically as remains of water plants and mollusc and ostracod shells (Figure 20), (ii) microscopically as diatom concentration, and (iii) instrumentally as variations of chlorophyll concentration (Figure 25) estimated by VNIR spectral scanning.

Carbonatic shells

During sample processing we have found various types of carbonatic shells enriched in different depths. We collect them mainly to get the material for radiocarbon dating; therefore we do not have any quantitative estimation of their abundance within the whole core. Two kinds of shells were found: ostracod and much more common mollusc shells.

Mollusc shells were present in various shapes (Figure 23) corresponding to several mollusc taxa that have been identified according to Fillippov and Riedel (2009). The most massive and the most often used for dating was *Cerastoderma sp.* Unfortunately very often the shells were broken and their identification was not possible, however we produce few points about the distribution of mollusc shells within the core. *Dreissena sp.* occurs in 17-29, and 164-210 cm. Abundance of *Cerastoderma sp.* and *Caspiohydrobia sp.* co-occur in the core intervals: topmost part, 105-126, and 315-330 cm. According to DRIFTS analysis mollusc shells are mainly formed by aragonite.

Ostracod shells have been found especially enriched in 120, and 315 cm. We did not perform their complete objective quantification, e.g., by sieving. We found several colour types of ostracod shells: colourless, almost black, and brown spotted (Figure 17, Attachment 2.5), whereas commonly ostracod shells in Aral Sea are colourless (I. Boomer, personal communication, 2008). We perform EDX analysis of several colour variable shells from

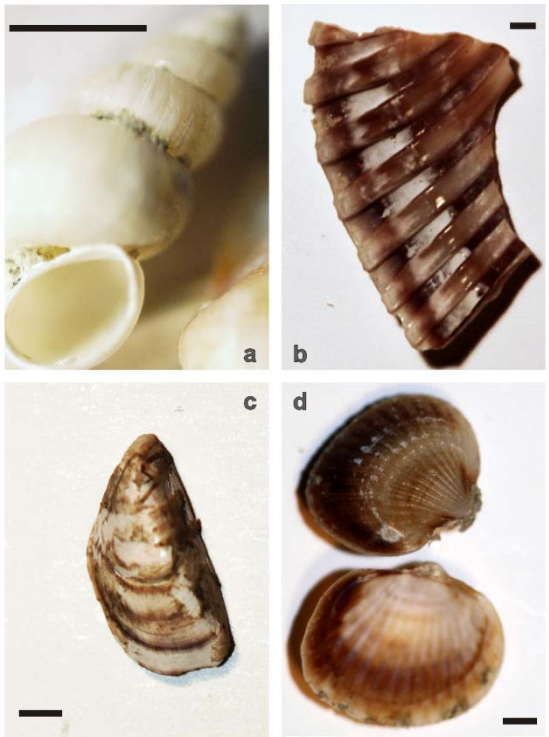

Figure 23 Major types of mollusc shells found in the core: a) *Caspiohydrobia sp.*; b) *Cerastoderma sp.* (most probably *C. rhomboides)*; c) *Dreissena sp.*; d) *Cerastoderma sp.* The scale = 1 mm.

different layers in order to find out the origin of the dark colour. Brownish spots are caused by iron and manganese impurities but the origin of black colour remains unexplained – it is caused neither by high carbon content nor by any metallic impurities unless the colouring layer is thinner than EDX penetration depth. The elemental composition of colourless shell and both sides of black ostracod shells are identical. We did not perform ostracod species identification which could be rather useful and we suggest ostracod analysis as a possible direction of further work for some ostracod specialist.

Plant macro remnants

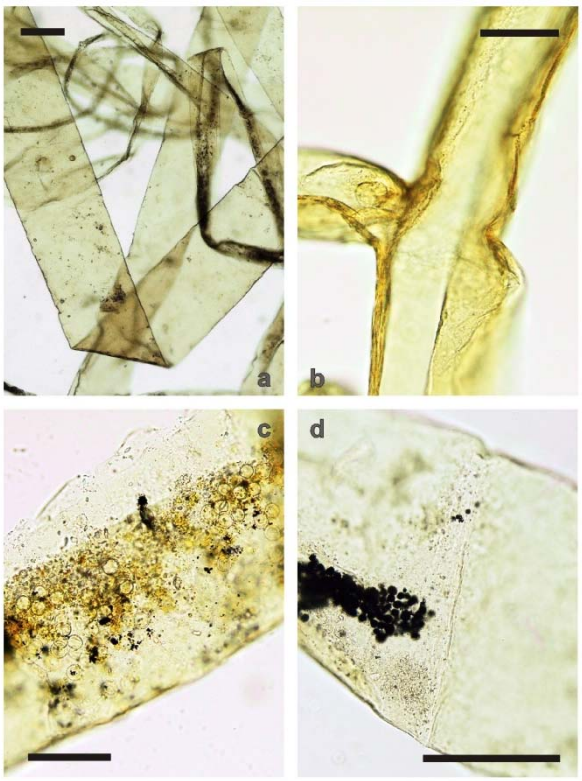

Figure 24 Organic macro remnants: a) cell walls; b) branching; c) *Vaucheria* - like microstructures; d) micro structure - cell divider. The scale = 100 µm.

Present macro remnants are plant fragments accumulated in certain parts of the core where they often set off the lamination (Figure 20). We found mixture of algae and other plant remains, e.g. moss protonema. The most common fragments, also used for dating, has width of about 200 µm, are occasionally branching and remains of pigmentation (greenish, reddish) in some cases even the micro structures of cell walls are still visible. Thank to micro structures (cell divisions) that are not perpendicularly (Figure 24d) oriented we can exclude the algae group (personal communication J. Veselá, Institute of Botany, PřF UK, Praha).

We wanted to know whether *Vaucheira sp.* (algae) that was abundant in Aral Sea in the last 2 ky (Sorrel et al 2006) but also in the last 50 years (Miradbulayev *et al.* 2004) is present in our core. *Vaucheria* spp. is rarely distinguishable in sediments because of poor preservation of needed micro-structures (gametangs). However some remains looking similar to *Vaucheria sp.* (Figure 24c) likely belongs to that group (personal communication J. Veselá, Institute of Botany, PřF UK, Praha). Possible Vaucheria fragments are concentrated especially in the interval 105-125 cm. Present macro remnants most probably belong to plants that live attached to the lake floor.

Chlorophyll and diatom concentration

The diatom concentration with TOC values and chlorophyll abundance match, except in 0-15 cm, where only chlorophyll show higher values, quite well (Figure 25). If we consider these values to be a measure for biological activity, than the lake primary productivity was reduced in the topmost 15 cm, 52-98, 125-150, and 220-300 cm.

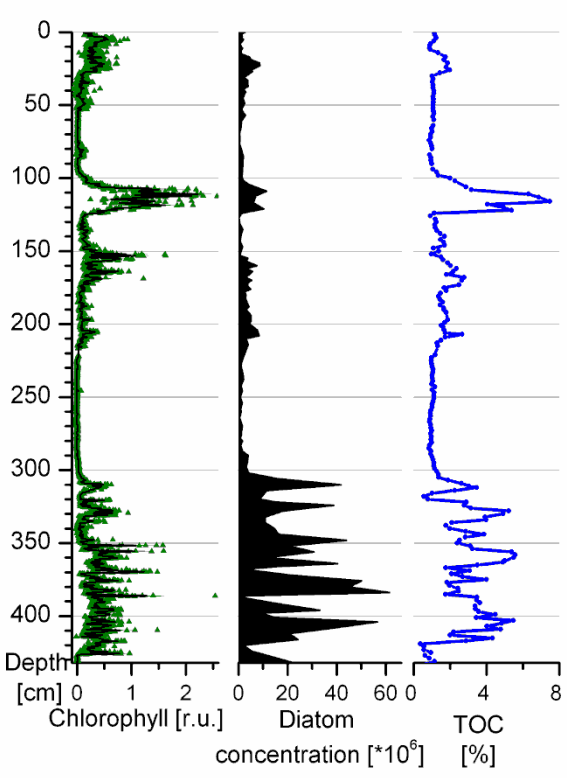

Figure 25 Comparison of chlorophyll, diatom concentration and TOC. TOC was provided by H. Oberhänsli, unpublished results.

We established 11 diatom assemblage zones (DAZ) on the base of changes of diatom concentration and prevailing taxa. List of diatom species is presented in Attachment 2.7. Characteristics and depths of the zones are shown in Table 8 and Figure 29, respectively. The concentration of diatoms ranged between $0.18x10^6$ and $61.5x10^6$ frustules per g. The highest concentrations were observed in the lowermost part of the core (~315 cm to the bottom of the core - DAZ 11). Additionally the species variability was higher than in the upper part (0 to 315 cm - DAZ 1 – 10). Twenty one most abundant diatom species are listed in Table 8. Diatom concentration is generally dramatically reduced in the intervals with gypsum layers.

During periods of low biological activity (DAZ 1, 3, 5, 6, and 8) diatom concentration is below 2.10^6 frustules per g, water plants are missing and the number of mollusc shells is strongly reduced (except for DAZ 1). Importantly in these zones sediment lamination is absent or only faintly visible (DAZ 1, 5). In the topmost zone the lamination could have been disturbed by coring at the youngest, least consolidated sediment.

On the other hand the biological activity is high between 16 and 51, 99 and 124, 151 and 219 and 301 and 432 cm, corresponding to DAZ 2, 4, 7, 9, 10 and DAZ 11 as reflected by gradually growing chlorophyll contents and diatom concentration. Similarly mollusc shells appeared and the amount of the water plant residues increased, which formed well visible lamination in the sediment. Filamentous algae are more common in the layers with the highest chlorophyll concentration (Figure 25). Algae-rich layers with a thickness of 2 mm to 3 cm contain mollusc and ostracod shells at various amounts, size and diversity. They concentrate in the following core sections: 10-35, 144-147, 155-205 cm and are exceptionally enriched in shell remains at depths of 7.5, 11, 53-63, 98-123, and 330-333 cm. The highest concentration of chlorophyll with massive accumulation of mollusc shells, and also a local maximum of the diatom valves (~$10x10^6$ frustules per g) is in DAZ 4. Gypsum is absent in the levels with water plants or shell rich layers.

Diatom assemblage zones

Competition among diatom species always results in a few dominant species whose alternation could be a signal of some environmental change. Environmental categorization of the most abundant diatoms is listed in Table 9. Most of present species are alkalophilous and eutraphentic (Van Dam *et al.* 1994). Diatom species composition between DAZ 1-10 and DAZ 11 is markedly different (). In the upper 3 m of the core the planktonic diatoms with preference to higher salinity environment, *A. octonarius* and *Cyclotella sp.* are dominant. In the lower part of the core smaller mainly tychoplanktonic epontic and benthic species with various salinity demands prevail (*C. placentula, N. sigma, N. fonticola, O. krumbeinii)* (Table 8, Figure 29).

We observed four periods with higher assemblage of euhalobous diatoms (DAZ 1, 4, 6, 8) (Table 8, Figure 29) with following species: *D. smithii* (Figure 26b), *A. octonarius* (Figure 28a), *T. compressa* (Figure 27a), *G. marina* (Figure 26c), and *S. fastuosa* (Figure 27b). The salinity preference of these species is wide. Reported salinity optimum for *A. octonarius* for example ranges from 36 ‰ (Wood 1973) to ~ 100‰ (Sapozhnikov *et al.* 2009) whereas *S. fastuosa* bloomed at salinity 130 ‰ (Sapozhnikov *et al.* in prep.). The crucial role in successive trends plays a replacing of planktonic *A. octonarius* by smaller *T. compressa* (Figure 29, Figure 31) representing probably not only salinity but also water temperature increase and nutrient availability decrease. This succession repeats at DAZ 1, 4, and 7 and in two cases (DAZ 1, 7) it is followed by a gypsum layer; therefore we took it as a base of our salinity trend indicating transition toward hypersaline environment. DAZ 10 (315-298 cm) was the only period with dominant abundance of *G. marina* which indicates warm and highly saline shallow water with low nutrient availability (Munda 2005; Resende *et al.* 2007). *G. marina* is followed by a bloom of *D. smithii* with lower salinity tolerance (Schrader and Gersonde, 1978) together with mesohalobous *T. lacustris* (Figure 26a) (DAZ 9). The most recent part of the core (DAZ 1) is the only period of presence and prevalence of euhalobous *S. fastuosa*.

The transition towards lower salinity (~DAZ 2, 4, 7) was rather rapid in the diatom record and it was evidenced by dramatically lower presence of hypersaline species (the darkest red in Figure 29). The species succession inside the mesohalobous group (Figure 29) representing some environmental change follows the order of *N. frustulum*, *N. digitoradiata* (Figure 28b), *P. salinarum*, *D. bombus* (Figure 28c), *Cyclotella sp., T. lacustris*, and *N. navicularis* (Figure 27c),. Diatom species *T. compressa* and

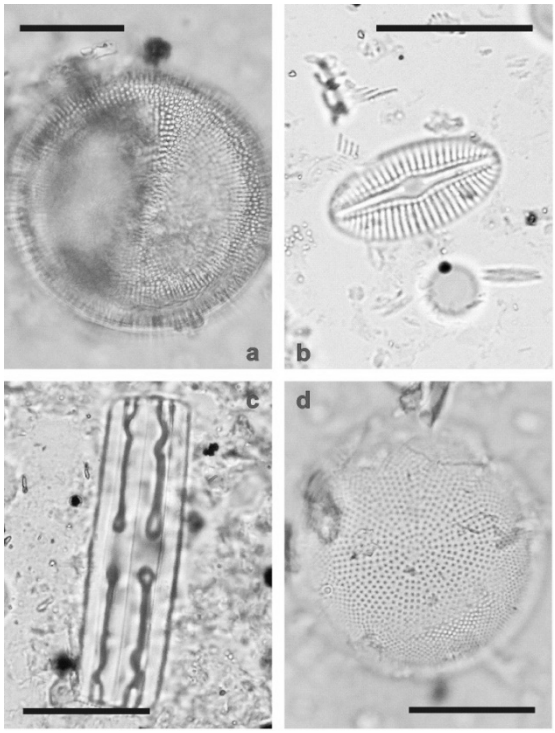

Figure 26 Diatoms from DAZ 9, 10: a) *Thallassiosira lacustris* – typical hemispherically depressed areas on both sides of the diatom centre; b) *Diploneis smithii*; c) *Grammatophora marina* – girdle view; d) *Actinocyclus octonarius*. The scale = 20 µm.

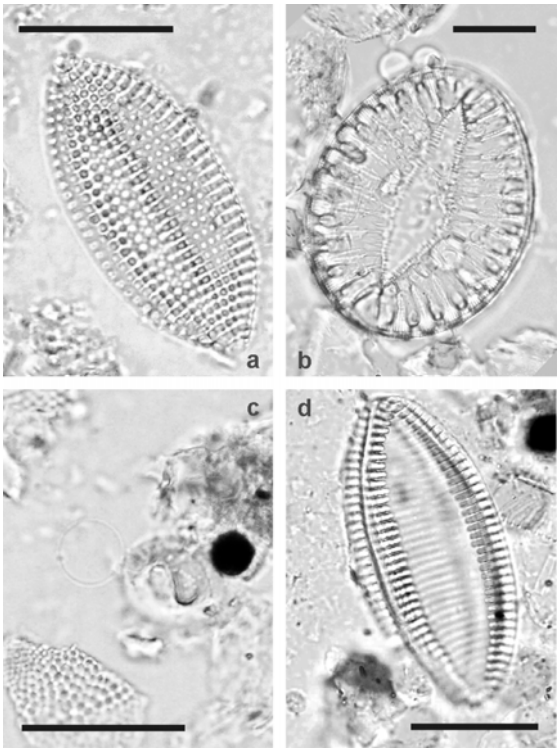

Figure 27 Diatoms representing assemblages occured in low diatom concentration: a) *Tryblionella compressa*; b) *Surirella fastuosa*; c) *Cyclotella choctawhatchaeana*; d) *Nitzschia navicularis*. The scale= 20 µm.

N. navicularis are simultaneously abundant in DAZ 4. It is not clear what their growth limiting factor is in this case, because these species differs by salinity and temperature optimum. *N. navicularis* could indicate rainy or winter period (Resende *et al.* 2007). Abundance of *N. digitoradiata* and *D. bombus* coincide in DAZ 2 and 7.

The periods of the lowest diatom concentration (65-80, 130-140, and 245-285 cm) are often accompanied by high relative abundance of *Cyclotella sp.* and the lowest species variability (not shown). In absolute numbers the concentration of this species are almost the same thorough the core, however relative prevalence of *C. choctawhatcheena* could point to the periods of low nutrients and low silica availability.

Diatoms which are generally known as oligohalobous (*C. placentula, N. fonticola*) (Table 9) and frequently used as low salinity indicators are present in recent Aral Sea with salinity exceeding 100 ‰. We therefore suggest that abundance of these species is limited rather by nutrients than by salinity. *N. fonticola* additionally indicate high oxygenated water (>75% sat.) and low state of trophy (Van Dam *et al.* 1994).

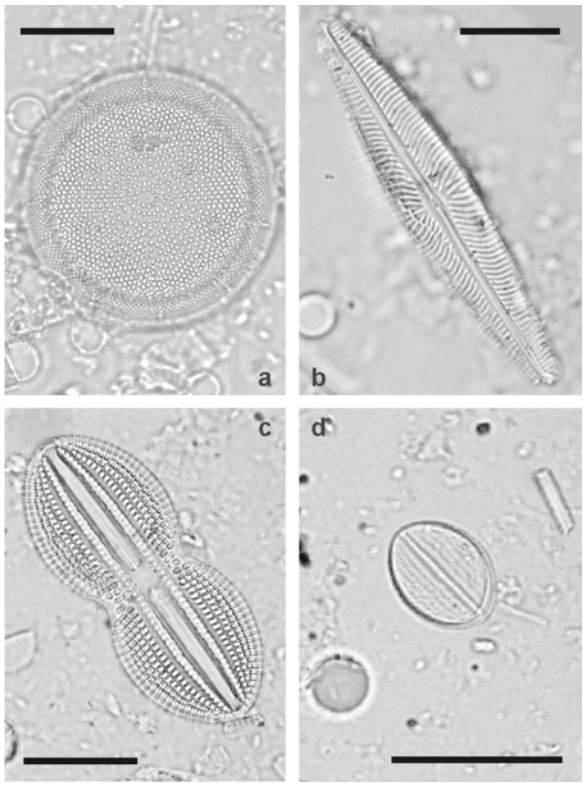

Figure 28 Diatoms representing assemblages occuring in zones with high diatom concentration: a) *Actinocyclus octonarius*; b) *Navicula digitoradiata*; c) *Diploneis bombus*; d) *Cocconeis placentula*. The scale= 20 µm.

Table 8 Diatom assemblage zones (DAZ) with diatom concentration and relative abundances of the most common species. Taxa having 20% or more in any sample within DAZ are classified as dominant (taxa that reached 50% is underlined), taxa having at least 10 % in any sample within DAZ are subdominant (tahta that reached 10 % more than once is underlined). Diatom concentration values: ■ < $3 \cdot 10^6$ frustules/g, ■■ 1 to $10 \cdot 10^6$ frustules/g, ■■■ $10 \cdot 10^6$ to $45 \cdot 10^6$ frustules/g, ■■■■ >$45 \cdot 10^6$ frustules/g

DAZ		DEPTH (cm)	Diatom conc.	DOMINANT TAXA	SUBDOMINANT TAXA
1		0-15	■	*S. fastuosa, A. octonarius, T. compressa var elongata*	*T. compressa, N. navicularis, C. placentula, D. finnica, D. smithii, N. digitoradiata, N. hungarica*
2		17-64	■■	*A. octonarius, D. smithii*	*N. digitoradiata, P. salinarum, D. bombus, N. navicularis, C. choctawhatcheena*
3		65-98	■	*C. choctawhatcheena, N. navicularis, T. compressa*	*A. octonarius*
4		99-123	■■	*A. octonarius, N. hungarica, C. placentula*	*N. fonticola*
5		124-146	■	*A. octonarius, T. compressa, C. choctawhatcheena, N. cocconeiformis*	*D. bombus, N. navicularis*
6		147-152	■	*N. sigma, A. octonarius*	*T. compressa C. placentula, N. digitoradiata, M. braunii*
7		153-227	■■	*A. octonarius*	*N. digitoradiata, T. compressa C. choctawhatcheena, D. bombus, P. elongatum, E. turgida*
8		228-283	■	*C. choctawhatcheena, D. bombus*	*A. octonarius, T. compressa, D. smithii, N. cocconeiformis*
9		284-297	■	*D. smithii*	*T. lacustris, A. octonarius, A. pediculus, E. turgida*
10		298-314	■■■	*G. marina, A. octonarius*	*N. digitoradiata, C. choctawhatcheena*
11	a	316-343	■■■	*O. krumbeii, A. octonarius, D. bombus, N. digitoradiata*	
	b	344-366	■■■■	*N. sigma, C. placentula Cyclotella sp., A. coffeaformis, N. digitoradiata*	*M. braunii, N. fonticola*
	c	367-372	■		*A. octonarius, O. krumbeii, C. choctawhatcheena, G. balticum*
	d	374-385	■■■■	*N. sigma, A. coffeaformis, N. fonticola*	*F. fasciculata, N. frustulum, C. placentula*
	e	386-402	■	*A. octonarius, N. digitoradiata*	*O. krumbeii, Cyclotella sp., D. bombus*
	f	403-417	■■■	*N. frustulum, C. placentula, N. fonticola*	*F. fasciculata, A. coffeaformis*
	g	418-425	■	*Cyclotella sp., N. frustulum*	*A. coffeaformis, N. digitoradiata, N. phyllepta*
	h	426-433	■■■■	*Cyclotella sp., O. krumbeii*	

Figure 29 Diatom concentration and relative abundance of diatoms in DAZ. Figure includes all diatom species that appear with an abundance of >20% on more than one occasion (with an exception of lower concentrated *P. salinarum* and *T. lacustris* whose abundance was markedly concentrated to the one period only). Note the change on the x scale at 300 cm in the plot of total diatom concentration.

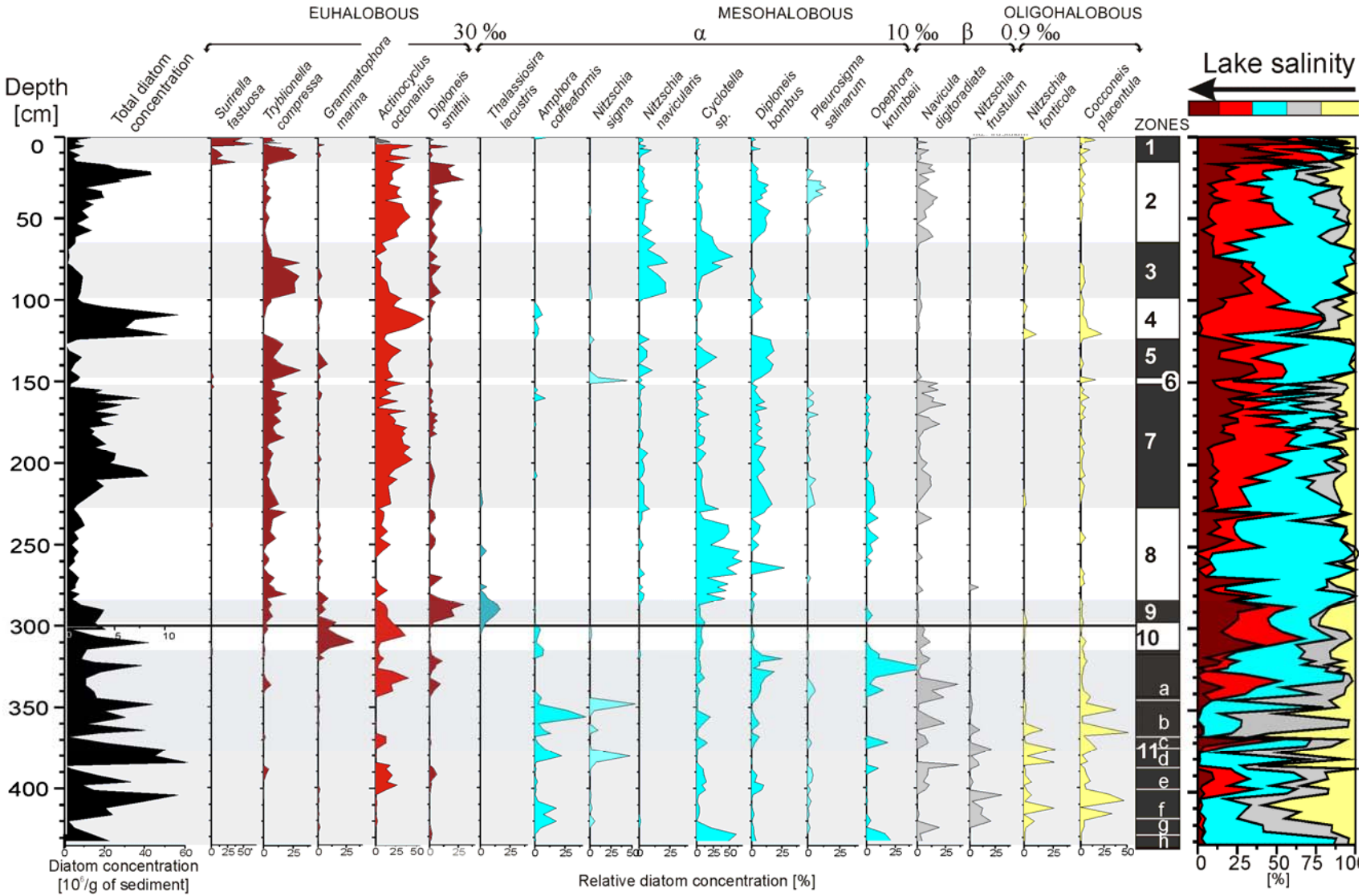

Table 9 Environmental characteristics of the most abundant diatom species. 1 – Witak *et al.* 2006, 2 – Espinosa *et al.* 2006, 3 – Hassan *et al.* 2006, 4 – Horton *et al.* 2007, 5 – Van Dam *et al.* 1994, 6 – Lie *et al.* 1988, 7 – Barnett 1997, 8 – Witak and Jankovska 2005, 9 –Horton *et al.* 2006, 10 – Austin *et al.* 2007, 11 – Hamilton *et al.* 2005, 12 – Schrader and Gersonde 1978, 13 – Sapozhnikov *et al.* 2009, 14 – Aladin *et al.* 2006, 15 – Horton *et al.* 2004, 16 – Melack *et al.* 2003, 17 – Jankowska *et al.* 2005, 18 – Parsons *et al.* 1999, Pestrea *et al.* 2002, 19 – Vos and Wolf 1993, 20 – Laird *et al.* 2007, 21 – Denys 1992, 22 – Korol 2005, 23 – Inda *et al.* 2006, 24 – Zalat and Vildary 2007, 25 – Wilson *et al.* 2005, 26 – Andrén *et al.* 1999, 27 – Hecky and Kilham 1973, 28 – Burić *et al.* 2007, 29 – Stager *et al.* 2003, 30 – Sawai *et al.* 2004, 31 – Munda 2005, 32 – Krivograd Klemenčič *et al.* 2007; 33 – Siqueiros Beltrones and López Fuerte 2006, 34 – Witkowski *et al.* 2005, 35 – Wood 1973, 36 – Wasmundl 1996, 37 – Gromisz and Szymelfenig 2005, 38 – Resende *et al.* 2007.

DIATOM TAXA	LIFEFORM			SALINITY				ADDITIONAL REQUIREMENTS
	Planktonic	Tycho-planktonic	Benthic	Euhalobous	Meso-halobous	β-meso halobous	Oligo-halobous	
A. octonarius	13, 21, 26			1, 2, 35	10			High silica conc.29, sublittoral 35, autumn bloom 36,37, higher amount of nitrates, volatile solids 38, low temperature (optimum ~13.5 °C) 38, 13
A. coffeaformis		3, 13, 21			3, 4, 14			Summer/autumn sp 14
A. pediculus		19	13, 21, 22				1, 5, 14	
C. placentula		3, 13, 21	1	13			1, 4, 5, 6, 9, 18, 19, 20	High nutrients and oxygen 19, 21
C. choctawhat.	13, 21, 26				1, 10, 18			Low silica and nutrients, temp. optimum 8-18 °C 28 Meromicric lakes 20
D. smithii	21		12, 13, 19, 22, 23	3, 4, 6, 8, 9, 18, 19	14, 1	10	26	
E. turgida		22	13	13			11, 14, 22	
F. fasciculata	13				7, 16			
G. marina		13, 24	19	14, 16, 24				
M. braunii		13, 21			5	12		
N. digotoradiata	21	19	13		5, 6, 11	10		Low saltmarsh 25, 30
N. fonticola		21	13, 17, 22				6, 9	High oxygen 5
N. frustulum			13, 17, 27			10, 17	14	High nitrogen27
N. navicularis	21	25	13, 19		7, 15, 19			Tidal flats 25, 30, high amount of volatile solids 38
N. sigma			14, 19, 27		4, 6, 14			
O. krumbeinii	21		1, 13	1	34			
P. salinarum	13, 32				14, 32			
S. fastuosa	21	33	13	13				
T. lacustris	13, 21				14			
T. compressa	21		13, 17, 23	8, 17, 18				Tidal flats 25, 30
T.hungarica		21	3, 13	6	14			

6.3. Discussion

6.3.1. Inorganic sedimentary components

Response to the regression phase in the last 50 years

The lake regression in the last 50 years is well documented: the lake level has fallen by more than 23 m (from 53 m a.s.l., Zavialov 2005), and salinity has increased from 10 ‰ (Mirabdullayev *et al.* 2004) to more than 100 ‰ (Sapozhnikov *et al.* 2009) in the Western Basin. The subdivision of single water body of Aral Sea resulted in separate development of physical properties, i.e. salinity, water level, density, temperature, in individual basins. Salinity values in Western Basin are higher at the lake surface and a minimum they reached at the depth of about 20-25 m of water depth (corresponding to a temperature minimum, Zavialov *et al.* 2009). Chernyshov Bay in the north of the western basin is meromictic. Below a strong pycnocline at the depth of 5 m huge anoxic water body has developed and below 10 m, the water contains hydrogen sulphide (Friedrich and Oberhänsli 2004).

Alkaline chemistry of the lake governs the mineral precipitation sequence with following main minerals: calcite and/or aragonite ($CaCO_3$), gypsum ($CaSO_4$), and halite (NaCl) indicating salinity increase. Schutter and Dukhovny (2003) stated that saturation of the Aral Sea water with calcium sulphate and precipitation of gypsum occur at the salinity level exceeding 25 ‰. However, an extensive precipitation of gypsum takes place at the salinity level higher than 35 ‰. Regarding salinity changes in the last 50 years (see Table 6) the gypsum saturation point was reached after 1985. Recently, gypsum form crusts at many places at the bottom: large gypsum deposits are visible on the lake shores (Attachment 2.2). According to Létolle *et al.* (2005) the lake has already lost most of its calcium in form of calcite and gypsum. Halite, as expected precipitated mineral after gypsum, is mainly coprecipitating with mirabilite ($Na_2SO_4.10H_2O$) that begins to precipitate at salinity of 100 ‰ in winter. Mirabilite often redissolves in summer and is eventually transformed on shores into thenardite (Na_2SO_4). Thenardite is then easily blown away by wind from the exposed shores. Nevertheless mirabilite was never observed in Chernyshov Bay. Halite deposits are in Aral Sea much less common than gypsum (Létolle *et al.* 2005).

Interpretation of variations in the last 2 ky

Based on our results we can see that the core C2/2004 is rich in evaporites (Figure 30). We did not observe their expected sequence of carbonates - sulphates – chlorides. However we have found minerals from these groups separately in discreet layers. We found gypsum to be an indicator of the highest salinity and calcite to be the most common evaporite mineral. Unexpected was a high concentration of halite observed in a documented high stand period (1650-1909 AD) and also in sediments dated to 1190-1330 AD. These periods had the highest organic content. Müller *et al.* (1996) quoted that halite ions could be deposited in sediment with high organic content in anoxic conditions where bacterial decomposition of organohalogen leads to release halite ions. Therefore we suggest that Cl-rich intervals indicate the periods of the presence of absorbable organic halogens rather than low stands (with high halite content). On the other hand, the gypsum rich periods (2000-1870, 1045-970 AD) with a coprecipitation of Mg-rich mineral (also formed in 180-0 AD) indicate periods of increased salinity. As was already mentioned

the gypsum precipitation in Aral Sea has started not earlier than 1980. Therefore we have to interpret our topmost (15 cm) gypsum rich interval (beginning in 1870 AD, according to the age model) either by contamination or more likely by the shift due to the reservoir effect. We have done a correlation between C2/2004 and CH2/1 comparing gypsum layers similarly as it was performed by Le Callonec *et al.* (2005). Our gypsum layer in the period 970-1045 AD can be probably compared with one of the gypsum layers in ~1180 AD (according to Sorrel *et al.* 2007b). This layer can be correlated to the most dramatic lake lowstand of the last 1.6 ky, which occurred at about 1000 AD (according to Maev and Karpychev 1999), in 1200-1300 AD (according to Boroffka *et al.* 2006), and in 900-1350 AD (according to Boomer *et al.* 2008), respectively. The calcite presence can be used as a proxy for changes in chemical properties of water linked to reduced or enhanced evaporation in the surface waters (Sorrel *et al.* 2007b).

Aral Sea regressions were previously very often related to the changes in Amu Darya river flow. Le Callonec *et al.* (2005) described high Fe contents to be chemical fingerprint of Amu Darya inflow (common in regressions older than 3 ky). Whenever the water was rich in carbonates, sulphates and also sodium leading to precipitation of gypsum, aragonite and calcite, respectively, the authors suggest that Amu Darya River has been diverted. Sorrel et al (2007) interpreted variations in Al and Ti within their core as the result of changes in the intensity of aeolian transport. Our variations in Fe, Ti, and Al are in accordance with the simultaneous trend of minerogenic elements (Figure 30). When comparing curves of minerogenic elements and the presence of evaporites we have found that these are complementary to each other. Basically the periods with low amount of evaporites and usually relatively high CEC values can be interpreted as lake level recovery connected with salinity decrease and higher riverine inflow.

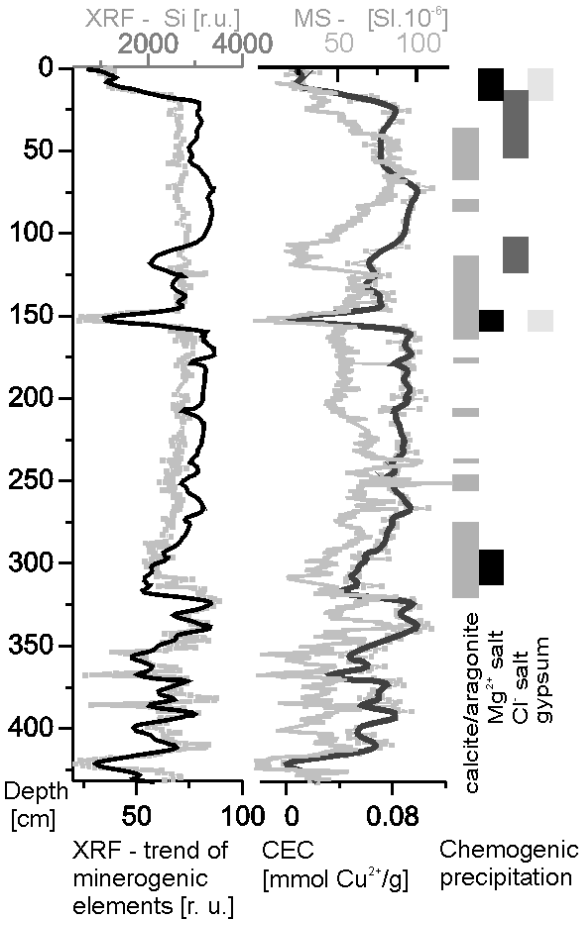

Figure 30 Changes in allochthonous and autochthonous inorganic sedimentary components obtained by XRF, CEC, and MS methods.

6.3.2. Organic sedimentary components

Response to the regression phase in the last 50 years

Several studies on recent diatom assemblages from various parts of Aral Sea have been published. Most authors (e.g., Kawabata *et al.* 1997, Mirabdullayev *et al.* 2004) merely related diatom assemblage composition to salinity as the principle forcing variable. According to Mirabdullayev *et al.* (2004) species diversity and productivity of the biological communities decreased at the transition from oligosaline to hypersaline conditions. Primary productivity limiting factors are variable in time. Aladin *et al.* (1998) stated that changes in the structure of the first trophic level were clearly determined by salinity during the initial stages of regression but later the changes in nutrient concentration, light conditions, coastline formation, and the redistribution of bottom sediments are more important than salinity. Due to high water transparency and shallow depths in the Aral Sea, most organics have been produced by phytobenthos (90% in 1975), and not by phytoplankton - as it is usual in other large water bodies. Dominant phytobenthos species in 1960 were Charophytes (*Tolypella aralica*), chlorophyte (*Vaucheria dichotoma*) and many others. Species variability decreased more than twice till 1995, presently (2002) only *Vaucheria* sp. and *Cladophora fracta* can be found. Reduction of species diversity was observed also in the case of phytoplankton – *Actinocyclus ehrenbergii* (older name of *A. octonarius*): it was dominant in 1960th and later it has vanished being replaced by *Amphora coffeaformis*, *Synedra tabulata* etc. (Mirabdullayev *et al.* 2004). Sapozhnikov *et al.* (2009) provide the most comprehensive study on recent diatom assemblages, including a comparison of water column and sediment samples from many sites. They have found discrepancies between published salinity demands of certain diatom species and their abundance in hypersaline conditions. In addition, they illustrate the importance of water depth for the composition of diatom communities. At 10 m water depth, the large mobile diatom *S. fastuosa* living on the salt crust (almost bare of silt) dominated the assemblage and with increasing depth and silt contents its abundance decreased independently on the temperature and salinity changes in the profile. Increasing amounts of silt may have favoured the small mobile *Nitzschia* species, which became more abundant with depth. The centric diatom *A.octonarius* was dominant in autumn 2003 in anoxic environment at a depth of 24.6 m and abundant up to a depth of 15 m. The relative abundance of *A.octonarius* increased with depth (Sapozhnikov *et al.* 2009).

Distribution and species composition of mollusc shells was also affected by hydrological changes of the last 50 years. For example *Dreissena* spp. was abundant in the late 1960th in all sedimentary depths and around 1980 it disappeared – it can survive salinities up to 20 ‰. On the other hand *Cerastoderma* spp. is not dependent on salinity but it need a soft substrate to filter and usually did not grow below 30 m. *Caspiohydrobia* spp. usually benefits from salinity increase (tolerate salinities at about 80 ‰) and is observed until 1960th in high numbers. However the spatial distribution of this species is closely connected with the distribution of aquatic plants (Fillippov and Riedel, 2009). By the end of 1980th almost all *Ostracod* species in Aral Sea disappeared (Aladin *et al.*1998). These studies allow us to understand better what happened during the last lake regression as well as in the more remote past. However, current analogues for transgressive phases or a stable lake level are not available.

Interpretation of variations in the last 2 ky

The present macro remnants most probably belong to the plants that live attached to the lake floor. Water depth during high stands would be less than 30 m in the place of the coring, which is still sufficient for the light. Water plants occurrence is hence sensitive to water turbidity and probably also salinity increase periods. Ecological interpretations of macro-remains are disabled by their low preservation. High presence of *Dreissena* spp. in our core (1890-1810 and 935-635 AD) could point to lower salinity values within these periods and its disappearance in Aral Sea in 1980 could correlate with last appearance in our core at 17 cm (1890 AD) (see age shift at top of the core discussed in the previous chapter).

The only available study on fossil diatom assemblages in the Aral Sea of the last 1.6 ky was that published by Austin *et al.* (2007). Using a salinity training set derived from the European Diatom Database, they obtained a paleoconductivity reconstruction for a core from Chernyshov Bay about 25 km NW from C2/2004. Their salinity reconstruction was confounded by changes in basin morphology with falling level (Boomer *et al.* 2009). In deposits corresponding to the last 1.6 ky we found much lower diatom concentrations and substantially different assemblages from those reported by Austin *et al.* (2007). They described a dominance of small benthic species (*Amphora pediculus*, *Nitzschia fonticola*, *Karayeva clevei*) which occur rarely in DAZ 1-10 of C2/2004. However, similarities exist between both records with regard to the abundance of large planktonic species (*A. octonarius*, and *Thalassiosira* sp.). The most remarkable correlation feature of these two cores is the maximum of *A. octonarius* concentration centred at the 109 cm in our core, dated at 1290 AD, which correlates with a single maximum of this species shown by Austin *et al.* (2007) at 490 cm (1310 AD according to their chronology). Less evident is the correlation of a high abundance of *Thalassiosira* spp. which is in their core centered at 420 AD and at 115 AD in ours. Nevertheless, given the dating uncertainty these peaks may well be coeval, as well.

Interpretation using (http://craticula.ncl.ac.uk/Eddi/jsp/datasets.jsp) conductivity transfer function similarly to Austin *et al.* (2007) was not possible in our case because the combined salinity dataset that included Spanish, Caspian, North and East African datasets do not correspond with our diatom assemblage. Neither of the datasets includes *A. octonarius* and other diatoms dominant in our core. Only North African datasets contains *N. digitoradiata*, *D.smithii*, and *G. marina* but in the maximum abundance of 5% and less. At the beginning of our interpretation we grouped the most abundant diatoms according to their salinity requirements (Figure 29). Usage of different halobian systems (see Table 5) and more importantly differences in categorization of the same diatom taxa within one system by various authors (see Table 9) aggravated the interpretation.

We have changed our interpretation from salinity inferred in accordance with observations by Sapozhnikov *et al.* (2009) who pointed to the diatom assemblage changes with the high of the water column (Figure 31). This new point of view enabled us to understand why we have such differences in diatom assemblage comparing to Austin *et al.* (2007) – their sedimentary core represents almost by 20 m deeper environment. Therefore such species that occur mainly in water depths of 10 m (i.e. *T. compressa*, *N. navicularis*) could be hardly found in their core. Moreover we have added to salinity and water level requirements also another limitation of growth of

individual diatom species - e.g. turbulence and amount of volatile solids. We can therefore interpret diatom assemblage changes in a more complex way.

Crucial for understanding of the diatom assemblage is the interpretation of the *A. octonarius* abundance. This species is mainly abundant when the sediment contains a very high diatom concentration that point to a relatively low dissolution rate of the frustules within the water column. Although *A. octonarius* is a marine diatom it was a dominant species in the Aral Sea in 1960 (Mirabdullayev *et al.* 2004). Sapozhnikov *et al.* (2009) observed that *A. octonarius* is abundant in the Western Basin today, but that it does not occur where water depth is less than 10 m and reaches its highest abundance in sediments in a depth of 20 m. Similar observation was published by Wood (1973), who reported preferred *A. octonarius* depth range of 20-130 m. The abundance of *A. octonarius* should also correlate with low oxygen periods which are apparently influenced by mixing dynamics because recently it has been found to survive anoxia (Sapozhnikov *et al.* 2009). Based on the observations of Sapozhnikov *et al.* (2009) we interpret the replacement of *A. octonarius* by *T. compressa* repeated in DAZ 1-2, 3-4, and 7 as a lake level fall. This interpretation is supported by the gypsum layers that occur in DAZ 1 and 7. Period rich in *T. compressa* is then followed by the reduction of diatom concentration and a relatively high abundance of *Cyclotella spp*. (DAZ 3 and 5) and *S. fastuosa* (DAZ 1). The bloom of *S. fastuosa*, which we captured in DAZ 1, was reported by Sapozhnikov *et al.* (2009) in the last decade. This observation confirms that the topmost part of our core represents the most recent period of sedimentation.

Figure 31 Total diatom concentrations and concentrations of *Tryblionella compressa*, *Actinocyclus octonarius* and *Cocconeis placentula, respectively,* compared to simplified core lithology (dark triangles = gypsum layers, white rectangles = absence of laminations) and CEC results plotted against depth and age. Low lake-level periods are shaded and, for comparison, chronology of the regression phases by Boomer *et al.* (2009) are ilustrated on the right side.

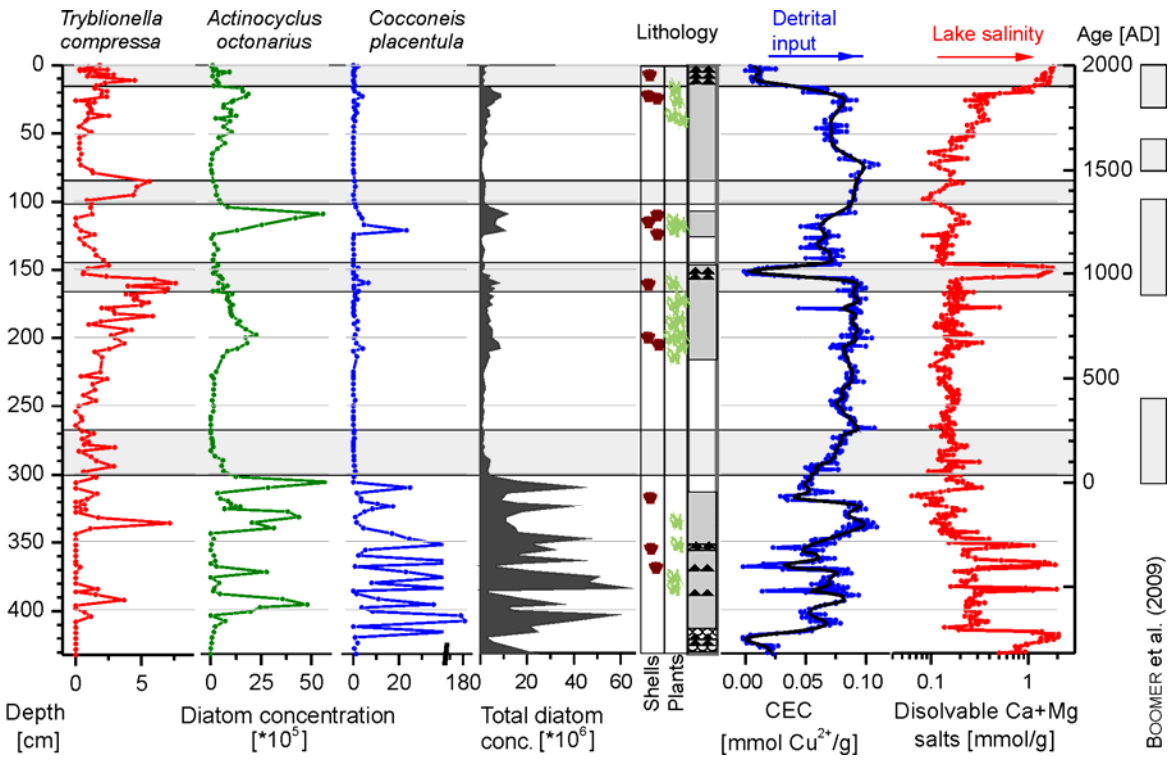

The lake level regressions associated with the succession *A. octonarius* to *T. compressa* and *S. fastuosa* resulted in following periods: 1900-2000, 1330-1450, 910-1060, 0-250 AD (3σ error ~100 years). Non-laminated sediments with low diatom concentrations and usually high CEC values were interpreted as major lake level transgressions.

6.3.3. Interpretation of water level variation

Period ~3000 B.C. (DAZ 11)

Environmental reconstructions based on pollen and archaeological data suggest that the Younger Dryas was featured in Central Asian deserts by colder winter temperatures, cool summers and greater aridity. Arid conditions changes during global Holocene optimum, locally known as Liavliakan pluvial around 6 ky BP, when the annual precipitation in this region was three times higher than at present and the desert landscapes were possibly entirely replaced by mesophytic steppes, with well developed forest vegetation along the river valleys. A general trend of aridization that started approximately 5000 years B.P. was interrupted by multiple minor climatic fluctuations in this region at a finer temporal scale (Lioubimtseva *et al.* 2005). Aridization of tropical and subtropical regions was in this period typical for large areas all over the world, e.g. Sahara region, South America (Acot 2005).

We believe that the sediments between ~315 cm and 432 cm represent continuous sedimentation from the period of ~5-6 ky BP. The change in the diatom assemblages below and above the possible hiatus in core C2/2004 is an proof of a substantial difference in the lake conditions in the last 1800 years and in the period ~5 ky BP. Higher diatom concentration and larger species variability during DAZ11 in comparison with DAZ1-10 could mean larger past availability of nutrients, lower salinity, and/or more available niches - in such case the lake must have been larger than in the last 2 ky. Similarities of diatom assemblages of DAZ11 and CH2/1 (Austin *et al.* 2007) could also lead us to the conclusion that our core must have been in deeper environment (such as now is CH2/1). The idea of Large Aral Sea during the Holocene optimum with the highest lake terrace of 72 m a.s.l. as was proposed by Boomer *et al.* (2000) was recently inspected by Reinhardt *et al.* (2008) and described in detail in Boomer *et al.* (2009). From geomorphologic evidences of these works can be concluded that Aral Sea water level during Holocene have probably never been higher than 55 m a.s.l. with the modelled highest potential water level of 65 m a.s.l. Higher water level would trigger overflow into the Caspian Sea (Boomer *et al.* 2009). However, the Aral Sea connection via Uzboy valley with Caspian Sea and therefore major high stand of Aral Sea is estimated from mollusc shells to the period from 5800 to 5250 BP (Leroy *et al.* 2007). Taking into account also tectonic instability of the region with uplifting rates up to 12 mm/year (Nurtaev 2004) and conclusion of Létolle and Mainguet (1993) that recent 72 m a.s.l. terrace have been in past tectonically uplifted of about 15-20 m the explanation of observed diatom assemblages is obvious. Aral Sea bottom was probably filled or may be even overfilled in the period of ~ 5 ky BP with the water level corresponding to recent 72 m a.s.l. (that time level ~ 55 m a.s.l.) but Aral Sea basin was about 15-20 m deeper than now. The three thin gypsum layers alternating with the clayey sediment with relatively high abundance of freshwater diatom species (Figure 29) could indicate that the overall chloride based salinity of the lake was much lower than today but gypsum was close to saturation at any lake level variations.

Period of hiatus ~3000 – 0 BC

Assuming presence of hiatus in the studied core C2/2004, there are two possible explanations of its origin. The lake level could fall below the level of the coring site in Chernyshov Bay and the older sediment has been removed by sheet wash erosion. Which would mean that the lake level was at least 3 m lower that today's if not influenced by tectonic; alternatively a tectonic movement or mass flows proceeded. Discontinuity in the same period was found in core CH2/1 also from Chernyshov Bay (Sorrel *et al.* 2006).

Post-Antiquity lake level minimum up to 250 AD (DAZ 9, DAZ8) and lake recovery - 250-525 AD (DAZ8)

Several authors confirmed that the most marked regression of the last few millennia occurred in the 0-4th century AD (Maev and Karpychev, 1999; Boomer *et al.* 2000, 2008; Boroffka *et al.* 2006) that timing is coeval with climate worsening after roman climatic optimum (Acot 2005). Maev and Karpychev (1999) estimated that the lake water level was ~20 m at maximum in that lowstand that would be about 10 m below recent water level resulting definitely in drying up our coring site (see the previous paragraph). Persistently growing but still low detritual input and increased concentration of calcite, aragonite, and other autochthonous minerals in the connection with high abundance of mainly euhalobous diatoms with succession mentioned in results proves slow rising of the water level from very low with simultaneous salinity decrease. Reconstruction of paleotemperatures for the whole Tibetan Plateau (Yang *et al.* 2003) resulted in rapid temperature fall from 200 to 300 AD and till ~500 AD temperatures remained much cooler than during the Little Ice Age. The cooling was evidenced by major glacier advance in Tien-Shan from 100 BC to 300 AD (Savoskul and Solomina, 1996) and in Western Tibetan Plateau in 300-500 AD (Yang *et al.* 2008). Cold climate could lower the meltwater formation in the upper course of the Aral Sea tributaries. During this period, it is believed that discharge from the Amu Darya was limited with much of the flow being diverted along old river beds and irrigation channel towards Lake Sarykamysh (Létolle *et al.* 2002 in Boomer *et al.* 2009). Above the hiatus (in DAZ11), the sediment bears signs of a stepwise onset of riverine input, stable lake hydrology with less pronounced stratification and less saline water according to both inorganic and biogenic proxy records. The biogenic and chemogenic input to the sediment was extremely low. Ancient Greeks called the Amu Darya the Oxus and the Syr Darya the Jaxartes. They were thus familiar with the area. However, they never mentioned the Aral Sea; probably because the lake was very small (UNESCO 1999). The extensive irrigation activities of the Persians that have been initiated in the 7th - 5th centuries BC along the Amu Darya and the Syr Darya are known up to 4th century AD (Boomer *et al.* 2009).

Pre-Medieval highstand/stagnation - 525-910 AD (DAZ7)

Our results clearly indicate during DAZ 7 stable and high riverine input with low biogenic and chemogenic sediment components. The lake sediment had still very large detritus input but at the end of the zone gypsum concentration started to appear in very thin laminas and water plant remnants were abundant. Sorrel *et al.* (2006) identified one of the longest and most pronounced low-salinity episodes from the last two millennia between 400 and 900 AD that corresponds also

with our increasing of *A. octonarius* with a local maximum at 190 cm (about 765 AD) pointing to the high water level.

Early Medieval regression - 910-1060 AD (DAZ7, 6)

The zone contains the prominent 3 cm thick gypsum layer, very low detritus and high chemogenic sediment component, in the latter stage (DAZ5) with much enhanced biogenic component. Lake level lowering was indicated by diatom analysis. During the early part of the whole period (800-1150 AD) glaciers advanced in Himalayas (Yang *et al.* 2008). Tien-Shan glaciers advanced a bit earlier at 700-900 AD (Savoskul and Solomina, 1996), but their enhanced melting followed in the period of Medieval Warm Optimum, i.e., enhanced input of meltwater should have entered to the lake tributaries. This is quite contradictory to the timing of the Early Medieval regression. Boomer *et al.* (2008) dated the regression to 900-1350 AD and attributed it to the climate change. Its timing coincided with the Medieval Warm Optimum when an increased evaporation due to warming can be expected in the entire Aral depression in that time. According to Le Callonec *et al.* (2005) the regression phase started at ~1030 AD in connection with Amu Darya river flow displacement into the Sarykamysh depression. On the other hand, this avulsion could also be the effect and not the reason of the local climate change. Sorrel *et al.* (2007b) found increased aridity in the Aral Sea basin in period 900-1200 AD, and this fact that could not be explained by Amu Darya avulsion.

Medieval lake recovery - 1060-1200 AD (DAZ5), and highstand 1200-1330 (DAZ4)

There was evident increase of the *A. octonarius* presence and the decrease in the lake salinity since the start of this zone. Diatom composition also suggests high nutrient availability, probably related to the increase of the detritus input to sediment started at the bottom of the zone. The lake transgression was similar as in the Post-Antiquity period as follows from similarity of the sediment character. Decrease in the lake salinity was also proven by dinoflagellate (Sorrel *et al.* 2006) and diatom analyses (Austin *et al.* 2007) after 1300-1350 AD, with low salinity period lasting to 1500 AD (Sorrel *et al.* 2007a). Increasing moisture and warm climate was also evidenced by the plants in the lake watershed (Sorrel *et al.* 2007b). Temperature maximum was found in period from 1200 to 1400 in Tibetan Plateau connected with a glacier regression (Yang *et al.* 2008). Two important events around a year 1220 AD have been evidenced. First was the destruction of irrigation systems by Mongol invasion (Létolle and Mainguet 1993) and second was the major earthquake (Boomer *et al.* 2000) both these events resulted in Amu Darya discharge into Aral Sea. 1320 was a period of Wolf solar activity minimum (Bard *et al.* 1996), while the solar activity was high in the preceding several centuries.

Late Medieval lake regression 1330-1450 AD (DAZ3)

At the beginning of the zone maximum of *A. octonarius* was followed by maximum of *T. compressa* similarly to the DAZ7 suggesting the gypsum saturation point approach (Figure 31). While diatom assemblage is pointing to the high salinity period, low autochthonous component concentration coeval with high values of CEC would show the opposite. However only during this period Si pattern (XRF) show significant differences from the CEC curve (Figure 30). That means that the ratio of expandable clay minerals and other Si-bearing minerals has been

changed. Sorrel *et al.* (2007a) stated between 1350 and 1420 AD the maximum of aeolian activity. In the maps used by Christopher Columbus (1490), the Aral Sea is not depicted while the Caspian Sea is shown accurately (UNESCO 1999). Shortly after the Mongol invasion irrigation systems and large dams were reconstructed (Boroffka *et al.* 2006) and gypsum bed and Kerderi settlement at an attitude of 32 m a.s.l. occurring during 13th and 14th century was observed. However in the period from 1300 to 1800 most of the lake level reconstruction patterns disagree (Figure 11).

Subrecent lake transgression 1450-1600 AD (DAZ3, DAZ2)

Boomer *et al.* (2009) dated to 1500-1650 AD lake level regression. There were several possible causes of that regression, e.g. avulsion of Amu Darya to Sarykamysh depression south of Aral Sea and decreased temperature in Tien-Shan Mountains at around 1600 AD (Esper *et al.* 2002). The first of three steps of glacier advance in Tien-Shan during Little Ice Age was identified in 1400-1500 AD, and the subsequent ones in 1700-1750 and 1800-1850 AD (Savoskul and Solomina 1996). Old stumps dated to 300 years ago have been found on the recently receded shore (UNESCO 1999). Nevertheless in the sediment of that zone low diatom concentration with the highest CEC values occurred proving the enhanced detritus input.

Subrecent lake highstand 1600-1900 AD (DAZ2) and recent lake regression (DAZ1)

Increase in the lake productivity was found in DAZ2 and high abundance of *A. octonarius* accompanied by high chlorine concentration resembles medieval highstand (DAZ4). At the end of the zone (21 cm ~1865 AD) diatom succession implying lake level lowering (the same to DAZ7 and DAZ3) followed by gypsum layer occurred. About 1690 AD there was the most significant solar activity minimum (Maunder) of the last millennium (Bard *et al.* 1996). We already stated that the topmost part of the sediment core (DAZ1) possibly corresponds to the recent lake level regression known from 1960th. Our interpretation is in agreement to the 19th century (references in Boomer *et al.* 2008) and early 20th century lake level highstand (53 m at 1911 and 1960, Peneva *et al.* 2004). Aral Sea water level was high at least from 1853 (see map in Attachment 2.1) probably until 1961, with secular variations of the water level less than 3 m (Kawabata 1997).

6.3.4. Driving force of Aral Sea fluctuations

The most recent regression of the Aral Sea, which was initiated in the 1960's (e.g., Peneva *et al.* 2004), had possibly two precedents in the last 2 millennia: at the beginning of the first millennium AD and at the beginning of 2nd millennium. Sorrel *et al.* (2007a) obtained a good correlation between the plant response in Aral Sea basin to cold and arid periods and the past Aral Sea lowstands (Figure 32). Boomer *et al.* (2008) assigned the causes of the two past lowstands to climate worsening, possibly enhanced by human activity. It seems obvious that on aridization of the regional climate people were to enhance irrigation causing a positive feedback in the local environment. This was confirmed also by these previous studies, which compared not numerous records of the humidity along the trajectory of the westerly winds from Mediterranean area (the most important humidity source). The past Amu Darya avulsions seem not to play the primary role in the lowstands, or perhaps they were a secondary cause enhancing the climate forcing. Moreover, human presence and irrigation canals in the area are known for 5000 years and during these years there were several low- and high-level episodes (Boomer *et al.* 2000).

Figure 32 Review of forcings that could be linked with Aral Sea lake level lowering.

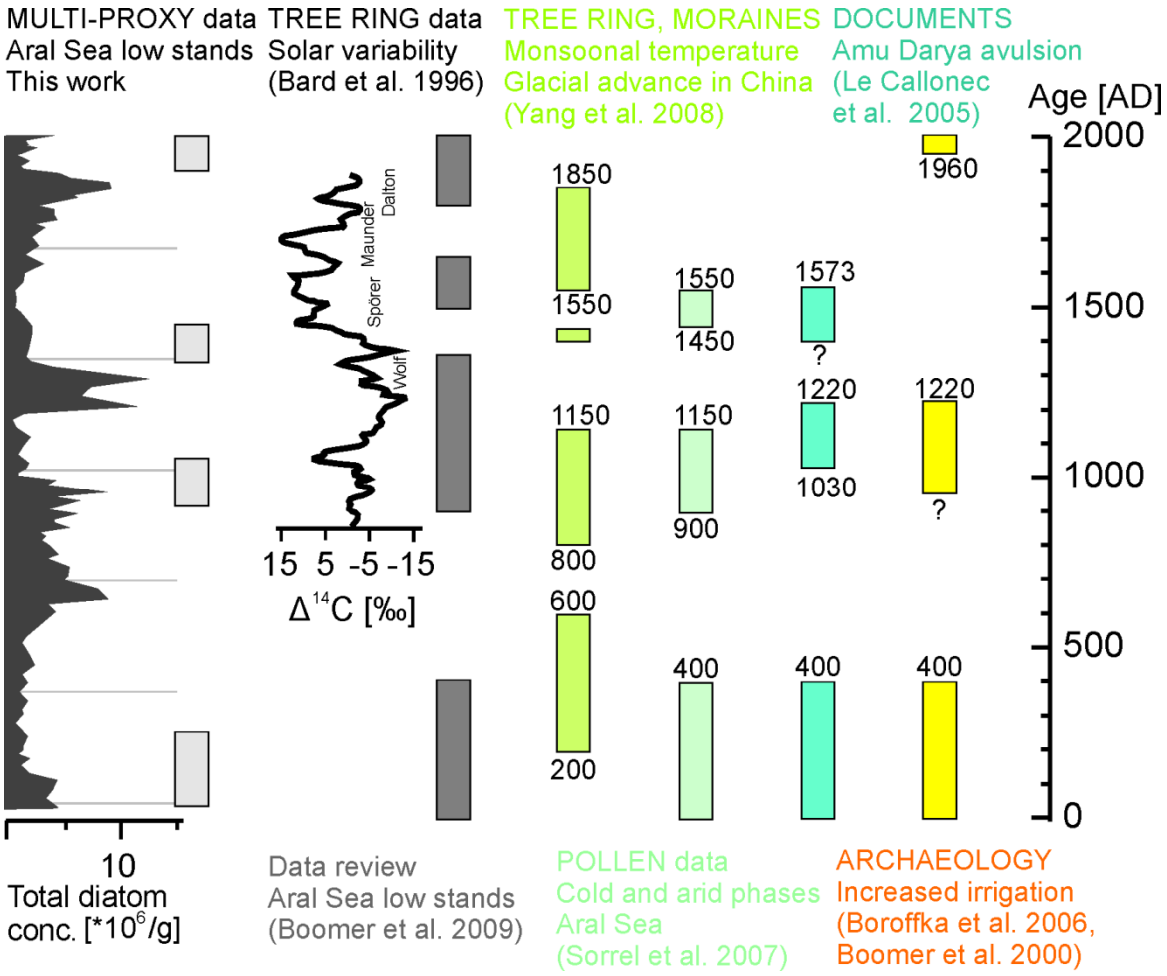

6.4. Conclusions

We proved that radiocarbon dating of mollusc shells is a reliable tool for dating the sediments. We produced the age model comparable with the previous studies (mainly based on picked organic matter) with the differences well within the limit of the reservoir effect and uncertainty of the radiocarbon dating method. Our age model points to a minor effect of reworking of older materials that is confirms that coring site represents a valuable continuous sedimentation archive of at least the last 1.8 ky.

We subjected sedimentary core C2/2004 from Aral Sea to a combination of diatom, clay mineral and salt analyses, and VNIR spectral scanning. It resulted in the characterization of changes of both autochthonous and allochthonous sedimentary components. The best resolution was achieved with VNIR spectral scanning, i.e., about 2 mm, which in combination with the mean sedimentation rate of about 0.17 cm/y, is formally equal to 1 year. A combination of methods always contribute to understanding some yet unexplained features, which are essential to the interpretation story, although in many cases the pattern of different methods seems similar. Especially the combination of organic and inorganic analytical methods is effective because it tells the story on the same environment from complementary points of view and it enables to evaluate the environmental information in a complex, holistic manner.

The interpretation of diatom assemblages using automatic routines (an evaluation software) must be done with a great care and only in cases when majority (at least 50%) of abundant species is reliably incorporated in the database with trustful information on the ecological demands of diatoms. Our diatom record did not fulfil this requirement and, moreover, we have found several discrepancies between the database information and ecological demands of individual species taken from different authors. Our interpretation of diatom assemblages was based on the diatom environmental requirements and the observation of the species within modern Aral Sea. High water levels in Aral Sea were traced by a high abundance of planktonic diatom *A. octonarius*, which needs sufficiently high water column. The lake level regressions were associated with the succession *A. octonarius* to *T. compressa* and *S. fastuosa* in the following periods: 1900-2000, 1330-1450, 910-1060, and 0-250 AD (3σ error ~100 years). All these three diatoms belong to the category with the highest salinity tolerance (euhalobous group) and so their succession would not be assigned to the salinity change using automatic procedures.

Non-laminated sediments with low diatom concentrations and usually high concentrations of siliciclastics were interpreted as major lake level transgressions. Low diatom concentrations disable environmental interpretation of diatom assemblages because their analysis has a low statistical significance; moreover, if the reason of the low diatom concentration was an enhanced dissolution of their valves, the original fossil diatom assemblage could hardly reflect the original situation.

Timings and duration of our lake lowstands have been carefully compared with other published interpretations of the past lake levels. There is an agreement on four major regressions in the last 2 ky, however the generally agreed pattern of past lake level changes is still missing. Our regressions in comparison with various lake level reconstructions appear to be shorter and slightly

shifted toward older ages. There are not many studies on sedimentary cores, in fact only one core have been subjected to multi-proxy analysis as the result of large European project (CLIMAN). Our multi-proxy study therefore provides another step in extending our knowledge on the Aral Sea history. To provide a consistent pattern representing the whole lake development, would be required more experimental work on other cores from different parts of Aral Sea.

We observed diatom assemblages representing a much deeper water column and a less saline environment in our lowermost 1 m of the core, which was radiocarbon dated to the age of about 5-6 ky BP, contrarily to the rest of the core (from 1.8 ky BP to the present time). The deeper sedimentation supports the hypothesis of a tectonic uplift of the whole basin by about 20 m published earlier by Létolle and Mainguet (1993). This uplift would be one the most reasonable explanations of recently discussed questions about the existence of terrace I (72 m a.s.l.) that previously led to conclusions that Aral Sea has been much larger at ~5 ky BP than during any known high level phase in the last 2 ky. We suggest that Aral Sea basin have been deeper by about 20 m but not necessarily larger by area; this would be in agreement with recent geomorphologic models excluding the existence of Aral Sea water level at recent 72 m a.s.l.

Lakes in semi arid climates such as Aral Sea amplifies even moderate changes in the global climate, therefore their water level is often highly variable in time. In addition to this environmental sensitivity, people have influenced the Aral Sea hydrology regime since pre-historic times by using the water of its tributaries to irrigation. We suggest that Aral Sea is not suitable for deciphering of anthropogenic and natural forcings because their individual components, which have operated in this area in the last 5 ky, are hardly distinguishable. Although people have strongly influenced the water inflow by overusing the river water, there are no evidences, that it was the primary forcing factor of Aral Sea variations in the past two millennia.

EXPERIMENTAL PART
BAIKAL LAKE

7. EXPERIMENTAL PART — BAIKAL LAKE

7.1. Materials - Core 98-1-13

Samples for analysis were obtained from pilot and piston cores VER 98-1-13 with a composite length of about 12 m from the Academician Ridge (latitude 53.5618N, longitude 108.0118E) at a water depth of 335 m (Figure 33) (Grygar *et al.* 2006). The core was stored in a sealed Al tube at 4 °C and than sampled using plastic cubic boxes with an inner volume of 6.7 cm^3 (Natsuhara Giken Co., Japan) producing a continuous series of samples with a mean vertical distance of 2.2 cm between the box centres (Grygar *et al.* 2007). Core sampling (Attachment 1) has been provided in Department of Paleomagnetism, Institute of Geology, AS CR, v.v.i. We obtained the boxes filled with sediment after their magnetic analyses for chemical, mineralogical, and diatom analyses in our laboratories. Despite their permanent storage in closed boxes in a fridge, some samples have already dried up and in some cases even their contamination by a recent material has been visible. Therefore for our sampling for biogenic (diatoms), minerogenic (clay minerals) and chemical components we chose yet unopened and not contaminated boxes.

Figure 33 The position of the coring site at Academian Ridge, Baikal Lake.

We composed the photo documentation (only 1122 cm) of the Core 98-1-13 provided in Department of Paleomagnetism, Institute of Geology, CAS, v.v.i. (Attachment 3.1). For lithology of the topmost 6 m see Grygar *et al.* (2006). Complete lithologic description was disabled by having only partly fresh and sampled core material. The material was fine clayey sediment with rare changes in grain size. Colour varied from light greyish-yellow to greenish-brown. The observed colour changes were mostly caused by relative amount of diatoms.

7.2. Results

7.2.1. Chronology

The bottom of Lake Baikal has never been directly affected by glaciations providing valuable uninterrupted sedimentary archive (Mackay *et al.* 2002) covering the Upper Pliocene, the entire Pleistocene, and the Holocene (e.g. Grachev *et al.* 1998). Baikal's mid latitude location in the centre of Asia makes it sensitive to changes in insolation patterns caused by orbital forcings (Peck *et al.* 1994 in Mackay *et al.* 2002). Academician Ridge, where our core was retrieved, is isolated from turbidites and river influence and receives only a slow "rain" of hemipelagic sedimentation. Sedimentation rates on the ridge appear to be remarkably constant (~ 4 cm/ky) (Colman *et al.* 1999). Although the whole area is tectonically active (see chapter 4.2.2) our coring

Figure 34 Left: Age model obtained by orbital tuning (solid line, Grygar *et al.* 2007) and its comparison to a palaeointensity age model developed for the upper part of the core (squares, Grygar *et al.* 2006). Right: Correlation of total diatom concentration correlation with orbital forcings (eccentricity and insolation) that was a base of the orbital tuning and produced age model.

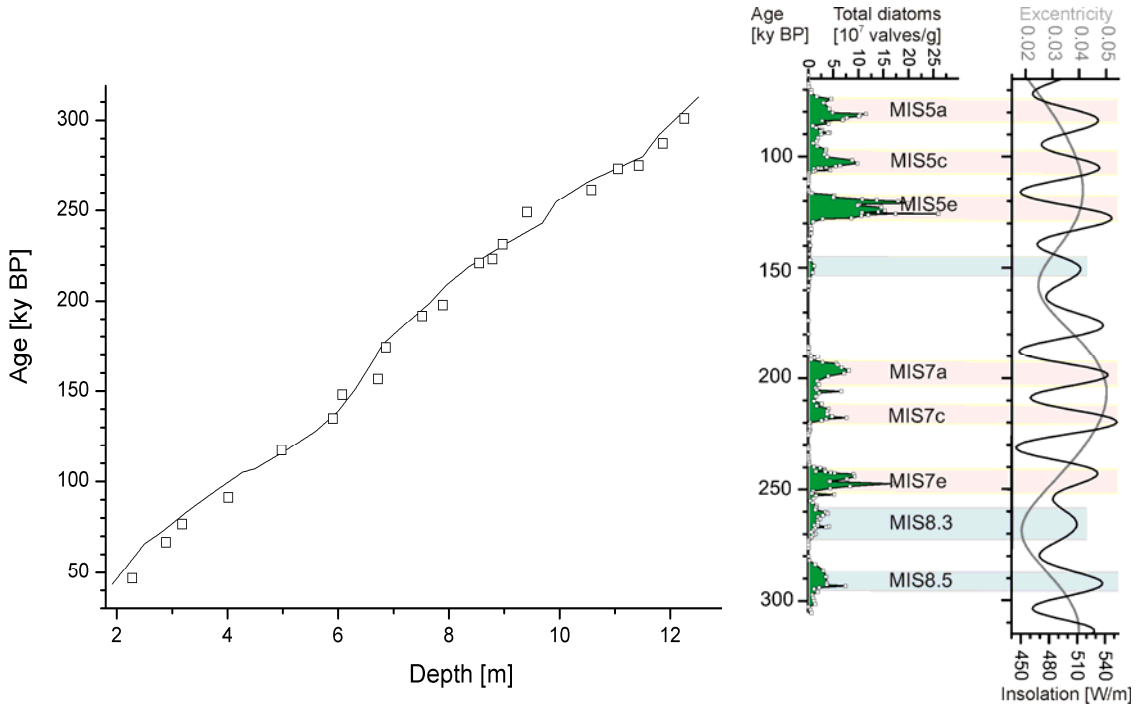

site is undisturbed in the range of top 10 m so our core represents a continuous sedimentary record.

An independent age model was created by correlating palaeoenvironmental proxies to the Northern Hemisphere summer insolation, calculated according to the Berger solution (Berger 1978). Similar technique have been used to derive an age model for the long diatom record from Lake Baikal cores BDP96-2 (Prokopenko et al 2001a) and BDP-96-1 and -2 (Prokopenko *et al.* 2006). The resulting age model for core VER98-1-13 is in good agreement with other cores from the Academician Ridge in which the age model was obtained by comparing some palaeoproductivity proxy to a marine $\delta^{18}O$ records (Peck *et al.* 1994, Fagel *et al.* 2003, Sakai *et al.* 2005). To obtain an orbitally tuned age model during the Brunhess, Prokopenko *et al.* (2001a) tied Northern Hemisphere summer insolation maxima and the onset of the main interglacial (interstadial) diatom booms. The application of the same approach resulted in recognition of 300 ky record in the 12 m of our core (Figure 34). Moreover after building our age model we have correlated diatom peaks of the total diatom concentration with oxygen isotopic stages MIS5a – MIS 8.5. That orbitally tuned model was then confirmed by paleointensity dating (Grygar *et al.* 2007, Figure 34).

7.2.2. Inorganic sedimentary components

Magnetic and spectral methods

Measurements of magnetic susceptibility (MS) and anhysteretic remanence magnetization (ARM) appeared to be very useful because minima of these curves reflecting decrease in the concentration of magnetic minerals point to warmer and/or more humid periods and therefore

the minima can be correlated to interglacial or interstadial periods (Peck *et al.* 1994, Demory *et al.* 2005, Grygar *et al.* 2005, Grygar *et al.* 2006). The most likely explanation for this is enhanced chemical weathering of Fe-bearing minerals, i.e. dark micas and amphiboles, and ferrimagnetic magnetite, in more humid climate. MS (reflecting the sum of ferro-, para-, and diamagnetic properties of the sediments) and ARM (reflecting mainly ferrimagnetic mineral properties) do not display the same patterns over the analysed interval (Figure 35), showing that in some parts of the section the minima of ferrimagnetics are broader than the minima influenced by higher concentration of the paramagnetics. This difference probably indicates that ferrimagnetic minerals are more easily weathered in the Lake Baikal watershed than paramagnetic minerals and/or that some extra paramagnetics are formed by the weathering of ferrimagnetics. Periods with lowered ferrimagnetics and high paramagnetics likely represent periods of moderate chemical weathering (Grygar *et al.* 2007).

The diffuse reflectance electron spectra (DRS) produced three proxies, R_{Vis}, R_{UV}, and B/C. R_{Vis} is the mean reflectivity in the Vis region, i.e. the lighter samples have higher values of R_{Vis}. The main coloured minerals in sediments from the Academician Ridge are amphiboles and dark micas (Grygar *et al.* 2005, Grygar *et al.* 2006), both of which are very sensitive to chemical weathering in a humid climate. There is a good correlation between R_{UV} and total diatoms or biogenic silica (Figure 37), showing that white and highly light-scattering SiO_2 can contribute to the pattern of high R_{UV} in humid/warm climates. R_{UV} is a mean reflectivity at 270 nm, which is inversely proportional to the total Fe (Fe_{TOT} as obtained by chemical analysis) in the sediments; Fe_{TOT} decreased in interglacials or interstadials (Grygar *et al.* 2006). B/C ratios have been shown to be a useful proxy for the oxidation state of Fe in alumosilicates, assuming that only a small fraction of Fe is bound in Fe^{3+} oxides (Grygar *et al.* 2006). This indicator is very sensitive to chemical weathering: if Fe^{2+} bearing micas are weathered to expandable clay minerals only a small fraction of Fe is mobilized while the majority is oxidized to Fe^{3+} and retained in the structure of the alumosilicates. This process is accompanied by a decrease in the B/C ratio. Generally, if all Fe-based proxies change "in phase", i.e. if R_{Vis} increased and R_{UV}, B/C, MS and ARM simultaneously decreased, chemical weathering was highly intensive and *vice versa*.

Figure 35 Inorganic proxies plotted against depth with the approximate intervals of marine isotopic stages (MIS). Even numbers for glacial, and odd for interglacial periods.

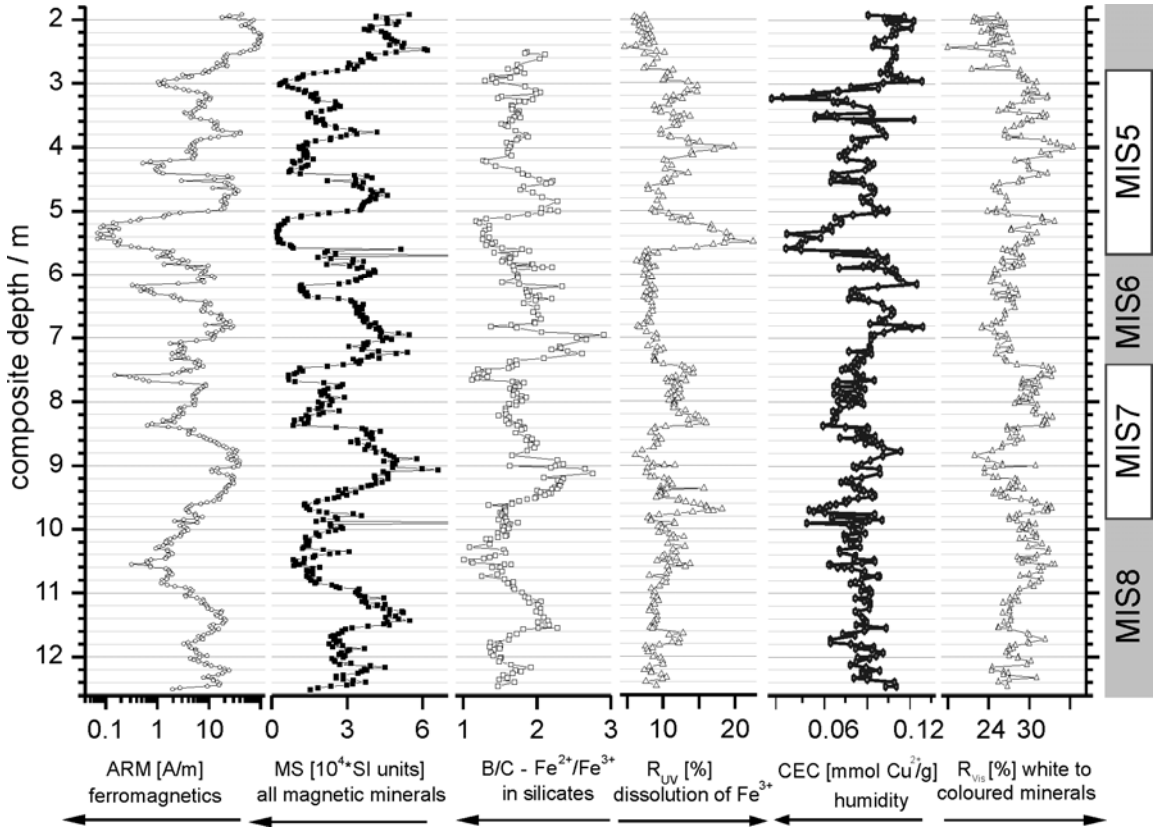

Clay mineral analysis

Clay minerals presence as well as their mineralogical composition are very useful indicators of weathering processes especially important when analyzing clayey rich material as is often the case of lake sediments. We used several methods for characterization of clay mineral content – the results of p-XRD, as a basic method for mineral analysis have been supplemented by high-temperature XRD measurement resulting in characteristics of clay mineral assemblage with resolution ~12 cm. Higher resolution (3.3 cm) has been achieved by fast chemical analytical method (Cu-trien method) tracing cation exchange capacity (CEC). CEC is one of the specific properties of expandable clay minerals, i.e. smectites, vermiculite and inter-stratified clay minerals with expandable components. CEC is directly proportional to the total concentration of expandable clay structures and does not need empirical calibration, as it is required by p-XRD analysis of clay minerals (Yuretich *et al.* 1999, Fagel *et al.* 2003). Contrarily to our initial expectations expandable clay mineral content decreased in a warm/humid climate (Sakai *et al.* 2005, Grygar *et al.* 2005). This pattern is obvious from the comparison of environmental proxies in Figure 35 and it has two reasonable explanations: either hydrolysis (dissolution) of expandable clay minerals is occurring under humid and warm climates in interglacials and major interstadials, or some environmentally controlled shift is occurring in the sediment source area. In any case, CEC minima are located in periods of increased diatom concentration, although not all diatom maxima are coincident with CEC minima Grygar *et al.* (2007).

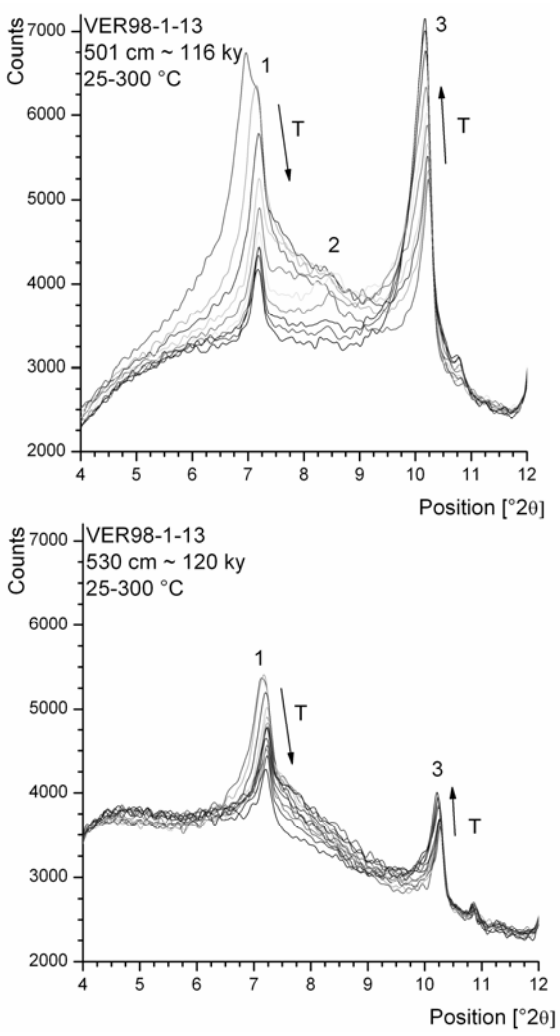

Figure 36 HT-XRD pattern common for samples from cooler (MIS 5d) – top and warmer periods (MIS 5e) – bottom, respectively. Black lines represents shift in temperature by 50 °C.

Bulk mineralogical composition derived from p-XRD show that all the sediment samples consists of quartz, muscovite, feldspars and kaolinite and additionally variable amount of amphibole, illite, chlorite, and assemblage of expandable clay minerals are present.

We have performed in total 30 HT-XRD scans. Evaluation of the HT-XRD is described in details by Grygar *et al.* (2005). All HT-XRD patterns were analysed using deconvolution into gaussians and diffraction line positions, intensities and FWHM have been evaluated. Basically we observed three places of interests in the most important area of 001 basal diffraction lines of clay minerals (Figure 36). Expandable clay mineral (1) with d-spacing 1.49 nm, most probably smectite or smectite rich illite-smectite has typical thermal behaviour of 2 layer hydrated smectite with two dehydratation steps (first ~1.19 nm (2) and second ~1 nm (3)). Next to the (001) of expandable component lies (001) of chlorite (~1.42 nm) and/or vermiculite (d (001) – 14,3). Place 2 (~1.19 nm) represents according to Grygar *et al.* (2005) triplet of thermally unstable phases corresponding to expandable structures, i.e. Mg,Ca smectite, vermiculite, and finally interstratified illite-smectite. Place 3 with d-spacing 1 nm with asymmetrical diffraction line was identified as overlain illite, macroscopic mica, and dehydrated expandable mineral.

The results of HT-XRD show that in periods with enhanced chemical weathering and high diatom productivity, the relative percentage of chlorite increased and micas decreased, showing that the later is preferentially consumed by chemical weathering (Grygar *et al.* 2005, 2007). In stadials and glacials, a well-ordered expandable clay mineral is present; CEC pattern resembles variations in mica content estimated by p-XRD that confirms the inter-layering of illite-smectite and vermiculite (the major expandable clay minerals found by Fagel *et al.* (2003) and Grygar *et al.* (2005) with the parent mica.

Diatom record

We have analysed 222 samples with resolution depending on the sample position in the core. We choose higher resolution where MS was lowest and lower resolution where MS was highest, i.e. at "interglacial" and "glacial" sediments, respectively. By next sampling series we increased the resolution if needed. We have identified 13 most abundant planktonic species mainly from *Stephanodiscus*, *Cyclotella*, and *Aulacoseira* genera. All benthic taxa have been counted together because in most of samples they were not present and if so they form not more than 2 % of the assemblage. For photo tables of identified species and SEM details of some diatom frustules see attachment 3.3, 3.2, respectively. Two types of information have been obtained from diatom analysis, the concentration of total diatom species, and a record of changes in species diversity over time. Changes in total diatom concentrations have a similar pattern to other proxies including magnetic susceptibility, R_{UV}, and the amount of biogenic opal estimated by p-XRD (Figure 35, Figure 37) because diatom frustules increase the content of p-XRD amorphous components and strongly scatter UV and Vis light thus increasing R_{Vis} and R_{UV}. The regression coefficients of correlations between diatoms and the non-biogenic proxies improve in zones dominated by smaller sized *Cyclotella* and *Aulacoseira* species.

Table 10 The most common diatom taxa in the core BDP98-1-13 with their characteristics. Environmental characterization of extinc taxa is based on recent analogues, as reported by Rioual and Mackay 2005.

DIATOM TAXA	Endemic	Extinct	Recent	Favourable growth conditions
Stephanodiscus grandis (Khurs. and Log.)	X	X		Low light conditions, high phosphorus loading, moderate silica abundance – highly silicified, associated with periods of deep mixing in spring.
Stephanodiscus carconeiformis (Khurs. and Log.)		X		
Stephanodiscus formosus (Khurs. and Log.)		X		
Stephanodiscus formosus var. minor (Khurs. and Log.)		X		
Stephanodiscus flabellatus (Khurs. and Log.)		X		
Aulacoseira baicalensis (Meyer) Simonsen	X		X	Offshore waters, spring months, narrower tolerated temperature range.
Aulacoseira skwortzowii (Edlund, Stoermer & Taylor)	X		X	Near shore waters, it blooms under ice cover, winter-spring months, 5-15°C optimum.
Cyclotella minuta (Skv.) Antipova	X		X	Pelagic condition, summer and autumn.
Cyclotella ornata (Skv.) Flower	X		X	
Cyclotella baicalensis (Meyer) Skv.	X			

Figure 37 Comparison of several proxies that traced diatom presence.

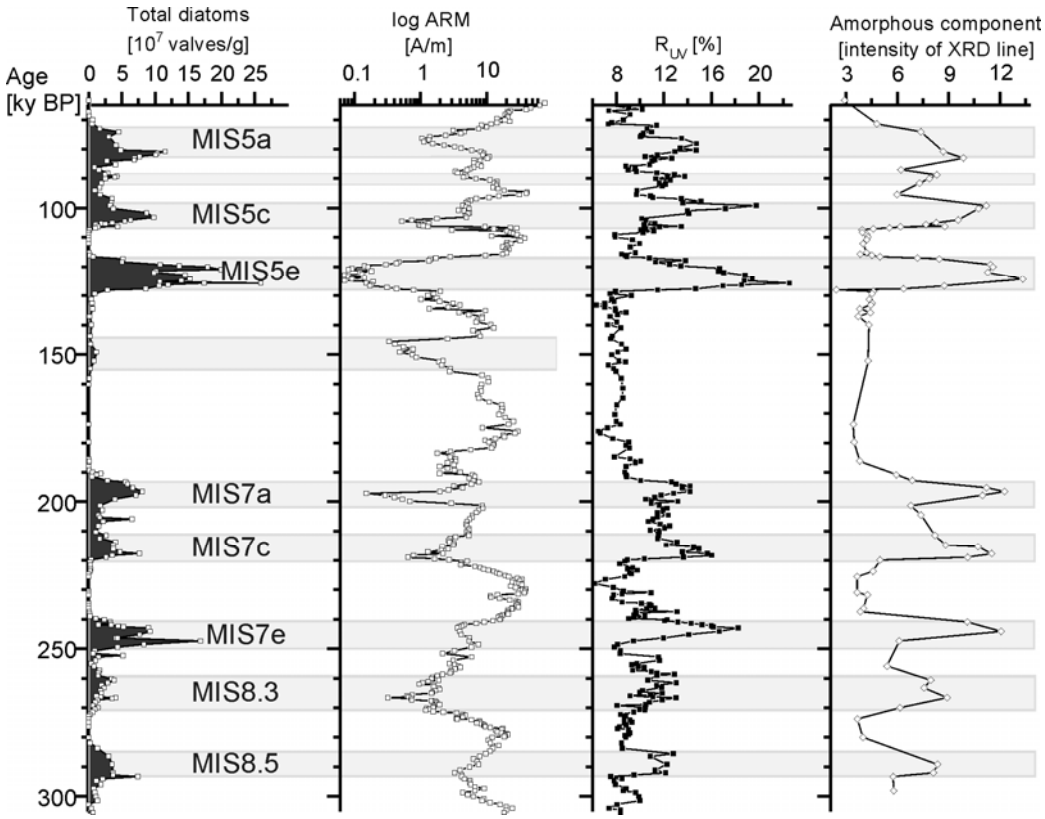

Figure 38 Total diatom concentration and distribution of diatom species in the core BDP98-1-13 covering last 60-300 ky. *S.* = *Stephanodiscus*, *C.* = *Cyclotella*, *A.* = *Aulacoseira*.

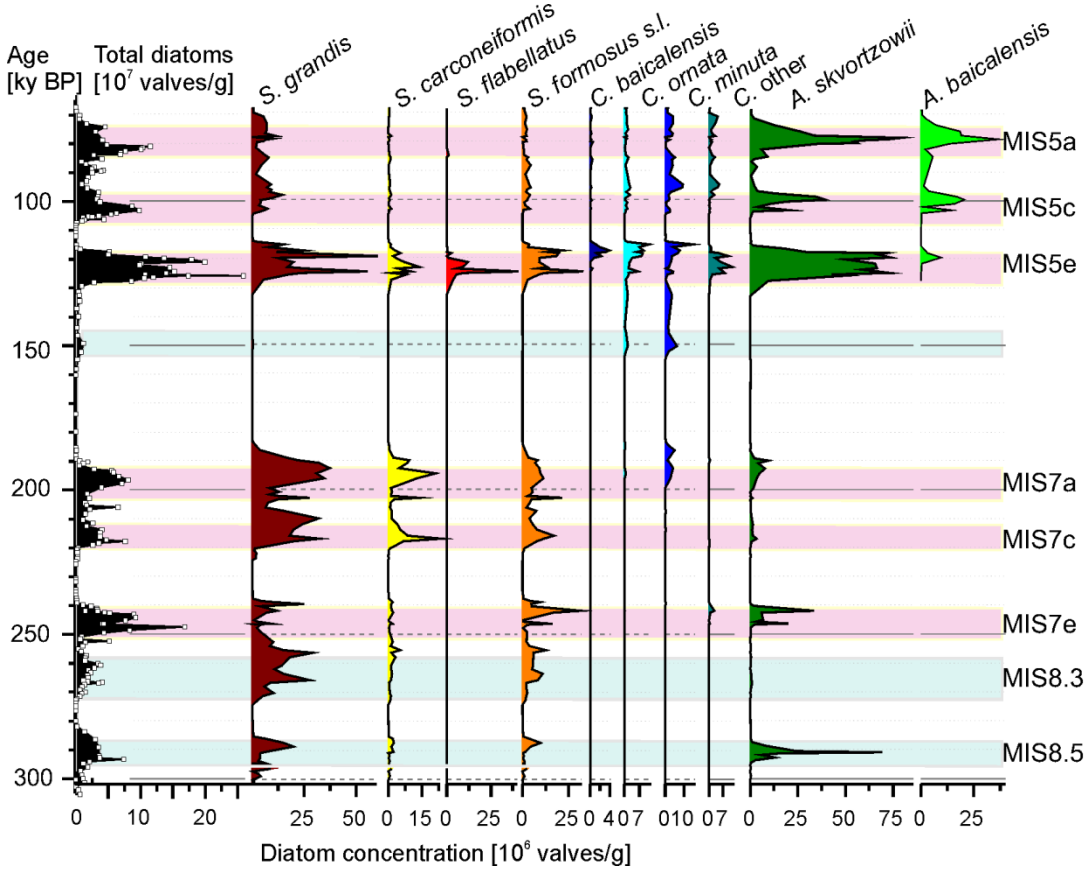

Several important features in the diatom diversity are in agreement with previous reports. In general glacial diatom assemblages contain only minimal numbers of diatom valves except for MIS 8. In the upper part of MIS 8 the glacial assemblages are almost solely composed of *S. grandis*, *S. carconeiformis*, *S. formosus*, and *S. formosus var. minor* (also reported by Khursevich *et al.* 2001) and in MIS 6 and Termination II mostly by *C. minuta* and *C. ornata* (also reported by Edlund and Stoermer 2000, Khursevich *et al.* 2001, and Rioual and Mackay 2005). As expected, more diverse and larger diatom populations were found in interglacials and interstadials due to the increased solar insolation and subsequent reduction on seasonal ice-cover and snow cover over the lake.

While the abundance and presence of *Aulacoseira* taxa varies throughout the analysed interval, large-celled *Stephanodiscus* taxa are present throughout. The ecological requirements of these extinct *Stephanodiscus* taxa remain unknown, though an important requirement is from recent analogous species believed to be deep water mixing and turbulence in the water column (Edlund and Stoermer 2000; Rioual and Mackay 2005). In addition their presence, even in glacial aged samples, may indicate a wide tolerance range and an ability to adapt even to different, more inhospitable, conditions. Alternatively, it may indicate the robustness of these taxa to dissolution in the water column relative to other Lake Baikal taxa. Both *A. baicalensis* and *A. skvortzowii* are cold water taxa requiring clear winter ice permitting deep water mixing in late winter and early spring. According to Rioual and Mackay (2005) both taxa have a similar ecology developing under the ice during the spring months. However, blooms of *A. skvortzowii* start to develop in near shore waters before extending into pelagic/offshore locations during the spring months while *A. baicalensis* primarily occurs in offshore waters (Mackay *et al.* 2000; Richardson *et al.* 2000).

The seasonal distribution of solar radiation during insolation peaks in MIS 8, MIS 7 and MIS 5 was different to today with increased eccentricity of Earth orbit leading to decreased winter insolation and increased summer insolation, producing faster spring warming (and probably also much faster autumn cooling). These seasonal continental climatic contrasts gradually reduced from MIS 8 to MIS 5. The concentrations of extinct small-sized *C. minuta*, medium-sized *C. ornata*, and extinct small-sized *S. formosus var. minor* peak at the end of periods of high diatom abundance (Figure 38), i.e. in periods approaching the Northern Hemisphere summer insolation minima. *S. formosus var. mino*r, in addition to *C. minuta* and *C. ornata*, also peaked in some stadials, such as 208-200 ky BP (MIS 7b) and 94-90 ky BP (MIS 5b). High concentrations of the large *S. grandis* and *S. carconeiformis* were followed by peaks in *S. formosus var. minor* in the lower part of MIS 8 and the later part of MIS 7, with a mean lag of ~3 ky, and by peaks of *C. minuta* in the uppermost sections of MIS 7 and by both *C. minuta* and *C. ornata* in the lowermost peaks of MIS 5 with a mean lag of ~4 ky. Similar successions trends have also been found in sediments from the Academician Ridge during the climatic optima corresponding to MIS 5c and MIS 5a (Chebykin *et al.* 2004, Grygar *et al.* 2006), MIS7 and the Kazantsevo (Khursevich *et al.* 2001), and at Continent Ridge during the Kazantsevo interglacial (Rioual and Mackay 2005).

The prevalence of *C. minuta* and *C. ornata* at the end of diatom peaks close to Northern Hemisphere summer insolation minima and in a period of rather stable Northern Hemisphere

summer insolation maximum in late MIS 6, together with the abundance of these taxa in Lake Baikal in the Holocene and today, suggest that these taxa can adapt to the decreased inter-seasonal insolation contrasts which may have been more unfavourable for larger *Stephanodiscus* taxa. In the early Kazantsevo *A. skvortzowii* prevailed, while in the latter parts of the interglacial *A. baicalensis* appeared. This *Aulacoseira* succession was also found by Edlund and Stoermer (2000) at Buguldeika Saddle, Khursevich *et al.* (2001) at the Academician Ridge and by Rioual and Mackay (2005) at Continent Ridge, suggesting it reflects a reduction in snow/ice cover throughout the North Basin. Following the early Kazantsevo, *A. baicalensis* then prevailed during the later part of MIS 5.

Today, the Holocene seasonal insolation contrasts are lowest within the last 300 ky, and accordingly the current Lake Baikal diatom flora is of a similar low diversity as that experienced during MIS 13-MIS 9e (Khursevich *et al.* 2001). The extinction of *S. grandis* and *S. carconeiformis* occurred at some point in the last glacial after MIS 5, perhaps in response to the changes in seasonal insolation described above. This kind of insolation forcing in diatom species development is in agreement with the long Pleistocene record of Khursevich *et al.* (2001) who found that major diatom variations/extinctions were aligned to variations in the Earth's orbit eccentricity.

7.3. Discussion

7.3.1. Inorganic sedimentary components

The glacial–interglacial changes of clay mineral composition are of immediate interest because of their potential to record past changes of weathering intensity in the Lake Baikal watershed. Lake Baikal as nonmarine archive at high latitude has not as strong response to hydrolysis of rock-forming silicates to climatic forcings as it is observed in archives in tropical and subtropical regions (Yuretich *et al.* 1999). Our mineralogical analysis of the core VER 98-1-13 (quartz, muscovite, feldspars, kaolinite, amphibole, illite, chlorite, and assemblage of expandable clay minerals) is in good agreement with previous reports from nearby cores (Yuretich *et al.* 1999, Fagel *et al.* 2003, Fagel and Boes 2008). However, identification of the type of expandable clay mineral and its interpretation in these works differs. High values of expandable components occur preferably during cold and glacial periods when weathering intensities are low. First explanation of this feature was that the high presence of vermiculite is intermediate stage of mica weathering and predominant physical weathering in Lake Baikal watershed during glacial–interglacial transitions (Fagel *et al.* 2003, Fagel and Boes 2008). Recent detailed study by Solotchina *et al.* (in press) proved that vermiculite is not present at all and the main expandable component is interstratified illite-smectite (I-S), which was identified also earlier by Yuretich *et al.* (1999). Solotchina *et al.* (in press) also explains I-S decreasing concentration during warmer periods by enhanced illitization processes. Higher seasonal temperatures and stronger 'wetting–drying cycles' in soils during interglacials are conducive to the irreversible fixation of K-cations, and illitization may proceed faster than neoformation of clay minerals, thereby resulting in the net loss of expandable layers in clays (Solotchina *et al.* in press). Regarding this new interpretation it seems that the signals of the abundance of expandable layers in illite–smectite and of the total abundance of illite are reflecting the intensity of chemical weathering in the watershed and significance of the abundance of illite and the abundance of expandable layers in illite–smectite are perhaps the most meaningful signals of paleoclimate in the mineralogical records of Lake Baikal.

Chemical weathering within the Lake Baikal watershed is an essential source of silicic acid for the water column. The oxidation of Fe^{2+} in alumosilicates to Fe^{3+} is explicitly related to the oxidation and other weathering processes. B/C, however, is not correlated to the diatom proxies and total Fe content. In several zones the B/C parameter decreases before the onset of large diatom concentrations, as if certain levels of silicate weathering were required to supply sufficient silicic acid to allow the subsequent diatom boom, although after a few ky lag. That lag has been related to the seasonal shifts of the perihelion and perhaps different humidity and temperature optima in the interglacials (Prokopenko *et al.* 2006). This trend is obvious in MIS 6 from 160 ky BP and in MIS 8 from 280 ky BP. However, it remains unclear at present whether the increase in diatoms at the beginning of interglacials was in response to levels in silicic acid and other nutrients rising above a critical threshold following increased watershed weathering in addition to insolation related change or, if diatom increases occurred only in response to insolation forced changes in ice/snow cover over the lake. Glacial periods are characterized by

high magnetic susceptibility values, which reflect increased input of wind-blown loess, as climates in Asia became colder, drier, and windier (Velichko *et al.* 1984 in Mackay *et al.* 2002).

7.3.2. Organic sedimentary variations in last 300 ky

All peaks in diatom concentrations occurred in periods of enhanced chemical weathering of primary minerals as indicated by spectral, mineralogical and rock magnetic analyses. Consequently, to exclude a possible direct inter-relationship of diatom and mineralogical records in further analysis, it is important to estimate which mineralogical or rock-magnetic parameters are not explicitly related to the lake bioproductivity by post-depositional processes, in other words, which mineral parameters are likely to reflect only chemical weathering in the watershed. The concentration of ferrimagnetic particles, evaluated by ARM, is not safe from this point of view because post-depositional reductive dissolution of magnetite by organic matter can decrease ARM in periods of increased lake productivity. Fe_{TOT}, R_{vis} and R_{uv} reflectance were also excluded from further interpretation as they are strongly related to the concentration of diatom frustules within the sediment (Grygar *et al.* 2007).

First who used biogenic silica in the sediment record as an indicator of glacial cycles have been Granina *et al.* (1993 in Mackay *et al.* 2002). During interglacial periods diatoms are major primary producers in the lake, accounting for ~ 98 % of all sedimentary silica. However, during glacial periods, diatom production decreases resulting in decreased sedimentary concentrations (Colman *et al.* 1995). Battarbee *et al.* (2005) highlight that only c.1% of the diatom crop makes it into the sedimentary record. Furthermore, the extent of dissolution appears to be species-specific, affecting more finely silicified, cosmopolitan taxa to a greater degree than the more robust endemic species (Oberhänsli and Mackay 2005). Despite these problems diatom concentrations in Lake Baikal have been most commonly directly related to changes in insolation as discussed by Prokopenko *et al.* (2001a), Khursevich *et al.* (2001). As Khursevich et al (2001) noticed, the diatom assemblage from MIS 9a to MIS 5 was highly stable with no dramatic taxa extinctions. This interval is marked by a well defined insolation pattern with interglacials and interstadials falling into periods of high seasonal differences caused by high eccentricity, i.e. resulting in summer insolation above and winter insolation below present levels. This increased seasonality, or climate continentality would have enhanced the vertical mixing of the water column during spring and early summer, believed to be pre-requisites for the growth of large-cell taxa *S. grandis*, *S. carconeiformis,* and *C. baicalensis* (in MIS 5e), and enabled fast transportation of nutrients into the photic zone. Edlund and Stoermer (2000) and Rioual and Mackay (2005) supposed that the extant large cell diatoms required clear winter ice cover and deep water mixing. Since *S. grandis* and *S. carconeiformis* were present throughout the analysed section including the MIS 8 glacial, we assume that they are able to prevail even in environmentally poor condition when turbulence may not have been high. Alternatively, it is also possible that these extinct taxa are more resistant to dissolution than other taxa.

Concentrations of *C. minuta*, *C. ornata*, and *S. formosus var. minor* peaked in periods with decreased seasonality, i.e. low Northern Hemisphere summer insolation minima (Figure 38). Their maxima after the peak for the larger *Stephanodiscus* taxa can imply a decrease in the deep mixing of the water but may also reflect a reduced supply of nutrients due to climatic worsening

in the later part of the interglacial or interstadial. CEC decreased in humid environment, with peaks in *Aulacoseira* taxa in MIS 5 coincident with humidity maxima (CEC minima) at 105-100 and 85-78 ky BP. Conversely, peaks in *Cyclotella* taxa at 99-96 and 76-72 ky BP coincided with high CEC values, i.e. a probably drier climate but with chemical weathering still relatively high as indicated by low amounts of magnetic minerals, Fe_{TOT}, and relatively low level of Fe^{2+}/Fe^{3+} in silicates. The same pattern of high CEC and low Fe^{2+}/Fe^{3+} is also found in MIS 7a during a shallow local maximum of *C. minuta*. The characteristic succession of *Cyclotella* species in the Kazantsevo interglacial was also accompanied by the same CEC and Fe^{2+}/Fe^{3+} pattern with less abundant concentrations of expandable clay minerals in the early stage of MIS 5e at 128 ky BP coincident with low numbers of *C. minuta*. After 123-122 ky BP, however, the amount of *C. minuta* and *C. ornata* started to increase with a peak between 121 and 117 ky BP.

7.3.3. Climatic changes in the period 60-350 ky BP recorded in Lake Baikal

Although our periods of the harshest glacial climate did not coincide with $\delta^{18}O$ maxima in marine foraminifera records, sharp climatic changes documented in the high latitude North Atlantic region between the middle of MIS5e and MIS5a are well expressed in the Lake Baikal sediment record (Figure 39). The extent and magnitude of local glaciation in the Baikal watershed obviously do not correspond well with the average extent of global glaciation. According to pollen data (Shichi et al. 2007) the glaciation of the Baikal Lake region is rather specific with strong differences in northern and southern parts of the basin due to geographical characteristics of the regions, i.e., the mountains around the northern region and the plains around the Selenga River in the southern region. Forests during interstadial and some interglacial (MIS5c, 5a) periods appeared primarily in the southern region. The local environment of Baikal and perhaps the entire

Figure 39 Climatic changes in the period 60-350 ky BP recorded in Lake Baikal in comparison with marine and glacial records.

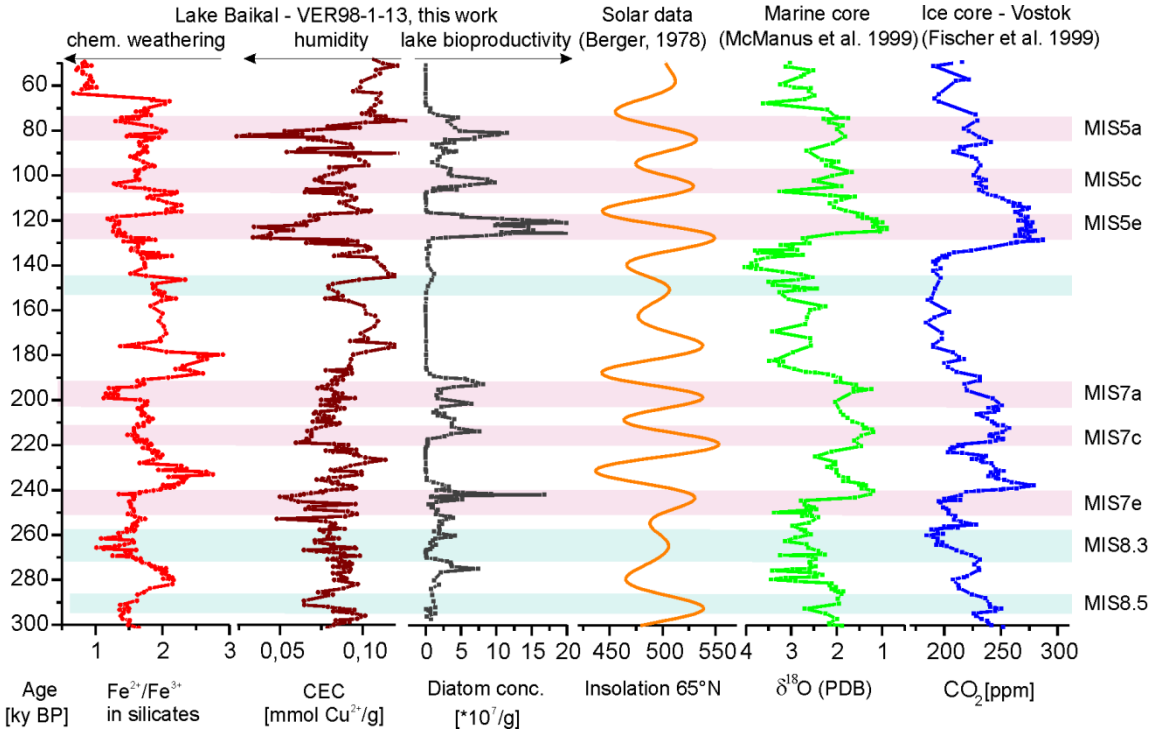

Central Siberia obviously amplified the insolation extremes during MIS5 expressed as high continental seasonal contrasts (Figure 39).

The combination of diatom analysis and weathering indices indicate that within the interval from MIS8.5 to MIS4, humidity was highest in MIS5e and in the short periods between MIS 5c and MIS 5a and moderate in MIS7e, MIS8.5 and the early MIS 8 interstadial. In contrast, the least humid/warm periods were the interstadials MIS 5c, MIS7c and MIS7a. Unusually the MIS 8 glacial was very moderate compared to the early half of MIS6, the climatically harshest period in the Lake Baikal region within the studied period (up to 300 ky). Furthermore, in contrast to MIS 8 which was interrupted by two interstadials of relatively intensive chemical weathering and increases in lake productivity, MIS6 was interrupted by only a single, very weak, increase in lake productivity.

7.4. Conclusions

The orbital forcing can be easily recognized in the amount of fossil diatoms in sediment; namely, diatom peaks correlate with the high latitude Northern hemisphere summer insolation maxima, especially in periods of low obliquity. This was used to construct one of our age models, while the other one was obtained by the palaeomagnetic dating. The results of the both dating approaches were similar with a difference of several ky. The studied core represents clayey sedimentation of the period of 300-60 ky BP.

We performed several methods related to the oxidation state of Fe in Fe-containing silicates and oxides and also to the concentration of expandable clay minerals, both indicating changes in the intensity of chemical weathering in the Baikal Lake watershed. Inorganic analytical methods enabled us recognising the humid phases, phases with enhanced chemical weathering and we also independently characterized the lake bioproductivity thanks to diatom analysis. Surprisingly low values of the concentration of expandable clay minerals within the warmest/most humid periods were observed. This surprising pattern has recently been explained by illitization via pedogenetic processes and attributed to pronounced continental and relatively dry climate in interglacials. Interstadial and interglacial periods in Baikal watershed are characterized by a higher proportion of illite, low concentration of expandable clay minerals and maxima of diatom concentrations as well as increased diatom species diversity. These indicators had extreme values during the MIS5e, known as Kazantsevo (the analogue of the European Eemian), which was therefore the most important climatic optimum in the period from 300 to 60 thousand years before presence.

Diatoms were abundant not only in interglacials and interstadials, but also in the insolation maxima of the MIS 8 and MIS 6 glacials. Increased diatom diversity indicates the enhancement of lake productivity and climatically more favourable environmental conditions during the climatic optima of MIS 7e, MIS 5e and some shorter periods between MIS 5c and MIS 5a. We have provided palaeoenvironmental interpretations of diatom assemblages partly based on the known ecological demands and partly (for the extinct species) we estimated their ecological requirements based on their abundance in periods specified by inorganic methods. E.g. extinct *Stephanodiscus grandis* as one of the most frequent diatoms despite its large frustule had probably a very wide tolerance range to nutrient availability and was able to adapt even to less hospitable conditions occurring in glacial periods.

The absence of diatom frustules within colder periods could be caused either by their lack in the lake related to the decreased light irradiance through a snow cover on the frozen lake or by their enhanced dissolution. Therefore neither the total number of diatom valves nor the amount of biogenic opal alone can be used to interpret the palaeoclimate/paleoenvironment. Instead, the past conditions can be evaluated from combining mineral proxies of chemical weathering and taxonomic diatom analysis to the species level.

Therefore as the main result of our work we have compared each climatic period in Baikal Lake watershed with marine isotopic stages (MIS) in the interval 300-60 ky complementary to numerous previous studies that were focused mainly to the characterization of climate in the Baikal Lake area in the last 150 ky or to several My with a much lower resolution than ours.

CONCLUSIONS

8. CONCLUSIONS

This thesis was aimed to investigate diatom assemblage variability and related parameters in sedimentary cores from Lake Baikal and Aral Sea and to provide a complex paleoenvironmental reconstruction of these two particular Asian sites.

Partial conclusions have been reported within chapters 6.4 and 7.4. We want to further generalize several points, to which this work led to.

One of the most important outcomes of this study is a successful application of diatom analysis for the palaeoenviromental interpretations. We have passed successfully from the methodology of diatom slide preparation, diatom species identification to the assemblage interpretation based on various sources. Despite its high demands for time and experience of a researcher, diatom analysis is a very powerful method that characterizes changes in autochthonous biogenic part of the lake sediments especially while reconstructing the past environmental changes. We proved the reliability of diatom analysis in competition with faster and easier methods in two different lake environments.

Concerning diatom analysis performed on the lake sediments we recommend:

- To avoid redundant steps in diatom slides preparation. When analysing organic poor lake sediments no leaching step (e.g. removing of organic matter) is needed.
- To count at least 300 diatom valves per slide to get statistically significant results.
- To use internal standard (in our case divinylbenzen microspheres in suspension of a known concentration) in order to get absolute numbers of the diatom concentration.
- For the interpretation of diatom analysis to use the definition of species ecological requirements mainly from the studies available from the same lake.
- To complement diatom analysis by other methods, especially those unravelling allochthonous sediment components.

We combined diatom analysis with various independent methods focusing more on the inorganic part of the sediments. We used especially spectral, and X-ray diffraction methods, and methods characterising clay minerals as one of the most relevant climate-sensitive components in the lake sediments. The clay mineral identification was performed using high temperature XRD, and the quantitative changes of the amount of expandable clay minerals in samples was achieved by using Cu-trien method to the determination of cation exchange capacity of clay minerals.

We recommend using as many proxies as possible (preferring fast methods that do not require large amount of the sample) because climatic unravelling is a very complex task. Each method can add some missing and crucial piece of a final mosaic and it is very difficult to predict *a priori*, which method will be the most valuable one to propose the palaeoenvironmental reconstruction.

ACKNOWLEDGMENTS

This thesis is a part of team work research. I am eternally grateful to all my co-workers.

I would like to thank to opposers of this work. I apologize for mistakes in my English.

9. PODĚKOVÁNÍ

Chtěla bych touto cestou poděkovat Univerzitě Karlově, že umožňuje studentům doktorského studia působit na pracovištích Akademie věd České republiky. Můj velký dík náleží Ústavu anorganické chemie AV ČR, v.v.i., který mi poskytl nenahraditelné zázemí již od prvního ročníku studia. Všichni členové oddělení Analytiky určitým způsobem přispěli k formování mého vztahu k vědě a ovlivnili tak i tuto práci.

Nejvíce chci poděkovat Tomáši Grygarovi, který mě vedl a nutil neustále přemýšlet o nových možnostech interpretace výsledků, o dalších metodách, i o jiných pohledech na svět. Srdečně mu děkuji za jeho všestrannou a neutuchající podporu, bez které by tato práce nevznikla. Děkuji mu za to, že se aktivně podílel na finalizaci této práce, ale zpětně zejména za to, že stál u jejího zrodu, když v roce 2005 v Řeži inicioval zavedení rozsivkové analýzy. Práci s rozsivkami se tehdy naučila Kateřina Novotná na týdenním kurzu v Londýně a před jejím odjezdem na roční stáž do Potsdam mi předala základy techniky i veškeré studijní materiály. Jelikož mě rozsivková analýza oslovila, již jsem u ní zůstala. Postupně jsem rozšiřovala své znalosti a zkušenosti až jsem neváhala změnit téma své disertační práce, abych mohla v rozsivkové analýze pokračovat. Děkuji tímto Kateřině Novotné, že umožnila zrod této práce. Děkuji Veronice Grünvaldové a Silvii Švarcové za pomoc s elektronovou mikroskopii. Děkuji Petru Bezdičkovi za možnost zpracovávat vysokoteplotní rentgenová měření. Děkuji i všem laborantům, díky nimž byly vzorky kvalitně zpracovány a výsledky analytických metod dosáhly vysokého rozlišení. V neposlední řadě děkuji svému školiteli Davidu Hradilovi, který mě nechal jít svou cestou a na jejím konci přispěl k finalizaci textu práce.

Druhý domov k rozsivkové činnosti mi poskytla Katedra botaniky PřF UK, kde jsem mohla užívat výborného mikroskopického vybavení. Rovněž se mi zde dostalo bezpočtu konzultací k identifikacím rozsivkových druhů a to zejména od Jany Veselé. Velmi si cením i bezděčné pomoci, kterou mi poskytli i další rozsivkoví specialisté. Nejvíce z nich mi pomohl George Swann s identifikací druhů v sedimentech Bajkalského jezera. Ze zahraniční spolupráce a pomoci nemohu opomenout Hedi Oberhänsli, díky Hedi jsme získali studijní materiál z obou jezer. Vděčím jí rovněž za mnohé plodné a poučné debaty a její zkušenosti.

Za finanční podporu vděčím Grantové agentuře Akademie věd ČR a to konrétně za jednoletý juniorský grantový projekt KJB300320901 s tématem: Datování a interpretace paleoklimatického záznamu ze sedimentu Aralského jezera z posledních 2000 let. V letech 2006-2008 byla tato práce podporována tematicky podobnými grantovými projekty KJB307020601 a IAAX00130801 jejichž řešitelům tímto děkuji. Velkou zásluhu na odevzdání této disertační práce má Aloisie Poulíčková, která jakožto šéfredaktorka časopisu Fottea přijala do tisku můj článek ve velmi krátkém čase.

Již od počátku mě v práci podporovala celá má rodina a nejvíce můj manžel, Vladimír Píška, který neváhal a kromě duchovní podpory pomáhal řešit i technické problémy. Jím navržená databáze k vyhodnocování rozsivkové analýzy mi ušetřila spoustu času a nervů. V kritickém období dokončování disertační práce spolu s mým bratrem Janem Bláhou pomáhali s řešením technických problémů s dokumentem. Za jejich obětavost, čas a trpělivost jim patří můj dík.

Děkuji oponentům této práce za jejich čas a posudky ať budou jakékoliv. Děkuji i Tobě poctivý čtenáři, který jsi došel až sem. Ať se Ti v Tvé další životní pouti daří.

REFERENCES

10. REFERENCES

Acot, P., **2005**. History of climate change (In Czech: Historie a změny klimatu: od velkého třesku ke klimatickým katastrofám), Praha, Karolinum, 237 pp.

Aladin, N.V., Fillippov, A.A., Plotnikov, I.S., Orlova, M.I., and Williams, W.D., **1998**. Changes in the structure and function of biological communities in the Aral Sea, with particular reference to the northern part (Small Aral Sea), 1985-1994: A review. International Journal of Salt Lake Research 7, p. 301–343.

Aladin, N.V., Plotnikov, I.S., Bolshov, A., and Pichugin, A., **2006**. Biodiversity of the Caspian Sea. Report of Caspian Sea Biodiversity Project under umbrella of Caspian Sea Environment Program.

Allen, P.A., and Collinson, J.D., **1986**. "Lakes." In Sedimentary Environments and Facies, 2nd ed. Oxford, U.K.: Blackwell Scientific Publications, 680 pp.

Alley, R.B., Marotzkr, J., Nordhaus, W.D., Overpeck, J.T., Peteet, D.M., Pielke, R.A., Pierrehumbert, R.T., Rhines, P.B., Stocker, T.F., Talley, L.D., and Wallace, J.M., **2003**. Abrupt Climate Change. Science 299, p. 2005–2010.

Anderson L., Abbott, M.B., and Finney, B.P., **2001**. Holocene Climate Inferred from Oxygen Isotope Ratios in Lake Sediments, Central Brooks Range, Alaska. Quarternary Research 55 (3), p. 313–321.

Andrén, E., Shimmield, G, and Brand, T., **1999**. Environmental changes of the last three centuries indicated by siliceous microfossil records from the southwestern Baltic Sea. The Holocene 9 (1), p. 25–38.

Audustin, L., Barbante, C., Barnes, P.R.F., Barnola, J.M., Bigler, M., Castellano, E., Cattani, O., Chappellaz, J., Dahl-Jensen, D., Delmonte, B., Dreyfus, G., Durand, G., Falourd, S., Fischer, H., Fluckiger, J., Hansson, M.E., Huybrechts, P., Jugie, G., Johnsen, S.J., Jouzel, Kaufmann, P., Kipfstuhl, J., Lambert, F., Lipenkov, V.Y., Littot, G. C., Lorrain, R., Maggi, V., Masson-Delmotte, V., Miller, H., Mulvaney, R., Oerlemans, J., Oerter, H., Orombelli, G., Parrenin, F., Peel, D.A., Petit, J.-R., Raynaud, D., Ritz, C., Ruth, U., Schwander, J., Siegenthaler, U., Souchez, R., Stauffer, B., Steffensen, J.P., Stenni, B., Stocker, T.F., Tabacco, I.E., Udisti, R., van de Wal, R.S.W., van der Broeke, M., Weiss, J., Wilhelms, F., Winther, J.-G., Wolff, E.W., and Zucchelli, M., **2004**. Eight glacial cycles from an Antarctic ice core. Nature 429, p. 623–628.

Austin, P., Mackay, A., Palagushkina, O., and Leng, M., **2007**. A high-resolution diatom-inferred palaeoconductivity and lake level record of the Aral Sea for the last 1600 yr. Quaternary Research 67: 383–393.

Barber, H.G, and Hawort, E.Y., **1994**. A guide to terminology of the diatom frustule, with a Key to the British Freshwater Genera. Freshwater Biological Assn., 112 pp.

Bard, E., Raisbeck, G.M., Yiou, F., and Jouzel, J., **1996**. Solar modulation of nuclide production over the last millennium: comparison between ^{14}C and ^{10}B records. Earth and Planetary Science Letters 150, p. 450–463.

Barnett, E.T., **1997**. Potential for coastal flooding due to coseismic subsidence in the central Cascadia margin (Master thesis). Portland State University.

Battarbee, R.W., L. Carvalho, V. J. Jones, R. J. Flower, N. G. Cameron, H. Bennion, and S. Juggins, **2001**: Diatoms. In: Tracking Environmental Changes Using Lake Sediments. Volume 3: Terrestrial, Algal and Siliceous Indicators [J. P. Smol, H. J. B. Birks, and W. M. Last (eds.)]. Kluwer Academic Publishers, Dordrecht, The Netherlands, 2–47 from 240 pp.

Battarbee, R.W., Mackay, A.W., Jewson, D.H., Ryves, D.B., and Sturm M., **2005**. Differential dissolution of Lake Baikal diatoms: correction factors and implications for palaeoclimatic reconstruction. Global Planetary Change 46, p. 75-86.

Berger A., **1978**. Long-term variations of daily insolation and Quaternary climatic changes. J. Atmospheric Sci. 35, p. 2362–236.

Boomer, I., Aladin, N., Plotnikov, I., and Whatley, R., **2000**. The palaeolimnology of the Aral Sea: a review. Quaternary Science Reviews 19. p. 1259–1278.

Boomer, I., Wünnemann, B., Mackay, A.W., Austin, P., Sorrel, P., Reinhardt, Ch., Keyser, D., Guichard, F., and Fontugne, M., **2009**. Advances in understanding the late Holocene history of Aral Sea region. Quaternary International 194 (1-2), p. 79–90.

Boroffka, N., Oberhänsli, H., Sorrel, P., Demory, F., Reinhardt, Ch., Wünnemann, B., Alimov, K., Baratov, S., Rakhimov, K., Saparov, N., Shirinov, S., Krivonogov, S.K., and Röhl, U., **2006**. Archaeology and Climate: Settlement and Lake-Level Changes at the Aral Sea. Geoarchaeology: An International Journal 21 (7), p. 721–734.

Brunello, A.J., Molotov, V.C., Dugherkhuu, B., Goldman, Ch., Khamaganova, E., Strijhova, T., and Sigman, R., **2006**. Lake Baikal. Experience and Lessons Learned Brief, 16 pp.

Burić, Z., Kiss, K.T., Ács, É., Viličić, D., Mihalić, K.C., and Carić, M., **2007**. The occurrence and ecology of the centric diatom Cyclotella choctawhatcheeana Prasad in a Croatian estuary. Nova Hedwigia 84 (1-2), p. 135–153.

Caroll, A.R., and Bohacs, K.M., **1999**. Stratigraphic classification of ancient lakes: Balancing tectonic and climatic controls. Geology 27 (2), p. 99–102.

Chebykin, E.P., Edgington, D.N., Goldberg, E.L., Phedorin, M.A., Kulikova, N.S., Zheleznyakova, T.O., Vorob'yova, S.S., Khlystov, O.M., Levina, O.V., Ziborova, G.A., and Grachev M.A., **2004**. Uranium-series isotopes as proxies of Late Pleistocene climate and geochronometers in bottom sediments of Lake Baikal. Geologia i Geofizika 45, p. 539–556.

Chivas, A.T, De Deckker, P., and Shelley, M.G., **1985**. Strontium content of ostracods indicates lacustrine palaeosalinity. Nature 316, p. 251–253.

Cohen, A.S., **2003**. Paleolimnology: The History and Evolution of Lake Systems. Oxford University press, 500 pp.

Colman, S.M., Peck, J.A., Karabanov, E.B., Carter, S.J., Bradbury, J.P., King, J.W., and Williams, D.F., **1995**. Continental climate responce to orbital forcing from biogenic silica records in Lake Baikal. Nature 378, p. 769–771.

Colman, S.M., Peck, J.A., Hatton, J., Karabanov, E.B., and King, J.W., **1999**. Biogenic silica records from the BDP93 drill site and adjacent areas of the Selenga Delta, Lake Baikal, Siberia. Journal of Paleolimnology 21, p. 9–17.

Cullen, H.M., Kaplan, A., Arkin, P.A., de Menocal, P.B., **2002**. Impact of the North Atlantic Oscillation on Middle Eastern climate and streamflow. Climatic Change 55, p. 315–338.

D'Arrigo, R., Mashig, E., Frank, D., Wilson, R., and Jacoby, G., **2005**. Temperature variability over the past millennium inferred from Northwestern Alaska tree rings. Climate Dynamics 24, p. 227–236.

Dawson, A.G., **1992**. Ice age Earth: Late Quarternary geology and climate. Routledge, London and New York, 279 pp.

Demory, F., Nowaczyk, N.R., Witt, A., and Oberhänsli, H., **2005**. High-resolution magneto stratigraphy of late quaternary sediments from Lake Baikal, Siberia: timing of intracontinental paleoclimatic responses. Global Planetary Change 46, p. 167–186.

Denys, L., **1992**. A check list of the diatoms in the Holocene deposits of the western Belgian Coastal Plain with a survey of their apparent ecological requirements: I. Introduction, ecological code and complete list. Service Geologique de Belgique 1992; Professional Paper 246, p. 1–41.

Derbyshire, E., Kemp, R.A., and Meng, X., **2009**. Climate change, loess and palaeosols: Proxy measures and resolution in North China. Journal of the Geological Society. FindArticles.com., available online from: http://findarticles.com/p/articles/mi_qa3721/is_199709/ai_n8758515/

Edlund, M.B., and Stoermer E.F., **2000**. A 200,000-year, high-resolution record of diatom productivity and community makeup from Lake Baikal shows high correspondence to the marine oxygen-isotope record of climate change. Limnol. Oceanogr. 45, p. 948–962.

Einsele, G., **2000**. Sedimentary Basins-Evolution, Facies, and Sediment Budget. Springer-Verlag Berlin Heidelberg New York, 792 pp.

Elderfield, H., and Ganssen, G. **2000**. Past temperature and ^{18}O of surface ocean waters inferred from foraminiferal Mg/Ca ratios. Nature 405, p. 442–445.

Epstein, S., Buchsbaum, R., Lowenstam, H.A., and Urey, H.C., **1953**. Revised Carbonate-Water Isotopis Temperature Scale. Geological Society of America Bulletin 64 (11), p. 1315–1326.

Esper, J., Shiyatov, S.G., Mazepa, V.S., Wilson, R.J.S, Graybill, D.A., and Funkhouser, G., **2002**. Temperature-sensitive Tien Shan tree ring chronologies show multi-centennial growth trends Climate Dynamics 21, p. 699–706.

Espinosa, M.A., Hassan, G.S., and Isla, F.I., **2006**. Diatom Distribution across Temperate Microtidal Marsh, Mar Chiquita Coastal Lagoon, Argentina. An International Journal of Marine Sciences, Thalassas 22 (2), 9–16.

Evans, M.N., Fairbanks, R.G., and Rubenstone, J.L. **1998**. A Proxy Index of ENSO. Teleconnections, Nature 394, p. 732–733.

Fagel, N., Boski, T., Likhoshway, L., and Oberhänsli, H., **2003**. Late Quaternary clay mineral record in Central Siberia Lake Baikal (Academician Ridge, Siberia). Palaeogeography Palaeoclimatology Palaeoecology 193, p. 159–179.

Fagel, N., and Boës, X., **2008**. Clay-mineral record in Lake Baikal sediments: The Holocene and Late Glacial transition. Palaeogeography, Palaeoclimatology, Palaeoecology 259 (2-3), p. 230-243.

Falkner, K.K., Measures, Ch.I., Herbelin, S.E., Edmond, J.M., and Weiss, R.F., **1991**. The major and minor element geochemistry of Lake Baikal, Limnology and Oceanography 36 (3), p. 413–423.

Fischer, H., Wahlen, M., Smith, J., Mastroianni, D., and Deck, B., **1999**. Ice core records of Atmospheric CO_2 around the last three glacial terminations, Science 283, p. 1712-1714.

Folland, C.K., Karl, T.R., Christy, J.R., Clarke, R.A , Gruza, G.V., Jouzel, J., Mann, M.E., Oerlemans, J., Salinger, M.J., and Wang, S.-W, **2001**: Observed Climate Variability and Change. In: Climate Change 2001: The Scientific Basis. Contribution of Working Group I to the Third Assessment Report of the Intergovernmental Panel on Climate Change [Houghton, J.T.,Y. Ding, D.J. Griggs, M. Noguer, P.J. van der Linden, X. Dai, K. Maskell, and C.A. Johnson (eds.)]. Cambridge University Press, Cambridge, United Kingdom and New York, NY, USA, 881 pp.

Freund, H., Gerdes, G., Streif, H., Dellwig, O., and Watermann, F., **2004**. The indicative meaning of diatoms, pollen and botanical macro fossils for the reconstruction of palaeoenvironments and sea-level fluctuations along the coast of Lower Saxony; Germany. Quarternary International 112, p. 71–87.

Friedrich, J., and Oberhänsli, H., **2004**. Hydrochemical properties of the Aral Sea water in summer 2002. Journal of Marine Systems 47, p. 77–88.

Geiss, E.Ch., Umbanhowar, Ch. E., Camill, P., and Banerjee, S.K., **2003**. Sediment magnetic properties reveal Holocene climate change along the Minnesota prairie-forest ecotone. Journal of Paleolimnology 30, p. 151–166.

Giorgi, F., B. Hewitson, J. Christensen, M., Hulme, H., Von Storch, P. Whetton, R. Jones, L. Mearns, C. FuIn, **2001**. Regional Climate Information – Evaluation and Projections. In: Houghton, J.T.,Y. Ding, D.J. Griggs, M. Noguer, P.J. van der Linden, X. Dai, K. Maskell, and C.A. Johnson (eds.). Climate Change 2001: The Scientific Basis. Contribution of Working Group I to the Third Assessment Report of the Intergovernmental Panel on Climate Change. Cambridge University Press, Cambridge, United Kingdom and New York, NY, USA, 881 pp.

Glantz, M.H. (ed.) **1999**. Creeping Environmental Problems and Sustainable Development in the Aral Sea Basin. Cambridge University Press, Cambridge, 283 pp.

Glantz, M.H. (ed.), Jing-lu, I., Hong, Y., Luecke, A., and Su-Min, W., **2001**. Modern climatic signals deduced from stable isotope in shells. In: Su-Min, W., Lake sediments, east Tibetan Plateau, China. 2001. Modern Chinese Geographical Science Chinese Geographical 11 (3), p. 246–251.

Grachev, M.A., Vorobyova, S.S., Likhoshway, Y.V., Goldbers, E.L., Ziborova, G.A., Levina, O.V., and Khlystov, O.M., **1998**. A high-resolution diatom record of the palaeoclimates of east Siberia for the last 2.5 My from Lake Baikal. Quarternary Science Reviews 17, p. 1101–1106.

Granina, L., **1997**. The chemical budget of Lake Baikal: a review. Limnology and Oceanography 42 (2), p. 373–378.

Gromisz, S., and Szymelfenig, M., **2005**. Phytoplankton in the Hel upwelling region (The Baltic Sea). Oceanological and Hdyrobiological Studies 34 (2), p. 115–135.

Grottoli, A.G., and Eakin, C.M., **2007**. A review of modern coral $\delta^{18}O$ and $\Delta^{14}C$ proxy records. Earth-Science Reviews 81, p. 67–91.

Grygar, T., Dědeček, J., Kruiver, P., Dekkers, M. J., Bezdička, P., and Schneeweiss, O., **2003**. Iron Oxide Mineralogy in Late Miocene Red Beds from La Gloria, Spain: Rock-magnetic, Voltametric and Vis Spectroscopy Analyses, Catena 53, p. 115–132.

Grygar, T., Bezdička, P., Hradil, D., Hrušková, M., Novotná, K., Kadlec, J., Pruner, P., and Oberhänsli, H., **2005**. Characterization of expandable clay minerals in Lake Baikal sediments by thermal dehydration and cation exchange. Clays and Clay Minerals 53, p. 389–400.

Grygar, T., Kadlec, J., Pruner, P., Swann, G., Bezdička, P., Hradil, D., Lang, K., Novotná, K., and Oberhänsli, H., **2006**. Paleoenvironmental record in Lake Baikal sediments: Environmental changes in the last 160 ky. Palaeogeography, Palaeoclimatology, Palaeoecology 237 (2–4), p. 240–254.

Grygar, T., Bláhová, A., Hradil, D., Bezdička, P., Kadlec, J., Schnabl, P., Swann, G., and Oberhänsli, H., **2007**. Lake Baikal climatic record between 310 and 50 ky BP: Interplay between diatoms, watershed weathering and orbital forcing. Palaeogeography, Palaeoclimatology, Palaeoecology 250 (1–4), p. 50–67.

Hamilton, S.K., Bunn, S.E., Thoms, M.C., and Marshall, J.C., **2005**. Persistence of aquatic refugia between flow pulses in a dryland river system (Cooper Creek, Australia). Limnology and Oceanography 50, p. 743–754.

Hammer, U.T., **1986**. Saline Lake Ecosystems of the World. Springer, 616 pp.

Hassan, G.S., Espinosa, M.A., and Isla, F.I., **2006**. Modern diatom assemblages in surface sediments from estuarine systems in the southeastern Buenos Aires Province, Argentina. Journal of Paleolimnology 35, p. 39–53.

Hecky, R.E., and Kilham, P., **1973**. Diatoms in alkaline, saline lakes: Ecology and geochemical implications. Limnology and Oceanography 18 (1), p. 53–71.

Hinrichs, K.-U., Rinna, J., Rullötter, J., and Stein, R., **1997**. A 160-kyr Record of Alkenone-Derived Sea-Surface Temperatures from Santa Barbara Basin Sediments. Naturwissenschaften 84, p. 126–128.

Horton, B. P., Innes, J. B., Shennan, I., Lloyd, J. M., and McArthur, J. J., **2004**. Holocene coastal change in East Norfolk, UK: palaeoenvironmental data from Somerton and Winterton Holmes, near Horsey. Proceedings of the Geologists' Association 115, p. 209–220.

Horton, B.P., Corbett, R., Culver, S.J., Edwards, R.J., and Hillier, C., **2006**. Modern saltmarsh diatom distributions of the Outer Banks,North Carolina, and the development of a transfer function for high resolution reconstructions of sea level. Estuarine, Coastal and Shelf Science 69, p. 381–394.

Horton, B. P., Zong, Y., Hillier, C., and Engelhart, S., **2007**. Diatoms from Indonesian mangroves and their suitability as sea-level indicators for tropical environments. Marine Micropaleontology 63 (3-4), p. 155–168.

Hradil, D., Grygar, T., Hrušková, M., Bezdička, P., Lang, K., Schneeweiss, O., and Chvátal, M., **2004**. Green earth pigment from Kadan region, Czech Republic: Use of rare Fe-rich smectite. Clays and Clay Minerals 52, p. 767–778.

Hulme, M., Conway, D., and Lu, X., **2003**. Climate Change: An Overview and its Impact on the Living Lakes. A report prepared for the 8 Living Lakes Conference, 7-12 September 2003, Norwich, UK, 40 pp.

Hurrell, J.W., Kushnir, Y., Visbeck, M., **2001**. The North Atlantic Oscillation. Science 291, p. 603–605.

Hustedt, F ., **1937-1939** . Systematische and Skologische Untersuchungen fiber die Diatomeen-Flora von Java, Bali, Sumatra. Arch . Hydrobiol. (Suppl .) 15–16.

Inda, H., García-Rodríguez, F., del Puerto, L., Acevedo, V., Metzeltin, D., Castiñeira, C., Bracco, R., and Adams, J.B., **2006**. Relationships between trophic state, paleosalinity and climatic changes during the first Holocene marine transgression in Rocha Lagoon, southern Uruguay. Journal of Paleolimnology 35, p. 699–713.

Issar, A.S., **2003**. Climate change during the Holocene and their impact on hydrological systems. Cambridge University Press, 123 pp.

Jankowska, D., Witak, M.,and Huszczo, D., **2005**. Paleoecological changes of the vistula lagoon in the last 7,000 y BP based on diatom flora. Oceanological and Hydrobiological Studies 24 (4), p. 109–129.

Johnson, T.C., Brown, E.T., McManus, J., Barry, S., Barker, P., and Gasse, F., **2002**. A High-Resolution Paleoclimate Record Spanning the Past 25 000 Years in Southern East Africa. Science 296 (5565), p. 113–116.

Kawabata, Y., Nakahara, H., Katayama, Y., and Ishida, N., **1997**. The phytoplankton of some saline lakes in Central Asia. International Journal of Salt Lake Research 6, p. 5–16.

Khursevich G.K., Karabanov E.B., Prokopenko A.A., Williams D.F., Kuzmin M.I., Fedenya S.A., and Gvozdkov A.A., **2001**. Insolation regime in Siberia as a major factor controlling diatom production in Lake Baikal during the past 800,000 years, Quaternary International 80–81, p. 47–58.

Khursevich, G.K., Prokopenko, A.A., Fedenya, S.A., Tkachenko, L. I., Williams, and D.F., 2005. Diatom biostratigraphy of Lake Baikal during the past 1.25 Ma: new results from BDP-96-2 and BDP-99 drill cores. Quaternary International 136 (1), p. 95-104.

Kilic, Ö., and Kilic, A. M., **2005**. Recovery of salt co-products during the salt production from brine. Desalination 186, p. 11–19.

King, J., and Peck, J., **2006**. Use of Paleomagnetism in Studies of Lake Sediments. In Last, W.M., and Smol, J.P. (eds.), 2001. Tracking Environmental Change Using Lake Sediments. Volume 1: Basin Analysis, Coring, and Chronological Techniques. Kluwer Academic Publishers, Dordrecht, The Netherlands. p. 371–389.

Kolbe, R., W., **1927**. Zur Okologie. Morphologie and Systematik der Brackwasser-Diatomeen. Die Kieslealgen des Sperenberger Salzgebietes. Pflanzenforschung 7, p. 1–46.

Korol, G., **2005**. Diatom flora from the Zhidini section and its palaeogeographic and biostratigraphic significance. Palynology 49, p. 29-39.

Krammer, K., and Lange-Bertalot, H. **1986**. Bacillariophyceae. 1. Teil: Naviculaceae. in Ettl, H., Gerloff, J., Heynig, H. and Mollenhauer, D. (eds) Süsswasser flora von Mitteleuropa, Band 2/1. Gustav Fischer Verlag: Stuttgart, New York. 876 pp.

Krammer, K., and Lange-Bertalot, H. **1988**. Bacillariophyceae. 2. Teil: Bacillariaceae, Epithemiaceae, Surirellaceae. in Ettl, H., Gerloff, J., Heynig, H. and Mollenhauer, D. (eds) Süsswasserflora von Mitteleuropa, Band 2/2. VEB Gustav Fischer Verlag: Jena. 596 pp.

Krammer, K., and Lange-Bertalot, H. **1991a**. Bacillariophyceae. 3. Teil: Centrales, Fragilariaceae, Eunotiaceae. in Ettl, H., Gerloff, J., Heynig, H. and Mollenhauer, D. (eds) Süsswasserflora von Mitteleuropa, Band 2/3. Gustav Fischer Verlag: Stuttgart, Jena. 576 pp.

Krammer, K., and Lange-Bertalot, H. **1991b**. Bacillariophyceae. 4. Teil: Achnanthaceae, Kritische Ergänzungen zu Navicula (Lineolatae) und Gomphonema, Gesamtliteraturverzeichnis Teil 1–4. in Ettl, H., Gärtner, G., Gerloff, J., Heynig, H. and Mollenhauer, D. (eds) Süsswasserflora von Mitteleuropa, Band 2/4. Gustav Fischer Verlag: Stuttgart, Jena. 437 pp.

Krivograd Klemenčič, A., Vrhovšek, D., and Smolar-Žvanut, N., **2007**. Microplanktonic and Microbenthic Algal Assemblages in the Coastal Brackish Lake Fiesa and the Dragonja Estuary (Slovenia). Nat. Croat. 16 (1), p. 63–78.

Kuzmin, Y.V., Nevesskaya, L.A., Krivonorov, S.K., and Burr, G.S., **2007**. Apparent ^{14}C ages of the 'pre-bomb' shells and correction values (R,DR) for Caspian and Aral Seas (Central Asia). Nuclear Instruments and Methods in Physics Research B 259, p. 463–466.

Labeyrie, L., Cole, J., Alverson, K., and Stocker. **2003**. The History of Climate Dynamics in the Late Quarternary. In: Alverson, K.D., Bradley, R.S., Pedersen, T.F., (eds.). Paleoclimate, Global Change and the future. Springer – Verlag Berlin, Heidelberg, New York, p. 33–61.

Laird, K., Michels, A., Stuart, Ch.T.L., Wilson, S.E., Last, W.M., and Cumming, B.F., **2007**. Examination of diatom-based changes from a climatically sensitive prairie lake (Saskatchewan, Canada) at different temporal perspectives. Quaternary Science Reviews 26, p. 3328–3343.

Le Callonnec, L., Person, A., Renard, M., Létolle, R., Nebout, N., Khelifa, L.B., and Rubanov, I., **2005**. Preliminary data on chemical changes in the Aral Sea during low-level periods from the last 9000 years. Comptes Rendus Geosciences 337, p. 1035–1044.

Lecointe, C., Coste, M., and Prygiel, J., **1993**. "Omnidia": software for taxonomy, calculation of diatom indices and inventories management. Hydrobiologia 269-270, p. 509-513.

Leng, J.M., and Marshall, J.D., **2004**. Palaeoclimate interpretation of stable isotope data from lake sediment archives. Quarternary Science Reviews 23, p. 811–831.

Leroy, S.A.G., Marret, F., Gibret, E., Chalié, F., Reyss, J.-L.M., and Arpe, K., **2007**. River inflow and salinity changes in the Caspian Sea during the last 5500 years. Quarternary Science Reviews 26, p. 3359–3383.

Létolle, R., and Mainguet, M., **1993**. Aral (In French). Springer-Verlag, Paris, 355 p.

Létolle, R., Aladin, N., Filipov, I., Boroffka, N.G.O., **2005**. The future chemical evolution of the Aral Sea from 2000 to the years 2050. Mitigation and Adaptation Strategies for Global Change 10, p. 51–70.

Liand, Y., and Blake, R.E., **2005**. Phosphate oxygen isotope ratio proxy for specific microbial activity in marine sediments (Peru Margin). American Geophysical Union, Fall Meeting 2005, abstract #PP43B-0672.

Lie, S.E., Stabell, B., and Mangerud, J., **1988**. Diatom stratigraphy related to Late Weichselian Sea-level Changes in Sunnmore, Western Norway. Norges Geologiske Undersokelse Bulletin 380, p. 203–219.

Lioubimtseva, E., Cole, R., Adams, J.M., and Kapustin, G., **2005**. Impacts of climate and land-cover changes in arid lands of Central Asia. Journal of Arid Environments 62, p. 285–308.

Lojka, R., Drábková, J., Zajíc, J., Sýkorová, I., Franců, J., Bláhová, A., and Grygar, T., **in press**. Climate variability in the Stephanian B based on environmental record of the Mšec Lake deposits (Kladno–Rakovník Basin, Czech Republic), Palaeogeography, Palaeoclimatology, Palaeoecology.

Mackay, A. W., Flower, R. J., Kuzmina, A. E., Granina, L. Z. , Rose1, N. L., Appleby, P. G. , Boyle, J. F., and Battarbee, R. W., **1998**. Diatom succession trends in recent sediments from Lake Baikal and their relation to atmospheric pollution and to climate change. Phil.Trans. R. Soc. Lond. B 353, p. 1011–1055.

Mackay, A.W., Battarbee, R.W., Flower, R.J., Jewson, D., Lees, J.A., Ryves, D.B., and Sturm, M., **2000**. The deposition and accumulation of endemic planktonic diatoms in the sediments of Lake Baikal and an evaluation of their potential role in climate reconstruction during the Holocene. Terra Nostra, 9, p 34–48.

Mackay, A.W., Flower, R.J., and Granina, L.Z., **2002**. Lake Baikal. In: The Physical Geography of Northern Eurasia: Russia and Neighbouring States. Ed. by M. Shahgedanova, and A. Goudie. Published by OUP, Oxford. (Chapter 17), p. 403–421.

Mackensen, A., **2004.** Changing Southern Ocean palaeocirculation and effects on global climate. Antarctic Science 16 (4), p. 369–386.

Mackereth, F.J.H., **1958**. A portable core sampler for lake deposits. Limnology and Oceanography 3, p. 181-191.

Maev, E.G., and Karpychev, Y.A., **1999**. Radiocarbon dating of bottom sediments in the Aral Sea age of deposits and sea level fluctuations. Water Resources 26 (2), p. 212–220.

Martius, C., Lamers, J., Ibrakhimov, M., and Vlek, P.L.G., **2004**. Towards a sustainable use of natural resources in the Aral Sea Basin. In: Bogena, H., Hake, J.-F. and H. Vereecken (eds.). Water and Sustainable Development. Schriften des Forschungszentrums Jülich. Reihe Umwelt/Environment 48, p. 117–134.

McManus, J. F., Oppo, D. W., Cullen, J. L., **1999**. A 0.5-million-year record of millennial-scale climatic variability in the North Atlantic. Science 283, p. 971-975.

Melack, J.M., Jellison, R., and Herbst, D.B. (editors), **2003**. Saline Lakes. Kluwer Academic Publisher, Boston, 360 pp.

Michalopoulos, P., Aller, R.C., and Reeder, R.J., **2000**. Conversion of diatoms to clays during early diagenesis in tropical, continental shelf muds. Geology 28 (2), p. 1095–1098.

Micklin, P., **2007**. The Aral Sea disaster. The Annual Review of Earth and Planetary Science 35, p. 47-72.

Milius S., **2008**. New dating finds oldest coral yet. Science News 173 (9), 142 pp.

Mirabdullayev, I.M., Joldasova, I.M., Mustafaeva, Z.A., Kazakhbaev, S., Lyubimova, S.A., and Tashmukhamedov, B.A., **2004**. Succession of the ecosystems of the Aral Sea during its transition from oligohaline to polyhaline water body. Journal of Marine Systems 47, p. 101–107.

Montagna, P., McCulloch, M., Taviani, M., Mazzoli, C., and Vedrell, B., **2006**. Phosphorus in Cold-Water Corals as a Proxy for Seawater Nutrient Chemistry. Science 312 (5781), p. 1788–1791.

Morley, J.J., and Heusser, L.E., **1997**. Role of orbital forcing in east Asian monsoon climates during the last 350 kyr : Evidence from terrestrial and marine climate proxies from core RC14-99. Paleoceanography 12 (3), p. 483–493.

Müller, G., Nkusi, G., and Schöler, H.F., **1996**. Natural Organohalogens in Sediments. Journal für Praktische Chemie/Chemiker-Zeitung 338 (1), p. 23–29.

Müller, R.D., Roest, W.R., Royer, J-Y., Gahagan, L.M., and Sclater, J.G., **1997**. Digital isochrons of the world's ocean floor. Journal of Geophysical Research 102, B2, p. 3211–3214.

Müller, J., Oberhänsli, H., Melles, M., Schwab, M., Rachold, V., and Hubberten, H.-W., **2001**. Late Pliocene sedimentation in Lake Baikal: implications for climatic and tectonic change in SE Siberia. Palaeogeography, Palaeoclimatology, Palaeoecology 174 (4), p. 305–326.

Munda, I.M., **2005**. Seasonal fouling by diatoms on artificial substrata at different depths near Piran (Gulf of Trieste, Northern Adriatic). Acta Adriatica 46 (2), p. 137–157.

NeWater project report, **1995.** Transboundary diver basin management regimes: The Amu Darya basin cae study. Ecologic – Institute for International and European Environmental Policy, Berlin, Germany, 27 pp.

Nurtaev, B., **2004**. Aral Sea Basin evolution: Geodynamic aspect. In: Nihoul, J.C.J., Zavialov, P.O., and Micklin, P.P. (eds.), Dying and Dead Seas climatic versus anthropic causes. Proceedings of the NATO Advanced Research Workshop. NATO Science Series: IV: Earth and Environmental Science 36, Berlin, Springer-Verlag, 91-97 pp.

Oberhänsli, H., and Mackay, A.W., **2005**. Introduction to "Progress towards reconstructing past climate in Central Eurasia, with special emphasis on Lake Baikal". **2005**, Global and Planetary Change 46, p. 1–7.

Oberhänsli, H., Weise, S.M., Stanichny, S., **2009**. Oxygen and hydrogen isotopic water characteristics of the Aral Sea, Central Asia. Journal of Marine Systems 76, p. 310–321.

Okada, A., Yabuki, S., and Liu, C-Q., **1994**. Salt mineralization in saline lands around the desert areas in Xinjiang, China. RIKEN Review 5, p. 3–4.

Oldfield, F., **2005**. Environmental Change: Key Issues and Alternativ Perspectives. Cambridge University Press, Cambridge, United Kingdom and New York, NY, USA, 363pp.

Orland, I.J., Bar-Matthews, M., Kita, N.T., Ayalon, A., Matthews, A., and Valley, J.W., **2009**. Quarternery Research 71, p. 27-35.

Paeth, H., Scholten, A., Friederichs, P., and Hense, A., **2008**. Uncertainties in climate change prediction: El Nino-Southern Oscillation and monsoons. Global and Planetary Change 60, p. 265–288.

Parsons, M. L., Dortch, G., Turner, R.E., and Rabalais, N.N., **1999**. Salinity history of coastal marshes reconstructed from diatom remains. Estuaries 22 (4), p. 1078-1089.

Peck, J.A., King, J.W., Colman, S.M., and Kravchinsky, V.A., **1994**. A rock-magnetic record from lake Baikal, Siberia - Evidence for Late Quaternary climate change, Earth Planetary Sci. Letters 122, p. 221–238.

Peinerud, E.K., Ingri, J., and Ponter, C. **2001**. Non-detrital Si concentrations as an estimate of diatom concentrations in lake sediments and suspended material. Chemical Geology 177, p. 229–239.

Peneva, E.L., Stanev, E.V., Stanychni, S.V., Salokhidinov, A., and Stulina, G., **2004**. The recent evolution of the Aral Sea level and water properties: analysis of satellite, gauge and hydrometeorological data. Journal of Marine Systems 47, p. 11–24.

Pestrea S., Blanc-Valleron M.-M., and Rouchy J.-M. **2002**. Les assemblages de diatomées des niveaux infra-gypseux du Messinien de Méditerranée (Espagne, Sicile, Chypre), in Néraudeau D., and Goubert E. (eds), l'Événement messinien : approches paléobiologiques et paléoécologiques. Geodiversitas 24 (3), p. 543–583.

Petit, J.R., Jouzel, J., Raynaud, D., Barkov, N.I., Barnola, J.-M., Basile, I., Bender, M., Chappellaz, J., Davis, M., Delaygue, G., Delmotte, M., Kotlyakov, V.M., Legrand, M., Lipenkov, V.Y., Lorius, C., Pépin, L., Ritz, C., Saltzman, E., and Stievenard, M., **1999**. Climate and atmospheric history of the past 420,000 years from the Vostok ice core, Antarctica. Nature 399, p. 429–435.

Prokopenko, A.A., Karabanov, E.B., Williams, D.F., Kuzmin, M.I., Shackleton, N.J., Crowhurst, S.J., Peck, J.A., Gvozdkov, A.N., and King, J.W., **2001a**. Biogenic silica record of the Lake Baikal response to climatic forcing during the Brunhes, Quaternary Res. 55, p. 123–132.

Prokopenko, A.A., Williams, D.F., Karabanov, E.B., and Khursevich, G.K., **2001b**. Continental response to Heinrich events and Bond cycles in sedimentary record of Lake Baikal, Siberia, Global Planetary Change 28, p. 217–226.

Prokopenko, A.A., Hinnov, L.A., Williams, D.F., and Kuzmin, M.I., **2006**. Orbital forcing of continental climate during the Pleistocene: a complete astronomically tuned climatic record from Lake Baikal, SE Siberia. Quaternary Science Reviews 25 (23-24), p. 3431–3457.

Rahmstorf, S., **2001**. Climate: Abrupt. In: Encyclopedia of Ocean Sciences, edited by J. Steele, S. Thorpe, and K. Turekian, Academic Press, London, p. 1–6.

Reed, J.M., **1998**. Diatom preservation in the recent sediment record of Spanish saline lakes: implications for palaeoclimate study. Journal of Paleolimnology 19, p. 129–137.

Reinhardt, Ch., Wünnemann, B., and Krivonogov, S.K., **2008**. Geomorphological evidence for the Late Holocene evolution and the Holocene lake level maximum of the Aral Sea. Geomorphology 93, p. 302–315.

Resende, P., Azeiteiro, U.M., Gonçalves, F., and Pereira, M.J., **2007**. Distribution and ecological preferences of diatoms and dinoflagellates in the west Iberian Coastal zone (North Portugal). Acta Oecologica 32, p. 224–235.

Richardson, T.L., Gibson, C.E., and Heaney, S.I., **2000**. Temperature, growth and seasonal succession of phytoplankton in Lake Baikal, Siberia. Freshw. Biol. 44, p. 431–440.

Richey, J.N., Poore, R.Z., Flower, B.P., and Quinn, T.M., **2007**. A 1400-year multi-proxy record of climate variability from the Northern Gulf of Mexico. Geology 35 (5), p. 423–326.

Rioual, P., and Mackay, A.W., **2005**. A diatom record of centennial resolution for the Kazantsevo Interglacial stage in Lake Baikal (Siberia), Global Planetary Change 46, p. 199–219.

Round, F. E., Crawford, R.M., and Mann, D.G., **1990**. The Diatoms. Cambridge University Press, Cambridge. 747 pp.

Sakai, T., Minoura, K., Soma, M., Tani, Y., Tanaka, A., Nara, F., Itoh, N., and Kawai, T., **2005**. Influence of climate fluctuation on clay formation in the Baikal drainage basin. J. Paleolimnology 3, p. 105–121.

Sampei, Y., and Matsumoto, E., **2001**. C/N ratios in a sediment core from Nakaumi Lagoon, southwest Japan. Usefulness as an organic source indicator. Geochem. J. 35 (3), p. 189–205.

Sapota, T., Aldahan, A., Possnert, G., Peck, J., king, J., Prokopenko, A., and Kuzmin, M., **2004**. A late Cenozoic Earth´s crust and cliamte dynamics record from Lake Baikal. Journal of Paleolimnology 32, p. 341–349.

Sapozhnikov, F.V., Simakova, U.V., and Ivanishcheva, P.S., **2009**. Modern assemblage changes of benthic algae as a result of hypersalinisation of the Aral Sea. Journal of Marine Systems 76 (3), p. 343–358.

Savoskul, O.S., and Solomina, O.N., **1996**. Late Holocene glacier variations in the frontal and inner ranges of Tian Shan, Central Asia. The Holocene 6, p. 25–35.

Sawai, Y., Horton, B.P., and Nagumo, T., **2004**. The development of a diatom-based transfer function along the Pacific coast of eastern Hokkaido, northern Japan – an aid in paleoseismic studies of the Kuril subduction zone. Quarternaty Science Reviews 23, p. 2467–2483.

Schiemann, R., Glazirina, M.G., Schär, Ch., **2007**. On the relationship between the Indian summer monsoon and river flow in the Aral Sea basin. Geophysical Research Letters 34, p. 1-6.

Schneider, D.A., Backman, J., Curry, W.B., and Possnert, G. **1996**. Paleomagnetic Constraints on Sedimentation Rates in the Eastern Arctic Ocean. Quarternary Research 46 (1), p. 62–71.

Schrader, H., and Gersonde, R., **1978**. The late Messinian Mediterranean brackish to freshwater environment diatom floral evidence, In Zachariasse et al. Microplaeontological counting methods, Hsü, K., Montadert, L., et al. Init. Repts DSDP, 42 (Pt. 1): Washington (U.S. Govt. Printing Office), p. 761–775.

Schutter, J., and Dukhovny, V. (eds.), **2003**. South PreAralie - new perspectives. Project: Science for Peace, Ekotec Resource. SIC ICWC, Tashkent, 150 pp.

Scourse, J.D., Hall, I.R., McCave, I.N., Young, J.R., and Sugdon, C., **2000**. The origin of Heinrich layers: evidence from H2 for European precursor events. Earth and Planetary Science Letters 182, p. 187–195.

Shichi, K., Kawamuro, K., Takahara, H., Hase, Y., Maki, T., and Miyoshi, N., **2007**. Climate and vegetation changes around Lake Baikal durign the last 350,000 years. Palaeogeography, Palaeoclimatology, Palaeoecology 248, p. 357–375.

Simonsen, R., **1962**. Untersuchungen zur Systematik and Okologie der Westlichen Ostsee. Int. Revue Hydrobiol .,Syst. Beih. 1, p. 1–144.

Sims, P.A., Mann, D.G., and Medlin, L.K., **2006**. Evolution of the diatoms: insights from fossil, biological and molecular data. Phycologia 45 (4), p. 361–402.

Siqueiros Beltrones, D.A., and López Fuerte, F.O., **2006**. Epiphytic diatoms associated with red mangrove (Rhizophora mangle) prop roots in Bahía Magdalena, Baja California Sur, Mexico. Rev. Biol. Trop. (Int. J. Trop. Biol.) 54 (2), p. 287–297.

Smol, J.P., **1987**. Methods in Quarternary ecology: Freshwater algae. Geoscience Canada 14 (4), p. 208–217.

Smol, J.P., and Cumming, B.F., **2000**. Tracking long-term changes in cliamte using algal indicators in lake sediments – review. J. Phycol. 36, p. 986-1011.

Solotchina, E.P., Prokopenko, A.A., Kuzmin, M.I., Solotchin, P.A., and Zhdanova, A.N., **in press**. Climate signals in sediment mineralogy of Lake Baikal and Lake Hovsgol during the LGM-Holocene transition and the 1-Ma carbonate record from the HDP-04 drill core. Quaternary International (2009).

Sorrel, P., Popescu S.-M., Head, M.J., Suc, J.P., Klotz, S., and Oberhänsli, H., **2006**. Hydrographic development of the Aral Sea during the last 2000 years based on a quantitative analysis of dinoflagellate cysts. Palaeogeography, Palaeoclimatology, Palaeoecology 234, p. 304–327.

Sorrel, P., Oberhänsli, H., Boroffka, N., Nourgaliev, D., Dulski, D., and Röhl, U., **2007a**. Control of wind strength and frequency in the Aral Sea basin during the late Holocene. Quaternary Research 67 (3), p. 371–382.

Sorrel, P., Popescu, S.-M., Klotz, S., Suc, J.-P., and Oberhänsli, H., **2007b**. Climate variability in the Aral Sea basin (CentralAsia) during the late Holocene based on vegetation changes. Quaternary Research 67 (3), p. 357-370.

Stager, J.C., Cumming, B.F., and Meeker, L.D., **2003**. A 10,000 year high-resolution diatom record from Pilkington Bay, Lake Victoria, East Africa. Quaternary Research 59, p. 172–181.

Šucha, V., **2001**. Clays in geological processes (in czech: Íly v geologických procesoch). Acta Geologica Univ. Com. Séria Monografie, 159 pp.

Sun, Y., S.C. Clemens, Z. An, and Z. Yu. **2006**. Astronomical timescale and palaeoclimatic implication of stacked 3.6-Myr monsoon records from the Chinese Loess Plateau. Quaternary Science Reviews, Vol. 25 p. 33–48.

Swann, G.E.A., Mackay, A.W., Leng, M.J., and Demory F., **2005**. Climatic change in Central Asia during MIS 3/2: a case study using biological responses from Lake Baikal, Global Planetary Change 46, p. 235–253.

Swann G.E.A., and Mackay A.W., **2006**. Potential limitations of biogenic silica as an indicator of abrupt climate change in Lake Baikal, Russia, J. Paleolimnol. 36, p. 81–89.

Sylvestre, F., Servant, M., Servant-Vildary, S., Causse, Ch., Fournier, M., and Ybert, J.-P., **1999**. Chronology on the Southern Bolivian Altiplano (18°–23°S) during Late-Glacial Time and the Early Holocene. Quaternary Research 51(1), p. 54–66.

Tarasov, P.E., Harrison, S.P., Saarse, L., Pushenko, M.Ya., Andreev, A.A., Aleshinskaya, Z.V., Davydova, N.N., Dorofeyuk, N.I., Efremov, Yu.V., Khomutova, V.I., Sevastyanov, D.V., Tamosaitis, J., Uspenskaya, O.N., Yakushko, O.F. and Tarasova, I.V, Ya, M., Elina, G.A., Elovicheva Ya. K., Filimonova, L.V., Gunova, V.S., Kvavadze, E.V., Nuestrueva, I.Yu., Pisareva, V.V., Shelekhova, T.S., Subetto, D.A., and Zernitskaya, V.P., **1996**. Lake Status Records from the Former Soviet Union & Mongolia: Documentation of the second version of the DATABASE, Paleoclimatology Publications Series Report #5, World Data Center -A for Paleoclimatology, 224 pp.

UNEP, 2005. Severskiy, I., Chervanyov, I., Ponomarenko, Y., Novikova, N.M., Miagkov, S.V., Rautalahti, E., Daler, D. Aral Sea, Global International Water Assessment Regional assessment 24. University of Kalmar, Kalmar, Sweden on behalf of United Nations Environment Programme, 71 pp.

UNESCO, 1999. Water related Aral Sea Basin vision for the year 2025. UNESCO Division of Water Sciences, 237 pp.

Valentini, K.L., Orolbaev, E.E., and Abylgazieva, A.K., **2004**. Water problems of Central Asia, Bishkek, 142 pp.

van Dam, H., Mertens, A., and Sinkeldam, J., **1994**. A coded checklist and ecological indicator values of freshwater diatoms from the Netherlands. Netherlands Journal of Aquatic Ecology 28 (1), p. 117–133.

von Grafenstein, U., Erlenkeuser, H., Brauer, A., Jouzel, J., and Johnsen, S., J. **1999**. A Mid-European Decadal Isotope-Climate Record from 15,500 to 5000 Years B.P. Scince 4, Vol. 284 (5420), p. 1654–1657.

von Rad, U., Schaaf, M., Michels, K.H., Schulz, H., Berger, W.H., and Sirocko, F., **1999**. A 5000-yr Record of Climate Change in Varved Sediments from the Oxygen Minimum Zone off Pakistan, Northeastern Arabian Sea, Quaternary Research 51 (1), p. 39–53.

Vos, P.C., and Wolf, H., **1993**. Diatoms as a tool for reconstructing sedimentary environments in coastal wetlands; methodological aspects. Hydrobiologia 269/270, p. 285–296.

Wasmundl, N., Breuel, G., Edler, L., Kuosa, H., Olsonen, R., Schultz, H., Pys-Wolska, M., Wrzolek, L., **1996**. CHAPTER IV - State of the marine Environment of the Baltic Sea Regions. 3rd Periodic Assessment of the State of the Marine Environment of the Baltic Sea, p. 27–45.

Wetzel, R. G., **2001**. Limnology – Lake and River Ecosystems. Elsevier, 1006 pp.

Williams, D.F., Peck, J., Karabanov, E.B., Prokopenko, A.A., Kravchinsky, V., King, J., and Kuzmin, M.I. **1997**. Lake Baikal Record of Continental Climate Response to Orbital Insolation Durign the Past 5 Million Years. Science 278, p. 1114–1117.

Wilson, G.P., Lamb, A.L., Leng, M.J., Gonzales, S., and Huddart, D. **2005**. $\delta^{13}C$ and C/N as potential coastal palaeoenvironmental indicators in the Mersey Estuary, UK. Guarternary Science Reviews 24: 2015–2029.

Winder, M., Reuter, J.E.E., and Schladow, S.G.G., **2009**. Lake warming favours small-sized planktonic diatom species. Proc Biol Sci 276(1656), p. 427–435.

Witak, A., and Jankowska, D., **2005**. The Vistula Lagoon evolution based on diatom records. Baltica 18 (2), p. 68–76.

Witak, M., Jankowska, D., and Piekarek-Jakowska, H., **2006**. Holocene diatom biostratigraphy of the southwestern Gulf of Gdansk, Sountern Baltic Sea (Part 1). Oceanological and Hydrobiological Studies 35 (4), p. 307–329.

Witkowski, A., Broszinski, A., Bennike, O., Janczak-Kostecka., B., Jensen, A.B., Lemke, W., Endler, R., and Kuijpers, A., **2005**. Darss Sill as a biological border in the fossil record of the Baltic Sea: evidence from diatoms. Quarternary International 130, p. 97–109.

Wood, **1973**. Relations of phytoplankton to the marine habitat in the straits of Florida and adjacent areas. Nova Hedwigia 24, p. 665–814.

Yang, B., Bräuning, A., and Yafeng, S., **2003**. Late Holocene temperature fluctuation on the Tibetan Plateau. Quarternary Science Rviews 22, p. 2335–2344.

Yang, B., Bräuning, A., Dong, Z., Zhang, Z., and Keqing, J., **2008**. Late Holocene monsoonal temperate glacier fluctuations on the Tibetan Plateau. Global and Planetary Change 60, p. 126–140.

Yuan, D., Chemg, H., Edwards, R.L., Dykoski, C.A., Kelly, M.J., Zhang, M., Qing, J., Lin, Y., Wang, Y., Wu, J., Dorale, J.A., An, Z., and Cai, Y., **2004**. Timing, Duration, and transitions of the last Interglacial Asian Monsoon. Science 304, p. 575–578.

Yuretich, R., Melles, M., Sarata, B., and Grobe, H., **1999**. Clay minerals in the sediments of Lake Baikal: A useful climate proxy. Journal of Sedimentary Research 69, p. 588–596.

Zalat, A., and Vildary, S.S., **2007**. Environmental change in Northern Egyptian Delta lakes during the late Holocene, based on diatom analysis. Journal of Paleolimnology 37, p. 273–299.

Zavialov, P.O., **2005**. Physical Oceanography of the Dying Aral Sea. Springer-Verlag / Praxis, Chichester, UK, 158 pp.

Zavialov, P.O., Ni, A.A., Kudyshkin, T.V., Kurbaniyazov, A.K., and Dikarev, S.N., **2009**. Five years of field hydrographic research in the Large Aral Sea (2002–2006). Journal of Marine Systems 76, p. 263–271.

Zelený, V., **2005**. Systematic botany; (in Czech). Česká Zemědělská Univerzita v Praze.

Zhamoida, V.A., Butylin, V.P., Popova, E.A., and Aladin, N.V., **1997**. Recent sedimentation processes in the Northern Aral Sea. International Journal of Salt Lake Research 6 (1), p. 67–81.

Zhao, Z., Yu, Z., Chen, F., Liu, X., and Ito, E., **2008**. Sensitive response of desert vegetation to moisture change based on a near-annual resolution pollen record from Gahai Lake in the Qaidam Basin, northwest China. Global and Planetary Change 62 (1-2), p. 107–114.

Online sources

bww.irk.ru, in the chapter 4.3.2: http://www.bww.irk.ru/baikalclimate/baikalclimate.html.

commons.wikimedia.org, in attachment 2.1:
http://commons.wikimedia.org/wiki/File:Arel_Sea.jpg

earthobservatory.nasa.gov, in the attachment 2.3:
http://earthobservatory.nasa.gov/IOTD/view.php?id=37626

eosnap.com, in the attachment 2.3:
http://www.eosnap.com/public/media/2009/02/aralsea/200090215-aralsesa-full.jpg

Halfman, B., **2006** – online. Lake Sediments. Available from:
http://fli.hws.edu/sos/main/documents/sosmanual/lake_sediments.pdf.

mapstor. com, in the chapter 4.2.3: http://mapstor.com/articles/topographic-maps-and-traveling/lake-baikal.html.

Laval, B., **2006** – online. Physical limnology – lake classification. Available from:
http://www.beltramiswcd.org/Aquatic%20Biology/Lake%20Classification.pdf.

Olney, M., **2002** – online. Diatoms. Available from:
http://www.ucl.ac.uk/GeolSci/micropal/diatom.html.

redorbit.com, in the attachment 2.3:
http://www.redorbit.com/modules/imglib/download.php?Url=/modules/imagegallery/gallery_images/0_93f7c531fd37dcb108eaae7307334d2a.jpg

Rohde, R.A., **2005** – online. Image: Milankovitch Variations.png. Available from:
http://www.globalwarmingart.com/wiki/Image:Milankovitch_Variations.png.

upload.wikimedia.org, in the attachment 2.3:
http://upload.wikimedia.org/wikipedia/commons/thumb/7/7b/Aralship2.jpg/800px-Aralship2.jpg

Williams, W.D., **2006** – online. The largest, highest and lowest lakes of the world: Saline lakes. Available from: http://lakes.chebucto.org/saline1.html.

Zanden, J.V., **2008** – online. Limnology – origin and morphology of lakes. Available from:
http://limnology.wisc.edu/courses/zoo315/lakeclassification08.pdf.

ATTACHMENTS

ATTACHMENTS

1. Core opening and sampling
2. Aral Sea
   - 2.1. Map of Aral Sea from 1853
   - 2.2. Aral Sea schrinkage from 1927 AD (geological map) to 2007 AD (satellite images).
   - 2.3. Aral Sea images:
   - 2.4. Core C2/2004, 434 cm
   - 2.5. Ostracod shells
   - 2.6. SEM images of diatom frustules
   - 2.7. List and photo tables of diatom species from Aral Sea
3. Baikal Lake
   - 3.1. Core 98-1-13, 0- 544 cm.
   - 3.2. SEM images of diatom frustules
   - 3.3. Photo tables of diatom species from Baikal Lake

1. CORE OPENING AND SAMPLING

a,b) core C2/2004, Aral Sea, photos taken in GFZ Potsdam by Kateřina Novotná and Anna Píšková, 2006, c,d) core VER98-1-13, Baikal Lake, photos taken in Institute of Geology AS CR by Stanislav Šlechta, 2003.

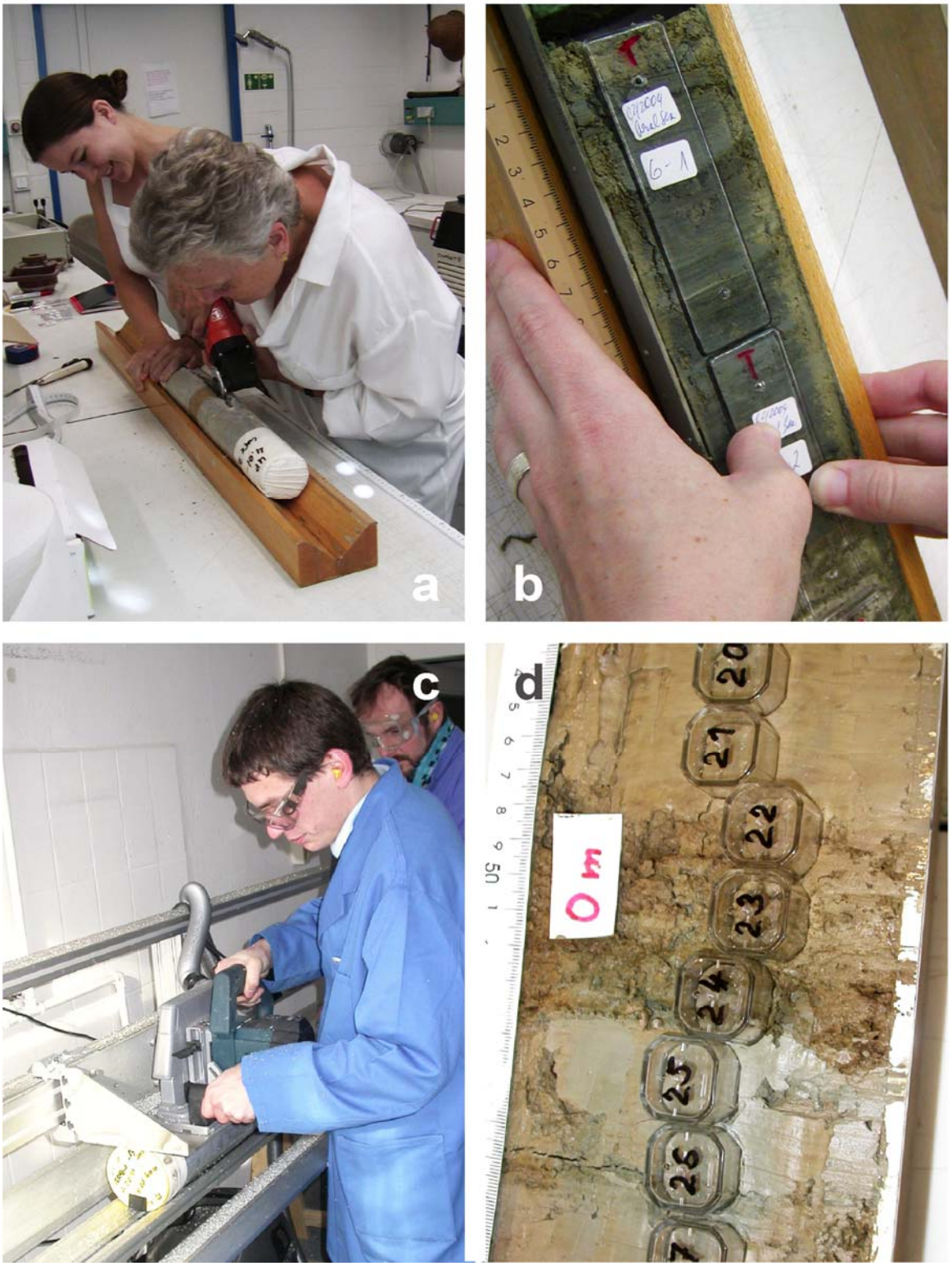

2. ARAL SEA

2.1. Map of Aral Sea from 1853

by Augustus Petermann in London for the Journal of the Royal Geographic Society in 1853, copy of the lithographed map based on the first Russian survey in 1848-49 (commons.wikimedia.org).

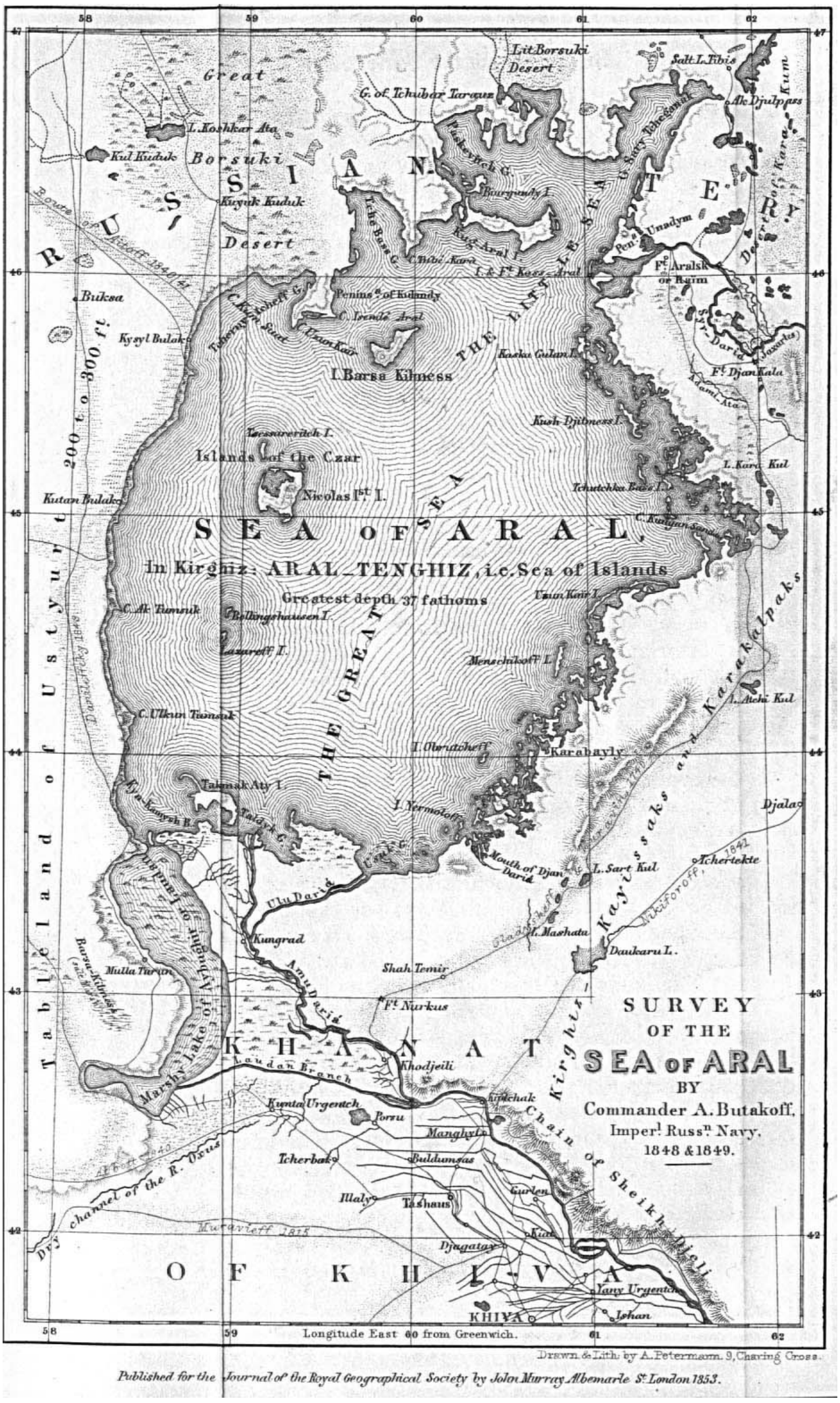

2.2. Aral Sea schrinkage from 1927 AD (geological map) to 2007 AD (satellite images).

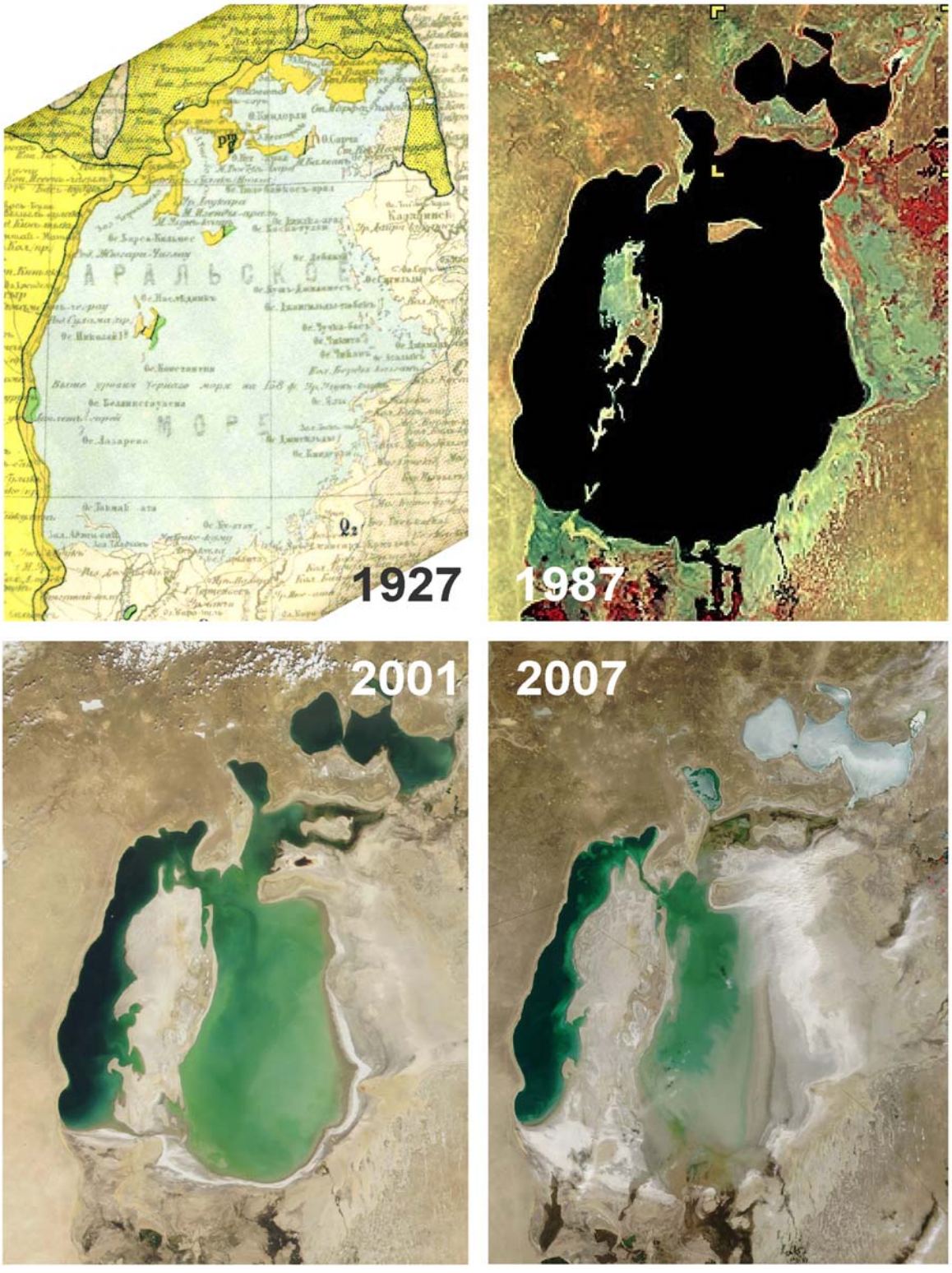

2.3. Aral Sea images:

a) dust storm (redorbit.com), b) snow cover acquired 15. 2. 2009 (eosnap.com), c) waveclouds acguired 12. 3. 2009 (earthobservatory.nasa.gov), d) abandoned ship (upload.wikimedia.org)

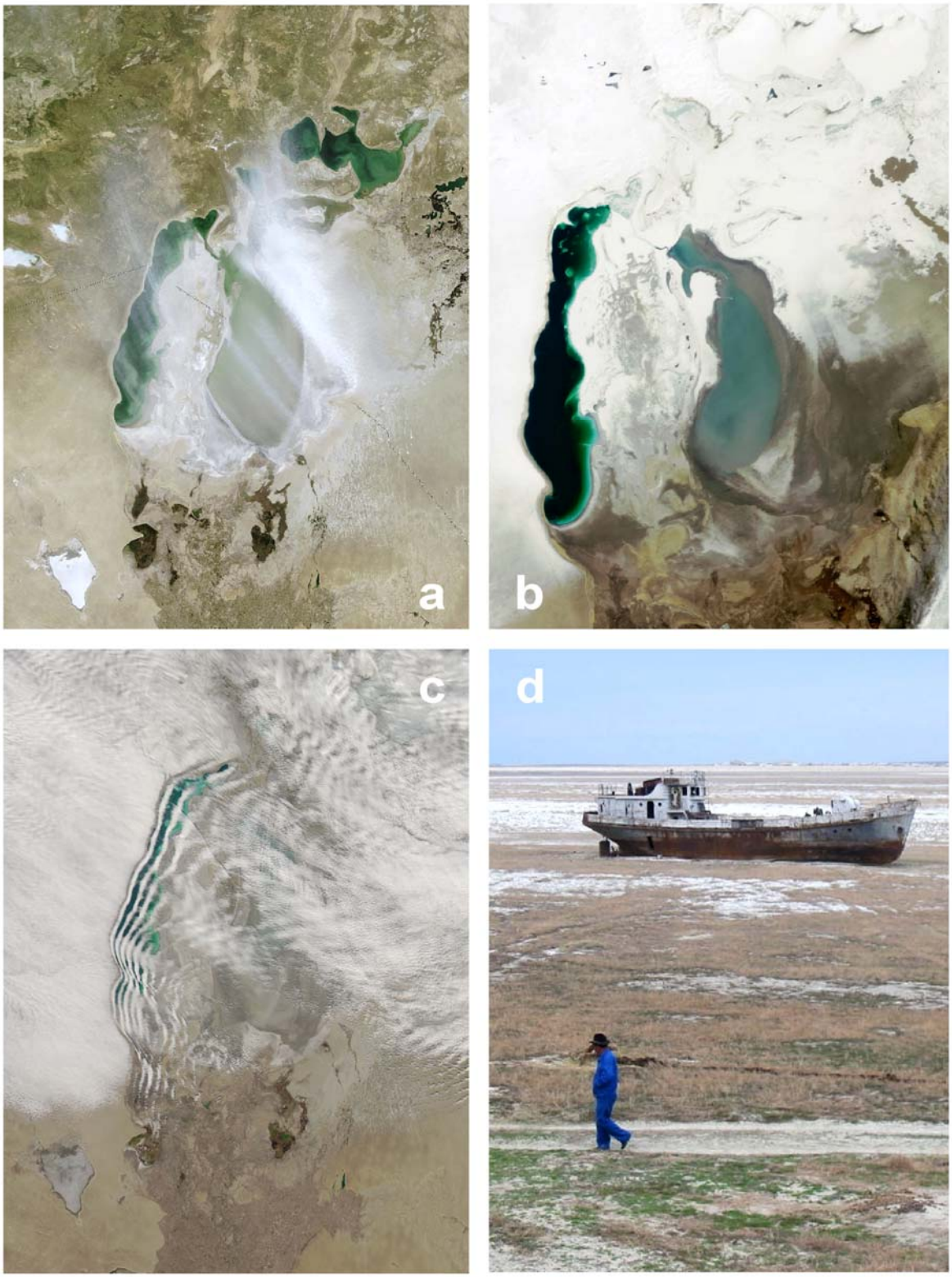

2.4. Core C2/2004, 434 cm

Photo taken in GFZ, Potsdam by Mgr. Kateřina Novotná, 2006. Modified by Anna Píšková, 2008.

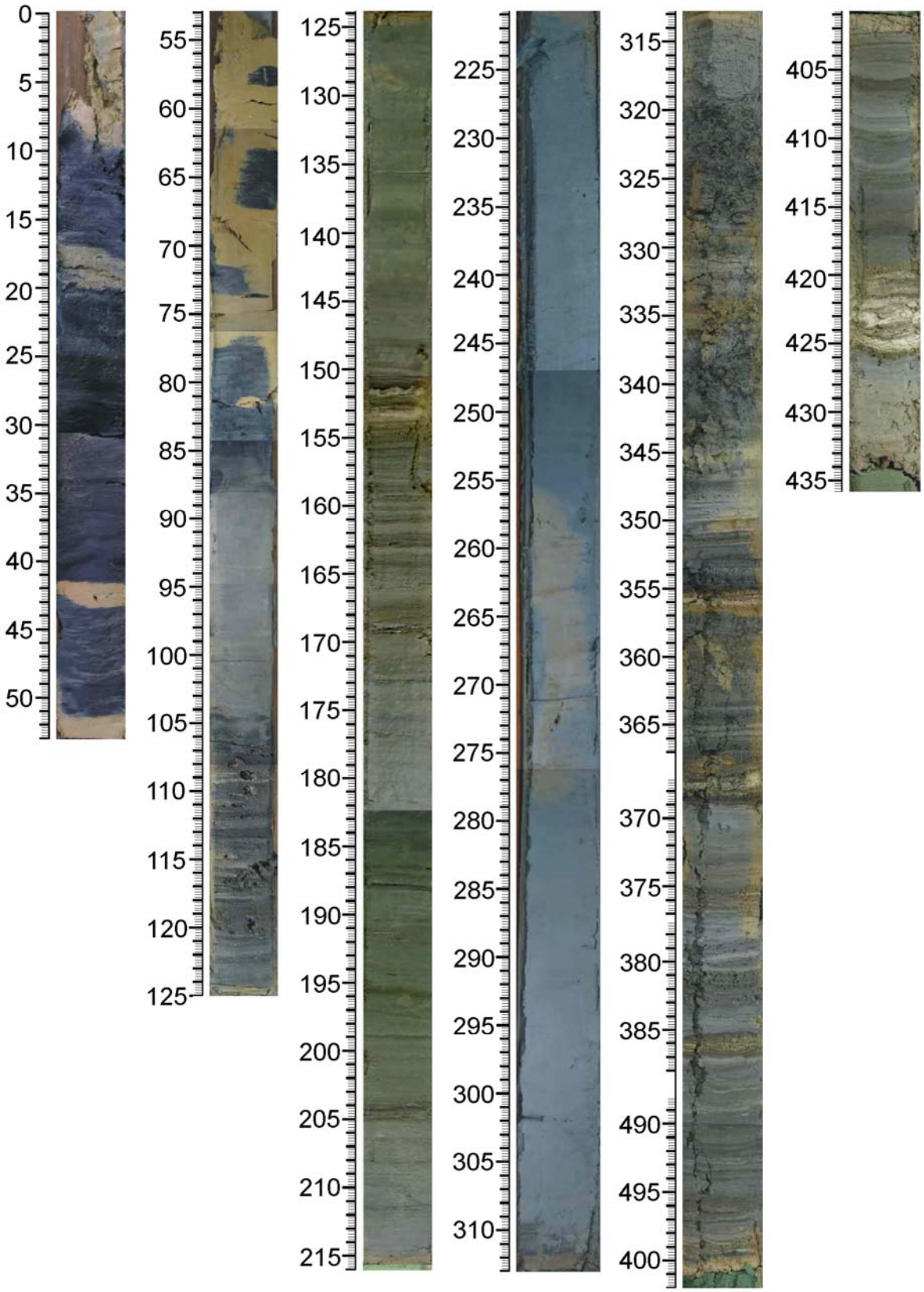

2.5. Ostracod shells

a, b) SEM images, c, d) Images from optical microscope: c)black and white shell, d) brownish spots on the white shells. Scale 200 µm.

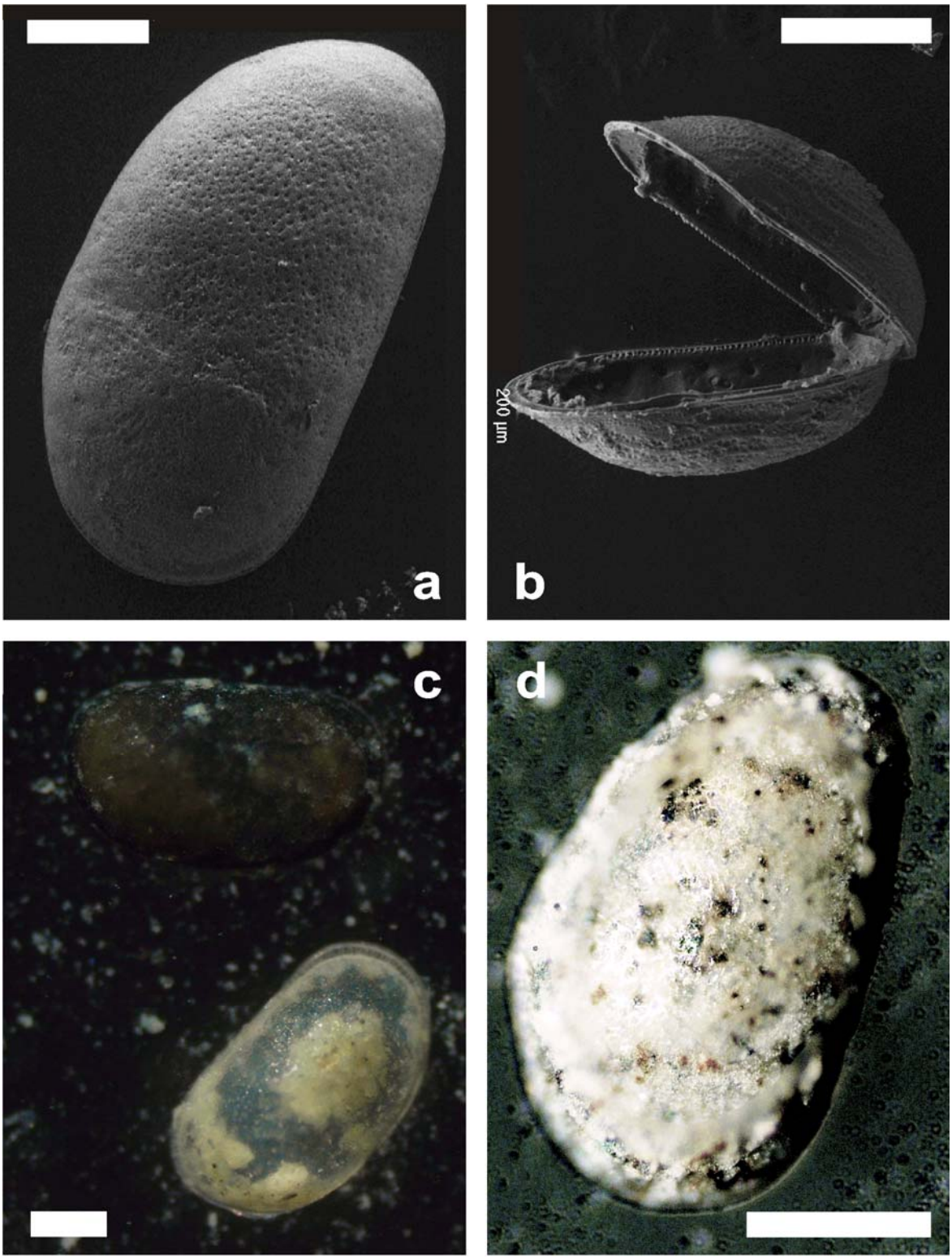

2.6. SEM images of diatom frustules

Actinocyclus octonarius: a) both valves, b) detail of the punctae structure (top right corner pseudonodus), c) Inner view to the frustule, d) detal of inner structures. Scale 5 µm.

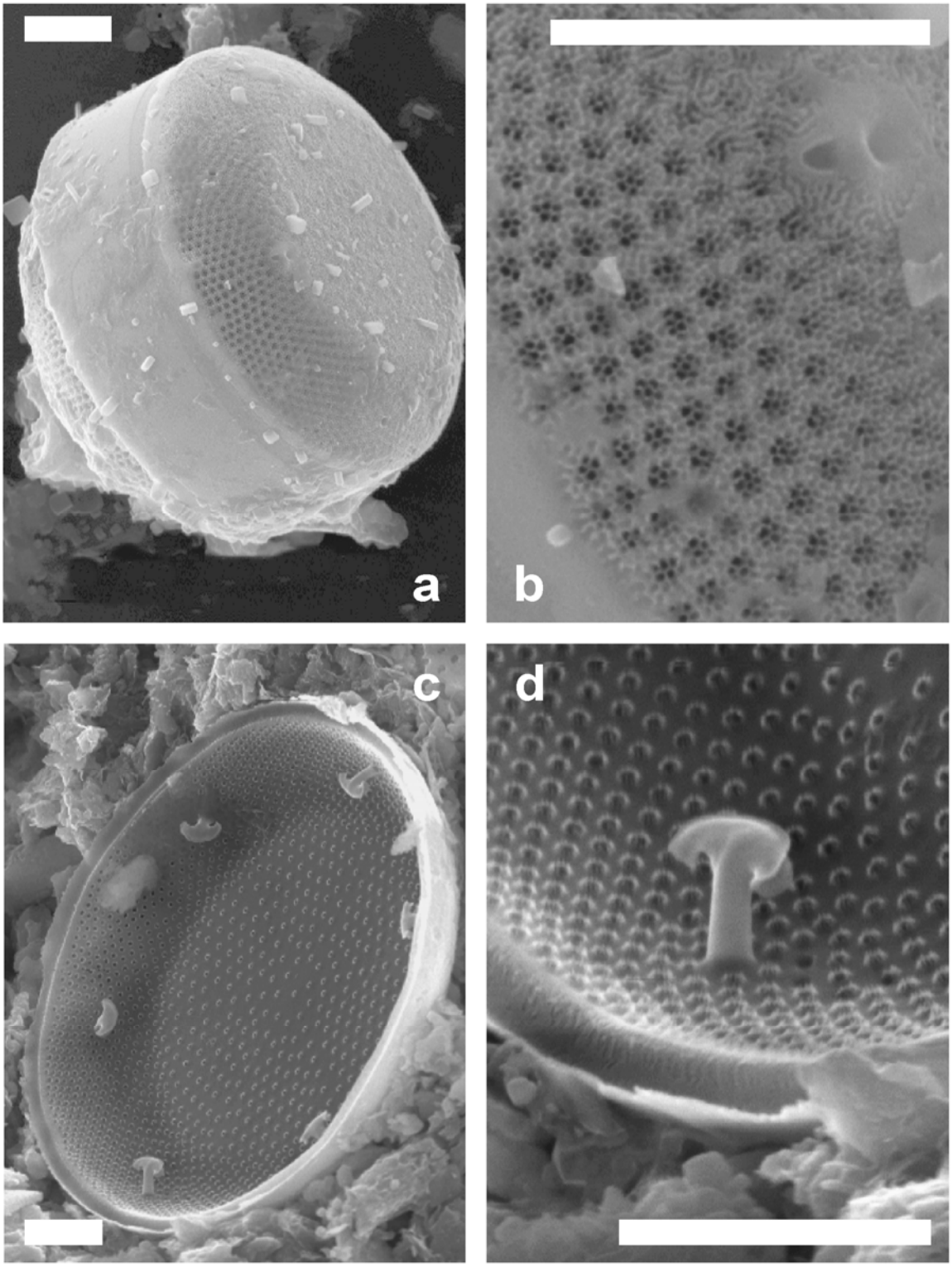

a,b) *Navicula digitoradiata*, c,d) *Diploneis bombus.* Scale 5 μm.

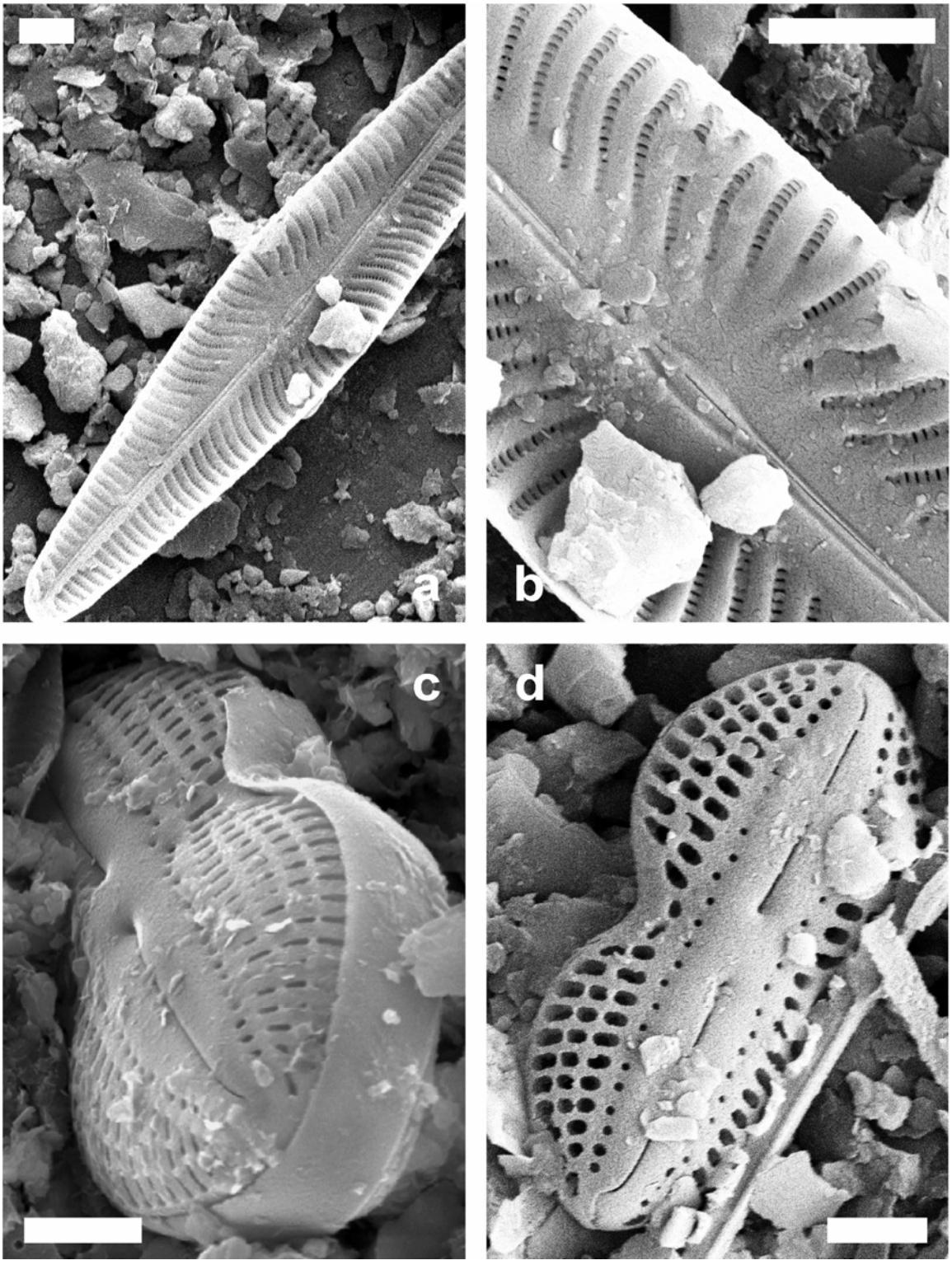

a,b) *Surirella fastuosa*, c,d) *Tryblionella compressa.* Scale 5 μm.

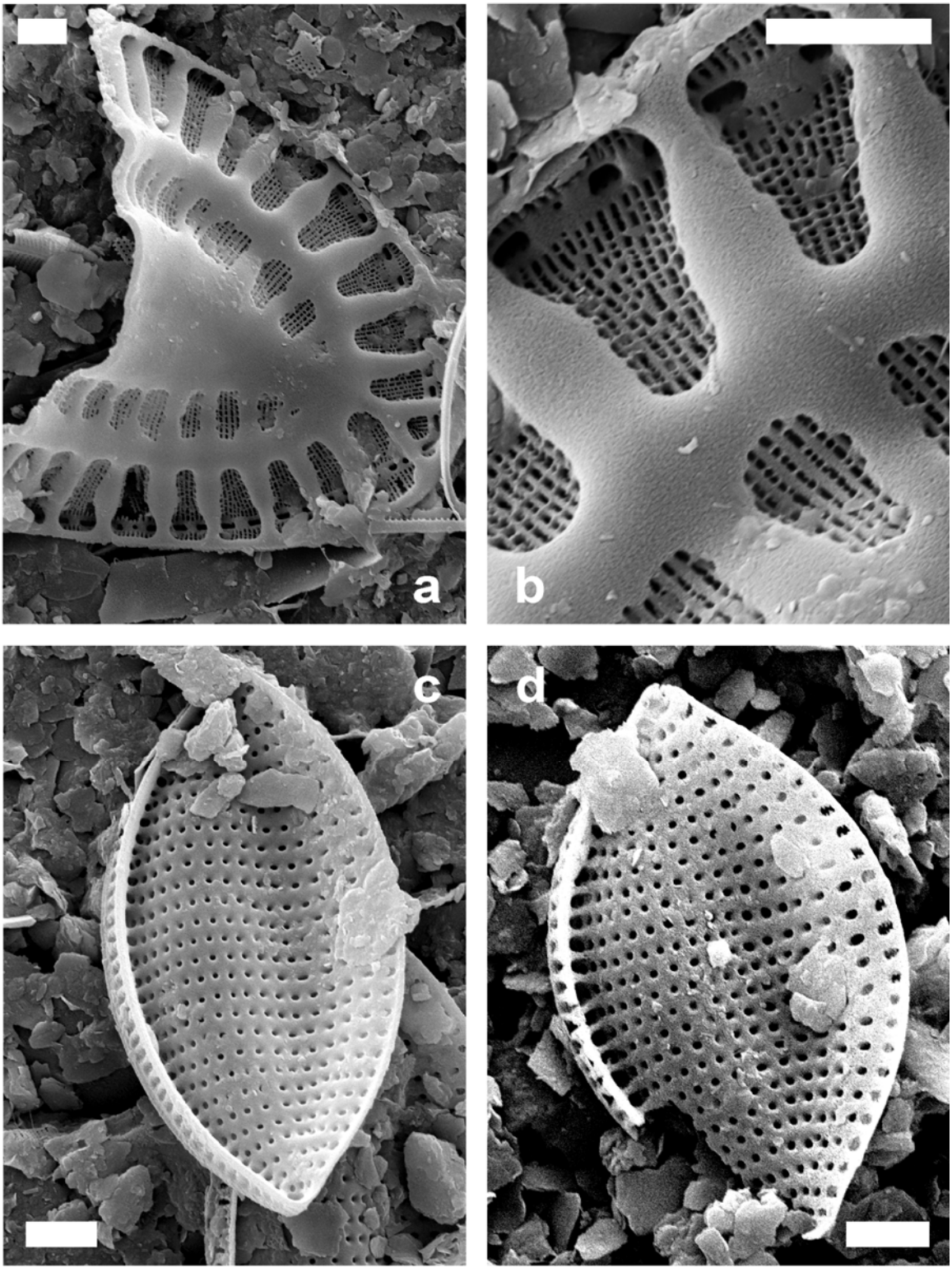

2.7. List and photo tables of diatom species from Aral Sea

A. Most of centric diatoms: *Actinocyclus*, *Thalassiosira*, *Aulacoseira*, and *Cyclotella* sp.

Actinocyclus octonarius Ehrenberg, *Thalassiosira baltica* (Grunow) Ostenfeld, *T. lacustris* (Grunow) Hasle, *T. proschkinae* Makarova, *Cylotella choctawhatcheeana* Prasad

B. *Nitzschia - Tryblionella* sp.

Nitzschia levidensis (W.Smith) Grunow in Van Heurck 1881, *N. amphibia* Grunow, *N. (Tryblionella) compressa* (Bailey) Boyer, *N. (Tryblionella) compressa var. elongata* Grunow) Lange-Bertalot, *N. fonticola* Grunow, *N. frustulum* (Kütz.) Grunow, *N. (Tryblionella) hungarica* Grunow, *N. insignis* Gregory, *N. littoralis G*runow, *N. navicularis* (Brébisson ex Kützing) Grunow, *N. obtusa* W. Smith, *N. sigma* (Kütz.) Grunow

C. *Diploneis*, *Amphora*, *Cocconeis* sp.

Diploneis bombus (Ehrenb.) Cleve, *D. ovalis* (Hilse) Cleve cf., *D. finnica* (Ehrenb.) Cleve 1891, *D. parma* Cleve 1891, *D. smithii* (Bréb.) Cleve, *Amphora communata* Grunow, *A. holsatica* Hustedt, *A. ovalis* Kützing, *A. pediculus (*Kütz.) Grunow, *A. coffeaformis* Kützing, *Cocconeis neodiminuta* Krammer, 1991, *C. placentula* Ehrenberg

D. *Navicula*, *Opephora*, *Rhopalodia*, *Cymbella* sp.

Navicula complanata Grunow, *N. digitoradiata* (Gregory) Ralfs in Pritchard (1861), *N. phyllepta* Kütz. 1844, *N. pygmaea* Kützing, *N. laterostrata* Hustedt, *Karayevia clevei* (Grunow in Cleve et Grunow), *Opephora krumbeinii* Witkowski, Witak & Stachura 1999, *O. olsenii* M. Müller, 1950, *Rhopalodia acuminata var. protracta* Grunow, *R. musculus* (Kützing) O. F. Müller, *Fragilaria brevistriata* Grunow

E. *Epithemia*, *Mastoglia*, *Grammatophora*, *Achnanthes* sp.

Epithemia adnata, (Kütz.) Bréb. 1838, *E. frickei,* Krammer, 1987, *E. turgida,* (Ehrenb.) Kütz. 1844, *Mastoglia braunii,* Grunow, *M. smithii,* Grunow, *Grammatophora marina,* Lyngbye, *Achnanthes brevipes* Agardh, *Petroneis marina* (Ralfs ex Pritchard) D.G. Mann

F. *Gyrosigma*, *Pleurosigma* sp.

Gyrosigma balticum (Ehrenb.) Rabenh. 1853, *G. scalproides* (Rabenhorst) Cleve, *G. Parkerii* (Harrison) Elmore 1921, *Pleurosigma elongatum* W. Smith, *P. salinarum,* Grunow

G. *Caloneis*, *Stauroneis* sp.

Caloneis latiuscula (Kütz.) Cleve 1938, *C. permagna* (Bailey) Cleve, *C. schumanniana var. biconstricta* Grunow, *C. amphisbaena* (Bory) Cleve, *Stauroneis phoenicenteron* Ehrenberg, *Petroneis humerosa* (Brébisson ex W. Smith) A. J. Stickle & D. G. Mann

H. *Surirella*, *Cymatopleura* sp.

Surirella fastuosa Ehrenberg, *Sur. ovalis* Bréb., *Sur. striatula* Turpin 1828, *Cymatopleura solea* Smith, *Tryblionella cocconeiformis* (Grunow) D.G. Mann 1990

A: 1, 3) *Actinocyclus octonarius*, 6, 7) *Actinocyclus spp.*, 2) *Thalasiossira lacustris*, 4) *T. baltica*, 8) *T. proschinae*, 5) *Aulacoseira spp.*, 9, 10, 11, 12) *Cyclotella spp.*, 11) *Cyclotella choctawhatcheena*

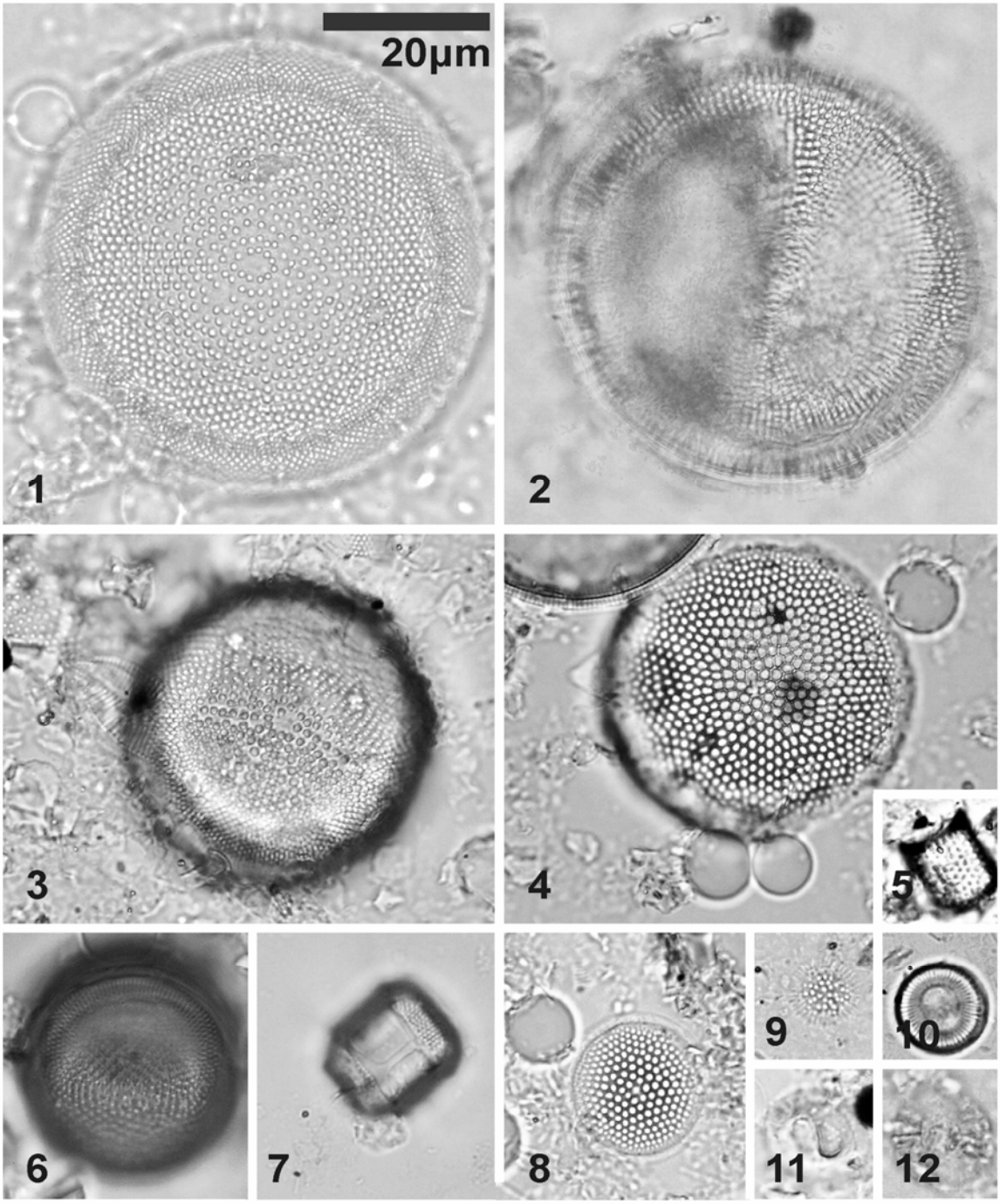

B: 13) *Nitzschia navicularis*, 14) *N. littoralis*, 15) *Tryblionella compressa*, 16) *T. compressa var. elongata*, 19) *T. compressa var. minor*, 17*) N. amphibia*, 18*) N. frustulum*, 20*) N. fonticula*, 21) *N. hungarica*, 22) *N. obtusa*, 23) *N. levidensis*, 24) *N. sigma*

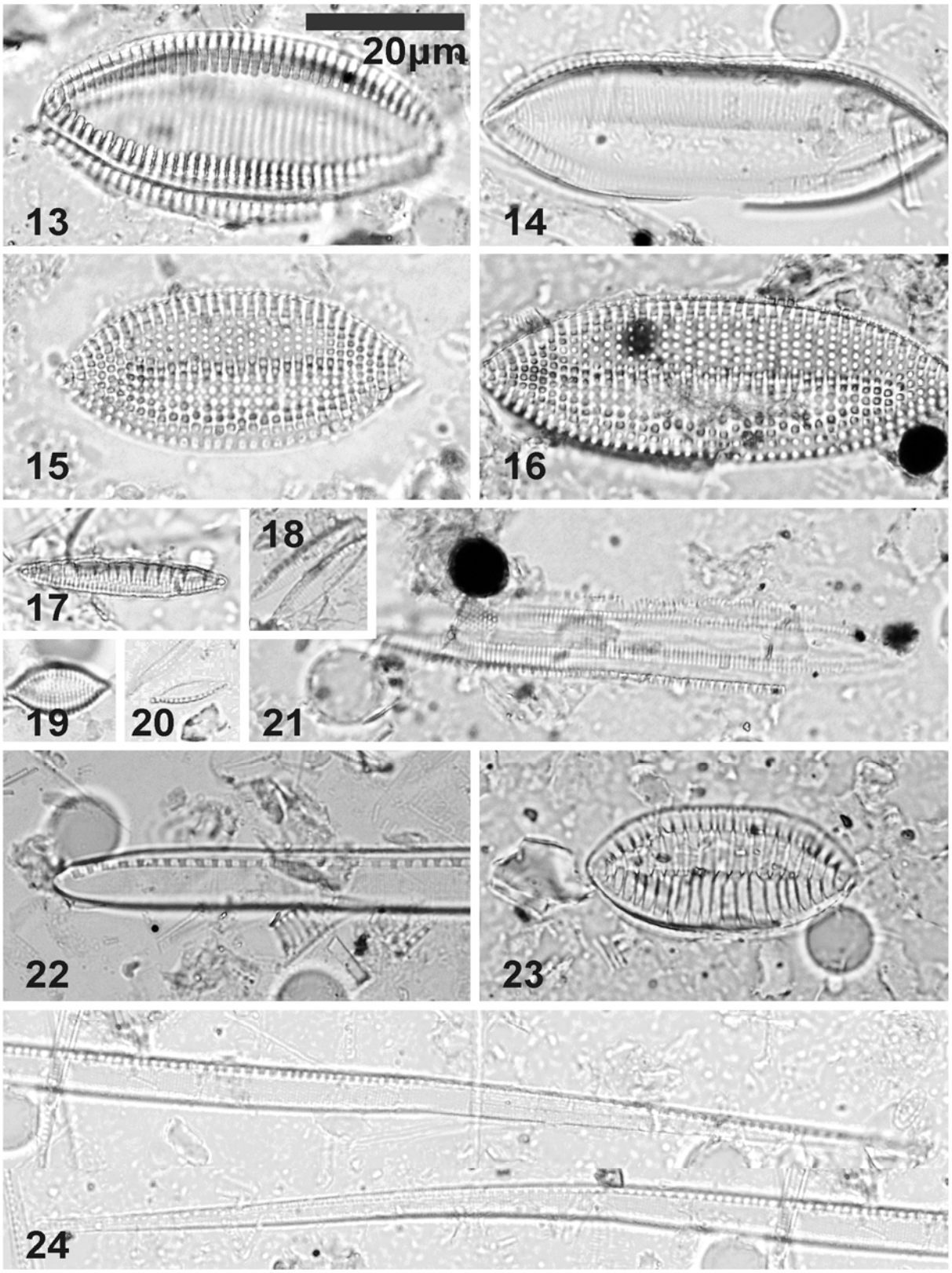

C: 25) *Diploneis bombus*, 26) *D. finnica*, 27) *D. ovalis*, 28) *D. smithii*, 30) *D. parma*, 29) *Amphora pediculus*, 31) *A. ovalis*, 32) *A. coffeaformis*, 34) *A. communata*, 35) *A. holsatica*, 36, 37) *Amphora* spp., 33) *Cocconeis placentula var. euglypta*, 38) *Cocconeis neodiminuta*

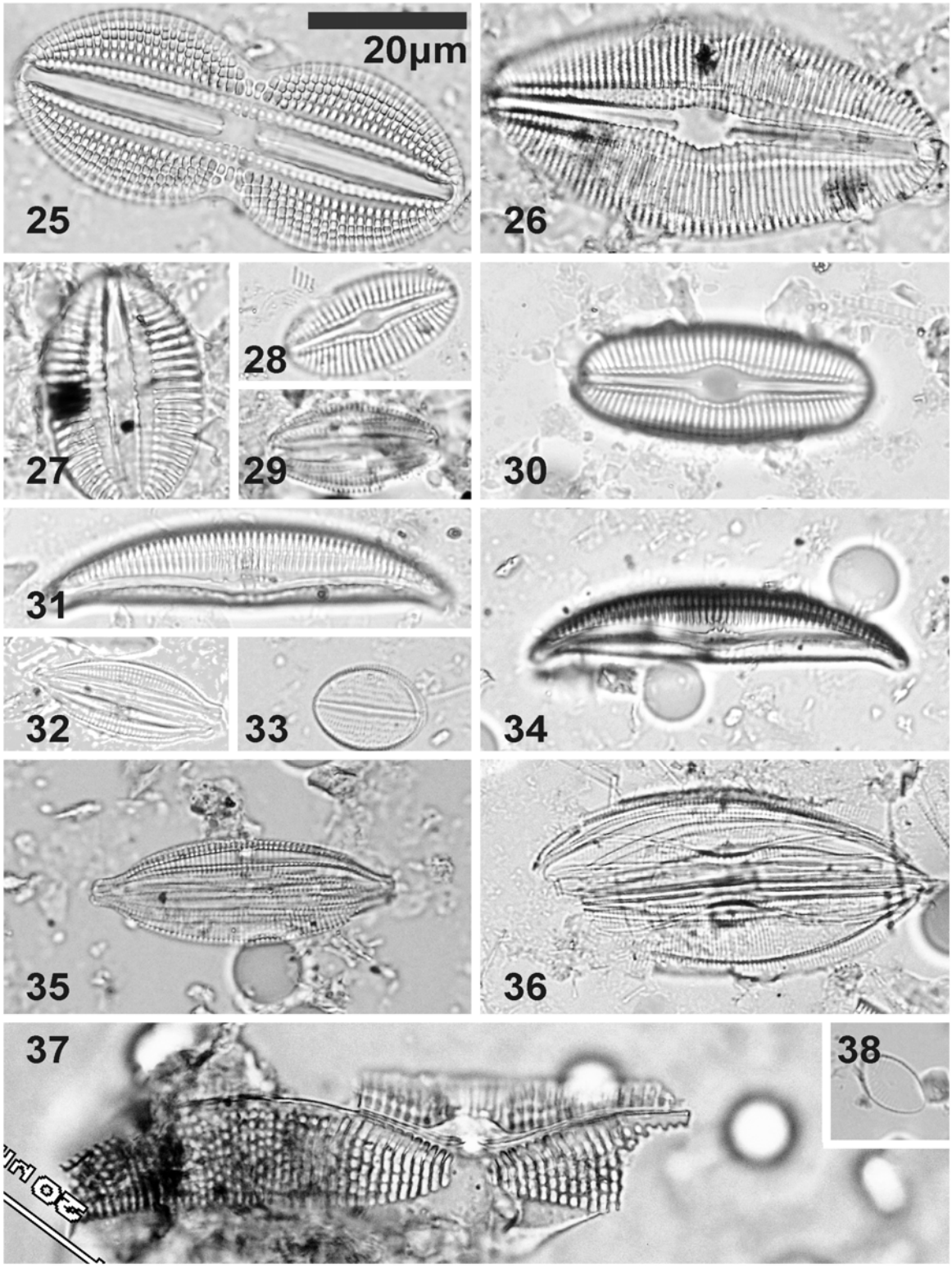

D: 39) *Navicula pygmaea*, 40) *N. digitoradiata*, 41) *Karaveia clevei*, 42, 47, 49, 50) *Navicula* spp., 43) *N. complanata*, 44) *N. laterostrata*, 46) *N. phyllepta*, 48) *Opephora krumbeii*, 51) *Rhopalodia acuminata var. protracta*, 52) *R. musculus*, 53) *Opephora olsneii*, 45, 54) *Cymbella* spp., 55) *Craticula* spp., 56) *Fragilaria brevistriata*

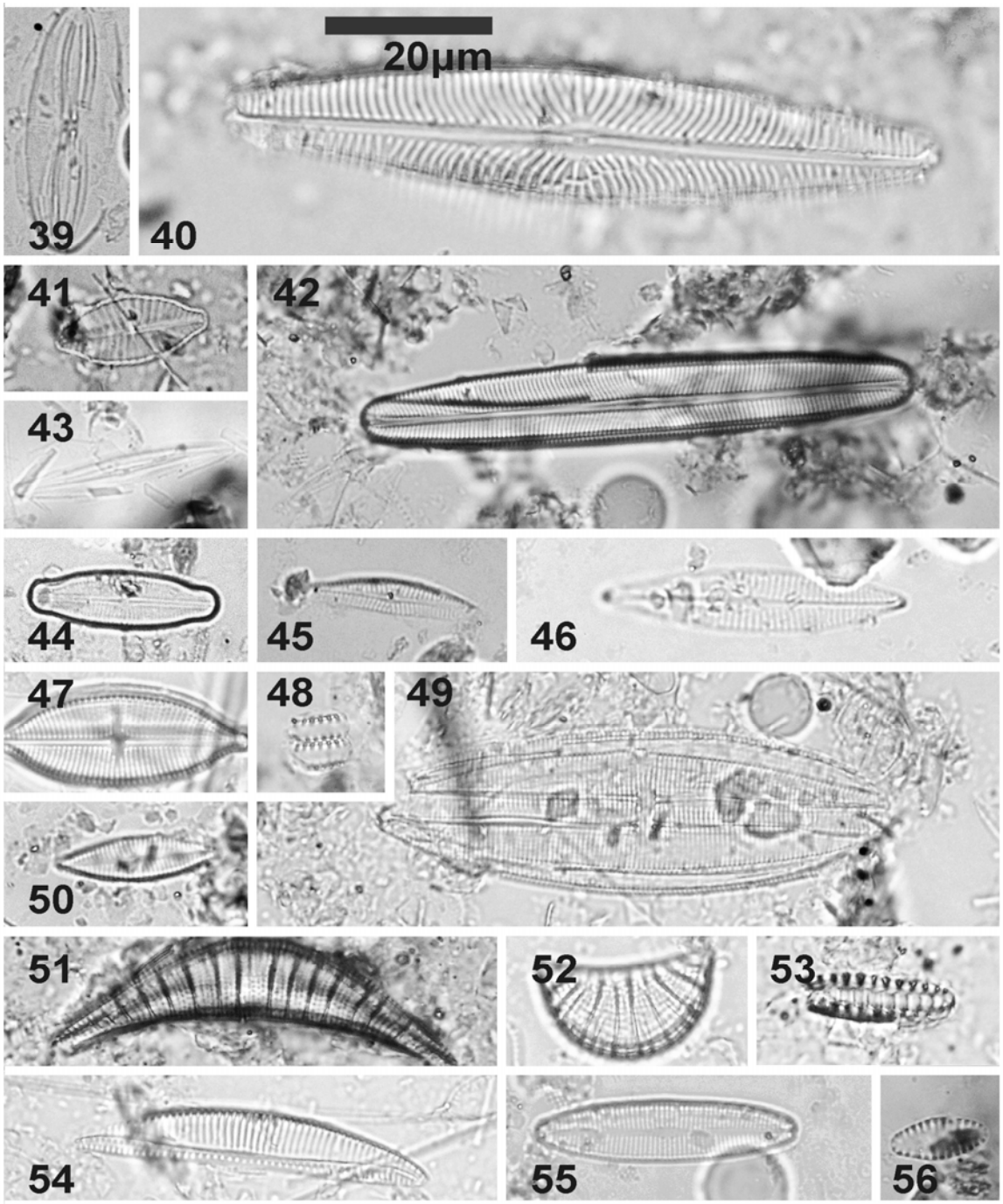

E: 57) *Epithemia turgida*, 58) *Petroneis marina*, 59) *Epithemia. adnata*, 60) *E. frickey*, 61) *Grammatophora marina*, 62) *Mastoglia braunii*, 64) *M. smithii*, 63, 65) *Achnanthes brevipes*

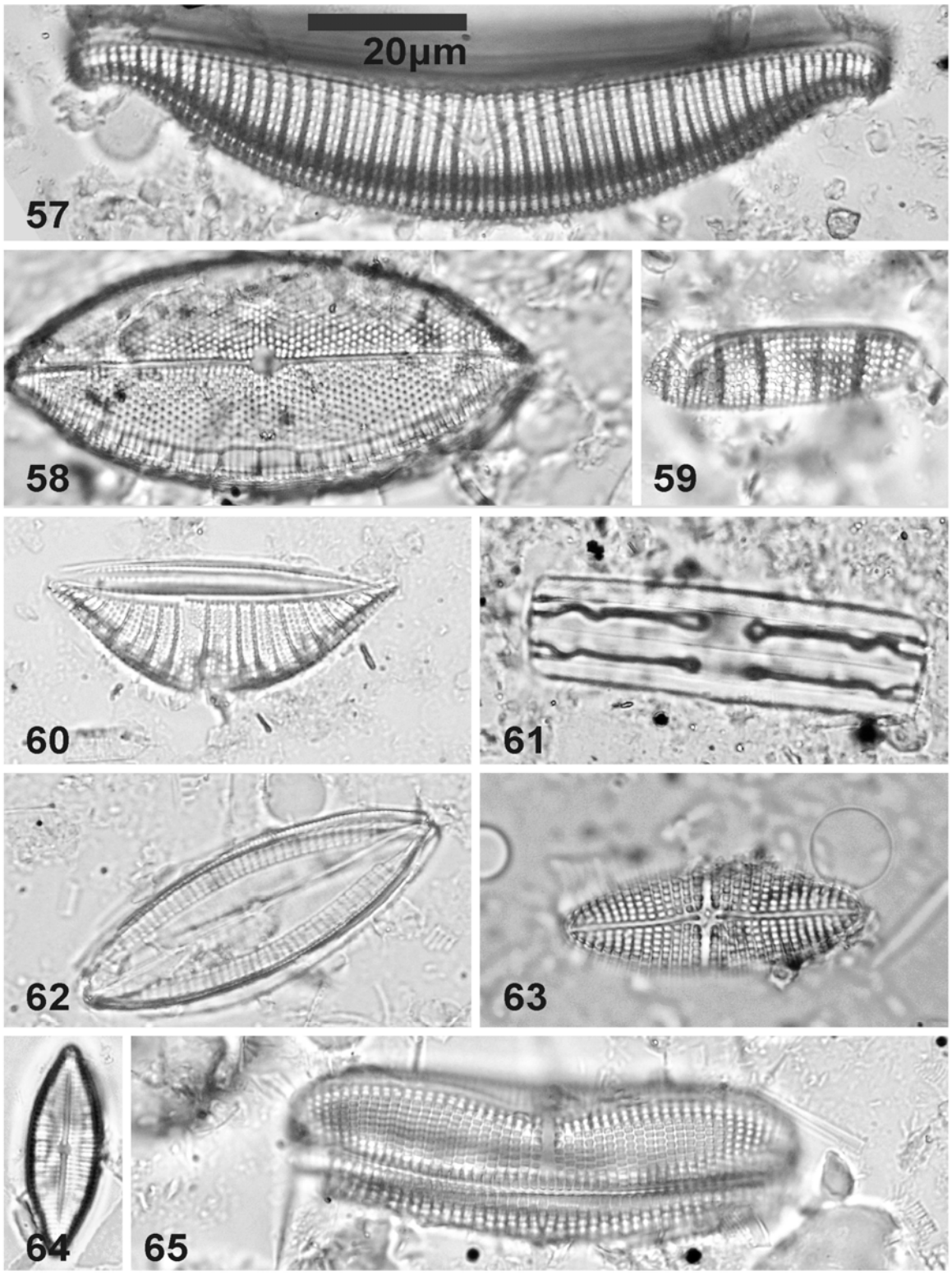

F: 66) *Pleurosigma salinarum*, 68) *P. elongatum*, 67) *Gyrosigma parkerii*, 69) *G. scalproides*, 70) *G. balticum*

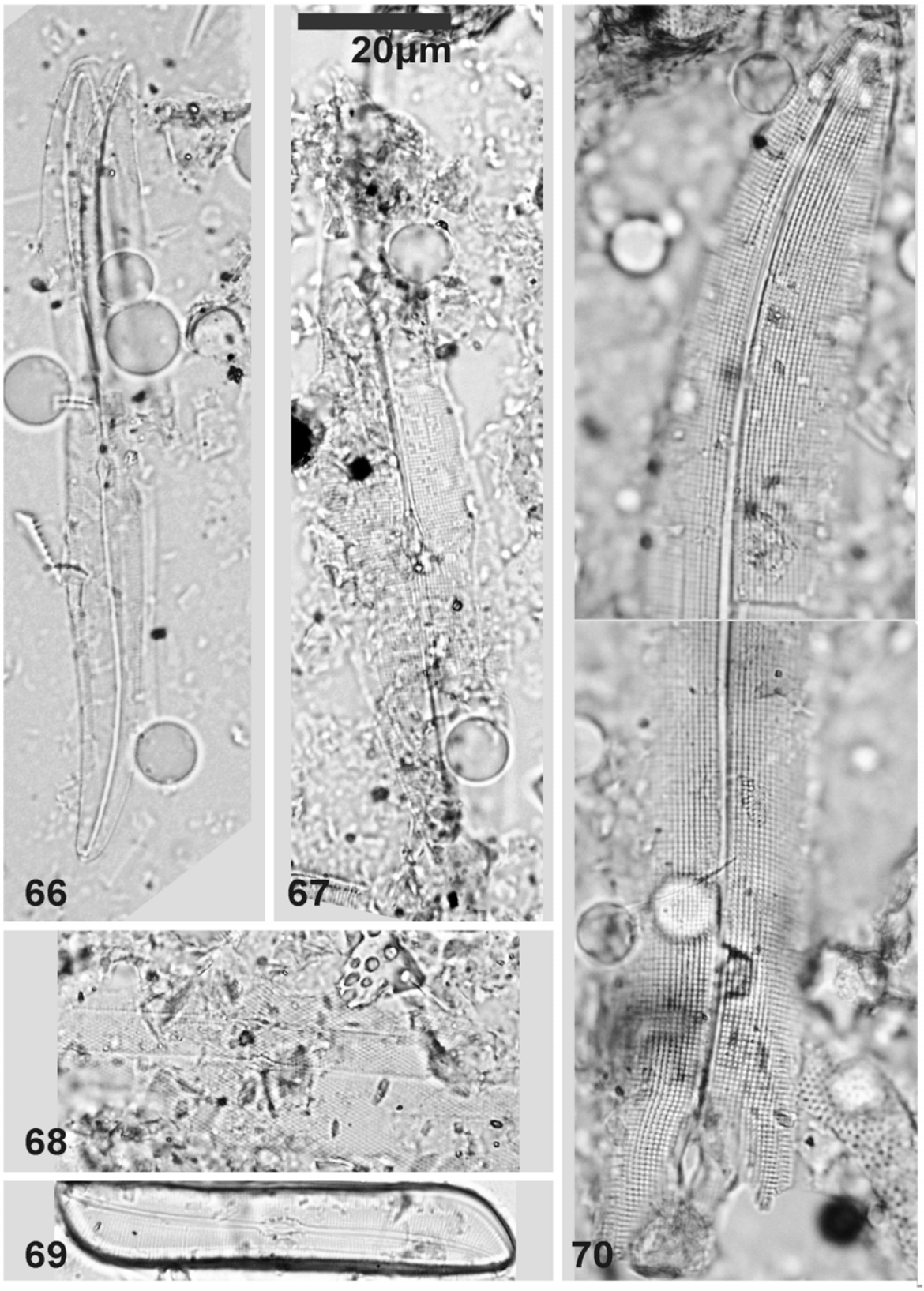

G: 71) *Caloneis cf. latiuscula*, 72) *Caloneis permagna*, 73) *C. amphisbaena*, 74) *Petroneis humerosa*, 75) *C. schumanniana var. biconstricta* 76) *Stauroneis phoenicenteron*

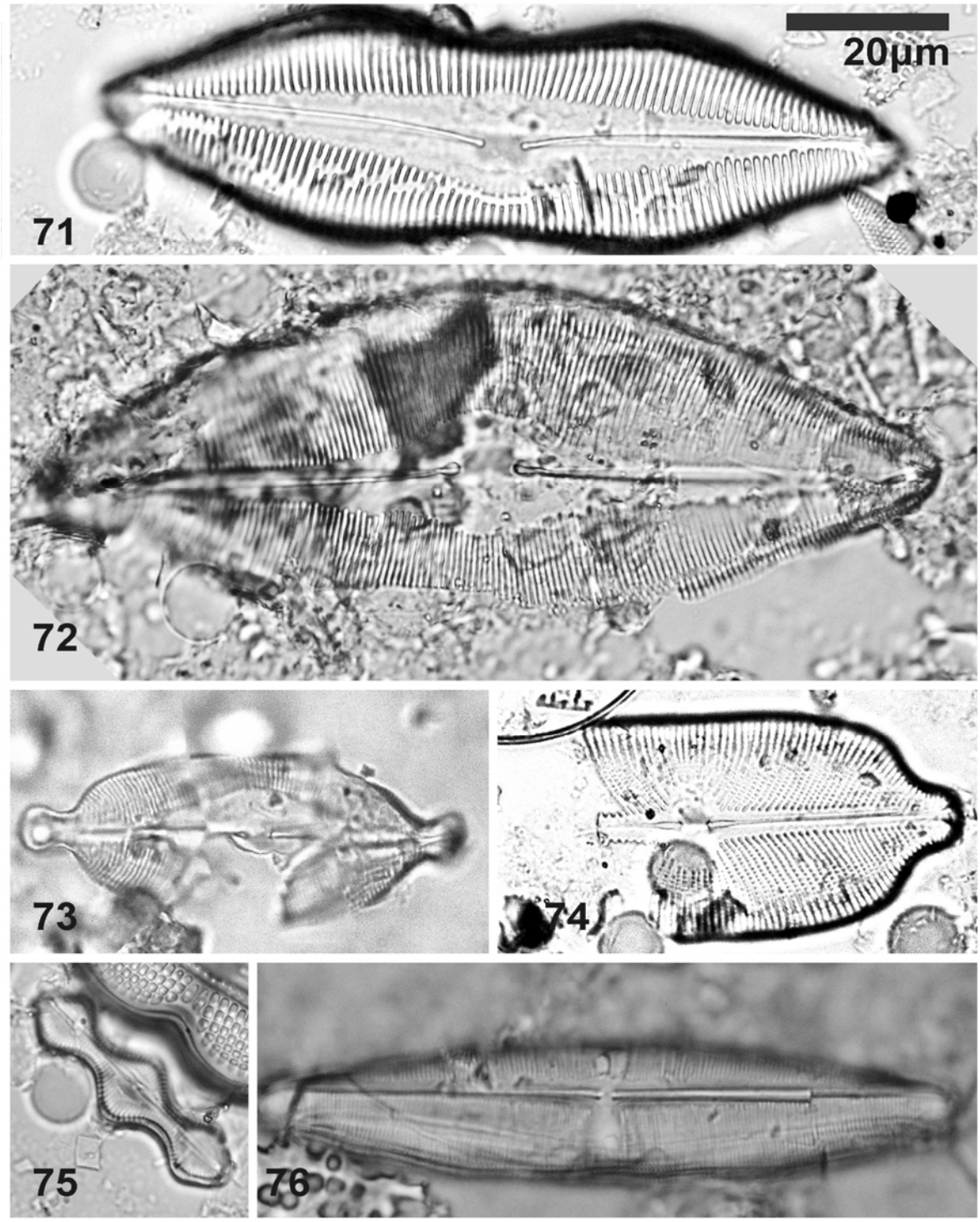

H: 77) *Surirella striatula*, 78) *S. fastuosa*, 79) *Sur. ovalis*, 80) *Tryblionella cocconeiformis*, 81) *Cymatopleura solea*

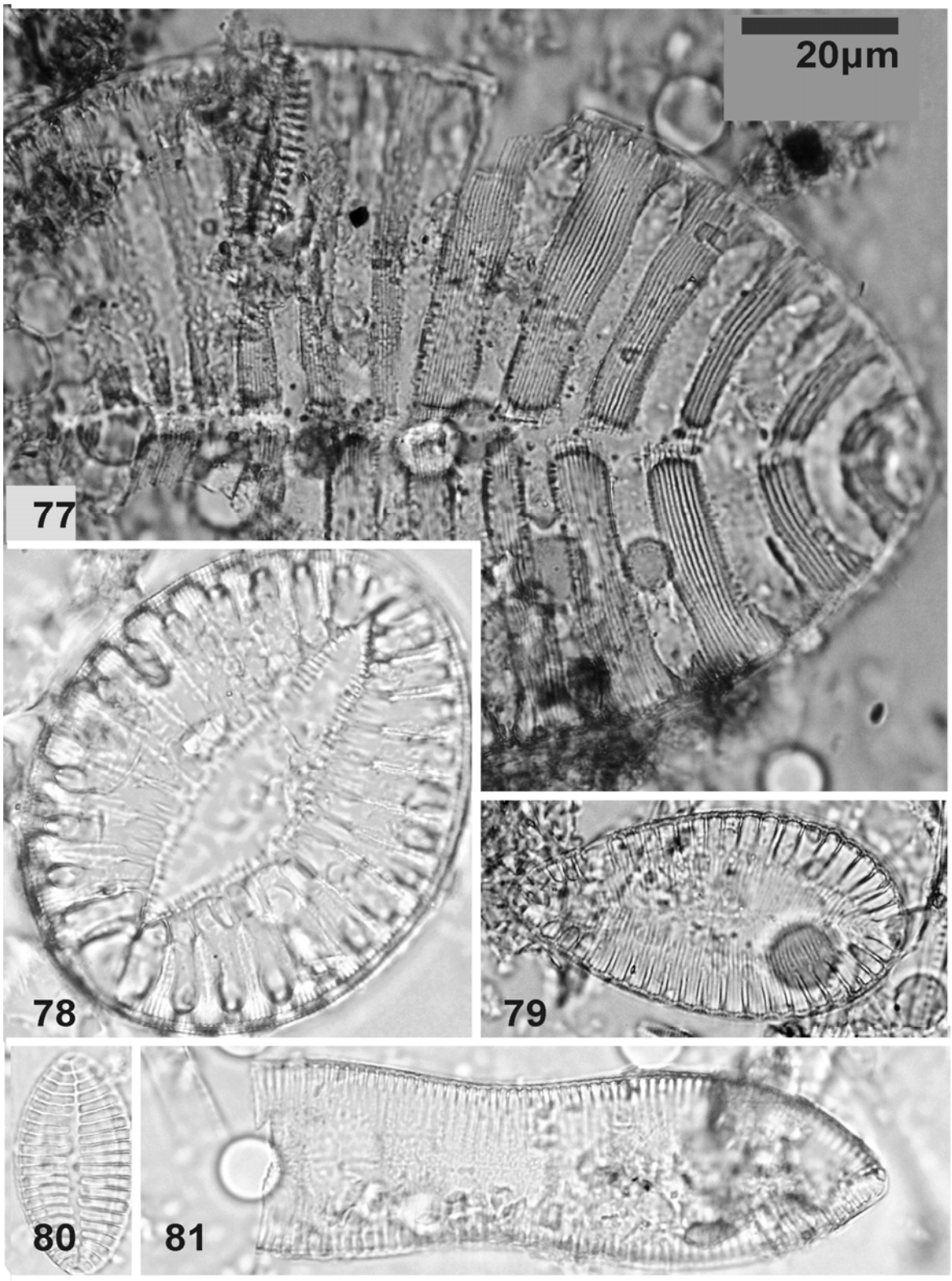

3. BAIKAL LAKE

3.1. Core 98-1-13, 0- 544 cm.

Photo taken in Geologic Institute AS CR by Stanislav Šlechta, 2003. Modified by Anna Píšková, 2009.

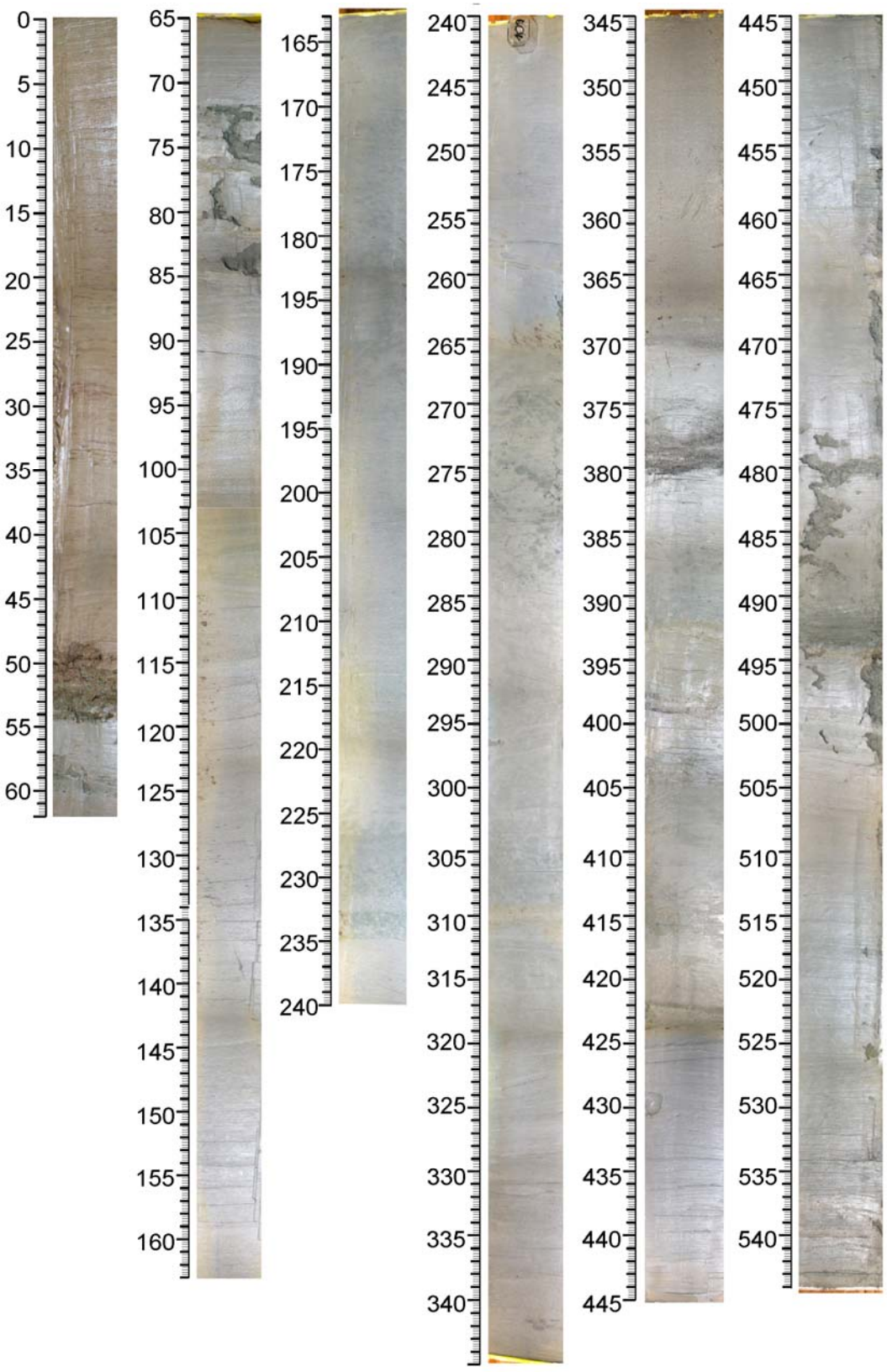

Core 98-1-13, 544-1122 cm.

Photo taken in Geologic Institute AS CR by Stanislav Šlechta, 2003. Modified by Anna Píšková, 2009.

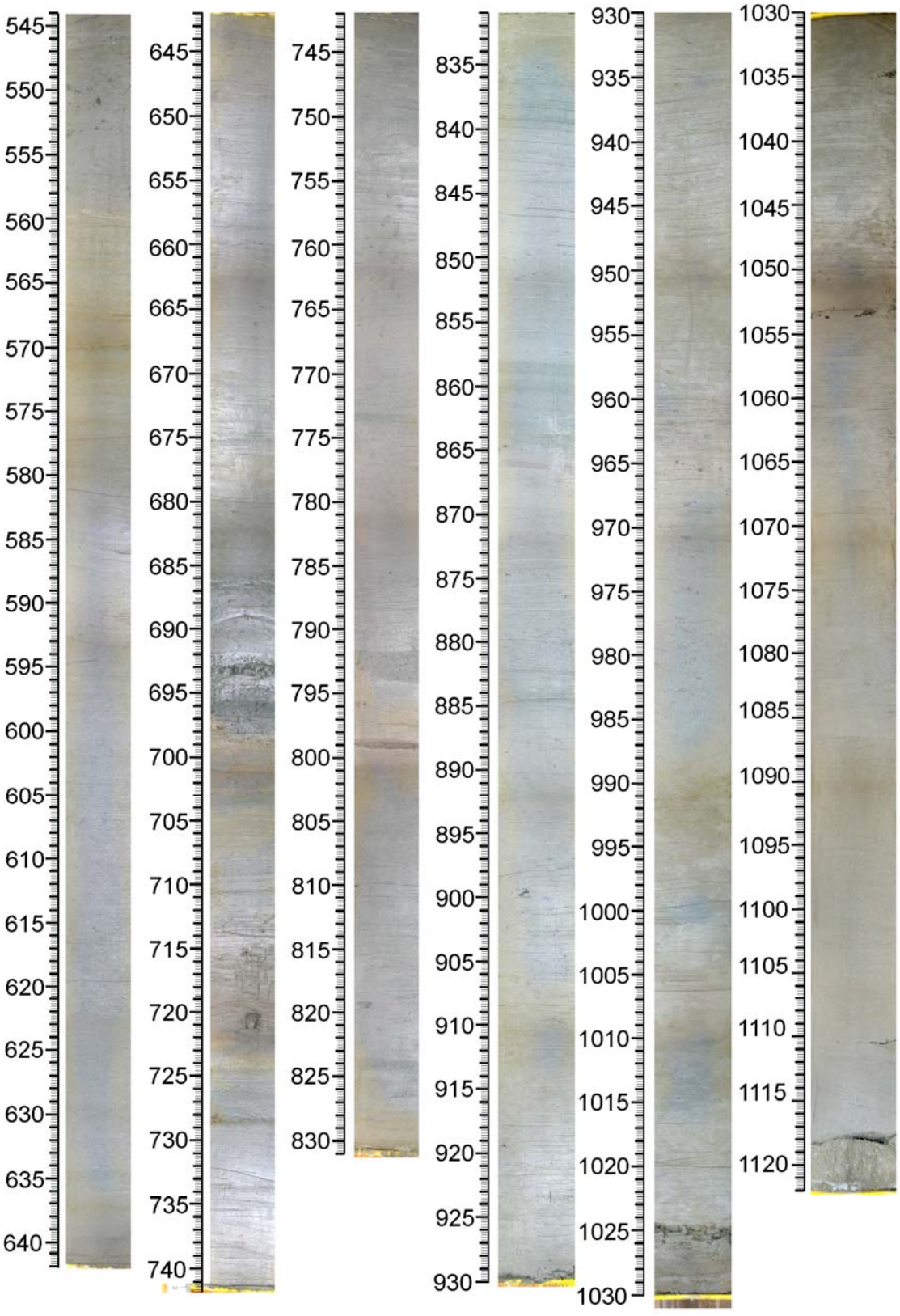

3.2. SEM images of diatom frustules

Stephanodiscus grandis. Scale 5 μm.

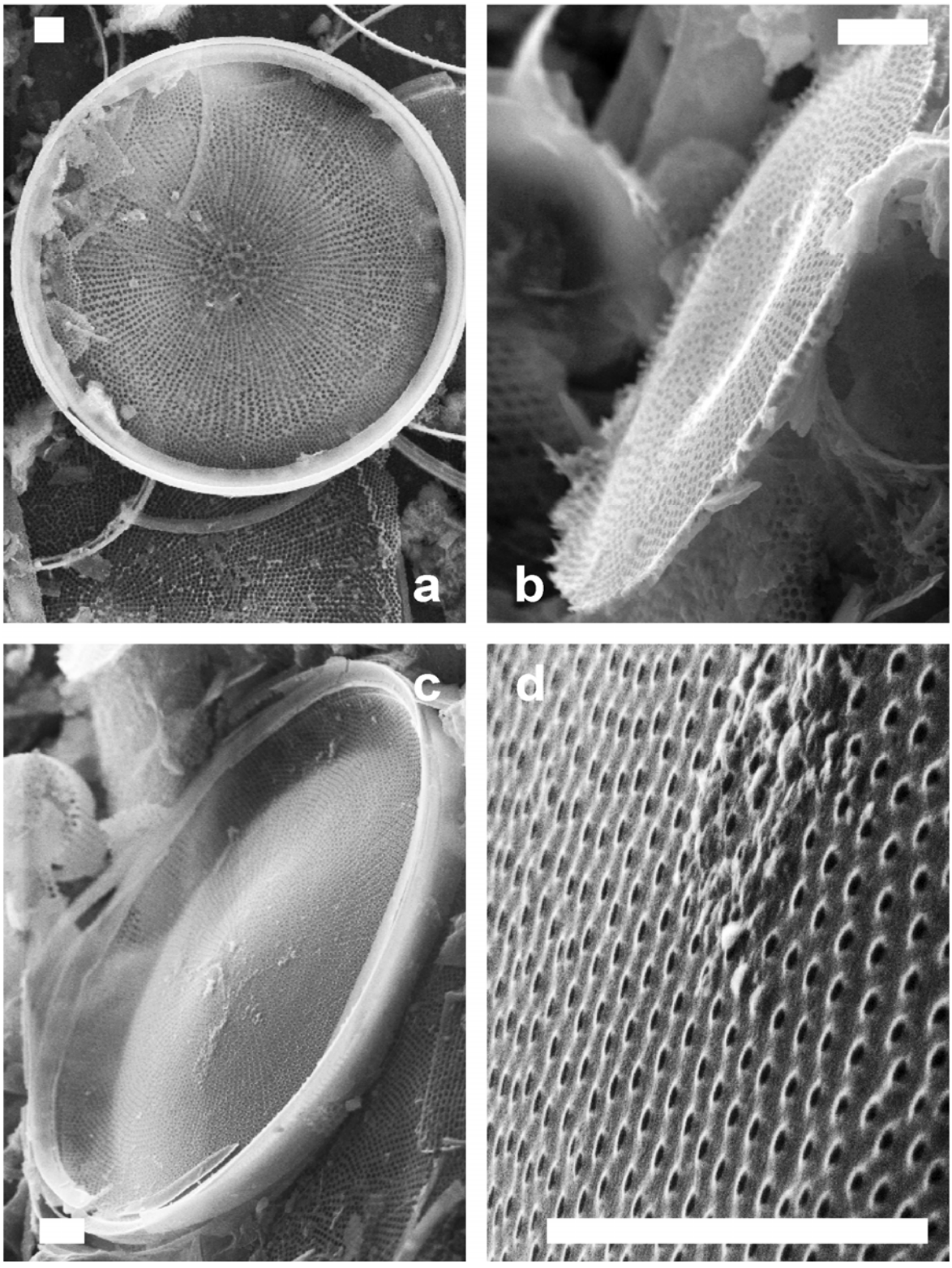

Aulacoseira skwortzowii. Scale 5 μm.

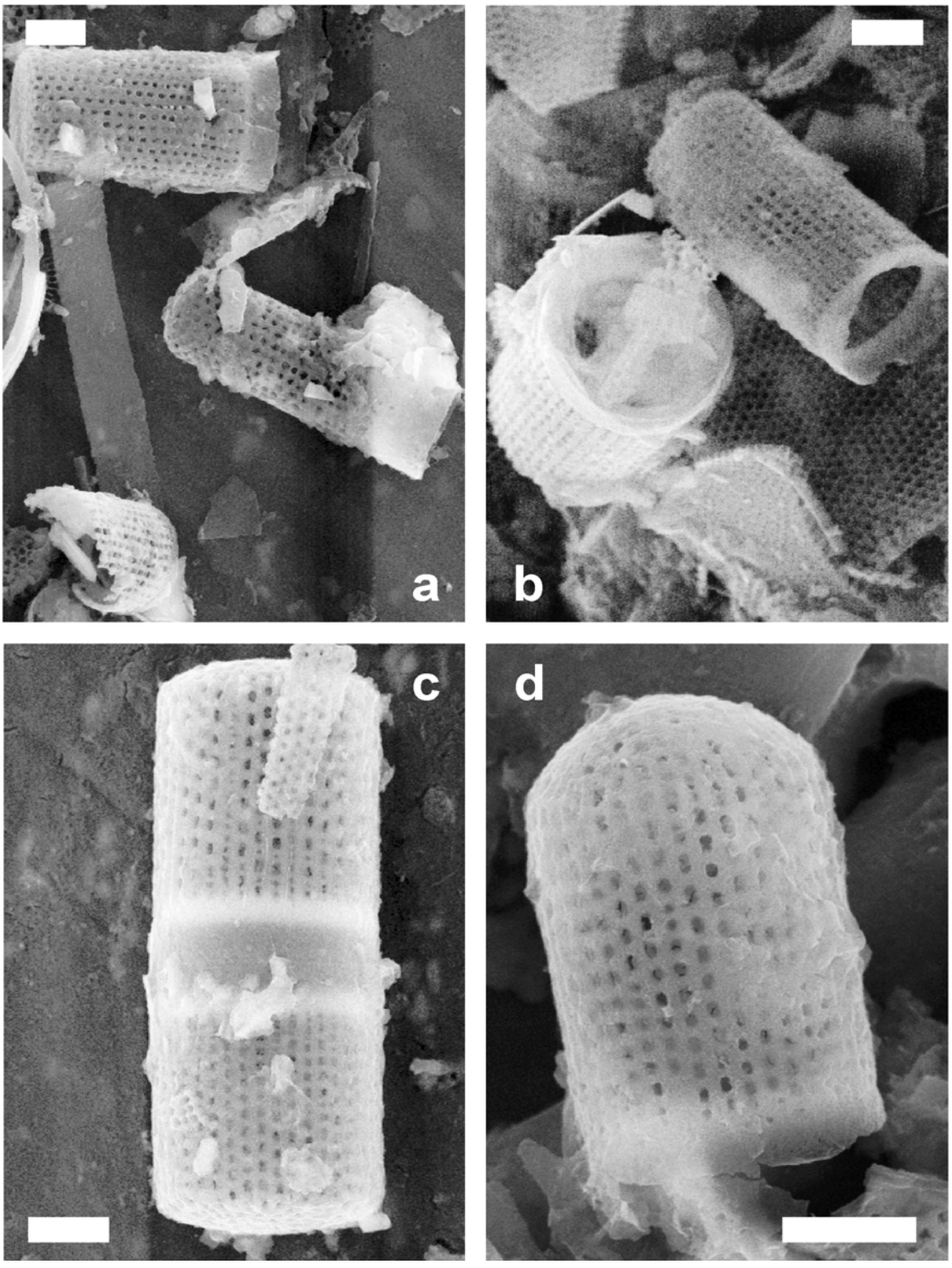

Cyclotella ornata: a) both valves, b) weathered central part of the frustule, c) *Stephanodiscus formosus*. Scale 5 μm.

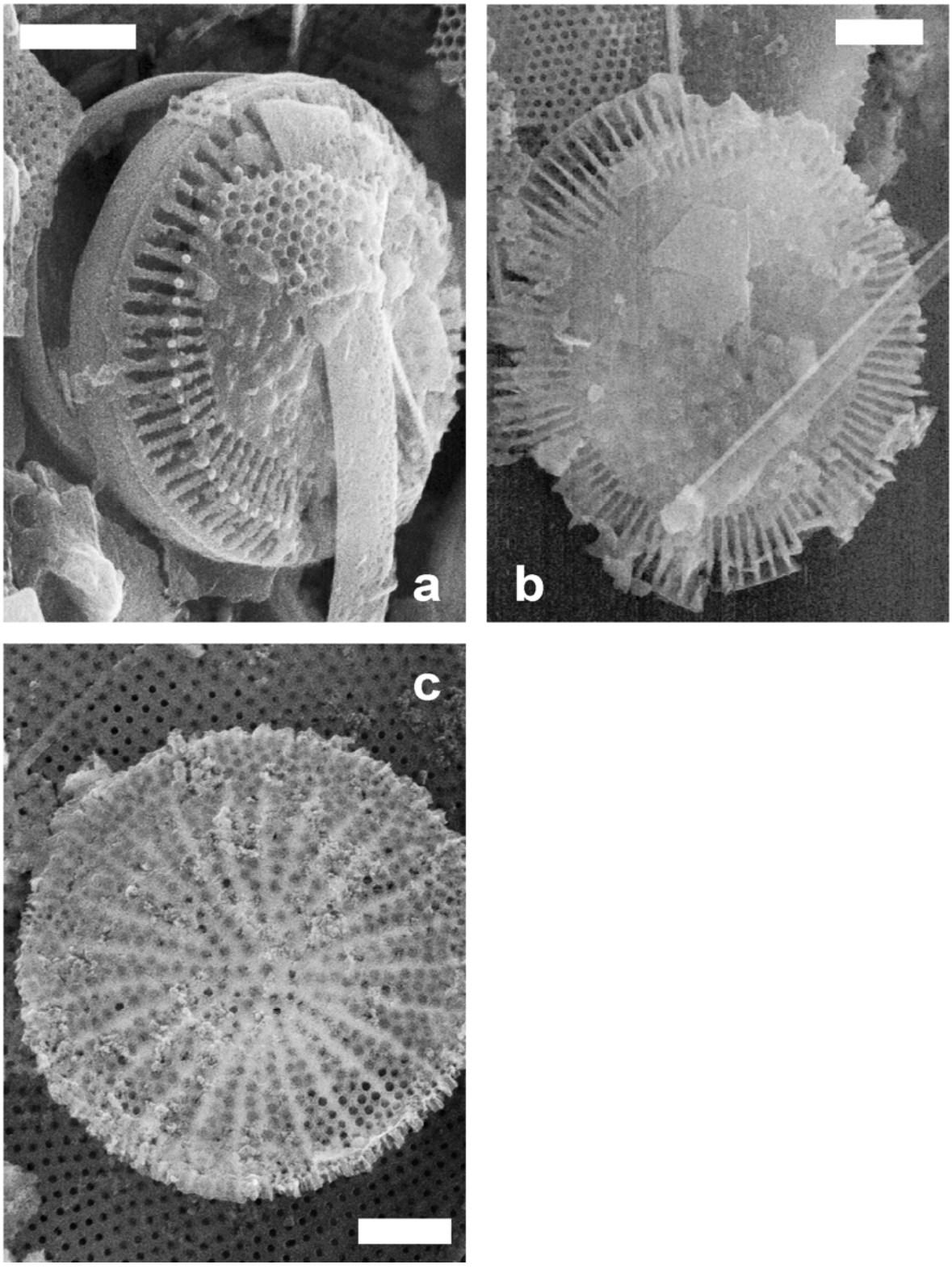

3.3. Photo tables of diatom species from Baikal Lake

1) *Stephanodiscus grandis*, 2) *Navicula spp.*, 4) *Stephanodiscus formosus var. minor*, 5) *S. carconeiformis*, 8) *S. formosus*

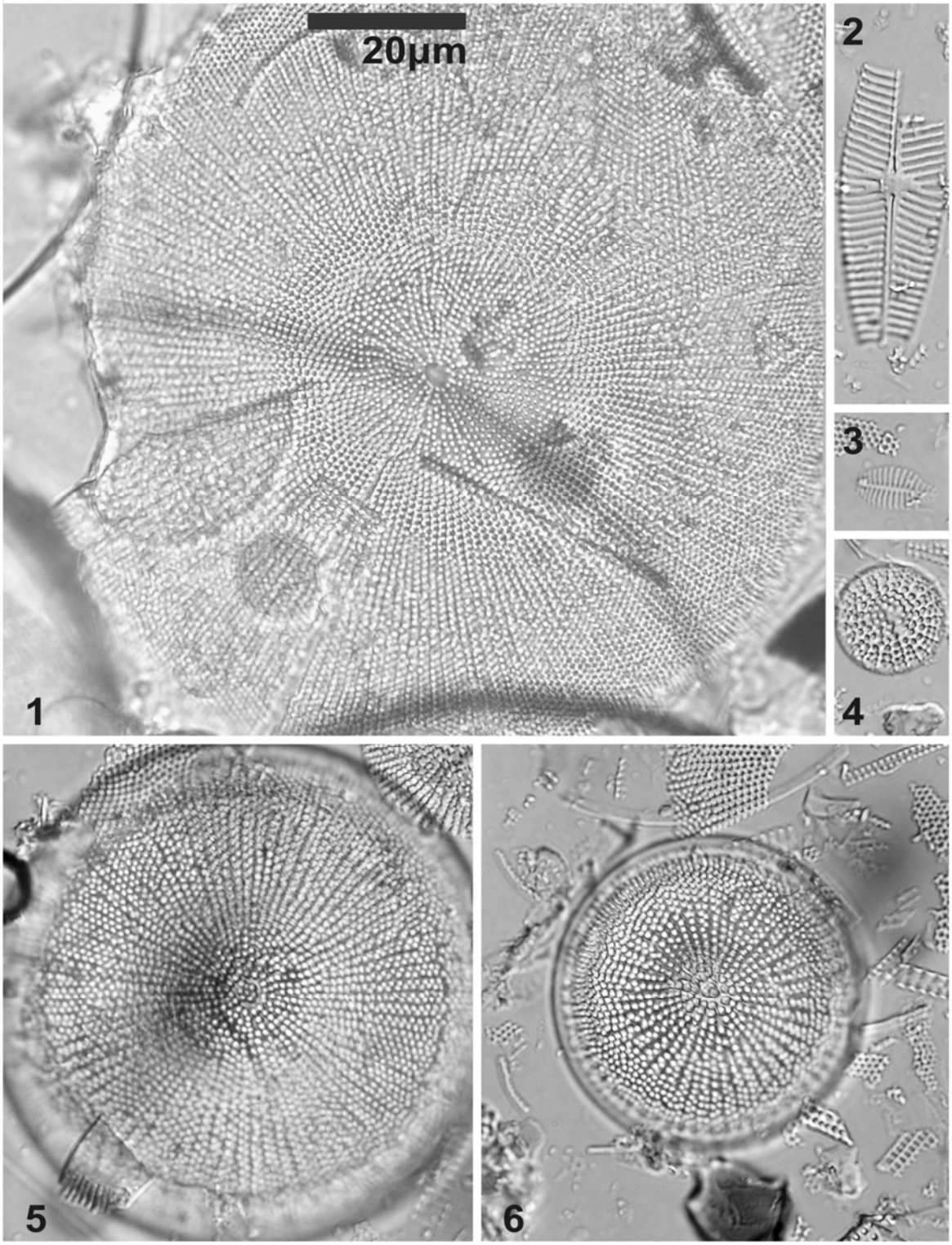

7) *Cyclotella baicalensis*, 8) *Synedra spp.*, 9) *Cyclotella* sp. cf. *operculata*, 10) *C. comtaeformica*, 11, 12) *Stephanodiscus flabellatus*, 13) *Stephanodiscus formosus var. minor*, 14) *Cyclotella* cf. *temperiana*

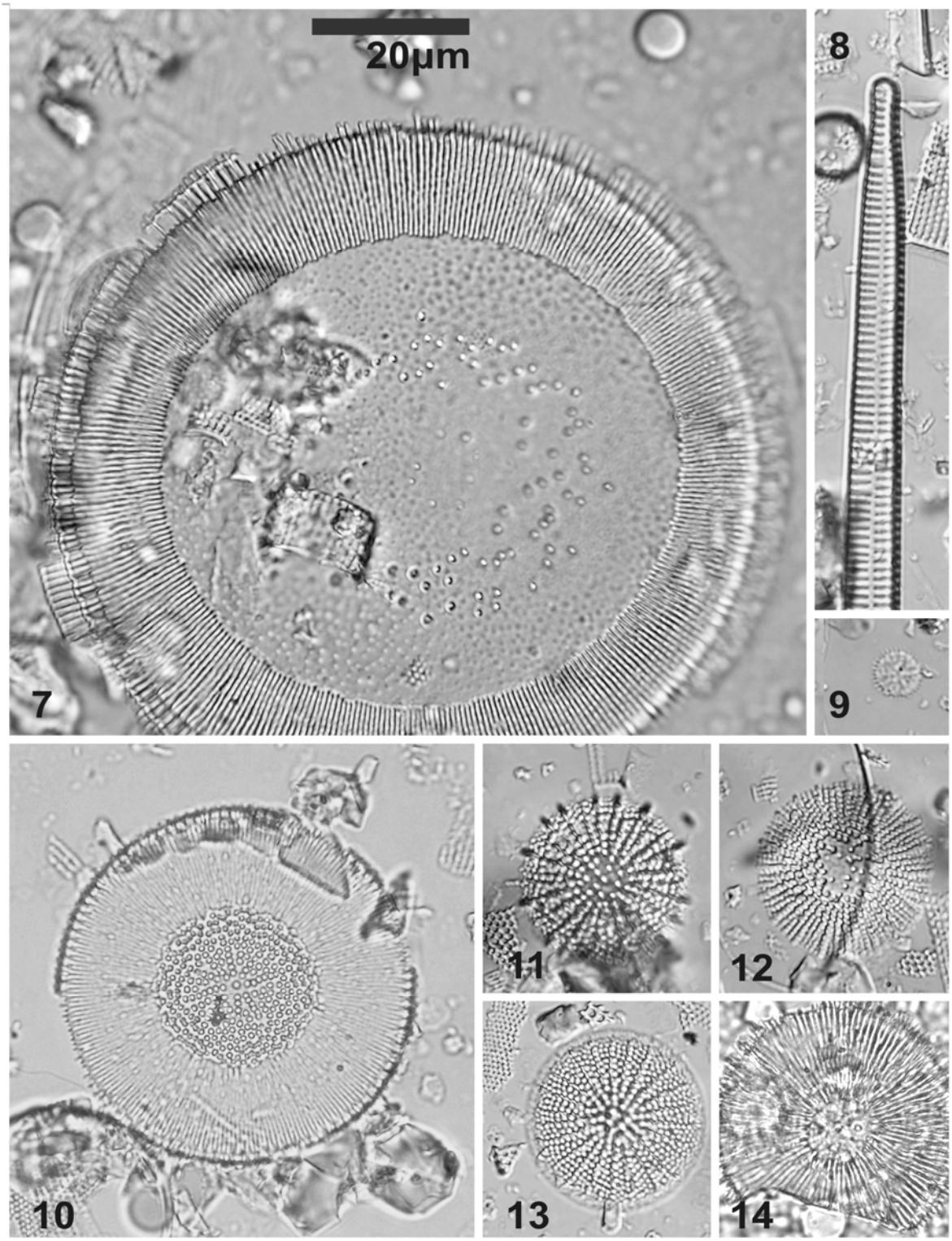

15, 16) *Cyclotella ornata*, 17, 18, 19) *C. minuta*, 20, 25) *Aulacoseira baicalensis*, 21-27 (except 25) *A. skvortzowii*: 21, 24) vegetative valve with fine areolae, 23, 26, 27) resting spore with coarse areolae, 22) auxospore